EXPLOITING DNA DAMAGE RESPONSE IN THE ERA OF PRECISION ONCOLOGY

EDITED BY: Yitzhak Zimmer, Christian Reinhardt and Michaela Medová
PUBLISHED IN: Frontiers in Oncology

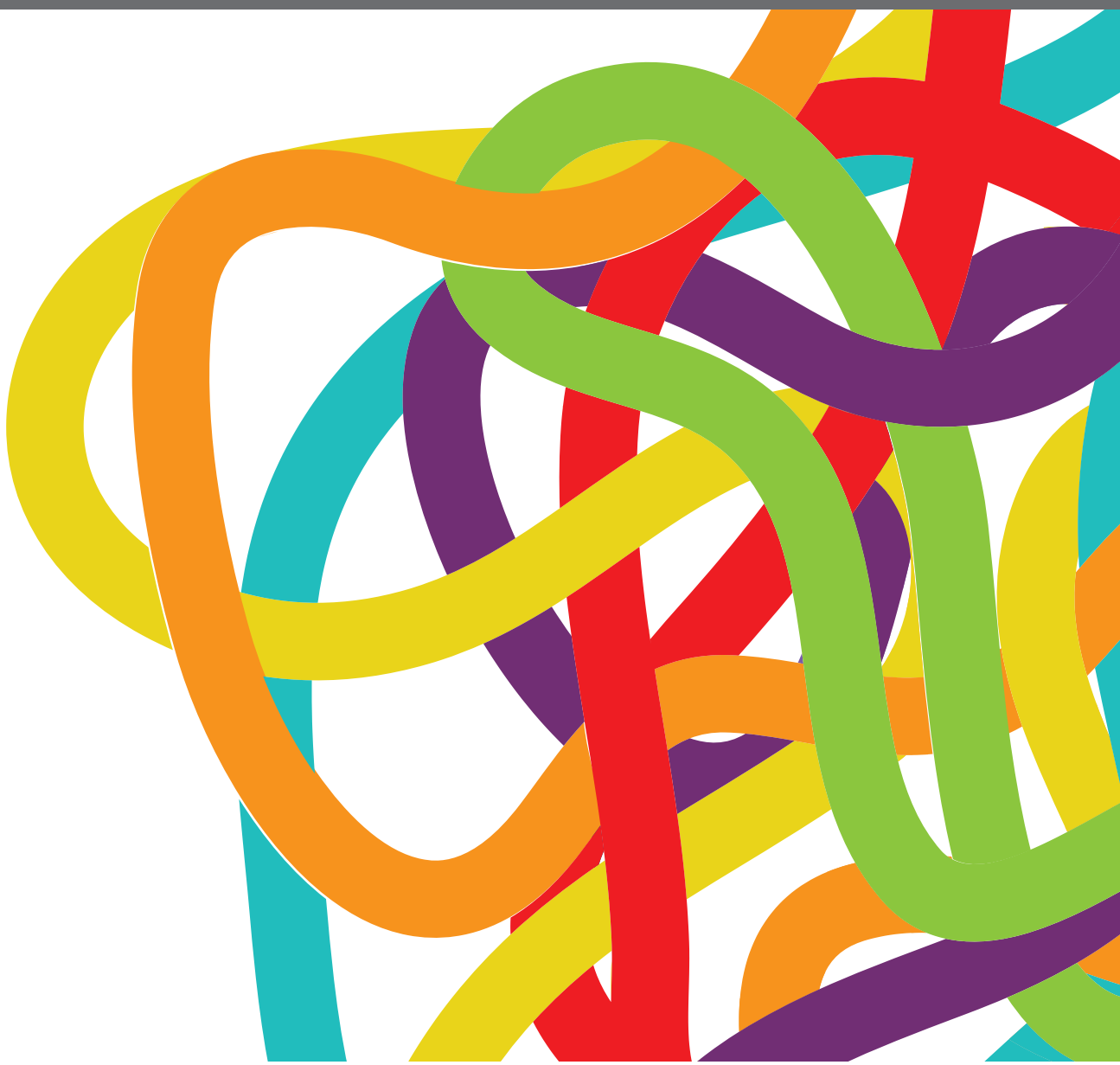

frontiers Research Topics

frontiers

ISSN 1664-8714
ISBN 978-2-88966-215-9
DOI 10.3389/978-2-88966-215-9

About Frontiers

Frontiers is more than just an open-access publisher of scholarly articles: it is a pioneering approach to the world of academia, radically improving the way scholarly research is managed. The grand vision of Frontiers is a world where all people have an equal opportunity to seek, share and generate knowledge. Frontiers provides immediate and permanent online open access to all its publications, but this alone is not enough to realize our grand goals.

Frontiers Journal Series

The Frontiers Journal Series is a multi-tier and interdisciplinary set of open-access, online journals, promising a paradigm shift from the current review, selection and dissemination processes in academic publishing. All Frontiers journals are driven by researchers for researchers; therefore, they constitute a service to the scholarly community. At the same time, the Frontiers Journal Series operates on a revolutionary invention, the tiered publishing system, initially addressing specific communities of scholars, and gradually climbing up to broader public understanding, thus serving the interests of the lay society, too.

Dedication to Quality

Each Frontiers article is a landmark of the highest quality, thanks to genuinely collaborative interactions between authors and review editors, who include some of the world's best academicians. Research must be certified by peers before entering a stream of knowledge that may eventually reach the public - and shape society; therefore, Frontiers only applies the most rigorous and unbiased reviews.
Frontiers revolutionizes research publishing by freely delivering the most outstanding research, evaluated with no bias from both the academic and social point of view. By applying the most advanced information technologies, Frontiers is catapulting scholarly publishing into a new generation.

What are Frontiers Research Topics?

Frontiers Research Topics are very popular trademarks of the Frontiers Journals Series: they are collections of at least ten articles, all centered on a particular subject. With their unique mix of varied contributions from Original Research to Review Articles, Frontiers Research Topics unify the most influential researchers, the latest key findings and historical advances in a hot research area! Find out more on how to host your own Frontiers Research Topic or contribute to one as an author by contacting the Frontiers Editorial Office: frontiersin.org/about/contact

EXPLOITING DNA DAMAGE RESPONSE IN THE ERA OF PRECISION ONCOLOGY

Topic Editors:
Yitzhak Zimmer, University Hospital Bern, Switzerland
Christian Reinhardt, University of Cologne, Germany
Michaela Medová, University Hospital Bern, Switzerland

Topic Editor Christian Reinhardt has received funding from companies Gilead, and lecture fees from Abbvie, Merck, and AstraZeneca. All other topic editors declare no competing interests with regards to the Research Topic subject.

Citation: Zimmer, Y., Reinhardt, C., Medová, M., eds. (2020). Exploiting DNA Damage Response in the Era of Precision Oncology. Lausanne: Frontiers Media SA. doi: 10.3389/978-2-88966-215-9

Table of Contents

frontiers in Oncology

EDITORIAL
published: 15 October 2020
doi: 10.3389/fonc.2020.611127

Editorial: Exploiting DNA Damage Response in the Era of Precision Oncology

Yitzhak Zimmer[1,2], *Hans Christian Reinhardt*[3,4] *and Michaela Medová*[1,2]*

[1] Department of Radiation Oncology, Inselspital, Bern University Hospital, University of Bern, Bern, Switzerland, [2] Department for BioMedical Research, Inselspital, Bern University Hospital, University of Bern, Bern, Switzerland, [3] Department of Hematology and Stem Cell Transplantation, University Hospital Essen, University of Duisburg-Essen, Essen, Germany, [4] German Consortium for Translational Cancer Research (DKTK), Medical Faculty, University of Duisburg-Essen, Essen, Germany

Keywords: DNA damage, precision oncology, synthetic lethality, DNA repair, personalized medicine

Editorial on the Research Topic

Exploiting DNA Damage Response in the Era of Precision Oncology

The main scope of precision oncology is providing a personally tailored cancer treatment that targets specific driver alterations identified *via* a next generation sequencing profiling of a patient tumor. The application of precision oncology is evolving dramatically and is constantly reshaping cancer treatment. The already routine implementation of trastuzumab and pertuzumab for treatment of breast cancer patients with HER2/neu amplification, imatinib in chronic myeloid leukemia and gastrointenstinal stromal tumors, dabrafenib and trametinib in $BRAF^{V600E}$-mutant melanoma, erlotinib and crizotinib for non-small cell lung cancer with the *EGFR* p.L858R mutation or the *ALK/EML4* rearrangement, respectively, serve as only few examples for the proof of principle (1).

Genome stability is critical for the maintenance of cellular physiology and is persistently sustained by the complex signaling networks of cell cycle checkpoint mediators and DNA repair effectors that together constitute the DNA damage response (DDR) network, which monitors and repairs damaged DNA (2–4). A major consequence of a compromised DDR function is cellular transformation and the onset and progression of cancer. Indeed, genomic instability is recognized as a major hallmark of cancer that commonly evolves on a defective DDR function background (5).

Targeting specific DDR signaling pathways in the context of precision oncology offers opportunities on two different, but complementary levels. Firstly, the vast majority of anti-cancer conventional approaches that consist of radiation therapy, as well as chemotherapeutic drugs as for example platinum compounds, topoisomerase inhibitors and temozolomide, elicit their cytotoxicity *via* DNA damage. Deregulated upregulation of particular DDR pathways by cancer cells may provide an escape mechanism that results in more efficient DNA repair with consequent treatment resistance and less favorable prognosis (6). Depending on a particular tumor landscape, a personalized targeted intervention within a specific relevant DDR pathway may therefore be instrumental for overcoming treatment resistance *via* chemo-radiosensitization. In that respect, effective and specific targeting of the three DDR master upstream kinases of the PIKK family, ATM, ATR and DNA-PK, is in the center of major research efforts in the last years (7–9). An additional targeting concept to effectively induce tumor cell death is blocking of cell cycle checkpoint mediators, such as CHK1, CHK2, and WEE1 in cancer cells with a high replication stress, allowing therefore cell cycle progression with a high burden of DNA damage (10).

OPEN ACCESS

Edited and reviewed by:
Paolo Pinton,
University of Ferrara, Italy

***Correspondence:**
Michaela Medová
michaela.medova@dbmr.unibe.ch

Specialty section:
This article was submitted to Molecular and Cellular Oncology, a section of the journal Frontiers in Oncology

Received: *28 September 2020*
Accepted: *30 September 2020*
Published: *15 October 2020*

Citation:
Zimmer Y, Reinhardt HC and Medová M (2020) Editorial: Exploiting DNA Damage Response in the Era of Precision Oncology. Front. Oncol. 10:611127. doi: 10.3389/fonc.2020.611127

The second major venue to utilize DDR targeting in personalized cancer treatment are tumors with loss-of-function mutations in genes encoding DDR components of a particular repair pathway. These mutations may create an ultimate dependency on an alternative pathway, which, if targetable, creates a tumor-specific vulnerability in the form of a synthetic lethal interaction exploitable in the clinic. Obviously, the dogma of targeting synthetic lethal interactions in the context of DDR signaling has been established through the integration of PARP inhibitors in the management of homologous recombination-deficient tumors due to *BRCA1/BRCA2* inactivating mutations (11–15). Motivated by this successful clinical implementation, functional genomic screens are profoundly used to identify novel synthetic interactions and drug targets in human cancers (16).

This Research Topic of Frontiers in Oncology entitled "Exploiting DNA Damage Response in the Era of Precision Oncology" aimed at bringing together contributions covering various aspects of DDR targeting in the context of precision oncology frameworks. The scopes of the research and review articles included in this collection are described below:

- Mohiuddin and Kang discuss in their review the biologic rationale for DNA-PK as a target in cancer. The roles of DNA-PK within the DDR, as well as in non-DDR signaling are described and an updated overview over the pharmacological efforts for generating effective inhibitors is provided.
- In the original research article by Lundgren Mortensen et al. the authors explore a tumor radiosensitization approach, which aims at increasing cellular p53 levels by using a stapled peptide, PM2, that interferes with the MDM2/X-dependent p53 downregulation. The effectiveness of PM2 together with external beam radiotherapy has been investigated in a panel of cancer cells.
- Das et al. have presented data of a computational approach to predict synthetic lethal interactions of somatic mutations in DDR genes within a TCGA-based pan-cancer cohort of patients. They have used various *in silico* approaches, including drug sensitivities responses, to validate the novel described synthetic lethal interactions.
- Carr et al. investigated in their research on acute myeloid leukemia a combination of the novel DNA-PK inhibitor M3814 and Mylotarg, an approved CD33 antibody conjugated with the DNA double strand break-inducing drug calicheamicin. The study demonstrated an enhanced anti-tumor activity of Mylotarg in the combined treatment modality, resulting from the inhibition of the DNA double strand break repair through non-homologous end-joining *via* M3814.
- Baldwin et al. explored the efficacy of a nano-formulation of the PARP inhibitor talazoparib in combination with temozolomide in xenograft models of Ewing Sarcoma. Their data suggest that the nanoparticle formulation of talazoparib reduces the toxicity of the combined treatment as compared to oral administration of the PARP inhibitor.
- Meng et al. reviewed the signaling interplay between DDR pathways, RNA processing and the generation of tumor-associated extracellular vesicles that are linked to treatment resistance and metastasis.
- The minireview by Trenner and Sartori focused on most recent updates concerning DNA double strand breaks repair pathways and how they could be exploited further for cancer treatment. Particular emphasis of this work is on combinatorial therapeutic approaches and the targeting of potentially newly discovered synthetic lethal interactions.
- Liptay et al. reviewed mechanisms of acquired drug resistance in tumors with DDR deficiencies. The authors of this study concentrated primarily on BRCA-deficient cancers and the emerging role of replication fork biology in acquired drug resistance in these tumors.
- Burgess et al. reviewed mechanisms involved in genomic instability of lung tumors and therapeutic opportunities in combination of DDR-based targeting with various modalities including immunotherapies.

Our understanding of the intricate and extremely complex network of the cellular DDR reshaped by groundbreaking discoveries in the last decades allowed numerous successful implementations of these findings into clinical practice. At the same time, the more we know, the more new questions arise. To one of them – who will profit from a specific therapy? –precision oncology will have to furnish answers all over again and again.

AUTHOR CONTRIBUTIONS

All authors contributed equally. All authors contributed to the article and approved the submitted version.

REFERENCES

1. Schwartzberg L, Kim ES, Liu D, Schrag D. Precision Oncology: Who, How, What, When, and When Not? *Am Soc Clin Oncol Educ Book Am Soc Clin Oncol Annu Meeting* (2017) 37:160–9. doi: 10.14694/EDBK_174176
2. Jackson SP, Bartek J. The DNA-damage response in human biology and disease. *Nature* (2009) 461:1071–8. doi: 10.1038/nature08467
3. Andor N, Maley CC, Ji HP. Genomic Instability in Cancer: Teetering on the Limit of Tolerance. *Cancer Res* (2017) 77:2179–85. doi: 10.1158/0008-5472.CAN-16-1553
4. Tubbs A, Nussenzweig A. Endogenous DNA Damage as a Source of Genomic Instability in Cancer. *Cell* (2017) 168:644–56. doi: 10.1016/j.cell.2017.01.002
5. Hanahan D, Weinberg RA. Hallmarks of cancer: the next generation. *Cell* (2011) 144:646–74. doi: 10.1016/j.cell.2011.02.013
6. Curtin NJ. DNA repair dysregulation from cancer driver to therapeutic target. *Nat Rev Cancer* (2012) 12:801–17. doi: 10.1038/nrc3399
7. Weber AM, Ryan AJ. ATM and ATR as therapeutic targets in cancer. *Pharmacol Ther* (2015) 149:124–38. doi: 10.1016/j.pharmthera.2014.12.001
8. Bradbury A, Hall S, Curtin N, Drew Y. Targeting ATR as Cancer Therapy: A new era for synthetic lethality and synergistic combinations? *Pharmacol Ther* (2020) 207:107450. doi: 10.1016/j.pharmthera.2019.107450

9. Medova M, Medo M, Hovhannisyan L, Maldonado CM, Aebersold DM, Zimmer Y. DNA-PK in human malignant disorders: Mechanisms and implications for pharmacological interventions. *Pharmacol Ther* (2020) 107617. doi: 10.1016/j.pharmthera.2020.107617
10. Smith HL, Southgate H, Tweddle DA, Curtin NJ. DNA damage checkpoint kinases in cancer. *Expert Rev Mol Med* (2020) 22:e2. doi: 10.1017/erm.2020.3
11. Golan T, Hammel P, Reni M, Van Cutsem E, Macarulla T, Hall MJ, et al. Maintenance Olaparib for Germline BRCA-Mutated Metastatic Pancreatic Cancer. *N Engl J Med* (2019) 381:317–27. doi: 10.1056/NEJMoa1903387
12. Litton JK, Rugo HS, Ettl J, Hurvitz SA, Goncalves A, Lee KH, et al. Talazoparib in Patients with Advanced Breast Cancer and a Germline BRCA Mutation. *N Engl J Med* (2018) 379:753–63. doi: 10.1056/NEJMoa1802905
13. Moore K, Colombo N, Scambia G, Kim BG, Oaknin A, Friedlander M, et al. Maintenance Olaparib in Patients with Newly Diagnosed Advanced Ovarian Cancer. *N Engl J Med* (2018) 379:2495–505. doi: 10.1056/NEJMoa1810858
14. Robson M, Goessl C, Domchek S. Olaparib for Metastatic Germline BRCA-Mutated Breast Cancer. *N Engl J Med* (2017) 377:1792–3. doi: 10.1056/NEJMc1711644
15. Robson M, Im SA, Senkus E, Xu B, Domchek SM, Masuda N, et al. Olaparib for Metastatic Breast Cancer in Patients with a Germline BRCA Mutation. *N Engl J Med* (2017) 377:523–33. doi: 10.1056/NEJMoa1706450
16. Huang A, Garraway LA, Ashworth A, Weber B. Synthetic lethality as an engine for cancer drug target discovery. *Nat Rev Drug Discov* (2020) 19:23–38. doi: 10.1038/s41573-019-0046-z

Conflict of Interest: The authors declare that the research was conducted in the absence of any commercial or financial relationships that could be construed as a potential conflict of interest.

frontiers in Oncology

MINI REVIEW
published: 17 July 2019
doi: 10.3389/fonc.2019.00635

DNA-PK as an Emerging Therapeutic Target in Cancer

*Ismail S. Mohiuddin and Min H. Kang**

Cancer Center, Department of Pediatrics, Pharmacology and Neuroscience, School of Medicine, Texas Tech University Health Sciences Center, Lubbock, TX, United States

The DNA-dependent protein kinase (DNA-PK) plays an instrumental role in the overall survival and proliferation of cells. As a member of the phosphatidylinositol 3-kinase-related kinase (PIKK) family, DNA-PK is best known as a mediator of the cellular response to DNA damage. In this context, DNA-PK has emerged as an intriguing therapeutic target in the treatment of a variety of cancers, especially when used in conjunction with genotoxic chemotherapy or ionizing radiation. Beyond the DNA damage response, DNA-PK activity is necessary for multiple cellular functions, including the regulation of transcription, progression of the cell cycle, and in the maintenance of telomeres. Here, we review what is currently known about DNA-PK regarding its structure and established roles in DNA repair. We also discuss its lesser-known functions, the pharmacotherapies inhibiting its function in DNA repair, and its potential as a therapeutic target in a broader context.

Keywords: DNA-PKcs, DNA-PK, DNA repair, chemotherapeutic target, *PRKDC*

OPEN ACCESS

Edited by:
Leonardo Freire-de-Lima, Federal University of Rio de Janeiro, Brazil

Reviewed by:
Alvaro Galli, Italian National Research Council, Italy
Christian Reinhardt, University of Cologne, Germany

****Correspondence:***
Min H. Kang
min.kang@ttuhsc.edu

Specialty section:
This article was submitted to Molecular and Cellular Oncology, a section of the journal Frontiers in Oncology

Received: *23 April 2019*
Accepted: *27 June 2019*
Published: *17 July 2019*

Citation:
Mohiuddin IS and Kang MH (2019) DNA-PK as an Emerging Therapeutic Target in Cancer. Front. Oncol. 9:635. doi: 10.3389/fonc.2019.00635

INTRODUCTION

The DNA-dependent protein kinase (DNA-PK) is a serine/threonine protein kinase consisting of a catalytic subunit (DNA-PKcs) and a Ku heterodimer that is made up of the Ku70 and Ku80 subunits. DNA-PK was accidentally discovered after researchers studying translation found that double-stranded DNA (dsDNA) contaminated their preparations, leading to the phosphorylation of specific proteins (1). Early work showed that DNA-PK phosphorylates Sp1 in the formation of Sp1 transcription complexes (2, 3). It was soon established that DNA-PK was involved in repairing double-strand breaks (DSBs) through non-homologous end-joining (NHEJ). Since then, DNA-PK's role in the DNA damage response (DDR) pathways has been expanded to include pathway choice between NHEJ and homologous recombination (HR) (4) and in the immune system through V(D)J and class-switch recombination (5). Given its critical function in DDR pathways, DNA-PK has been targeted in cancer therapy in concert with DNA-damaging agents (6). More recently, DNA-PK has been implicated in other cellular processes, including cell cycle progression (7) and telomere maintenance (**Table 1**) (33). These findings, combined with the transcriptional targets that associate with DNA-PK, suggest that DNA-PK is pivotal in pathways outside of the DDR that are critical to cellular survival and proliferation.

Cloning of the cDNA of DNA-PKcs showed significant homology with the phosphatidylinositol 3-kinase (PI3K) family, however it did not have any activity toward lipids (34). At 460 kDa, DNA-PKcs is the largest of six serine/threonine kinases in the phosphatidylinositol 3-kinase-related kinase (PIKK) family, consisting of 4,128 amino acids (35). The PIKK family share significant homology (**Figure 1**) (36, 37). Ku heterodimerization is essential to maintain the stability of both subunits, loss of one subunit leads to decreased levels of the other (38). Although there

is significant sequence divergence in the subunits in higher eukaryotes, especially compared to lower organisms, there is structural homology in both subunits (39). Ku70 and Ku80 contain three domains: an alpha helix/beta barrel von Willebrand A (vWA) domain on the N-terminus, a DNA-binding/dimerization core, and a helical domain at the C-terminus. The vWA domain functions as a surface for protein interactions, mediating binding between DNA-PK and factors involved in DNA repair, telomere regulation, and other functions (40). The C-terminal domain (CTD), where the majority of sequence divergence exists, contains the nuclear localization signal (NLS) on both subunits. Although Ku functions as a heterodimer, each subunit can independently import into the nucleus (38). The Ku70 CTD contains the SAP domain that increases the affinity of DNA-binding, whereas the Ku80 CTD houses the critical DNA-PKcs binding region (40).

DNA-PK IN DNA REPAIR

The role of DNA-PK in DNA repair has been extensively reviewed (41), and thus is briefly summarized here. Three main pathways exist to repair damaged DNA: classical NHEJ (C-NHEJ), alternative NHEJ (A-NHEJ), and HR. HR repairs DNA with the greatest fidelity because it uses sister chromatids to repair DSBs, but can only occur in the S and G2 phases of the cell cycle. Both NHEJ pathways can occur throughout the cell cycle, though A-NHEJ is more active during S phase (42). As opposed to the use of template strands in HR, NHEJ ligates two strands of DNA across a break. C-NHEJ is the primary form of DNA repair in higher eukaryotes, due to its simplicity and presence throughout the cell cycle. If C-NHEJ is unable to repair a DSB, the error-prone A-NHEJ becomes the dominant pathway (40, 43). But before a damage pathway is pursued, a cell must detect the presence of DSBs. H2A histone family member X (H2AX), is phosphorylated both by DNA-PKcs and ATM at its Ser139 residue to form γ-H2AX, a marker of DNA damage, that functions to retain factors involved in DSB repair (12).

DNA-PK in Non-homologous End-Joining

By recruiting specific enzymes, NHEJ can repair DSBs of varying complexity, like those with incompatible ends or damaged bases (44). The sequence of NHEJ can be described as: (a) DSB end-recognition and binding by Ku; (b) assembly of the components of the NHEJ machinery, such as DNA-PKcs, the XRCC4-DNA ligase IV complex, and XRCC4-like factor (XLF); (c) activation of DNA-PKcs kinase activity; (d) bridging and, if necessary, end-processing of the broken DNA strands; (e) end-ligation by the XRCC4-DNA ligase IV complex; and (f) dissociation of the NHEJ machinery (36, 44, 45). The order of events following Ku binding to DNA is unknown; NHEJ is a dynamic process involving multiple factors interacting simultaneously.

In the first step of NHEJ, the Ku heterodimer recognizes and binds to the free ends of the DSB and recruits the canonical factors involved in NHEJ, including XRCC4-DNA ligase IV (9), XLF (46), and DNA-PKcs. Caspase-2-mediated cleavage of Ku80 at Asp726 may allow for DNA-PKcs binding and formation of the DNA-PK complex (47), causing an inward translocation of the Ku heterodimer and DNA-PKcs activation through conformational changes in the FAT and FATC domains (45). The DNA-PK complex likely tethers broken DNA strands, thereby preventing their nucleolytic degradation (48). DNA-PKcs phosphorylates members of the NHEJ machinery, including Ku,

TABLE 1 | Protein targets of DNA-PK and their associated cellular functions.

Protein Target	Function	References
DNA DAMAGE RESPONSE		
Non-homologous end joining		
Artemis	Contributes to end-processing of DSB	(8)
DNA-PKcs	Phosphorylates factors involved in NHEJ	(8–11)
H2AX	Retains factors involved in DSB repair	(12)
Ku70/Ku80	Binds to DNA, recruits components of NHEJ machinery	(8, 9)
XLF	Stabilizes ends of DSBs	(8, 9)
XRCC4	Stabilizes ends of DSBs and ligates DSB with Ligase IV	(8, 9)
Homologous recombination		
BRCA1	Inhibits DNA-PKcs-mediated autophosphorylation	(13)
DNA-PKcs	Involved in DDR pathway choice via differential phosphorylation	(14, 15)
H2AX	Retains factors involved in DSB repair	(12)
RPA	Promotes HR after phosphorylation via recruitment of Rad51	(16, 17)
NON-DNA DAMAGE RESPONSE		
Cell cycle progression		
Chk2	Forms complex with BRCA1 to organize mitotic spindle	
DNA-PKcs	Localizes to centrosomes and kinetochores	(18–20)
MDM2/HDM2	Overcomes p53-mediated G1 phase cell cycle arrest	(21, 22)
p53	Causes cell cycle arrest in G1 phase	
PLK1	Regulates mitotic entry	(19, 23)
PP6	Regulates mitotic exit	(23)
Transcriptional regulation		
AR	Drives expression of prostate cancer-associated genes	(24)
NRE	Impairs glucocorticoid-induced MMTV transcription	(25)
OCT1 & OCT2	Drive expression of genes in multiple tissues	(26)
RNA Pol I	Involved in transcriptional elongation	(27)
Sp1	Functions as general transcription factor	(2)
TBP	Functions as general transcription factor	(28)
TFIIB	Functions as general transcription factor	(28)
TRIM28	Activates RNA Polymerase II to activate transcriptional elongation	(27)
Telomere maintenance		
DNA-PKcs	Facilitates telomere end-capping	(29–31)
hnRNP-A1	Maintains telomeric overhangs and activates telomerase	(29)
Ku70/Ku80	Maintains telomere length	(32)

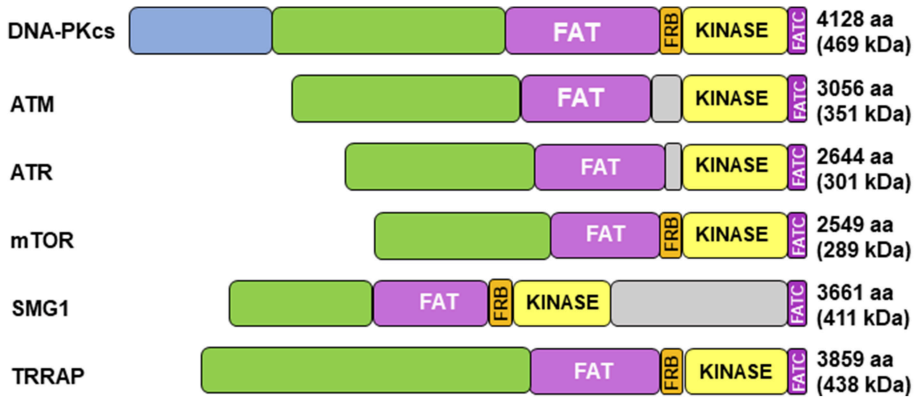

FIGURE 1 | Structure of DNA-PKcs and related members of the phosphatidylinositol 3-kinase-related kinase (PIKK) family. DNA-PKcs can be subdivided into three large structural units: a large N-terminal helical domain, followed by the Circular Cradle, which contains multiple HEAT (Huntingtin, Elongation Factor 3, PP2A, and TOR1) repeats and a number of well-conserved phosphorylation clusters, and a C-terminal Head, which contains the highly conserved catalytic kinase domain. The kinase domain is flanked on either side by the well-conserved FAT (named for its homology in FRAP, ATM, and TRRAP) and FATC (FAT at the C-terminus) domains. The FKBP12-rapamycin-binding (FRB) domain, which sits between the FAT and kinase domain, is essential for mTOR kinase activity and subsequent G_1 to S cell cycle progression, however, it may serve a different purpose in DNA-PK. The N-terminus contains HEAT repeats (blue) that make contact with other HEAT repeats (green). The FAT and FATC domains (purple) help stabilize the catalytic domain (yellow), which is adjacent to the FRB domain (orange). ATM, ataxia-telangiectasia mutated; ATR, ataxia telangiectasia and Rad3-related protein, mTOR, mammalian target of rapamycin; SMG1, one of the serine/threonine-protein kinases; TRRAP, transformation/transcription domain-associated protein.

XRCC4, XLF, DNA-PKcs itself, and Artemis, which is involved in DNA end-processing (8). DNA-PKcs autophosphorylation at Thr2609 and Thr2647 in the ABCDE cluster mediates a conformational change in DNA-PKcs allowing for DNA end-processing (10). Conversely, mutagenesis of Ser2056, another known autophosphorylation site in the PQR cluster, showed that it likely limits end-processing (11).

While autophosphorylation appears to be crucial in NHEJ, the importance of binding interactions and DNA-PKcs-mediated phosphorylation of components of the NHEJ machinery remains unclear (49). Ku80 is crucial in immobilizing the broken ends of chromosomes within the nucleus, allowing for proper alignment at the site of repair (50). Cells harboring a deletion of the Ku80 carboxyl terminus showed increased sensitivity to IR and decreased levels DNA-PKcs autophosphorylation at Thr2647 when compared with controls, but levels of the autophosphorylated Ser2056 residue were unchanged (51). Mutant Ku heterodimers containing alanine instead of serine or threonine at residues 6, 577, and 580 of Ku70 and 715 of Ku80 were still able to function in DNA-damage repair (52).

DNA-PK in Homologous Recombination

When faced with DNA damage-inducing stress, a cell has a choice between NHEJ and HR, but the competition between the two pathways is not fully understood. The availability of sister chromatids in the S and G2 phases of the cell cycle make HR a more favorable outcome, but some mechanism must exist to inhibit NHEJ, which can be activated at any point in the cell cycle. Breast Cancer 1, early onset (BRCA1), a canonical HR factor, functions in various capacities during DNA repair. In the context of pathway choice, BRCA1 prevents NHEJ in the S and G2 phases by inhibiting DNA-PKcs autophosphorylation at Ser2056. This interaction, mediated BRCA1's BRCT domain binding to DNA-PKcs, occurs in a phosphorylation-independent manner (13).

Beyond cell cycle considerations, other factors influencing the decision to pursue one DDR pathway over another remain unclear. Cells with inactivating mutations in Ku and DNA-PKcs will preferentially use HR as the primary DDR mechanism (14). Perhaps DNA repair pathway choice centers on whether DNA-PKcs is activated via phosphorylation: a phosphorylated/active form of DNA-PKcs favors NHEJ, while an unphosphorylated/inactive form favors HR. However, seemingly contradictory findings indicate a more nuanced mechanism. While mutagenesis and inactivation of DNA-PKcs that impaired NHEJ favored HR, pharmacological inhibition of DNA-PKcs impaired HR (15).

Replication protein A (RPA), a heterodimer that binds to single-stranded DNA (ssDNA), is an important modulator of HR. RPA complexes with tumor suppressor protein p53 and is hyperphosphorylated after DNA damage via DNA-PKcs (16). Coupled with the phosphorylation of p53, this hyperphosphorylation causes dissociation of the RPA-p53 complex and allows RPA to bind to ssDNA and promote HR via Rad51. Cells treated with camptothecin, followed by siRNA knockdown of DNA-PKcs-mediated phosphorylation of residues of RPA32, showed impaired HR (17).

FUNCTIONS OF DNA-PK OUTSIDE OF DNA REPAIR

Aside from its well-known role in two of the DDR pathways, DNA-PK functions in other cellular processes, such as cell cycle progression, transcription, and telomere maintenance. These

functions may be involved in tumor progression, highlighting DNA-PK's potential as a therapeutic target.

DNA-PK's Role in Cell Cycle Progression

Upon genotoxic stress, p53 causes cell cycle arrest in G1. Human/murine double minute 2 (MDM2; HDM2 in humans) overcome this blockade by complexing with p53. Since its discovery, MDM2—and its interplay with p53—has been targeted in cancer therapy (53). DNA-PKcs regulates this interaction by phosphorylating HDM2 at Ser17 to prevent binding with p53 (21). DNA-PK also acts on p53 by phosphorylating its Ser15 and Ser37 residues, inducing a conformational change that prevents HDM2 binding (22).

Cells are susceptible to DNA damage during S phase, which results in stalling or collapse of the replication fork. Replication stress leads to the formation of one-ended DSBs that are bound by RPA. Linked to its role in HR, DNA-PKcs-mediated phosphorylation of Ser4 and Ser8 of RPA32 causes growth arrest and delays mitotic entry (54).

DNA-PKcs has been implicated in the regulation of mitosis. Numerous studies have shown that reduction of DNA-PKcs enzymatic activity, either by pharmacological inhibition or by siRNA-mediated knockdown, leads to defects in chromosomal alignment and in nuclear morphology (7). Phosphorylation of DNA-PKcs at Ser2056, Thr2609, Thr2647, and Thr3950 causes DNA-PKcs localization to centrosomes. Phosphorylated Thr2609 is also seen at kinetochores during metaphase and cytokinesis (18, 19, 23). Phosphorylation at Thr2609 causes an association with polo-like kinase 1 (PLK1) in the mitotic phase, which regulates mitotic entry and exit, throughout mitosis at multiple subcellular structures. This interaction is essential for chromosomal segregation (19). Ser3205, another residue on DNA-PKcs that is likely essential for the overall success of mitosis, is phosphorylated by PLK1, allowing for the localization of DNA-PKcs to the midbody during cytokinesis. Dephosphorylation of Ser3205, via protein phosphatase 6 (PP6), occurs when cells exit mitosis (23), indicating that phosphorylation of this specific residue mediates mitotic entry and exit. DNA-PKcs also phosphorylates downstream targets involved in mitotic regulation. The Chk2-BRCA1 signaling pathway, which organizes the mitotic spindle, depends on DNA-PKcs activity. Chk2-mediated phosphorylation at Ser988 of BRCA1 ensures proper kinetochore-microtubule attachment. DNA-PKcs regulates Chk2 activity through the phosphorylation of its Thr68 residue. Knockdown of DNA-PKcs by siRNA inhibited phosphorylation of Thr68 on Chk2 and impaired microtubule growth during mitosis (55).

DNA-PK as a Regulator of Transcription

Once established, the critical role DNA-PK plays in the DDR pathways became the dominant focus of its study. However, DNA-PK is critical for efficient gene expression, both in mediating transcriptional machinery and in modulating transcription factors. *In vitro*, Chinese hamster ovarian cells with a Ku70/Ku80 or DNA-PKcs deficiency showed a 2–7-fold decrease in transcription with multiple promoters compared to controls (56). RNA polymerase II activity requires functional activity of the TRIM28 factor, which is phosphorylated by DNA-PKcs at Ser824 (27). DNA-PK is involved in the phosphorylation of the general transcription factors TATA-binding protein (TBP) and transcription factor IIB (TFIIB), allowing them to synergistically form complexes with RNA polymerase and transcription factor IIF to stimulate basal transcription (28). The earliest defined role of DNA-PKcs in transcription was its activity on the transcription factor Sp1, which activates cellular promoters by binding to GC-rich regions. Upon binding to promoters, multiple residues of Sp1 are phosphorylated by DNA-PKcs (2). DNA-PKcs is also involved in the phosphorylation and activation of the POU domains of octamer-binding transcription factors 1 and 2 (OCT1 and OCT2) (26). Serine residues of c-MYC, the oncoprotein responsible for transcription of ∼15% of the human genome (57), are phosphorylated by DNA-PKcs (58). DNA-PKcs also mediates the transcriptional activation of factors involved in metabolism. After feeding or in response to insulin, DNA-PK phosphorylates the upstream stimulatory factor-1 (USF-1) transcription factor at its Ser262 residue. The DNA-PK-USF complex induce transient breaks in the fatty acid synthase (FAS) promoter region immediately preceding transcriptional activation. Once transcribed, FAS can induce lipogenesis. DNA-PKcs-deficient mice fail to induce lipogenesis and are deficient in triglyceride levels (59). In 17β-estradiol (E_2)-treated Michigan Cancer Foundation (MCF)-7 cells, topoisomerase IIβ-induced DSBs of the *pS2* promoter appear to be critical component of signal-dependent activation of gene transcription. These transient DSBs activate the enzymatic activity of poly(adenosine diphosphate-ribose) polymerase-1 (PARP-1). DNA-PKcs and the Ku heterodimer were copurified with PARP-1, suggesting that DNA-PK may be involved in transcriptional activation at these transient breaks (60). Recent studies demonstrated that DNA-PKcs functions in the progression of hormone-driven cancers. In advanced prostate cancer, DNA-PKcs coactivates the androgen receptor (AR), promoting metastatic phenotypes. Depletion of DNA-PKcs reduced expression of AR-regulated genes, delaying the formation of metastases (24). In breast cancer, DNA-PKcs-mediated phosphorylation of the estrogen receptor-α (ERα) at Ser118, leads to its stabilization and transcriptional activation. Inhibition of DNA-PK, either pharmacologically or via siRNA, reduced activation of ERα as well as increased its ubiquitination and subsequent degradation (61).

DNA-PK and Telomere Maintenance

Given that telomeres are essentially endogenously occurring DSBs, it seems likely that DNA-PK would be intricately involved in their regulation. Paradoxically, DNA-PK's role in telomere maintenance is to protect against the processing and fusion associated with DSBs. The Ku70/Ku80 heterodimer has been implicated in several processes involving telomeres, including the silencing of telomere-proximal genes, tethering of telomeres to the nuclear periphery, and protecting telomeres from nucleolytic degradation (32, 62). Ku80 is critical for telomere length; siRNA-mediated knockdown of Ku80 led to significant telomere shortening (63). Similar results were produced in mice and human cells when DNA-PKcs activity was impaired (29, 33). Telomeric repeat-containing RNA (TERRA), a long non-coding

RNA transcribed from telomeric DNA, has been implicated in processes related to telomere maintenance, such as the formation of heterochromatin (64, 65), replication (65), and end-capping (66). TERRA activity is thought to be mediated by the heterogenous nuclear ribonucleoprotein A1 (hnRNP A1). DNA-PKcs-mediated phosphorylation of hnRNP A1 removes TERRA from chromatin, allowing for telomere replication. Inhibition of DNA-PKcs/hnRNP A1 activity resulted in TERRA accumulation at telomeres, impairing efficient replication (66). DNA-PKcs is instrumental in facilitating telomere end-capping, likely through an interaction with the kinase interacting protein (KIP) and the telomeric repeat-binding factor 2 (TRF2), a subunit of the shelterin complex (67). Phosphorylation of Ser2056 of DNA-PKcs mediates end-capping. In its absence, uncapped telomeres are seen as DSBs and are processed, leading to inappropriate fusion events (30). Pharmacological inhibition of DNA-PKcs showed similar results in a concentration-dependent manner (31).

DNA-PK AND CANCER

Deregulated DNA-PK activity is associated with a number of cancers. In melanoma, DNA-PKcs acts as a metastatic driver by stimulating angiogenesis and tumor migration. DNA-PKcs activity was associated with the secretion of pro-metastatic proteins through modification of the tumor microenvironment (68). Increased expression and deregulation of DNA-PKcs was demonstrated to drive the development of hepatocellular carcinoma (69, 70). Upregulation of DNA-PKcs has also been observed in multiple myeloma (71), and, along with increased expression of the Ku subunits, is associated with radioresistance in cancers of the thyroid (72), nasopharynx (73), oral cavity (74), and cervix (75). Coupled with its critical cellular functions, these findings have made DNA-PK a prime therapeutic candidate in the treatment of malignancy.

PHARMACOTHERAPIES TARGETING DNA-PK

The development of DNA-PK inhibitors relied on earlier studies that synthesized small molecules PI3K inhibitors. Quercetin, a naturally occurring bioflavonoid, acted as a competitive antagonist against the kinase domain of PI3K and other protein and lipid kinases. This non-selectivity proved to be useful, as quercetin was used as a model compound to develop targeted inhibitors. 2-(4-Morpholinyl)-8-phenyl-4H-1-benzopyran-4-one (LY294002), was developed as a selective and competitive inhibitor of PI3K activity. Unlike quercetin, LY294002 had zero activity against other kinases and had a 2.7-fold increase in potency ($IC_{50} = 1.5–2.0\,\mu M$) (76).

The specificity and potency of LY294002 against PI3K activity made it an ideal structural lead compound to develop new inhibitors that specifically target DNA-PKcs. This next generation of inhibitors, the 2,6-disubstituted pyran-4-one and thiopyran-4-one inhibitors, were more potent ($IC_{50} = 1.1$ and $0.72\,\mu M$, respectively) and selective for DNA-PKcs when compared to LY294002 (77). This led to the development of chromen-4-one derivatives, 2-*N*-morpholino-8-dibenzofuranyl-chromen-4-one (NU7427) and 2-*N*-morpholino-8-dibenzothiophenyl-chromen-4-one (NU7441). Compared to previous DNA-PKcs inhibitors, NU7427, and NU7441 were significantly potent ($IC_{50} = 40$ and 13 nM, respectively) and specific. At concentrations of $100\,\mu M$, NU7441 did not have an effect on ATM or ATR activity and showed minimal activity against PI3K and mTOR (78). NU7441 potentiates the effects of DNA damage-inducing chemotherapy in B-cell chronic lymphocytic leukemia (CLL) (79), breast (80), non-small cell lung carcinoma (NSCLC) (81), and nasopharyngeal carcinoma (NPC) (82) cell lines, as well increasing sensitivity to IR and chemotherapy in colorectal carcinoma cell lines (83). In an attempt to optimize the pharmacologic profile of NU7441, focused libraries were used to identify the biological activity of substitutions at the dibenzothiophene-1 position. The addition of water-soluble groups at this position proved to be effective, leading to the development of a new chromen-four-one derivative that has an even greater potency ($IC_{50} = 6$ nM). Unfortunately, this novel inhibitor may have some undesirable off-target effects (84). However, these findings highlight the ability to further modify known DNA-PKcs inhibitors, specifically with water-soluble groups, to develop more potent therapies. Another strategy to develop novel inhibitors was to use a homology model of the ATP-binding site of DNA-PK, based on the crystal structure of PI3Kγ. KU-0060648, a dual DNA-PKcs and PI3K inhibitor, has better bioavailability and a more favorable pharmacokinetic profile compared to NU7441 and also has limited activity against other PIKK family members. KU-0060648 is also more potent, with a 500-fold increase in solubility compared to NU7441 (85). DNA-PK inhibitors have also been demonstrated as effective single agents, taking advantage of synthetic lethality in ATM-deficient lymphoma models (86).

Another strategy taken to target DNA-PKcs activity in cancer is through the use of non-coding microRNAs (miRNAs). One study identified miR-101 as targeting both DNA-PKcs and ATM. Upregulation of miR-101 sensitized glioblastoma and non-small cell lung cancer cell lines to IR (87). Another study demonstrated that transfection with has-miR-96-5p and has-miR-874-3p combined with IR decreased survival of non-small cell lung cancer cell lines when compared to IR alone, and had a similar effect when compared to a DNA-PK inhibitor (NU7026) plus IR (88).

DNA-PK has been targeted with antibodies and inhibitors specific to the Ku heterodimer. Though antibodies are generally ineffective against intracellular targets, there has been success with ScFv 18-2, which conjugates with folate via a scissile disulfide linker and enters cells through folate receptor-mediated endocytosis. Lung cancer cell lines treated with ScFv 18-2 showed increased levels of γ-H2AX and decreased phosphorylation of Ser2056. Compared to controls, treated cell lines were more radiosensitive (89). Based on the crystal structure of the Ku70/Ku80 heterodimer (7-{[2-(3,4-dimethoxyphenyl)ethyl]amino}-3-(3-fluorophenyl)pyrimido[4,5-d]pyrimidine-2,4(1H,3H)-dione

(Compound L), was developed as an inhibitor that disrupts the Ku heterodimer binding to DNA. Compound L decreased phosphorylation of Ser2056 and downstream DNA-PK targets in glioblastoma cell lines (90).

The promising effects of DNA-PK inhibitors to sensitize tumors to chemotherapy and radiation has led to their implementation in clinical trials. M3814 is being tested with radiotherapy in advanced solid tumors (NCT02516813). CC-122, a pleiotropic pathway modulator with activity against DNA-PK, is in Phase 1 trials studying its effects in multiple myeloma, advanced solid tumors, and non-Hodgkin's lymphoma (NCT01421524). CC-115, a dual DNA-PK and mTOR inhibitor, is in Phase 2 studies to determine its efficacy in glioblastoma (NCT02977780).

CONCLUSIONS

Since its discovery, DNA-PK has proven to be an intriguing modulator of many cellular functions. Its instrumental role in regulating how cells respond to genotoxic insult has been the dominant focus of research. Though much has been discovered, key questions remain that will help elucidate DNA-PK's role in cancer. Are there other substrates of DNA-PK that are yet to be discovered? How does the activity of the Ku heterodimer and DNA-PKcs change in malignancy? Finally, can the specific interactions between DNA-PK and its many substrates be targeted? Thus, far, DNA-PK inhibitors have focused on potentiating DNA damage through inhibition of its kinase function, thereby blocking phosphorylation of key enzymes involved in DNA repair. But these therapies represent a small portion of the therapeutic strategies that may be implemented to target DNA-PK. Novel inhibitors that impair the protein-protein interactions between DNA-PK and its many substrates have the potential to be more targeted and potent. In order to develop this next generation of inhibitors, further study on the regions of DNA-PK that are crucial for substrate binding is warranted. Given the recent findings on its structural properties, the many functions and pathways it regulates, and its therapeutic potential, DNA-PK remains a subject of great importance that may contribute greatly to our overall understanding of cancer and to the discovery of novel therapeutics.

AUTHOR CONTRIBUTIONS

All authors listed have made a substantial, direct and intellectual contribution to the work, and approved it for publication.

FUNDING

This work was funded by National Cancer Institute, NIH (R01 CA168699 to MK), and by Cancer Prevention and Research Institute of Texas (individual investigator awards RP170470 to MK).

REFERENCES

1. Walker AI, Hunt T, Jackson RJ, Anderson CW. Double-stranded DNA induces the phosphorylation of several proteins including the 90 000 mol. wt. heat-shock protein in animal cell extracts. *EMBO J.* (1985) 4:139–45. doi: 10.1002/j.1460-2075.1985.tb02328.x
2. Jackson SP, MacDonald JJ, Lees-Miller S, Tjian R. GC box binding induces phosphorylation of Sp1 by a DNA-dependent protein kinase. *Cell.* (1990) 63:155–65. doi: 10.1016/0092-8674(90)90296-Q
3. Lees-Miller SP. The DNA-dependent protein kinase, DNA-PK: 10 years and no ends in sight. *Biochem Cell Biol.* (1996) 74:503–12. doi: 10.1139/o96-054
4. Shrivastav M, De Haro LP, Nickoloff JA. Regulation of DNA double-strand break repair pathway choice. *Cell Res.* (2008) 18:134–47. doi: 10.1038/cr.2007.111
5. Bjorkman A, Du L, Felgentreff K, Rosner C, Pankaj Kamdar R, Kokaraki G, et al. DNA-PKcs is involved in Ig class switch recombination in human B cells. *J Immunol.* (2015) 195:5608–15. doi: 10.4049/jimmunol.1501633
6. Davidson D, Amrein L, Panasci L, Aloyz R. Small molecules, inhibitors of DNA-PK, targeting DNA repair, and beyond. *Front Pharmacol.* (2013) 4:5. doi: 10.3389/fphar.2013.00005
7. Jette N, Lees-Miller SP. The DNA-dependent protein kinase: a multifunctional protein kinase with roles in DNA double strand break repair and mitosis. *Prog Biophys Mol Biol.* (2015) 117:194–205. doi: 10.1016/j.pbiomolbio.2014.12.003
8. Drouet J, Frit P, Delteil C, de Villartay JP, Salles B, Calsou P. Interplay between Ku, Artemis, and the DNA-dependent protein kinase catalytic subunit at DNA ends. *J Biol Chem.* (2006) 281:27784–93. doi: 10.1074/jbc.M603047200
9. Mari PO, Florea BI, Persengiev SP, Verkaik NS, Bruggenwirth HT, Modesti M, et al. Dynamic assembly of end-joining complexes requires interaction between Ku70/80 and XRCC4. *Proc Natl Acad Sci USA.* (2006) 103:18597–602. doi: 10.1073/pnas.0609061103
10. Cui X, Yu Y, Gupta S, Cho YM, Lees-Miller SP, Meek K. Autophosphorylation of DNA-dependent protein kinase regulates DNA end processing and may also alter double-strand break repair pathway choice. *Mol Cell Biol.* (2005) 25:10842–52. doi: 10.1128/MCB.25.24.10842-10852.2005
11. Jiang W, Crowe JL, Liu X, Nakajima S, Wang Y, Li C, et al. Differential phosphorylation of DNA-PKcs regulates the interplay between end-processing and end-ligation during nonhomologous end-joining. *Mol Cell.* (2015) 58:172–85. doi: 10.1016/j.molcel.2015.02.024
12. Stiff T, O'Driscoll M, Rief N, Iwabuchi K, Lobrich M, Jeggo PA. ATM and DNA-PK function redundantly to phosphorylate H2AX after exposure to ionizing radiation. *Cancer Res.* (2004) 64:2390–6. doi: 10.1158/0008-5472.CAN-03-3207
13. Davis AJ, Chi L, So S, Lee KJ, Mori E, Fattah K, et al. BRCA1 modulates the autophosphorylation status of DNA-PKcs in S phase of the cell cycle. *Nucleic Acids Res.* (2014) 42:11487–501. doi: 10.1093/nar/gku824
14. Neal JA, Dang V, Douglas P, Wold MS, Lees-Miller SP, Meek K. Inhibition of homologous recombination by DNA-dependent protein kinase requires kinase activity, is titratable, and is modulated by autophosphorylation. *Mol Cell Biol.* (2011) 31:1719–33. doi: 10.1128/MCB.01298-10
15. Allen C, Halbrook J, Nickoloff JA. Interactive competition between homologous recombination and non-homologous end joining. *Mol Cancer Res.* (2003) 1:913–20.
16. Shao RG, Cao CX, Zhang H, Kohn KW, Wold MS, Pommier Y. Replication-mediated DNA damage by camptothecin induces phosphorylation of RPA by DNA-dependent protein kinase and dissociates RPA:DNA-PK complexes. *EMBO J.* (1999) 18:1397–406. doi: 10.1093/emboj/18.5.1397
17. Serrano MA, Li Z, Dangeti M, Musich PR, Patrick S, Roginskaya M, et al. DNA-PK, ATM and ATR collaboratively regulate p53-RPA interaction to facilitate homologous recombination DNA repair. *Oncogene.* (2013) 32:2452–62. doi: 10.1038/onc.2012.257
18. Lee KJ, Lin YF, Chou HY, Yajima H, Fattah KR, Lee SC, et al. Involvement of DNA-dependent protein kinase in normal cell cycle progression through mitosis. *J Biol Chem.* (2011) 286:12796–802. doi: 10.1074/jbc.M110.212969

19. Huang B, Shang ZF, Li B, Wang Y, Liu XD, Zhang SM, et al. DNA-PKcs associates with PLK1 and is involved in proper chromosome segregation and cytokinesis. *J Cell Biochem.* (2014) 115:1077–88. doi: 10.1002/jcb.24703
20. Shang ZF, Huang B, Xu QZ, Zhang SM, Fan R, Liu XD, et al. Inactivation of DNA-dependent protein kinase leads to spindle disruption and mitotic catastrophe with attenuated checkpoint protein 2 Phosphorylation in response to DNA damage. *Cancer Res.* (2010) 70:3657–66. doi: 10.1158/0008-5472.CAN-09-3362
21. Mayo LD, Turchi JJ, Berberich SJ. Mdm-2 phosphorylation by DNA-dependent protein kinase prevents interaction with p53. *Cancer Res.* (1997) 57:5013–6.
22. Shieh SY, Ikeda M, Taya Y, Prives C. DNA damage-induced phosphorylation of p53 alleviates inhibition by MDM2. *Cell.* (1997) 91:325–34. doi: 10.1016/S0092-8674(00)80416-X
23. Douglas P, Ye R, Trinkle-Mulcahy L, Neal JA, De Wever V, Morrice NA, et al. Polo-like kinase 1 (PLK1) and protein phosphatase 6 (PP6) regulate DNA-dependent protein kinase catalytic subunit (DNA-PKcs) phosphorylation in mitosis. *Biosci Rep.* (2014) 34:e00113. doi: 10.1042/BSR20140051
24. Goodwin JF, Kothari V, Drake JM, Zhao S, Dylgjeri E, Dean JL, et al. DNA-PKcs-mediated transcriptional regulation drives prostate cancer progression and metastasis. *Cancer Cell.* (2015) 28:97–113. doi: 10.1016/j.ccell.2015.06.004
25. Giffin W, Torrance H, Rodda DJ, Prefontaine GG, Pope L, Hache RJ. Sequence-specific DNA binding by Ku autoantigen and its effects on transcription. *Nature.* (1996) 380:265–8. doi: 10.1038/380265a0
26. Lees-Miller SP, Chen YR, Anderson CW. Human cells contain a DNA-activated protein kinase that phosphorylates simian virus 40 T antigen, mouse p53, and the human Ku autoantigen. *Mol Cell Biol.* (1990) 10:6472–81. doi: 10.1128/MCB.10.12.6472
27. Bunch H, Lawney BP, Lin YF, Asaithamby A, Murshid A, Wang YE, et al. Transcriptional elongation requires DNA break-induced signalling. *Nat Commun.* (2015) 6:10191. doi: 10.1038/ncomms10191
28. Chibazakura T, Watanabe F, Kitajima S, Tsukada K, Yasukochi Y, Teraoka H. Phosphorylation of human general transcription factors TATA-binding protein and transcription factor IIB by DNA-dependent protein kinase–synergistic stimulation of RNA polymerase II basal transcription *in vitro*. *Eur J Biochem.* (1997) 247:1166–73. doi: 10.1111/j.1432-1033.1997.01166.x
29. Espejel S, Franco S, Sgura A, Gae D, Bailey SM, Taccioli GE, et al. Functional interaction between DNA-PKcs and telomerase in telomere length maintenance. *EMBO J.* (2002) 21:6275–87. doi: 10.1093/emboj/cdf593
30. Williams ES, Klingler R, Ponnaiya B, Hardt T, Schrock E, Lees-Miller SP, et al. Telomere dysfunction and DNA-PKcs deficiency: characterization and consequence. *Cancer Res.* (2009) 69:2100–7. doi: 10.1158/0008-5472.CAN-08-2854
31. Bailey SM, Brenneman MA, Halbrook J, Nickoloff JA, Ullrich RL, Goodwin EH. The kinase activity of DNA-PK is required to protect mammalian telomeres. *DNA Repair.* (2004) 3:225–33. doi: 10.1016/j.dnarep.2003.10.013
32. Fisher TS, Zakian VA. Ku: a multifunctional protein involved in telomere maintenance. *DNA Repair.* (2005) 4:1215–26. doi: 10.1016/j.dnarep.2005.04.021
33. Ruis BL, Fattah KR, Hendrickson EA. The catalytic subunit of DNA-dependent protein kinase regulates proliferation, telomere length, and genomic stability in human somatic cells. *Mol Cell Biol.* (2008) 28:6182–95. doi: 10.1128/MCB.00355-08
34. Smith GC, Jackson SP. The DNA-dependent protein kinase. *Genes Dev.* (1999) 13:916–34. doi: 10.1101/gad.13.8.916
35. Jeggo PA. DNA-PK: at the cross-roads of biochemistry and genetics. *Mutat Res.* (1997) 384:1–14. doi: 10.1016/S0921-8777(97)00009-8
36. Blackford AN, Jackson SP. ATM, ATR, and DNA-PK: the trinity at the heart of the DNA damage response. *Mol Cell.* (2017) 66:801–17. doi: 10.1016/j.molcel.2017.05.015
37. Sibanda BL, Chirgadze DY, Ascher DB, Blundell TL. DNA-PKcs structure suggests an allosteric mechanism modulating DNA double-strand break repair. *Science.* (2017) 355:520–4. doi: 10.1126/science.aak9654
38. Koike M, Shiomi T, Koike A. Dimerization and nuclear localization of ku proteins. *J Biol Chem.* (2001) 276:11167–73. doi: 10.1074/jbc.M010902200
39. Tuteja R, Tuteja N. Ku autoantigen: a multifunctional DNA-binding protein. *Crit Rev Biochem Mol Biol.* (2000) 35:1–33. doi: 10.1080/10409230091169177
40. Fell VL, Schild-Poulter C. The Ku heterodimer: function in DNA repair and beyond. *Mutat Res Rev Mutat Res.* (2015) 763:15–29. doi: 10.1016/j.mrrev.2014.06.002
41. Goodwin JF, Knudsen KE. Beyond DNA repair: DNA-PK function in cancer. *Cancer Discov.* (2014) 4:1126–39. doi: 10.1158/2159-8290.CD-14-0358
42. Guirouilh-Barbat J, Huck S, Lopez BS. S-phase progression stimulates both the mutagenic KU-independent pathway and mutagenic processing of KU-dependent intermediates, for nonhomologous end joining. *Oncogene.* (2008) 27:1726–36. doi: 10.1038/sj.onc.1210807
43. Betermier M, Bertrand P, Lopez BS. Is non-homologous end-joining really an inherently error-prone process? *PLoS Genet.* (2014) 10:e1004086. doi: 10.1371/journal.pgen.1004086
44. Davis AJ, Chen BP, Chen DJ. DNA-PK: a dynamic enzyme in a versatile DSB repair pathway. *DNA Repair.* (2014) 17:21–9. doi: 10.1016/j.dnarep.2014.02.020
45. Spagnolo L, Rivera-Calzada A, Pearl LH, Llorca O. Three-dimensional structure of the human DNA-PKcs/Ku70/Ku80 complex assembled on DNA and its implications for DNA DSB repair. *Mol Cell.* (2006) 22:511–9. doi: 10.1016/j.molcel.2006.04.013
46. Yano K, Morotomi-Yano K, Wang SY, Uematsu N, Lee KJ, Asaithamby A, et al. Ku recruits XLF to DNA double-strand breaks. *EMBO Rep.* (2008) 9:91–6. doi: 10.1038/sj.embor.7401137
47. Yan Q, Zhu H, Lan L, Yi J, Yang J. Cleavage of Ku80 by caspase-2 promotes non-homologous end joining-mediated DNA repair. *DNA Repair.* (2017) 60:18–28. doi: 10.1016/j.dnarep.2017.10.001
48. Cary RB, Peterson SR, Wang J, Bear DG, Bradbury EM, Chen DJ. DNA looping by Ku and the DNA-dependent protein kinase. *Proc Natl Acad Sci USA.* (1997) 94:4267–72. doi: 10.1073/pnas.94.9.4267
49. Wang C, Lees-Miller SP. Detection and repair of ionizing radiation-induced DNA double strand breaks: new developments in nonhomologous end joining. *Int J Radi Oncol Biol Phys.* (2013) 86:440–9. doi: 10.1016/j.ijrobp.2013.01.011
50. Soutoglou E, Dorn JF, Sengupta K, Jasin M, Nussenzweig A, Ried T, et al. Positional stability of single double-strand breaks in mammalian cells. *Nat Cell Biol.* (2007) 9:675–82. doi: 10.1038/ncb1591
51. Weterings E, Verkaik NS, Keijzers G, Florea BI, Wang SY, Ortega LG, et al. The Ku80 carboxy terminus stimulates joining and artemis-mediated processing of DNA ends. *Mol Cell Biol.* (2009) 29:1134–42. doi: 10.1128/MCB.00971-08
52. Douglas P, Gupta S, Morrice N, Meek K, Lees-Miller SP. DNA-PK-dependent phosphorylation of Ku70/80 is not required for non-homologous end joining. *DNA Repair.* (2005) 4:1006–18. doi: 10.1016/j.dnarep.2005.05.003
53. Shangary S, Wang S. Targeting the MDM2-p53 interaction for cancer therapy. *Clin Cancer Res.* (2008) 14:5318–24. doi: 10.1158/1078-0432.CCR-07-5136
54. Liu S, Opiyo SO, Manthey K, Glanzer JG, Ashley AK, Amerin C, et al. Distinct roles for DNA-PK, ATM and ATR in RPA phosphorylation and checkpoint activation in response to replication stress. *Nucleic Acids Res.* (2012) 40:10780–94. doi: 10.1093/nar/gks849
55. Shang Z, Yu L, Lin YF, Matsunaga S, Shen CY, Chen BP. DNA-PKcs activates the Chk2-Brca1 pathway during mitosis to ensure chromosomal stability. *Oncogenesis.* (2014) 3:e85. doi: 10.1038/oncsis.2013.49
56. Woodard RL, Anderson MG, Dynan WS. Nuclear extracts lacking DNA-dependent protein kinase are deficient in multiple round transcription. *J Biol Chem.* (1999) 274:478–85. doi: 10.1074/jbc.274.1.478
57. Gearhart J, Pashos EE, Prasad MK. Pluripotency redux–advances in stem-cell research. *N Engl J Med.* (2007) 357:1469–72. doi: 10.1056/NEJMp078126
58. Iijima S, Teraoka H, Date T, Tsukada K. DNA-activated protein kinase in Raji Burkitt's lymphoma cells. Phosphorylation of c-Myc oncoprotein. *Eur J Biochem.* (1992) 206:595–603. doi: 10.1111/j.1432-1033.1992.tb16964.x
59. Wong RH, Chang I, Hudak CS, Hyun S, Kwan HY, Sul HS. A role of DNA-PK for the metabolic gene regulation in response to insulin. *Cell.* (2009) 136:1056–72. doi: 10.1016/j.cell.2008.12.040
60. Ju BG, Lunyak VV, Perissi V, Garcia-Bassets I, Rose DW, Glass CK, et al. A topoisomerase IIbeta-mediated dsDNA break required for regulated transcription. *Science.* (2006) 312:1798–802. doi: 10.1126/science.1127196
61. Medunjanin S, Weinert S, Schmeisser A, Mayer D, Braun-Dullaeus RC. Interaction of the double-strand break repair kinase DNA-PK and estrogen receptor-alpha. *Mol Biol Cell.* (2010) 21:1620–8. doi: 10.1091/mbc.e09-08-0724

62. Sui J, Lin YF, Xu K, Lee KJ, Wang D, Chen BP. DNA-PKcs phosphorylates hnRNP-A1 to facilitate the RPA-to-POT1 switch and telomere capping after replication. *Nucleic Acids Res.* (2015) 43:5971–83. doi: 10.1093/nar/gkv539
63. Jaco I, Munoz P, Blasco MA. Role of human Ku86 in telomere length maintenance and telomere capping. *Cancer Res.* (2004) 64:7271–8. doi: 10.1158/0008-5472.CAN-04-1381
64. Deng Z, Norseen J, Wiedmer A, Riethman H, Lieberman PM. TERRA RNA binding to TRF2 facilitates heterochromatin formation and ORC recruitment at telomeres. *Mol Cell.* (2009) 35:403–13. doi: 10.1016/j.molcel.2009.06.025
65. Feuerhahn S, Iglesias N, Panza A, Porro A, Lingner J. TERRA biogenesis, turnover and implications for function. *FEBS Lett.* (2010) 584:3812–8. doi: 10.1016/j.febslet.2010.07.032
66. Le PN, Maranon DG, Altina NH, Battaglia CL, Bailey SM. TERRA, hnRNP A1, and DNA-PKcs interactions at human telomeres. *Front Oncol.* (2013) 3:91. doi: 10.3389/fonc.2013.00091
67. Khadka P, Lee JH, Baek SH, Oh SY, Chung IK. DNA-PKcs-interacting protein KIP binding to TRF2 is required for the maintenance of functional telomeres. *Biochem J.* (2014) 463:19–30. doi: 10.1042/BJ20131395
68. Kotula E, Berthault N, Agrario C, Lienafa MC, Simon A, Dingli F, et al. DNA-PKcs plays role in cancer metastasis through regulation of secreted proteins involved in migration and invasion. *Cell Cycle.* (2015) 14:1961–72. doi: 10.1080/15384101.2015.1026522
69. Evert M, Frau M, Tomasi ML, Latte G, Simile MM, Seddaiu MA, et al. Deregulation of DNA-dependent protein kinase catalytic subunit contributes to human hepatocarcinogenesis development and has a putative prognostic value. *Br J Cancer.* (2013) 109:2654–64. doi: 10.1038/bjc.2013.606
70. Cornell L, Munck JM, Alsinet C, Villanueva A, Ogle L, Willoughby CE, et al. DNA-PK-A candidate driver of hepatocarcinogenesis and tissue biomarker that predicts response to treatment and survival. *Clin Cancer Res.* (2015) 21:925–33. doi: 10.1158/1078-0432.CCR-14-0842
71. Herrero AB, San Miguel J, Gutierrez NC. Deregulation of DNA double-strand break repair in multiple myeloma: implications for genome stability. *PLoS ONE.* (2015) 10:e0121581. doi: 10.1371/journal.pone.0121581
72. Ihara M, Ashizawa K, Shichijo K, Kudo T. Expression of the DNA-dependent protein kinase catalytic subunit is associated with the radiosensitivity of human thyroid cancer cell lines. *J Radiat Res.* (2019) 60:171–7. doi: 10.1093/jrr/rry097
73. Lee SW, Cho KJ, Park JH, Kim SY, Nam SY, Lee BJ, et al. Expressions of Ku70 and DNA-PKcs as prognostic indicators of local control in nasopharyngeal carcinoma. *Int J Radi Oncol Biol Phys.* (2005) 62:1451–7. doi: 10.1016/j.ijrobp.2004.12.049
74. Shintani S, Mihara M, Li C, Nakahara Y, Hino S, Nakashiro K, et al. Up-regulation of DNA-dependent protein kinase correlates with radiation resistance in oral squamous cell carcinoma. *Cancer Sci.* (2003) 94:894–900. doi: 10.1111/j.1349-7006.2003.tb01372.x
75. Beskow C, Skikuniene J, Holgersson A, Nilsson B, Lewensohn R, Kanter L, et al. Radioresistant cervical cancer shows upregulation of the NHEJ proteins DNA-PKcs, Ku70 and Ku86. *Br J Cancer.* (2009) 101:816–21. doi: 10.1038/sj.bjc.6605201
76. Vlahos CJ, Matter WF, Hui KY, Brown RF. A specific inhibitor of phosphatidylinositol 3-kinase, 2-(4-morpholinyl)-8-phenyl-4H-1-benzopyran-4-one (LY294002). *J Biol Chem.* (1994) 269:5241–8.
77. Hollick JJ, Golding BT, Hardcastle IR, Martin N, Richardson C, Rigoreau LJ, et al. 2,6-disubstituted pyran-4-one and thiopyran-4-one inhibitors of DNA-Dependent protein kinase (DNA-PK). *Bioorg Med Chem Lett.* (2003) 13:3083–6. doi: 10.1016/S0960-894X(03)00652-8
78. Hardcastle IR, Cockcroft X, Curtin NJ, El-Murr MD, Leahy JJ, Stockley M, et al. Discovery of potent chromen-4-one inhibitors of the DNA-dependent protein kinase (DNA-PK) using a small-molecule library approach. *J Med Chem.* (2005) 48:7829–46. doi: 10.1021/jm050444b
79. Elliott SL, Crawford C, Mulligan E, Summerfield G, Newton P, Wallis J, et al. Mitoxantrone in combination with an inhibitor of DNA-dependent protein kinase: a potential therapy for high risk B-cell chronic lymphocytic leukaemia. *Br J Haematol.* (2011) 152:61–71. doi: 10.1111/j.1365-2141.2010.08425.x
80. Ciszewski WM, Tavecchio M, Dastych J, Curtin NJ. DNA-PK inhibition by NU7441 sensitizes breast cancer cells to ionizing radiation and doxorubicin. *Breast Cancer Res Treat.* (2014) 143:47–55. doi: 10.1007/s10549-013-2785-6
81. Yanai M, Makino H, Ping B, Takeda K, Tanaka N, Sakamoto T, et al. DNA-PK inhibition by NU7441 enhances chemosensitivity to topoisomerase inhibitor in non-small cell lung carcinoma cells by blocking DNA damage repair. *Yonago Acta Med.* (2017) 60:9–15.
82. Dong J, Ren Y, Zhang T, Wang Z, Ling CC, Li GC, et al. Inactivation of DNA-PK by knockdown DNA-PKcs or NU7441 impairs non-homologous end-joining of radiation-induced double strand break repair. *Oncol Rep.* (2018) 39:912–20. doi: 10.3892/or.2018.6217
83. Zhao Y, Thomas HD, Batey MA, Cowell IG, Richardson CJ, Griffin RJ, et al. Preclinical evaluation of a potent novel DNA-dependent protein kinase inhibitor NU7441. *Cancer Res.* (2006) 66:5354–62. doi: 10.1158/0008-5472.CAN-05-4275
84. Cano C, Barbeau OR, Bailey C, Cockcroft XL, Curtin NJ, Duggan H, et al. DNA-dependent protein kinase (DNA-PK) inhibitors. Synthesis and biological activity of quinolin-4-one and pyridopyrimidin-4-one surrogates for the chromen-4-one chemotype. *J Med Chem.* (2010) 53:8498–507. doi: 10.1021/jm100608j
85. Harnor SJ, Brennan A, Cano C. Targeting DNA-dependent protein kinase for cancer therapy. *ChemMedChem.* (2017) 12:895–900. doi: 10.1002/cmdc.201700143
86. Riabinska A, Daheim M, Herter-Sprie GS, Winkler J, Fritz C, Hallek M, et al. Therapeutic targeting of a robust non-oncogene addiction to PRKDC in ATM-defective tumors. *Sci Transl Med.* (2013) 5:189ra78. doi: 10.1126/scitranslmed.3005814
87. Yan D, Ng WL, Zhang X, Wang P, Zhang Z, Mo YY, et al. Targeting DNA-PKcs and ATM with miR-101 sensitizes tumors to radiation. *PLoS ONE.* (2010) 5:e11397. doi: 10.1371/journal.pone.0011397
88. Piotto C, Biscontin A, Millino C, Mognato M. Functional validation of miRNAs targeting genes of DNA double-strand break repair to radiosensitize non-small lung cancer cells. *Biochim Biophys Acta Gene Regul Mech.* (2018) 1861:1102–18. doi: 10.1016/j.bbagrm.2018.10.010
89. Xiong H, Lee RJ, Haura EB, Edwards JG, Dynan WS, Li S. Intranuclear delivery of a novel antibody-derived radiosensitizer targeting the DNA-dependent protein kinase catalytic subunit. *Int J Radi Oncol Biol Phys.* (2012) 83:1023–30. doi: 10.1016/j.ijrobp.2011.08.039
90. Weterings E, Gallegos AC, Dominick LN, Cooke LS, Bartels TN, Vagner J, et al. A novel small molecule inhibitor of the DNA repair protein Ku70/80. *DNA Repair.* (2016) 43:98–106. doi: 10.1016/j.dnarep.2016.03.014

Conflict of Interest Statement: The authors declare that the research was conducted in the absence of any commercial or financial relationships that could be construed as a potential conflict of interest.

frontiers in Oncology

ORIGINAL RESEARCH
published: 19 September 2019
doi: 10.3389/fonc.2019.00923

The Stapled Peptide PM2 Stabilizes p53 Levels and Radiosensitizes Wild-Type p53 Cancer Cells

Anja Charlotte Lundgren Mortensen[1], Diana Spiegelberg[1,2], Christopher John Brown[3], David Philip Lane[3,4] and Marika Nestor[1]*

*[1] Department of Immunology, Genetics and Pathology, Uppsala University, Uppsala, Sweden, [2] Department of Surgical Sciences, Uppsala University, Uppsala, Sweden, [3] Agency for Science, Technology and Research (A*STAR), Singapore, Singapore, [4] Science for Life Laboratory, Department of Microbiology, Tumor and Cell Biology, Karolinska Institutet, Stockholm, Sweden*

The tumor suppressor p53 is a key mediator of cellular stress and DNA damage response cascades and is activated after exposure to ionizing radiation. Amplifying wild-type p53 expression by targeting negative regulators such as MDM2 in combination with external beam radiotherapy (EBRT) may result in increased therapeutic effects. The novel stapled peptide PM2 prevents MDM2 from suppressing wild-type p53, and is thus a promising agent for therapeutic combination with EBRT. Effects of PM2 and potential PM2-induced radiosensitivity were assessed in a panel of cancer cell lines using 2D cell viability assays. Western Blot and flow cytometric analyses were used to investigate the mechanisms behind the observed effects in samples treated with PM2 and EBRT. Finally, PM2-treatment combined with EBRT was evaluated in an *in vitro* 3D spheroid model. PM2-therapy decreased cell viability in wild-type p53, HPV-negative cell lines. Western Blotting and flow cytometry confirmed upregulation of p53, as well as initiation of p53-mediated apoptosis measured by increased cleaved caspase-3 and Noxa activity. Furthermore, 3D *in vitro* tumor spheroid experiments confirmed the superior effects of the combination, as the only treatment regime resulting in growth inhibition and complete spheroid disintegration. We conclude that PM2 induces antitumorigenic effects in wt p53 HPV-negative cancer cells and potentiates the effects of EBRT, ultimately resulting in tumor eradication in a 3D spheroid model. This strategy shows great potential as a new wt p53 specific tumor-targeting compound, and the combination of PM2 and EBRT could be a promising strategy to increase therapeutic effects and decrease adverse effects from radiotherapy.

Keywords: p53, wild-type p53, radiosensitization, external beam radiation therapy (EBRT), PM2, spheroid apoptosis

OPEN ACCESS

Edited by:
Michaela Medová, University Hospital Bern, Switzerland

Reviewed by:
Franz Rödel, University Hospital Frankfurt, Germany
Magnus Olsson, Karolinska Institute (KI), Sweden

****Correspondence:***
Anja Charlotte Lundgren Mortensen
anja.mortensen@igp.uu.se

Specialty section:
This article was submitted to Molecular and Cellular Oncology, a section of the journal Frontiers in Oncology

Received: *12 June 2019*
Accepted: *03 September 2019*
Published: *19 September 2019*

Citation:
Mortensen ACL, Spiegelberg D, Brown CJ, Lane DP and Nestor M (2019) The Stapled Peptide PM2 Stabilizes p53 Levels and Radiosensitizes Wild-Type p53 Cancer Cells. Front. Oncol. 9:923. doi: 10.3389/fonc.2019.00923

INTRODUCTION

Today up to 50% of all cancer patients receive at least one dose of external beam radiotherapy (EBRT) (1–4). With continuous technological increases over the last few decades, it has evolved into one of the most well-established and successful non-invasive cancer therapy regimens (5, 6). Improvements to EBRTs such as intensity modulated radiotherapy (IMRT) and volumetric modulated arc therapy (VMAT) are undergoing continuous development, exemplifying that EBRT as a field still has room for improvement (5, 7–9). One such improvement is the use

of radiosensitizers, where sensitizing tumor cells to radiation damage may further increase the radiotherapy success rate. Tumor cell radiosensitization could also allow reductions in radiation dose, thus lowering the risk of adverse effects (10–12).

The transcription factor p53 is a promising target for radiosensitization, as it plays a key role in both DNA repair and radiation response mechanisms (13). p53 is upregulated after exposure to ionizing radiation and drives a variety of cellular responses in damaged cells, where the specific response depends quantitatively on the level of p53 accumulation (13–15). The outcome of p53 accumulation is complex and often cell type specific (16). While low levels of wt p53 leads to cell cycle arrest, higher levels may result in apoptosis, senescence or autophagy. In the event of apoptosis, it is linked to transcription of pro-apoptotic proteins such as Phorbol-12-myristate-13-acetate-induced protein 1 (Noxa) (14, 17, 18).

Due to its key role, p53 is commonly inactivated in cancer cells to avoid the induction of apoptosis, either through mutations in p53, or by accumulating mutations in p53 regulatory factors while still maintaining wild-type p53 (wt p53). While wt p53 expression remains intact in around 50% of all cancers, it is often suppressed by dysfunctional activation pathways, for example epigenetic silencing of p14 ARF expression or overexpression of negative feedback regulators such as murine double-minute 2 (MDM2) and its structural homolog, murine double-minute X (MDMX) (19, 20). MDM2/X are p53 target proteins that bind and block the transcriptional activity in an autoregulatory feedback loop and mark the p53 protein for ubiquitination (21).

Previous studies have demonstrated that wt p53 expression can be amplified by targeting MDM2/X, which has been shown to result in tumor regression *in vivo* (22). Inhibiting the MDM2-p53 protein-protein interaction causes wt p53 accumulation in the cancer cells, which may eventually lead to cell cycle arrest or cell death. Promising pre-clinical data has led to several MDM2/X-p53 inhibitors currently undergoing clinical trials (23, 24). However, none of the current clinical trials are exploring combined EBRT and MDM2/X-p53 inhibition therapy, which could PM2 therapy potentially provide further utility within the growing field of MDM2-p53 inhibitors.

The present study involves PM2, which is a novel stapled peptide targeting the MDM2/X-p53 interaction (25). Like most MDM2/X-p53 inhibitors, PM2 mimics the amino acid sequence of wt p53 that is bound by MDM2/X (26, 27). "Stapling" in this context means that a covalent hydrocarbon linker has been introduced between two non-adjacent amino acids, thus connecting turns of the peptide's α helix resulting in greater stability (21, 26, 27). The stabilization of the peptide's secondary structure, in addition to increasing its affinity for MDM2/X by reducing the entropic cost of binding, also results in an increase in its *in vivo* half-life. The use of staple peptides, which have a much more comprehensive network of interactions with MDM2 than small molecule inhibitors such as Nutlin-3, have been shown to bind to and antagonize Nutlin-3-resistant MDM2 (26, 27).

In a recent study we have established the *in vivo* potential of PM2 as a radiotherapy potentiator in a wt p53 colorectal cancer model (28). In mice carrying wt p53 tumors, PM2 combined with radiotherapy prolonged median survival by 50%, whereas effects on $p53^{-/-}$ tumors were negligible. This proof-of-concept study demonstrates the promise of this application *in vivo,* and suggests that a future clinical application of PM2 with radiotherapy in wt p53 cancers might improve tumor control. However, to enable such a scenario it is vital to thoroughly assess the effects of PM2 and EBRT on a larger scale, to validate p53-dependent effects, and most importantly to unravel the mechanisms behind the effects and the cellular fates of treated cells. Consequently, the aim of this study was to assess the potential antitumorigenic effects of the combination of EBRT and PM2 therapy as well as to determine the mechanisms behind the observed effects.

MATERIALS AND METHODS

Cell Lines

The human squamous cell carcinoma cell lines UM-SCC-74A and UM-SCC-74B were kindly provided by Professor TE Carey (University of Michigan, USA) and cultured in Dulbecco's Modified Eagle Medium (DMEM) with 10% fetal bovine serum, 1% L-glutamine, 1% antibiotics (100 IU penicillin and 100 μg/ml streptomycin) as well as 1% non-essential amino acids (all from Biochrom Kg, Berlin, Germany). UT-SCC-45 (kindly provided by Dr. R. Grenman, Turku University Central Hospital, Finland) was cultured in DMEM with the abovementioned additives. HCT116 and A431 were purchased from American Type Culture Collection (Manassas, VA, USA). HCT116 was cultured in McCoy's modified Eagle medium with 10% fetal bovine serum, 1% L-glutamine and 1% antibiotics (100 IU penicillin and 100 μg/ml streptomycin) and A431 was cultured in Ham's F10 with the same additives. H314 was purchased from the European Collection of Authenticated Cell Cultures (Salisbury, UK) in DMEM/Ham's F12 (1:1) with the abovementioned additives. Cells were incubated at 37°C with 5% CO_2, and cultivated for no longer than 2 months at a time.

PM2

The stapled MDM2-p53 antagonist, PM2 (MW = 1462.75Da), was produced at p53 Laboratory (A*STAR, Singapore) and dissolved in DMSO to a stock concentration of 10 mM and stored at −20°C.

NanoBIT Mdm2:p53 PPI Cell Based Assay

HEK293 FT cells were seeded at a cell density of $5*10^5$ cells per well into a six-well plate and incubated overnight at 37°C and 5% CO_2 in DMEM with 0.3 mg/ml glutamine, 100 IU/ml penicillin, 100 μg/ml streptomycin and 10% fetal calf serum. Each well was transfected with 2 μg of DNA consisting of a 1:1 ration of the sMBIT-Mdm2 fusion and LgBIT-p53 fusion vectors (PROMEGA). Each transfection was performed following the manufacturer's instructions with a 3:1 ratio of FuGene transfection reagent (PROMEGA) to DNA in 0% FCS Opti-MEM no red phenol media. Cells were incubated overnight and then washed with 1 ml of PBS, followed by trysinization and re-suspension in Opti-MEM media with 0% FCS. The cell suspension was then adjusted to 2.2×10^5 cells per ml.

Re-suspended HEK-293 FT cells were centrifuged at 1,000 rpm for 5 min at room temperature. Ninety microliter of the

cell re-suspension was added to the wells of a white opaque 96-well plate. Stapled peptides were then titrated onto the 96-well plate using a suitable 2-fold dilution series from a 10 × stock solution containing 10% *v*/*v* DMSO. Control wells were also treated with a 10% DMSO only stock solution to yield a final residual DMSO concentration of 1% *v*/*v*. The 96-well plates were incubated for 4 h at 37°C, with 5% CO_2. Wells were treated with a solution of Nano-Glo live substrate, which was prepared as per the manufacturer's instructions (PROMEGA). The plates were shaken for 1 min at 22°C and luminescence assessed after an additional 50 min using an Envision Multi-Plate reader (Perkin-Elmer, Waltham, MA, USA). NanoBit titration data was used to determine IC_{50} values for drug potency by fitting 4-parameter logistic curves using GraphPad Prism 7.0.

Radiation

Cells were irradiated using ^{137}Cs gamma-ray photons at a dose-rate of ∼1 Gy/min (Best Theratronics Gammacell® 40Exactor, Springfield, USA).

Cell Viability Assays, 2,3-Bis(2-Methoxy-4-Nitro-5-Sulfophenyl)-2H-Tetrazolium-5-Carboxanilide Salt (XTT)

Five-hundred to ten thousands cells were seeded in flat-bottomed 96-well plates and incubated for 48 h prior to irradiation with 2Gy. Three hours post-irradiation, PM2 was added in concentrations spanning 0–40 μM. Cells were incubated at 37° for 4–5 days until 80–90% confluence had been obtained. A mix of XTT Activation Reagent and XTT Reagent was added according to the American Type Culture Collection 30–1011 K protocol (Manassas, VA, USA). Plates were incubated for up to 6 h at 37° and absorbance was measured by using a BioMark Microplate Reader (Bio-Rad Laboratories AB, Solna, Sweden).

Western Blot

Cells were incubated for at least 24 h prior to irradiation (2 Gy) and/or PM2 treatment, where PM2 (20 μM) was added 3 h after irradiation. Whole-cell lysates were prepared according to standard protocols. Protein concentrations were measured using a DeNovix DS-11 spectrophotometer (DeNovix Inc., Wilmington, DE, USA). Samples were separated on 4–12% Bis-Tris SDS gels and transferred to a nitrocellulose membrane (ThermoFisher Scientific, Uppsala, Sweden) by wet-transfer blotting. The membrane was blocked for 1 h in PBS with 5% BSA before incubation with primary antibodies targeting p53, caspase-3, NaK-ATPase and GLB1 (DO-1 (ab1101), ab13847, ab76020 and ab128993, AbCam, Cambridge, UK) and β-actin (A5441, Sigma Aldrich Sweden, Stockholm, Sweden) at 4°C overnight. After washing with PBS with 1% Tween-20, the membrane was incubated with respective and species-specific Horse Radish Peroxidase-labeled secondary antibody (ThermoFisher Scientific, Waltham, MA, USA) and stained with electro-chemiluminescent solution (Immobilon, Millipore, Bedford, USA). Immunoreactive bands were visualized with a CCD camera (SuperCCD HR, Fujifilm, Japan) and analyzed in ImageJ version 1.48 (NIH, Bethesda, MD, USA).

Flow Cytometry

Cells were incubated for at least 24 h prior to irradiation and/or PM2 treatment. Twenty micrometer PM2 was added with a 3-h delay after irradiation. Cells were collected and fixed in 70% ethanol at 6, 12, 24, 48, 72, and 96 h post-irradiation and stored at −20°C. For cell cycle analyses, 6, 12, 24, and 48 h samples were rehydrated and washed twice with PBS and stained with DAPI (Sigma Aldrich Sweden, Stockholm, Sweden) using 1 μg/ml for 30 min. 24, 48, 72, and 96 h samples were stained with caspase-3 and Noxa (ab13847 (1:500) and ab13654 (1:1,000), AbCam, Cambridge, UK) overnight at 4°C, followed by incubation with fluorescent labeled secondary antibodies for 90 min (ab 1:400) at room temperature. Analyses were performed using a BD LSR Fortessa flow cytometer (Becton Dickinson Biosciences, San Jose, USA). Data analyses for cleaved caspase-3 and Noxa were performed with BD FACSDiVa (Becton Dickinson Biosciences, San Jose, USA), while cell cycle analyses of exclusively viable cells were performed using FlowJo (Becton, Dickinson Biosciences, San Jose, USA). Coefficient of variation (CV) values, were below seven for all samples.

3D Assays

For liquid overlay 3D spheroid formation, 96-well plates were coated with 0.15% agarose dissolved in PBS with 1% penicillin/streptomycin. 1000 UM-SCC-74B cells/well were seeded and incubated at 37°C for 3 days prior to treatment. The standard dose of 20 μM of PM2 was added 3 h after irradiation. Half of the medium was replaced every 48 h for the first 10 days, thereafter every 4 days. Samples with repeated PM2 treatments received a new 20 μM dose despite removing of half of the incubation medium. Images were obtained every 2–4 days using a Canon EOS 700D camera mounted on an inverted Nikon Diaphot-TMD microscope. The images were analyzed using ImageJ version 1.48 (NIH, Bethesda, MD, USA), by measuring the surface area of each spheroid and calculating the volume, assuming each spheroid retained a spherical form. Each spheroid was normalized to its own starting volume at the start of treatment (Day 0, growth ratio = 1). Spheroids exceeding a volume of 600 μm^3 were excluded (i.e., terminated) from further analyses as 600 μm^3 is the maximum size possible to obtain in these settings with uncompromised growth conditions.

Statistical Analyses

GraphPad Prism version 6.07 (GraphPad Software, San Diego, USA) was used for data processing and analysis. *p*-values were determined using unpaired student's *t*-test for comparison between two groups or one-way ANOVA followed by Tukey's multiple comparisons test, with $p < 0.05$ (*), $p < 0.01$ (**), $p < 0.001$ (***), and $p < 0.0001$ (****). For XTT assays cell viability was normalized for irradiated and unirradiated samples separately. Thus, an observed significant difference in viability between combination treated samples and solely PM2-treated samples, was considered as the result of PM2 potentiating the effects of radiation. A modified approach to the coefficient of

TABLE 1 | Panel of screened cell lines using 0–20 μM of PM2 and 0 or 2 Gy of EBRT.

Cell line	p53 status	HPV status	Cancer	PM2 effect	IC_{50}	Significant effect of combination
A431	Single base mutation (30)	Negative	Epidermal (vulva)	No	n/a	Yes
H314	Two mutations (31)	Negative	HNSCC (floor of mouth)	No	n/a	No
UT-SCC-45	Wild-type* (32)	Positive	HNSCC (floor of mouth)	No	n/a	No
UM-SCC-74A	Wild-type (33)	Negative	HNSCC (tongue)	Yes	16 μM	Yes
UM-SCC-74B	Wild-type (33)	Negative	HNSCC (larynx)	Yes	17 μM	Yes
HCT116	Wild-type (34)	Negative	Adenocarcinoma (colorectal)	Yes	14 μM	Yes

**Wild-type-status is only assessed for exon 4–8. n/a, not applicable.*

drug interaction (CDI) was determined as: CDI = AB/(A*B), where AB was the ratio of the combination treatment to controls and A or B was the ratio of radiation or PM2 treatment to controls. CDI $\leq$ 0.7 equaled significant synergistic effect, CDI $\leq$ 1 equaled additive effect and CDI $>$ 1 equaled antagonistic effect (29).

RESULTS

PM2 Treatment Decreases Cell Viability and Radiosensitizes wt p53 Cells in Monolayer Cultures

Viability assays (XTT) of six cancer cell lines treated with PM2, either with or without the addition of 2 Gy of external radiation, were performed to measure the efficacy of PM2 alone as well as its potential radiosensitizing effects (**Table 1**). PM2 treatment decreased significantly the viability of all confirmed wt p53, HPV negative cell lines at low doses, starting at ∼10 μM for both HCT116 and UM-SCC-74A and at a slightly higher dose for UM-SCC-74B (**Figure 1A**, green lines). Increasing concentrations of PM2 resulted in reduced viability. An inhibitory concentration of 50% decrease (IC_{50}) was measured at 16 and 17 μM of PM2 for UM-SCC-74A and UM-SCC-74B, respectively and 14 μM for HCT116. At concentrations of 20 μM of PM2, the average viability was reduced by 73 and 90% for UM-SCC-74A and UM-SCC-74B, respectively, and 75% for HCT116, compared to untreated controls. Combination treatment of PM2 and EBRT exhibited a significant drop in viability compared to PM2-monotherapy outcomes at low doses of PM2, starting at 10 μM for UM-SCC-74B cells (**Figure 1A**). The IC_{50} of the combination treatment was detected at 10 μM for UM-SCC-74B and 12 μM for HCT116. These IC_{50}-values correlate with the NanoBIT assays using PM2 (IC_{50} value of 14.8 ± 0.5 μM). The NanoBIT assay further verified the specificity of the antagonistic properties of PM2 to MDM2, with no effect obtained by the scrambled peptide $PM2^{SCRAM}$ (**Supplementary Figure 1A**). PM2 did not affect the two confirmed mutant p53 cell lines, A431 and H314 (**Table 1**; **Supplementary Figure 1B**). However, the combination therapy significantly decreased the viability of A431. The HPV positive cell line, UT-SCC-45, was unresponsive to PM2 therapy regardless of the addition of EBRT (**Table 1**; **Supplementary Figure 1B**).

PM2 and Radiation Treatment Results in G2/M Phase Shift and S-phase Depletion

To investigate underlying mechanisms of PM2 therapy associated cytotoxicity, cell cycle analysis of viable cells was performed on both UM-SCC-74B and HCT116. A distinct G2/M-shift was observed as early as 6 h post-irradiation with 2Gy for both HCT116 and UM-SCC-74B (**Figure 1B**). Single modality treatments with 20 μM of PM2 did not induce a G2/M-shift for either of the cell lines. More than twice as many cells comprised the G2/M-phase of the dual treated samples than untreated controls for both cell lines throughout the 48 h timeframe (**Table 2**). An S-phase reduction occurred as early as 12 h post-treatment for dual treated samples for UM-SCC-74B and HCT116, followed by S-phase depletion at 24 h post-treatment (**Table 2**).

PM2 Upregulates Cleaved Caspase-3, Noxa, wt p53, and GLB-1

The expression of wt p53, cleaved caspase-3 and GLB-1 following treatment with PM2 and/or radiation was visualized through Western Blotting. Western Blot analyses detected an increased expression of p53 in PM2-treated samples at 24 h post-treatment for both cell lines, with a significant increase between solely PM2-treated and combination treated samples (**Figures 2A,D**). Similarly, an increase in expression of the apoptotic marker cleaved caspase-3 was detected in all PM2-treated samples as well as irradiated samples, although the expression of the marker in the combination group was predominant (**Figures 2B,D**). Additionally, a significant increase of senescence marker, Galactosidase beta-1 (GLB-1), was detected at 72 h post-treatment in combination treated UM-SCC-74B samples compared to the irradiated samples. The same trend was observed in the HCT116 samples, where both the PM2-monotherapy and combination therapy resulted in a similar increase of GLB-1 compared to irradiated and control samples (**Figures 2C,D**). An increase in cleaved caspase-3 expression was confirmed through flow cytometry in PM2-treated samples at 48 h post-treatment, peaking at 72 and 96 h for UM-SCC-74B (40-fold increase compared to controls) and HCT116 (10-fold increase compared to controls), respectively (**Figure 2E**). The combination therapy samples had significantly higher expression levels of cleaved caspase-3 than PM2-treated samples for UM-SCC-74B ($p \leq 0.05$). A similar trend was

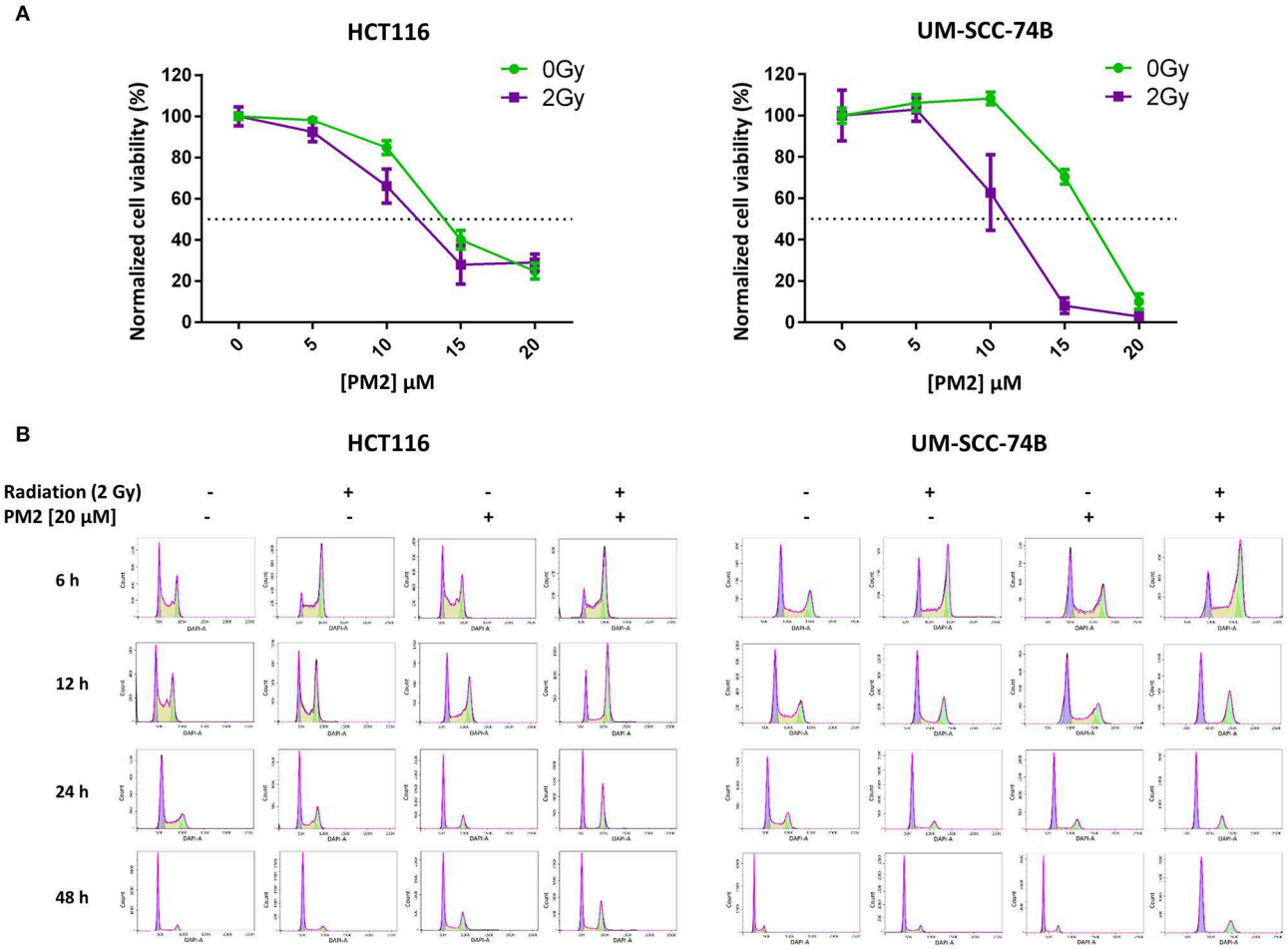

FIGURE 1 | (A) Cell viability (XTT) response to treatment with 0–20 µM of PM2 of UM-SCC-74B and HCT116 without external radiation (green) and in combination with 2 Gy of EBRT (purple). Error bars presented as 95% confidence intervals, $n = 6$. Please note that irradiated cells were normalized to survival at 2 Gy, 0 µM PM2, whereas un-irradiated cells were normalized to survival at 0 Gy, 0 µM PM2 in order to compensate for the effects of radiation. Dotted line indicated 50% viability of controls. **(B)** Cell cycle distribution of viable UM-SCC-74B and HCT116 cells at 6, 12, 24, and 48 h post-treatment with either 2 Gy, 20 µM of PM2, or the combination, fitted according to FlowJo cell cycle analysis software. CV-values for all cell cycle analyses were below 7.

observed for HCT116. Expression levels of the p53-dependent pro-apoptotic protein Noxa correlated with the increase in cleaved caspase-3 levels. Near-3-fold and 4-fold increases in Noxa levels were observed after combination therapy compared to PM2 therapy alone for UM-SCC-74B and HCT116, respectively ($p \leq 0.01$) (**Figure 2F**).

Radiation Potentiates the Effects of PM2 in an *in vitro* 3D Tumor Model

In order to establish whether the potentiating effects of combining PM2 and radiation, as observed in monolayer cultures that were present in a 3D multicellular tumor spheroid system, the growth of wt p53 UM-SCC-74B spheroids was measured over time. EBRT and PM2 therapy had similar inhibitory effects on cell growth at repeated treatments (**Figures 3A,B,D,E**). Five repeated treatments of EBRT at 48 h intervals resulted in an average size of 69% of controls at day 14, whereas five repeated doses of 20 µM of PM2 resulted in an average size of 57%. Combining a single dose of PM2 with EBRT resulted in greater inhibitory effects than either treatment alone. The growth inhibiting effect of one PM2 treatment and radiation treatment was rather persistent, and started to fade after day ten (**Figure 3C**). Repeated doses of PM2 (2–5 × 20 µM) in combination with either a single radiation dose (2 Gy) or repeated doses (2–5 × 2 Gy) resulted in increased inhibitory effects in a repeated-dose-dependent manner (**Figures 3C,F**). By day 14, the majority of treatments had resumed normal or near-normal growth ratios, with the exception of repeated treatments of 2 × 2 Gy/3 × 20 µM, 3 × 2 Gy/3 × 20 µM, and 5 × 2 Gy/5 × 20 µM (**Figure 3C**). However, spheroids treated with three and five fractionated radiation doses in combination with a single dose of PM2 were reduced to a size of 75 and 55%, respectively, of untreated controls. Treatment with 5 × 2 Gy/5 × 20 µM of PM2 resulted in spheroid disintegration and cell death, which persisted beyond the end of the assay (**Figures 3C,F**, **4**). Repeated

TABLE 2 | S-phase and G2/M-phase development 6–48 h post-treatment with 2 Gy, 20 μM of PM2, or the combination, of viable UM-SCC-74B and HCT116 cells.

UM-SCC-74B: S-phase					UM-SCC-74B: G2/M-phase				
Time post-treatment	**0 Gy**	**2 Gy**	**PM2**	**Combination**	**Time post-treatment**	**0 Gy**	**2 Gy**	**PM2**	**Combination**
6 h	34.7%	39.9%	41.6%	42.9%	6 h	23.6%	34.21%	19.7%	37.9%
12 h	37.9%	17.6%	18.3%	7.31%	12 h	19.5%	29.2%	18.3%	39.4%
24 h	33.4%	12.7%	12.9%	2.89%	24 h	16.8%	13.5%	16.7%	23.8%
48 h	20.4%	20.1%	17.4%	5.37%	48 h	11.9%	8.99%	10.8%	20.6%
HCT116: S-phase					**HCT116: G2/M-phase**				
Time post-treatment	**0 Gy**	**2 Gy**	**PM2**	**Combination**	**Time post-treatment**	**0 Gy**	**2 Gy**	**PM2**	**Combination**
6 h	55.1%	49.4%	55.8%	44.9%	6 h	19.5%	41%	19.4%	39.9%
12 h	50.7%	39.1%	35.1%	17.3%	12 h	18%	31.5%	30.1%	53.8%
24 h	33.7%	28%	10.7%	5.51%	24 h	14.3%	22.8%	21.1%	42.7%
48 h	16.5%	16.2%	23%	17.5%	48 h	10.8%	8.57%	20.6%	29.9%

Coefficient of variation (CV) values for all cell cycle analyses were below 7.

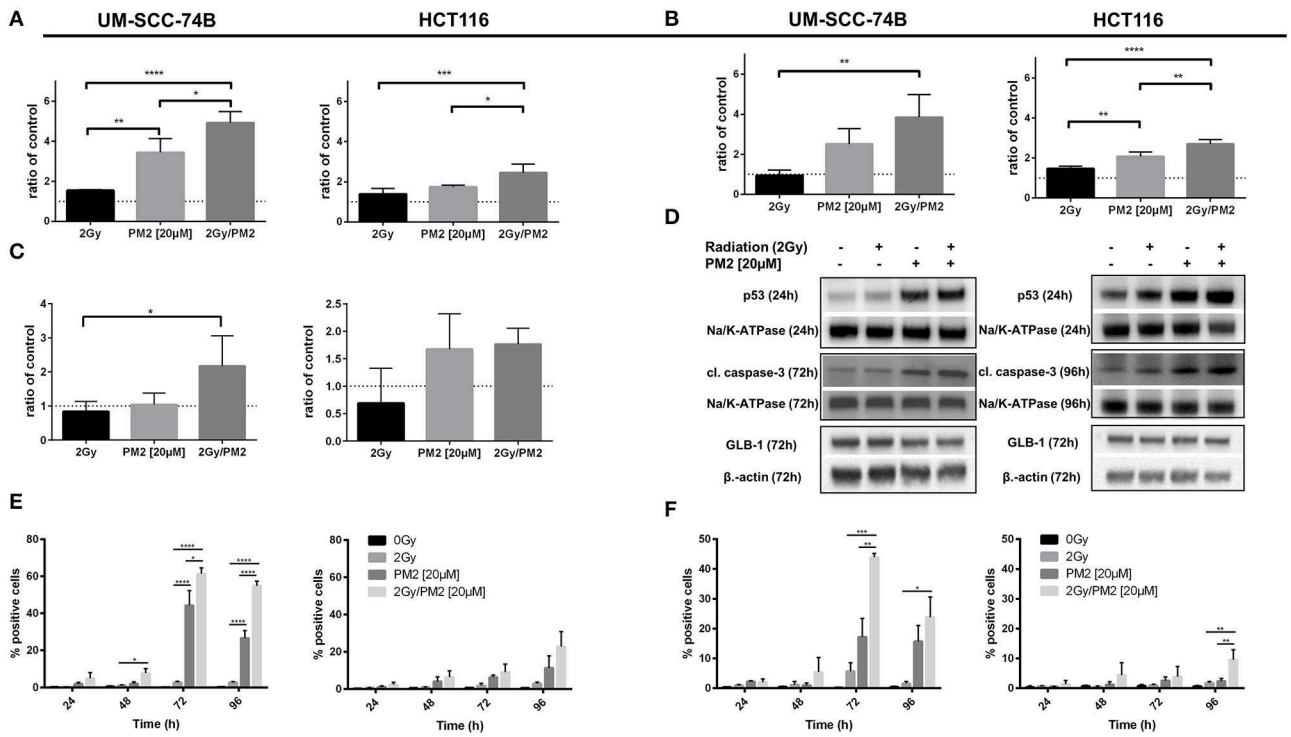

FIGURE 2 | Western Blot analyses of p53-expression **(A)** at 24 h post-treatment of UM-SCC-74B and HCT116 samples with either 2 Gy, 20 μM of PM2, or the combination and cleaved caspase-3 expression **(B)** as well as GLB-1 expression **(C)** of UM-SCC-74B and HCT116 samples at 72 and 96 h post-treatment, respectively. NaK-ATPase was used as loading control for p53 and cleaved caspase-3, β-actin for GLB-1 expression. All samples were normalized to controls, represented as a dotted line at y = 1. $n \geq 3$, error bars presented as SD. Representative Western Blot images **(D)** of p53, cleaved caspase-3 and GLB-1 expression of UM-SCC-74B at 24 h (p53) and 72 h (cleaved caspase-3, GLB-1) post-treatment, and HCT116 samples at 24 h (p53), 72 h (GLB-1), and 96 h (cleaved caspase-3) post-treatment. Flow cytometric analyses of cleaved caspase-3 **(E)** and Noxa-expression **(F)** of UM-SCC-74B and HCT116 samples at 24, 48, 72, and 96 h post-treatment with either 2 Gy, 20 μM of PM2, or the combination. $n \geq 3$, error bars represent SD. Significance was determined using one-way ANOVA: $p \leq 0.05$ (*), $p \leq 0.01$ (**), $p \leq 0.001$ (***), $p \leq 0.0001$ (****).

treatments of 2 × 2 Gy/3 × 20 μM and 3 × 2 Gy/3 × 20 μM of PM2 also resulted in continuous growth inhibition throughout day 14; however, this combination did not result in spheroid disintegration (**Table 3**; **Figure 4**). All combination treatments demonstrated synergistic inhibitory effects on the proliferation rate of UM-SCC-74B spheroids prior to day 14 (**Table 4**).

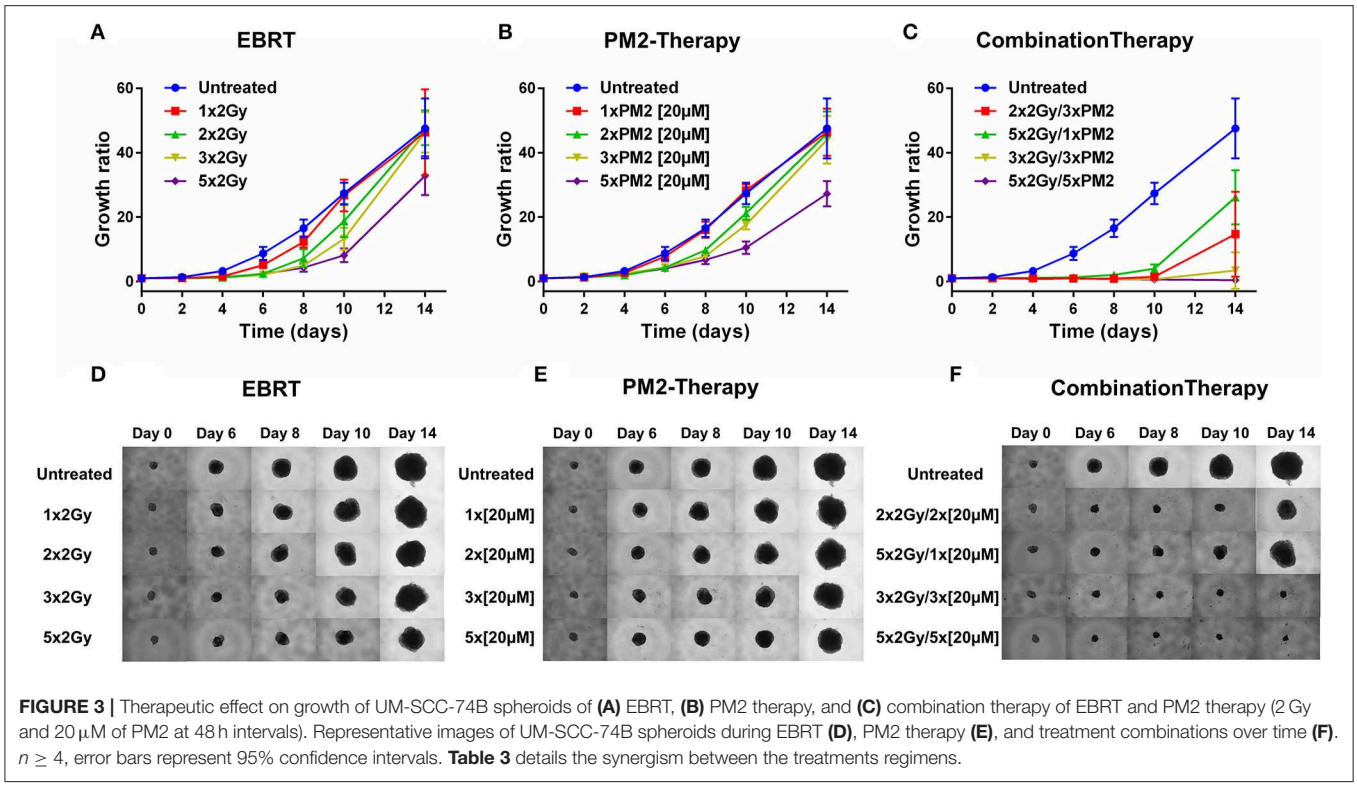

FIGURE 3 | Therapeutic effect on growth of UM-SCC-74B spheroids of **(A)** EBRT, **(B)** PM2 therapy, and **(C)** combination therapy of EBRT and PM2 therapy (2 Gy and 20 μM of PM2 at 48 h intervals). Representative images of UM-SCC-74B spheroids during EBRT **(D)**, PM2 therapy **(E)**, and treatment combinations over time **(F)**. $n \geq 4$, error bars represent 95% confidence intervals. **Table 3** details the synergism between the treatments regimens.

TABLE 3 | CDI-values of selected treatments of UM-SCC-74B spheroids on Day 10 and Day 14 post treatment.

	Day 10					Day 14			
Treatment	**1 × 2 Gy**	**2 × 2 Gy**	**3 × 2 Gy**	**5 × 2 Gy**	**Treatment**	**1 × 2 Gy**	**2 × 2 Gy**	**3 × 2 Gy**	**5 × 2 Gy**
1 × 20 μM	0.705	0.507	0.493	0.472	1 × 20 μM	1.03	0.93	0.821	0.815
2 × 20 μM	n/a	0.209	n/a	n/a	2 × 20 μM	n/a	0.51	n/a	n/a
3 × 20 μM	0.412	0.122	0.244	n/a	3 × 20 μM	0.944	0.333	0.182	n/a
5 × 20 μM	0.398	n/a	n/a	0.201	5 × 20 μM	0.568	n/a	n/a	0.023

CDI < 0.7 equaled a significant synergistic effect, CDI ≤ 1 equaled additive effect, and CDI > 1 equaled antagonistic effect. n/a, not assessed.

DISCUSSION

Several MDM2-p53 inhibitors are currently undergoing different stages of both preclinical and clinical evaluation. On the clinical level, the antagonists are primarily being tested either as single modality treatments or in combination with chemotherapeutic agents such as doxorubicin or cytarabine (23). Interestingly, even though wt p53 plays a central role in radiation response mechanisms, none of the current clinical trials are combining MDM2-p53 inhibitors with ionizing radiation. However, previous studies have demonstrated that stabilization of wt p53 may offer great potential to boost the therapeutic effects of radiotherapy (28, 35, 36). Consequently, the present study aimed to investigate whether the novel stapled MDM2/X-p53 inhibitor PM2 can potentiate the therapeutic effects of ionizing radiation in a panel of cell lines, the synergistic potential of various combinations of doses and fractionations, as well as the underlying mechanisms behind the effects.

In the present study, a single dose of PM2 (20 μM) impaired cell viability in all three wt p53 cell lines grown in monolayer. Furthermore, after a single dose of ionizing radiation (2 Gy), the effects of PM2 were significantly amplified (**Table 1**). The amplification resulted in differences between irradiated and un-irradiated samples at doses as low as 10 μM (**Figure 1A**). All three wt p53 HPV-negative cell lines responded in a similar fashion to PM2 therapy, with UM-SCC-74B demonstrating the most pronounced sensitivity with and without radiation. As expected, the two p53 mutated cell lines did not respond to PM2 monotherapy. Interestingly, even though A431 (which has a single point mutation of *TP53*) was unaffected by PM2 therapy alone, a significant decrease in viability was detected when combined with ionizing radiation (**Supplementary Figure 1B**). Some effect of Nutlin-1 on mutant p53 cells, albeit at considerably higher concentrations than required for wt p53 cell lines, has previously been shown in an *in vitro* study (37). Thus, it is possible that there

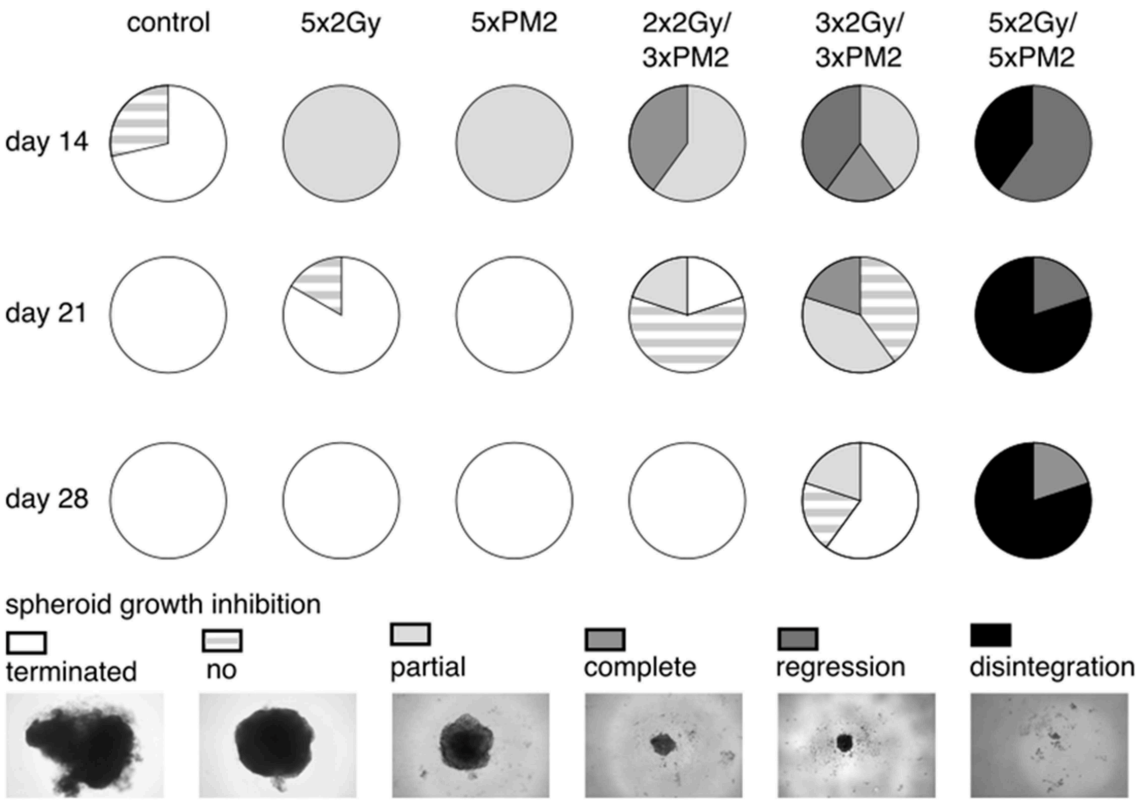

FIGURE 4 | Spheroid response to selected repeated treatments of 20 μM of PM2, 2 Gy of EBRT, or combinations of the treatment modalities at day 14, 21, and 28 post-start of treatment, presented as parts of whole with representative images of the different therapeutic responses. Terminated, maximum assay dependent spheroid size reached (>600 μm^3); no, no spheroid growth inhibition (spheroids with growth rates matching those of untreated controls); partial, partial growth inhibition (spheroids with reduced growth rates compared to untreated controls); complete, complete spheroid growth inhibition (spheroids with unchanged spheroid size post-start of treatment); regression, reclining spheroid size post-start of treatment; disintegration, dissolution of non-viable spheroids $n \geq 4$.

TABLE 4 | Median and maximum time (d) to spheroid termination due to excessive growth (volume >600 μm^3) of selected treatments.

Treatment	Control	2 × 2 Gy and 3 × PM2	3 × 2 Gy and 3 × PM2	5 × 2 Gy	5 × PM2	5 × 2 Gy and 1 × PM2	5 × 2 Gy and 5 × PM2
Median time to termination (d)	14	21	28	21	21	21	Not reached
Maximum time to termination (d)	17	25	35	25	21	25	Not reached

"Not reached" meaning no termination was present during the course of the assay.

is potential for combined PM2 and radiotherapy also for selected mutant p53 cancers. No response was observed on the HPV positive cell line UT-SCC-45 regardless of the addition of ionizing radiation. This is in line with previous studies indicating that the HPV E6 protein binds to p53, resulting in ubiquitin-dependent degradation and rendering MDM2-p53 inhibitors useless (38). In this study, only one HPV-positive cell line was investigated, and further studies are needed to confirm this finding. Furthermore, the lack of response when using the scrambled PM2 peptide ($PM2^{SCRAM}$) validates the specificity of PM2 to its target (**Supplementary Figure 1A**). Taken together, these results support and validate previous findings on the specific MDM2/X-p53 antagonistic properties of PM2 (25, 27, 28).

Two of the main cellular responses following p53 activation are cell cycle arrest and apoptosis, the latter through transcription of pro-apoptotic proteins such as Noxa (14, 17, 37). In the present study, combination therapy (EBRT and PM2) prolonged and increased the amount of viable cells in the radiosensitive G2/M-phase and resulted in S-phase depletion (**Table 2**; **Figure 1B**). The prolonged arrest in G2/M-phase and S-phase depletion suggests that the irradiated cells are unable to repair the DNA damage and are more likely to undergo cell death rather than proceed through mitosis, further preventing cell proliferation (39, 40). These results demonstrate that the combination therapy of PM2 and EBRT resulted in greater effects and potency than either treatment alone.

Western Blot results confirmed PM2 specificity through an extensive increase in p53-levels following PM2 therapy. The upregulation of p53-expression is in concordance with our previous study (28) as well as studies using Nutlin-3, where increased p53-expression was directly correlated to increasing concentrations of the MDM2-p53 inhibitor (37). Combination therapy further increased wt p53 levels in both UM-SCC-74B and HCT116 samples (**Figures 2A,D**). UM-SCC-74B samples presented a near 5-fold increase in wt p53 levels following combination therapy. The extensive increase could be the reason why UM-SCC-74B was more sensitive both to PM2 therapy and to the combination treatment compared to HCT116 throughout the study. Four-fold and near-three-fold increases in cleaved caspase-3 levels were detected in PM2-treated UM-SCC-74B and HCT116 samples, respectively, indicating elevated apoptotic activity (**Figures 2B,D**). Interestingly, elevated levels of senescence were also detected, through increased levels of GLB-1 (**Figures 2C,D**). The GLB-1 levels followed the same pattern as p53, cleaved caspase-3 and Noxa, meaning the greatest increase was observed for the combination treated samples. However, the increase was less pronounced and failed to reach significance in the HCT116 samples. These results warrant further investigation of the mechanisms behind the possible induction of p53-mediated senescence pathways following PM2 therapy.

Flow cytometric analyses confirmed the increased levels of cleaved caspase-3 in both cell lines (**Figure 2E**). Increased levels of Noxa were detected in both UM-SCC-74B and HCT116, where the levels following the combination of EBRT and PM2 therapy proved greater than EBRT or PM2-monotherapy (**Figure 2F**). Interestingly, in samples treated with only EBRT, neither cleaved caspase-3 nor Noxa-expression levels differed from untreated controls, whereas PM2 therapy resulted in distinct increases at 72 h post-treatment. The increased levels of Noxa-expression of the PM2-treated samples suggest that the observed cell death could be the result of p53-mediated apoptosis. Thus, we conclude that the apoptotic effects induced by PM2 therapy are further potentiated by a combination with EBRT in wt p53 cancer cell lines. Moreover, the present study is the first to demonstrate increased senescence and p53-mediated apoptosis in cells treated with a combination of PM2 and EBRT, and may provide an explanation to the synergistic therapeutic effects obtained.

While monolayer assays are suitable for mechanistic evaluations, often generating greater therapeutic responses, anti-tumorigenic properties are better assessed in assays simulating the 3D-structure of tumors, such as *in vitro* 3D tumor spheroid models. When switching from monolayer to 3D models, the treatment schedule must be changed accordingly to better emulate an *in vivo* setting. As such, PM2-treatments were incubated for 48 h in all 3D assay settings to simulate the biological elimination and excretion rates *in vivo*. Treatment with PM2 every second day is less frequent than other MDM2-p53 inhibitors in current clinical trials (41). However, PM2 offers an extended biological half-life as well as inhibition of both p53 negative regulators MDM2 and MDMX. Therefore, less frequent doses of PM2 therapy could potentially circumvent issues of resistance and toxicities as seen with other MDM2-p53 inhibitors, for example Nutlin-3 (23, 26). Furthermore, treatment resistance can be avoided by combining PM2 therapy with EBRT.

In the present study, UM-SCC-74B spheroids irradiated with one, two, three or five times 2 Gy at 48 h intervals resulted in dose-dependent growth inhibition (**Figure 3A**). Interestingly, a single dose (20 μM) of PM2 incubated for 48 h, which in monolayer assays was highly potent in reducing viability, failed to impair UM-SCC-74B spheroid growth. This difference in PM2-potency is likely due to the changes in treatment schedule from monolayer to 3D setting (42). However, repeated doses at 48 h intervals did inhibit growth in a dose-dependent manner similar to that of repeated EBRT (**Figure 3B**). When combining the two therapies, potentiating effects were observed; a single 20 μM dose of PM2 (48 h incubation) which previously rendered little or no effect as a monotherapy, resulted in synergistic growth inhibitory effects for all treatments until day 14, with CDI < 0.7 when combined with either single or fractionated radiation treatments (**Table 3**; **Figure 4**). A further evolution of the combination regimens with both repeated EBRT and PM2 doses resulted in synergism in all combinations (**Table 3**). While all combinations resulted in growth inhibition, the majority of the spheroids eventually regained normal growth patterns (**Figure 4**). However, the rate at which they did differed markedly between the treatment regimes. There was a strong repeated-dose-dependent response to combination therapy: two repeated doses of each treatment resulted in growth inhibition surpassing the standard 14-day assay (data not shown), while adding a third dose of PM2 further increased the time to spheroid progression (**Table 4**; **Figure 4**). Three repeated doses of each therapy further prolonged the inhibitory effects, extending the median time to spheroid termination due to excess size to 28 days post-start of treatment, a 2-fold increase compared to untreated controls (**Table 4**). Most strikingly, five repeated doses of both therapies resulted in 100% spheroid disintegration (**Figures 3C**, **4**). These findings demonstrate for the first time that, despite each treatment having an inhibitory effect alone, combining PM2 and EBRT can result in complete collapse of tumor spheroids and tumor cell death. This demonstrates the great potential of PM2 as a radiosensitizer in combination with fractionated EBRT, and may be especially suitable to increase the effect and reduce the frequency of recurrent tumors from small surviving subpopulations.

To conclude, the potential antitumorigenic effects of the combination of EBRT and PM2 therapy, as well as the mechanisms behind the effects and the cellular fates of treated cells were assessed in the present study. The study presents previously unknown data on PM2 and radiation treatment, demonstrating cell cycle arrest as well as upregulation of p53-mediated apoptosis. We therefore conclude that PM2 shows great promise as a future therapeutic cancer drug candidate, particularly as a radiosensitizer in combination with ionizing radiation.

DATA AVAILABILITY STATEMENT

All datasets generated for this study are included in the manuscript/**Supplementary Files**.

AUTHOR CONTRIBUTIONS

AM designed the study, acquired the majority of the data, performed data analyses, statistical analyses and interpretation and drafted the article. DS assisted with the design of the study, acquired data and performed analyses and interpretation, and revised the original draft. CB acquired data, performed data analyses and interpretation, and revised the original draft. DL assisted with the design of the study and performed interpretation of data as well as revised the original draft. MN designed the study with AM and performed data analyses and interpretation as well as revised the original draft. All authors have approved the submitted manuscript.

FUNDING

This study was supported by grants from the Swedish Research Council (2013-30876-104113-30) and the Swedish Cancer Society (CAN 2018/494, CAN 2015/1080).

ACKNOWLEDGMENTS

Flow cytometry was performed with equipment maintained by the BioVis Platform, Uppsala. The authors would like to thank Tabassom Mohajer Shojai for assisting with experimental work.

SUPPLEMENTARY MATERIAL

The Supplementary Material for this article can be found online at: https://www.frontiersin.org/articles/10.3389/fonc.2019.00923/full#supplementary-material

Supplementary Figure 1 | (A) Titrations of PM2 and PM2^{SCRAM} against HEK293 cells that are transiently transfected with the Mdm2:p53 NanoBIT system. Cells were treated for 4 h with either compound in 10% FCS containing DMEM cell media. IC_{50} of PM2 were determined to be 14.8 ± 0.5 μM using a 4-parameter model. Curve fitting was performed using Prism 8 (Graphpad). **(B)** Cell viability (XTT) response to treatment with 20 μM of PM2 of A431, H314, UT-SCC-45, and UM-SCC-74A cells with or without EBRT (2 Gy) $n \geq 4$. Please note that irradiated cells were normalized to survival at 2 Gy, 0 μM PM2, whereas un-irradiated cells were normalized to survival at 0 Gy, 0 μM PM2 in order to compensate for the effects of radiation.

REFERENCES

1. Borras JM, Lievens Y, Dunscombe P, Coffey M, Malicki J, Corral J, et al. The optimal utilization proportion of external beam radiotherapy in European countries: an ESTRO-HERO analysis. *Radiother Oncol*. (2015) 116:38–44. doi: 10.1016/j.radonc.2015.04.018
2. Dearnaley DP, Jovic G, Syndikus I, Khoo V, Cowan RA, Graham JD, et al. Escalated-dose versus control-dose conformal radiotherapy for prostate cancer: long-term results from the MRC RT01 randomised controlled trial. *Lancet Oncol*. (2014) 15:464–73. doi: 10.1016/S1470-2045(14)70040-3
3. Lumen N, Ost P, Van Praet C, De Meerleer G, Villeirs G, Fonteyne V. Developments in external beam radiotherapy for prostate cancer. *Urology*. (2013) 82:5–10. doi: 10.1016/j.urology.2013.03.043
4. Hall S, Rudrawar S, Zunk M, Bernaitis N, Arora D, McDermott CM, et al. Protection against Radiotherapy-Induced Toxicity. *Antioxid Basel Switz*. (2016) 5:22. doi: 10.3390/antiox5030022
5. Li T, Xing L. Optimizing 4D cone-beam CT acquisition protocol for external beam radiotherapy. *Int J Radiat Oncol*. (2007) 15:1211–9. doi: 10.1016/j.ijrobp.2006.10.024
6. McDonald SC, Rubin P. Optimization of external beam radiation therapy. *Int J Radiat Oncol*. (1977) 2:307–17. doi: 10.1016/0360-3016(77)90089-X
7. Birk Christensen C, Loft-Jakobsen A, Munck af Rosenschöld P, Højgaard L, Roed H, Berthelsen AK. 18F-FDG PET/CT for planning external beam radiotherapy alters therapy in 11% of 581 patients. *Clin Physiol Funct Imaging*. (2018) 38:278–84. doi: 10.1111/cpf.12411
8. Navran A, Heemsbergen W, Janssen T, Hamming-Vrieze O, Jonker M, Zuur C, et al. The impact of margin reduction on outcome and toxicity in head and neck cancer patients treated with image-guided volumetric modulated arc therapy (VMAT). *Radiother Oncol*. (2019) 130:25–31. doi: 10.1016/j.radonc.2018.06.032
9. Au KH, Ngan RKC, Ng AWY, Poon DMC, Ng WT, Yuen KT, et al. Treatment outcomes of nasopharyngeal carcinoma in modern era after intensity modulated radiotherapy (IMRT) in Hong Kong: A report of 3328 patients (HKNPCSG 1301 study). *Oral Oncol*. (2018) 77:16–21. doi: 10.1016/j.oraloncology.2017.12.004
10. Kumar S, Singh RK, Meena R. Emerging targets for radioprotection and radiosensitization in radiotherapy. *Tumour Biol*. (2016) 37:11589–609. doi: 10.1007/s13277-016-5117-8
11. Hirai T, Saito S, Fujimori H, Matsushita K, Nishio T, Okayasu R, et al. Radiosensitization by PARP inhibition to proton beam irradiation in cancer cells. *Biochem Biophys Res Commun*. (2016) 478:234–40. doi: 10.1016/j.bbrc.2016.07.062
12. Li Y, Liu F, Wang Y, Li D, Guo F, Xu L, et al. Rapamycin-induced autophagy sensitizes A549 cells to radiation associated with DNA damage repair inhibition. *Thorac Cancer*. (2016) 7:379–86. doi: 10.1111/1759-7714.12332
13. Lee C-L, Blum JM, Kirsch DG. Role of p53 in regulating tissue response to radiation by mechanisms independent of apoptosis. *Transl Cancer Res*. (2013) 2:412–21. doi: 10.3978/j.issn.2218-676X.2013.09.01
14. Goh AM, Lane DP. How p53 wields the scales of fate: arrest or death? *Transcription*. (2012) 3:240–4. doi: 10.4161/trns.21297
15. Meyn RE, Milas L, Ang KK. The role of apoptosis in radiation oncology. *Int J Radiat Biol*. (2009) 85:107–15. doi: 10.1080/09553000802662595
16. Speidel D. The role of DNA damage responses in p53 biology. *Arch Toxicol*. (2015) 89:501–17. doi: 10.1007/s00204-015-1459-z
17. Deben C, Wouters A, Beeck KO de, Bossche J van D, Jacobs J, Zwaenepoel K, et al. The MDM2-inhibitor Nutlin-3 synergizes with cisplatin to induce p53 dependent tumor cell apoptosis in non-small cell lung cancer. *Oncotarget*. (2015) 6:22666–79. doi: 10.18632/oncotarget.4433
18. Ploner C, Kofler R, Villunger A. Noxa: at the tip of the balance between life and death. *Oncogene*. (2009) 27:S84–92. doi: 10.1038/onc.2009.46
19. Mancini F, Di Conza G, Moretti F. MDM4 (MDMX) and its transcript variants. *Curr Genomics*. (2009) 10:42–50. doi: 10.2174/138920209787581280
20. Liu J, Zhang C, Feng Z. Tumor suppressor p53 and its gain-of-function mutants in cancer. *Acta Biochim Biophys Sin*. (2014) 46:170–9. doi: 10.1093/abbs/gmt144
21. Hoe KK, Verma CS, Lane DP. Drugging the p53 pathway: understanding the route to clinical efficacy. *Nat Rev Drug Discov*. (2014) 13:217–36. doi: 10.1038/nrd4236
22. Trino S, Iacobucci I, Erriquez D, Laurenzana I, De Luca L, Ferrari A, et al. Targeting the p53-MDM2 interaction by the small-molecule MDM2 antagonist Nutlin-3a: a new challenged target therapy in adult Philadelphia positive acute lymphoblastic leukemia patients. *Oncotarget*. (2016) 7:12951–61. doi: 10.18632/oncotarget.7339
23. Burgess A, Chia KM, Haupt S, Thomas D, Haupt Y, Lim E. Clinical overview of MDM2/X-targeted therapies. *Front Oncol*. (2016) 6:7. doi: 10.3389/fonc.2016.00007
24. Tisato V, Voltan R, Gonelli A, Secchiero P, Zauli G. MDM2/X inhibitors under clinical evaluation: perspectives for the management of hematological malignancies and pediatric cancer. *J Hematol Oncol*. (2017) 10:133. doi: 10.1186/s13045-017-0500-5
25. Brown CJ, Quah ST, Jong J, Goh AM, Chiam PC, Khoo KH, et al. Stapled peptides with improved potency and specificity that activate p53. *ACS Chem Biol*. (2013) 8:506–12. doi: 10.1021/cb3005148

26. Wei SJ, Chee S, Yurlova L, Lane D, Verma C, Brown C, et al. Avoiding drug resistance through extended drug target interfaces: a case for stapled peptides. *Oncotarget*. (2016) 7:32232–46. doi: 10.18632/oncotarget.8572
27. Wei SJ, Joseph T, Chee S, Li L, Yurlova L, Zolghadr K, et al. Inhibition of nutlin-resistant HDM2 mutants by stapled peptides. *PLoS ONE*. (2013) 8:e81068. doi: 10.1371/journal.pone.0081068
28. Spiegelberg D, Mortensen AC, Lundsten S, Brown CJ, Lane DP, Nestor M. The MDM2/MDMX-p53 antagonist PM2 radiosensitizes wild-type p53 tumors. *Cancer Res*. (2018) 78:5084–93. doi: 10.1158/0008-5472.CAN-18-0440
29. Zhao Y, Gao J-L, Ji J-W, Gao M, Yin Q-S, Qiu Q-L, et al. Cytotoxicity enhancement in MDA-MB-231 cells by the combination treatment of tetrahydropalmatine and berberine derived from Corydalis yanhusuo W. T. Wang. *J Intercult Ethnopharmacol*. (2014) 3:68–72. doi: 10.5455/jice.20140123040224
30. Bykov VJN, Issaeva N, Shilov A, Hultcrantz M, Pugacheva E, Chumakov P, et al. Restoration of the tumor suppressor function to mutant p53 by a low-molecular-weight compound. *Nat Med*. (2002) 8:282–8. doi: 10.1038/nm0302-282
31. Paterson IC, Davies M, Stone A, Huntley S, Smith E, Pring M, et al. TGF-beta1 acts as a tumor suppressor of human malignant keratinocytes independently of Smad 4 expression and ligand-induced G(1) arrest. *Oncogene*. (2002) 21:1616–24. doi: 10.1038/sj.onc.1205217
32. Busch C-J, Kriegs M, Laban S, Tribius S, Knecht R, Petersen C, et al. HPV-positive HNSCC cell lines but not primary human fibroblasts are radiosensitized by the inhibition of Chk1. *Radiother Oncol J Eur Soc Ther Radiol Oncol*. (2013) 108:495–9. doi: 10.1016/j.radonc.2013.06.035
33. Bradford CR, Zhu S, Ogawa H, Ogawa T, Ubell M, Narayan A, et al. P53 mutation correlates with cisplatin sensitivity in head and neck squamous cell carcinoma lines. *Head Neck*. (2003) 25:654–61. doi: 10.1002/hed.10274
34. Liu Y, Bodmer WF. Analysis of P53 mutations and their expression in 56 colorectal cancer cell lines. *Proc Natl Acad Sci USA*. (2006) 103:976–81. doi: 10.1073/pnas.0510146103
35. Shirai Y, Shiba H, Iwase R, Haruki K, Fujiwara Y, Furukawa K, et al. Dual inhibition of nuclear factor kappa-B and Mdm2 enhance the antitumor effect of radiation therapy for pancreatic cancer. *Cancer Lett*. (2016) 370:177–84. doi: 10.1016/j.canlet.2015.10.034
36. Feng FY, Zhang Y, Kothari V, Evans JR, Jackson WC, Chen W, et al. MDM2 inhibition sensitizes prostate cancer cells to androgen ablation and radiotherapy in a p53-dependent manner. *Neoplasia N Y N*. (2016) 18:213–22. doi: 10.1016/j.neo.2016.01.006
37. Vassilev LT, Vu BT, Graves B, Carvajal D, Podlaski F, Filipovic Z, et al. *In vivo* activation of the p53 pathway by small-molecule antagonists of MDM2. *Science*. (2004) 303:844–8. doi: 10.1126/science.1092472
38. Natarajan T, Anandhi M, Aiswarya D, Ramkumar R, Kumar S, Perumal P. Idaein chloride induced p53 dependent apoptosis in cervical cancer cells through inhibition of viral oncoproteins. *Biochimie*. (2016) 121:13–20. doi: 10.1016/j.biochi.2015.11.008
39. Qu A, Wang H, Li J, Wang J, Liu J, Hou Y, et al. Biological effects of 125I seeds radiation on A549 lung cancer cells: G2/M arrest and enhanced cell death. *Cancer Invest*. (2014) 32:209–17. doi: 10.3109/07357907.2014.905585
40. Lomazzi M, Moroni MC, Jensen MR, Frittoli E, Helin K. Suppression of the p53- or pRB-mediated G1 checkpoint is required for E2F-induced S-phase entry. *Nat Genet*. (2002) 31:190–4. doi: 10.1038/ng891
41. Andreeff M, Kelly KR, Yee K, Assouline S, Strair R, Popplewell L, et al. Results of the phase I trial of RG7112, a small-molecule MDM2 antagonist in leukemia. *Clin Cancer Res*. (2016) 22:868–76. doi: 10.1158/1078-0432.CCR-15-0481
42. Eke I, Cordes N. Radiobiology goes 3D: How ECM and cell morphology impact on cell survival after irradiation. *Radiother Oncol*. (2011) 99:271–8. doi: 10.1016/j.radonc.2011.06.007

Conflict of Interest: DL heads a collaboration with Merck on macrocyclic peptides. DL and CB have a patent EP3256484A1 pending. The authors declare no potential conflict of interest.

frontiers in Oncology

ORIGINAL RESEARCH
published: 25 October 2019
doi: 10.3389/fonc.2019.01136

Pan-Cancer Analysis of Potential Synthetic Lethal Drug Targets Specific to Alterations in DNA Damage Response

*Shaoli Das, Kevin Camphausen and Uma Shankavaram**

Radiation Oncology Branch, National Cancer Institute, National Institutes of Health, Bethesda, MD, United States

Alterations in DNA damage response (DDR) is one of the several hallmarks of cancer. Genomic instability resulting from a disrupted DDR mechanism is known to contribute to cancer progression, and are subjected to radiation, cytotoxic, or more recently targeted therapies with limited success. Synthetic lethality (SL), which is a condition where simultaneous loss-of-function of the genes from complementary pathways result in loss of viability of cancer cells have been exploited to treat malignancies resulting from defects in certain DDR pathways. Albeit being a promising therapeutic strategy, number of SL based drugs currently in clinical trial is limited. In this work we performed a comprehensive pan-cancer analysis of alterations in 10 DDR pathways with different components of DNA repair. Using unsupervised clustering of single sample enrichment of these pathways in 7,272 tumor samples from 17 tumor types from TCGA, we identified three prominent clusters, each associated with specific DDR mechanisms. Somatic mutations in key DDR genes were found to be dominant in each of these three clusters with distinct DDR component. Using a machine-learning based algorithm we predicted SL partners specific to somatic mutations in key genes representing each of the three DDR clusters and identified potential druggable targets. We explored the potential FDA-approved drugs for targeting the predicted SL genes and tested the sensitivity using the drug screening data in cell lines with mutation in the primary DDR genes. We have shown clinical relevance, for selected targetable SL interactions using Kaplan-Meier analysis in terms of improved disease-free survival. Thus, our computational framework provides a basis for clinically relevant and actionable SL based drug targets specific to alterations in DDR pathways.

Keywords: DNA damage response, synthetic lethality, single sample gene set enrichment analysis, mutual exclusivity, somatic mutations, drug sensitivity, disease-free survival, Kaplan-Meier analysis

OPEN ACCESS

Edited by:
Michaela Medová,
University Hospital Bern, Switzerland

Reviewed by:
Hamid Morjani,
Université de Reims Champagne-Ardenne, France
Matúš Medo,
University of Electronic Science and Technology of China, China

****Correspondence:***
Uma Shankavaram
uma@mail.nih.gov

Specialty section:
This article was submitted to Molecular and Cellular Oncology, a section of the journal Frontiers in Oncology

Received: *22 August 2019*
Accepted: *10 October 2019*
Published: *25 October 2019*

Citation:
Das S, Camphausen K and Shankavaram U (2019) Pan-Cancer Analysis of Potential Synthetic Lethal Drug Targets Specific to Alterations in DNA Damage Response. Front. Oncol. 9:1136. doi: 10.3389/fonc.2019.01136

INTRODUCTION

Responding to DNA damage from various internal or external stimuli is a crucial process for cell viability. Normally the DNA repair pathways guide the cell fate decisions for cells exposed to DNA damage; they can either be repaired and restored to normal function, or in cases where the damage is irreversible the cell is "sacrificed" by senescence via activation of certain DNA damage response (DDR) pathways (1). But in a third scenario, because of inefficient repair of damaged DNA, the affected cell evades senescence, which leads to proliferation of cells carrying oncogenic

alterations, and subsequently develops cancer (2). Genomic instability caused by driver mutations is a hallmark of cancer (3). A key function of the DDR machinery in cancer cells is to promote genomic stability and guiding cell fate decisions. Traditional cancer therapies involving radiation and cytotoxic chemotherapies induce DNA damage and exploit DDR pathways to facilitate tumor cell death. Thus, DDR pathways play a major role to determine response to these therapies (4).

DNA damage response (DDR) is a complex multi-level process involving sub-pathways like base-excision, nucleotide excision and mismatch repair for handling single-strand breaks, or homologous recombination repair, homology directed repair, non-homologous end joining, and Fanconi anemia pathways for handling double-strand breaks in DNA (5). Deficiency and alterations in various components of the DDR machinery is common in all types of cancers (6), but generally deficiency in one component can be compensated by other components of DDR (2, 7). Synthetic lethal (SL) interactions are formed between components which are compensatory between themselves. So, a better understanding of the SL relationships between components of DDR is a promising approach to tackle resistance to conventional cancer therapy. Guided by the knowledge of specific DDR alterations in individual patients, SL-based drug targets can be attractive choices for personalized cancer therapy.

The success of *PARP* inhibitors in treating *BRCA1/2* mutated tumors in clinical trials demonstrated the validity of the concept of SL (8). FDA approval of *PARP* inhibitor drugs for treating *BRCA1/2*-mutated ovarian and breast cancer patients has propelled interest in exploration of other potential SL associations between DDR components. Use of shRNA or CRISPR screenings in cancer cell lines is a viable approach for identifying synthetic lethal interactions specific to certain cancer genes of interest (9, 10), but running these screenings are costly when the number of the genes of interest is large. On the other hand, computational prediction of cancer-specific SL interactions can identify many potential candidates for SL interactions (11, 12), but without proper validation of these predictions it is hard to prioritize the targets. We tried to address this limitation by our previously published machine-learning based computational method called DiscoverSL that harnesses the large-scale tumor genomic and clinical data from cancer patients combined with the RNAi and drug screening data from cancer cell lines to infer statistical measures on predicted synthetic lethal interactions to prioritize clinically relevant and targetable candidates (13). Another computational method ISLE also prioritizes SL pairs by identifying those pairs that are predictive of patients' survival upon co-inactivation; but they use literature-derived SL interactions from shRNA-screening experiments (14). Driven by the need to identify potential SL based drug targets specific to alterations in certain DDR pathways in cancers, here we performed a pan-cancer analysis on enrichments or deficiencies of different DDR pathways and alterations in the DDR components from genomic data of 17 tumor types from The Cancer Genome Atlas (TCGA). Combining the existing knowledgebase on potential SL interactions from literature and the SL predictions from DiscoverSL algorithm with the FDA-approved drug targets, we propose clinically relevant, and potentially actionable, cancer specific network of SL DDR alterations, and drug interactions.

MATERIALS AND METHODS

Data Source and Pre-processing

The primary source of tumor genomic and clinical data of 17 tumor types is the cancer genome atlas (TCGA) project (15). Somatic mutation, and RSEM processed and Z-score normalized RNA-Seq v2 gene expression data of TCGA tumor samples are downloaded from cBioPortal (16). Additionally, raw RNA-Seq count data of TCGA tumor, and normal samples was collected from a published resource from Gene Expression Omnibus accession GSE62944, that processed TCGA raw RNA-Seq data using featurecount package to generate the gene-wise raw counts (17).

The gene-pathway associations for 10 DDR pathways were collected from the curated geneset (c2 version 6.2) in the MsigDB database (18).

For validation purposes, we collected processed shRNA screening data in 214 cancer cell lines from Achilles project version 2.4.3 in form of essentiality scores calculated using ATARiS (19). Genomic profiles (mutation) of these cancer cell lines are collected from the cancer cell line encyclopedia [CCLE (20)].

Drug-protein interaction data are collected from the databases DrugBank and DGIDB (21, 22). For drug sensitivity analysis we collected drug screening data from the genomics of drug sensitivity in cancer (GDSC) data portal (23). From this portal we collected the drug response data in cancer cell lines using LN-IC50 and AUC scores as well as the genomic mutation profiles of the corresponding cancer cells.

Computational and Meta-Data

Single sample enrichment scores for 10 DDR pathways across 7,272 tumor samples from 17 histology was calculated using ssGSEA analysis from R package GSVA (24). RSEM processed and Z-score normalized RNA-Seq v2 gene expression data of TCGA cohort, downloaded from cBioPortal, was used for ssGSEA analysis. Unsupervised clustering of tumor samples was performed using hierarchical clustering with spearman correlation as the similarity metric.

Synthetic lethal partners for DDR genes in 17 cancer types are calculated using recently published DiscoverSL algorithm. For each pair of potential synthetic lethal gene pairs and a given cancer type from TCGA, DiscoverSL uses *p*-values calculated from four parameters: (a) DiffExp: differential expression of the secondary gene in samples with vs. without mutation in the primary gene (calculated from TCGA RNA-Seq raw count data available from GSE62944, using EdgeR package) (b) Exp.correlation: expression correlation of the primary and secondary gene (calculated using Pearson's correlation) (c) Mutex: mutual exclusivity of mutation of the primary and secondary gene (calculated using a hypergeometric test described in the following section), and (d) SharedPathway: probability that the primary and secondary genes are part of common pathways (Also calculated using hypergeometric test using the c2 collection

from MSigDB). In DiscoverSL, these four parameters are used as features in a Random Forest model trained with a set of positive and negative examples of synthetic lethal interactions derived from literature. Detailed description for calculation of all four parameters and the Random Forest model can be found in the Supplementary Methods section of our previous publication (13).

Synthetic lethal interactions reported in previous literature or SL screens are collected from the database SynLethDB (25) and another recent publication that curated SL interactions obtained from SL screens in human cell lines (14).

Calculation of Mutual Exclusivity and Mutual Co-occurrence

The probability of a tumor sample belonging to a DDR cluster D (1, 2, or 3, derived from the unsupervised clustering of ssGSEA scores of 10 DDR pathways) and co-occurrence of a gene mutation event E for any DDR gene (*Gene1*) associated with 10 DDR pathways is calculated with a hypergeometric test. Let P_{Mutco} be the hypergeometric P-values for co-occurrence of mutation in *Gene1* and DDR cluster D. The formula for calculation of the hypergeometric P-value is as follows:

$$P_{Mutco} = \sum_{i=S_{12mut}}^{\min(S_{1mut},S_2)} \frac{\left(\frac{S_{1mut}}{i}\right)\left(\frac{S_T - S_{1mut}}{S_2 - i}\right)}{\left(\frac{S_T}{S_2}\right)}$$

Where,

S_{12mut} = Number of tumor samples belonging to DDR cluster D and carrying mutation in Gene1
S_{1mut} = Number of tumor samples with mutation in Gene1
S_2 = Number of tumor samples belonging to DDR cluster D
S_T = Total Number of tumor samples

Similarly, mutual exclusivity with genetic mutation in two DDR genes Gene1 and Gene2 is calculated with a hypergeometric test that calculates the probability of co-occurrence of mutation in Gene1 and Gene2 in patient samples (from TCGA) for a given cancer. Let P_{Mutex} be the hypergeometric P-values for co-occurrence of mutation for Gene1 and Gene2. The formula for calculation of the hypergeometric P-values is as follows:

$$P_{Mutex} = \sum_{i=S_{12mut}}^{\min(S_{1mut},S_{2mut})} \frac{\left(\frac{S_{1mut}}{i}\right)\left(\frac{S_T - S_{1mut}}{S_{2mut} - i}\right)}{\left(\frac{S_T}{S_{2mut}}\right)}$$

Where,

S_{12mut} = Number of cancer samples for a cancer type C with mutation in both *Gene1* and *Gene2*
S_{1mut} = Number of cancer samples for a cancer type C with mutation in *Gene1*
S_{2mut} = Number of cancer samples for a cancer type C with mutation in *Gene2*
S_T = Total Number of cancer samples for a cancer type C

For TCGA mutation data, cases with non-silent mutations are considered as gene mutation events. Opposite to the mutual co-occurrence, the mutual exclusivity P-values should represent the P-value for non-co-occurrence of mutations in Gene1 and Gene2. So, the mutual exclusivity P-value $Mutex_{Mut}$ is calculated as:

$$Mutex_{Mut} = 1 - P_{Mutex}$$

For $Mutex_{Mut}$, the null hypothesis is that the two genes are mutated in the same tumor samples. When $Mutex_{Mut}$ takes a higher value (e.g., 0.98) that means the null hypothesis cannot be rejected and the gene mutations are not mutually exclusive, while $Mutex_{Mut} < 0.05$ means that the null hypothesis can be rejected and the gene mutations are mutually exclusive, i.e., the two genes are not mutated in the same samples.

The mutual co-occurrence and mutual exclusivity p-values are adjusted for multiple testing correction by false discovery rate using Benjamini and Hochberg (26).

In-silico Validation of the Predicted Synthetic Lethal Interactions

We have used multiple methods to validate the significance of SL pair interactions. (1) To assess the effect of silencing the SL gene (gene2) in cancer cell lines where the primary gene (gene1) is mutated, significance of difference in shRNA score [essentiality calculated using ATARiS algorithm from shRNA screening of 214 cell lines (19)] is calculated by t-test using shRNA screening data from Achilles 2.4.3 project. We termed this parameter as *PvalRNAi*. (2) To assess the clinical outcome of under-expression vs. over-expression of the predicted SL gene (gene2) in cases with mutation in the primary gene (gene1), Kaplan Meier survival analysis was performed on disease free survival in TCGA clinical data. (4) To assess the potential drug sensitivity a p-value is calculated using t-test on the LNIC50 values between primary gene mutated vs. non-mutated cells from the Genomics of Drug Sensitivity in Cancer (GDSC) project data. We termed this parameter as *Drug Sensitivity*.

RESULTS

Somatic Mutations in the Components of DDR in a Pan-Cancer Context

To explore the association of 10 DDR pathway related alterations and gene mutations in pan-cancer context, we first identified the DDR pathway specific genes from Reactome and KEGG pathway database [MSigDB c2 collection v6.2 (18)]. These 10 pathways constitute 221 genes and represent different components of DDR handling including single strand breaks or double strand breaks in DNA as illustrated in **Figure 1A** and outlined in the introduction section. Next, we identified somatic mutations among the 221 genes in TCGA data comparing 17 cancer types. All cancer types had somatic alterations in one or more DDR genes. **Figure 1B** represents the somatic mutation in 17 TCGA cancer types. We considered genes having mutation in at least 1% samples in a given cancer, and present in any two or more cancers, resulting in 72 genes. Of all DDR genes, *TP53* was the most frequently mutated gene. The other frequently mutated DDR genes were *PRKDC, ATM, BRCA2, POLE, ATR,*

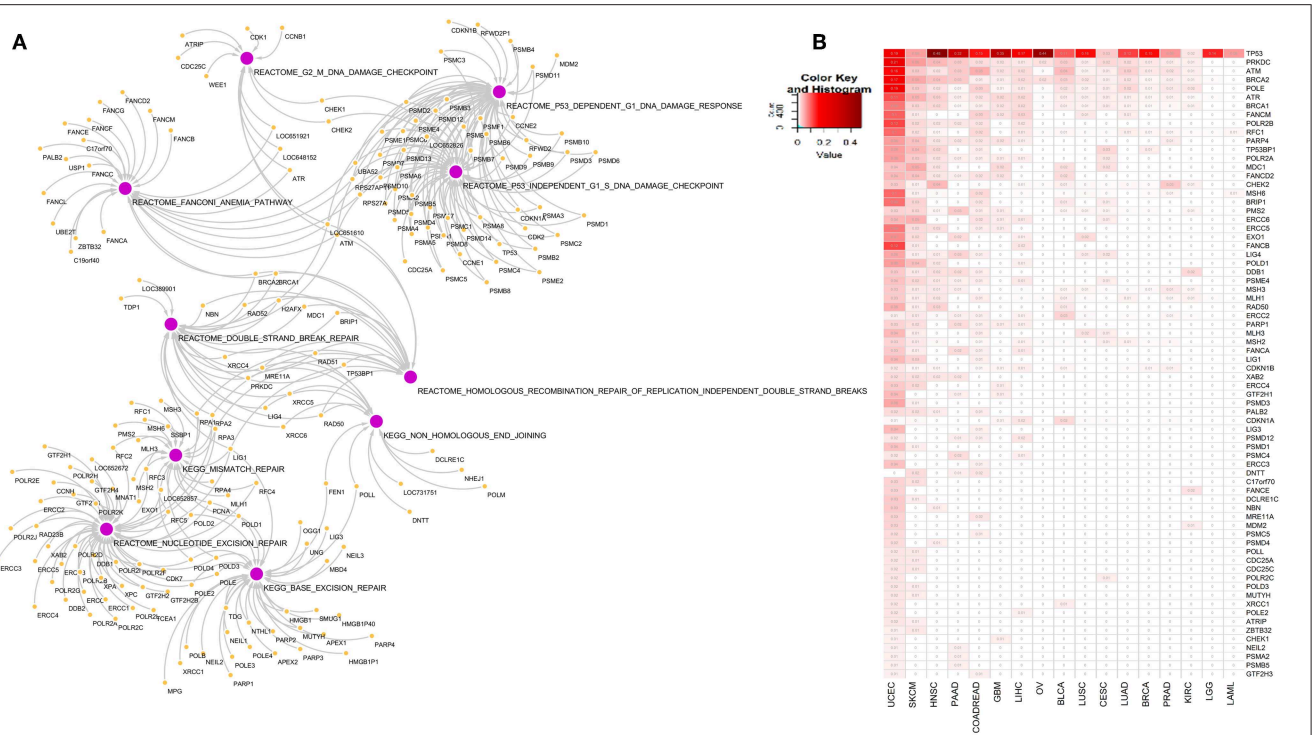

FIGURE 1 | (A) Network diagram of genes associated with 10 DNA damage response pathways at different level of DNA repair: base excision repair, nucleotide excision repair, mismatch repair, double strand break repair, homologous recombination repair of replication independent DNA double strand breaks, non-homologous end joining, G2-M DNA damage checkpoint, Fanconi anemia pathway, P53 dependent DNA damage response and P53 independent DNA damage response. **(B)** Somatic mutations in genes from the 10 DNA damage response pathways in 17 cancer types. We included genes that are mutated in at-least 1% of tumor samples in more than one tumor types. Numbers in each cell represents frequency of samples carrying mutation in corresponding gene in that cancer type. Rows and columns are sorted by the frequency of mutation of the DDR genes in the tumor types.

BRCA1, and *FANCM*. Among the 17 cancer types, uterine corpus cancer (UCEC), head and neck cancer (HNSC), and skin cutaneous melanoma (SKCM) had most frequent alterations in DDR genes.

Exclusive Pattern of Enrichment Is Observed Between Certain Components of DDR

To check the difference in enrichments of the 10 DDR pathways in the pan-cancer scenario, we did single sample geneset enrichment (ssGSEA) analysis on 7,272 tumor samples from 17 tumor types from TCGA. Using unsupervised clustering, we found three pathway clusters and three sample clusters of tumor samples (**Figure 2A**). The sample cluster 1 had enrichment of DNA double strand break repair associated pathways, while the sample cluster 2 had enrichment in single strand break repair related pathways and *p53* dependent or independent DNA damage response at G1. Sample cluster 3, had some similar attributes from cluster 1, but can be characterized by more enrichments in G2/M cell cycle checkpoints, Fanconi anemia and mismatch repair pathways. So, the cluster 1 and cluster 3 were mostly enriched for late-stage DDR (double strand break repair and late-stage cell cycle, respectively), and cluster 1 was more enriched in early-stage DDR (single strand break repair and *p53* dependent or independent G1 checkpoint). From the correlation analysis of pan-cancer wide enrichment scores (ssGSEA) as shown in **Figure 2B**, we observed exclusive pattern of enrichments between the DDR pathways from three groups; one consisting of pathways related to double strand break repair (group 1; enriched in cluster 1), one consisting of pathways related to late-stage cell cycle checkpoints (G2/M), Fanconi anemia and mismatch repair (group 2; enriched in cluster 3), and the other one consisting of single strand break repair and *p53* dependent or independent DNA damage response (group 3; enriched in cluster 2). Among the pathways in group 1 and group 2, non-homologous end joining had negative correlation with the pathways in group 2, while homologous recombination had a positive correlation with these pathways. Mismatch repair had weak positive correlation with not just the pathways from the same group (Fanconi anemia and G2/M checkpoint) but also homologous recombination repair pathway from group 1. This correlation can be attributed to the fact that many components of the Fanconi anemia pathway interacts with the mismatch repair related proteins (27). The correlation of the homologous recombination repair with G2/M DNA damage checkpoint is also expected as this pathway of double strand break repair is restricted to G2 phase or late

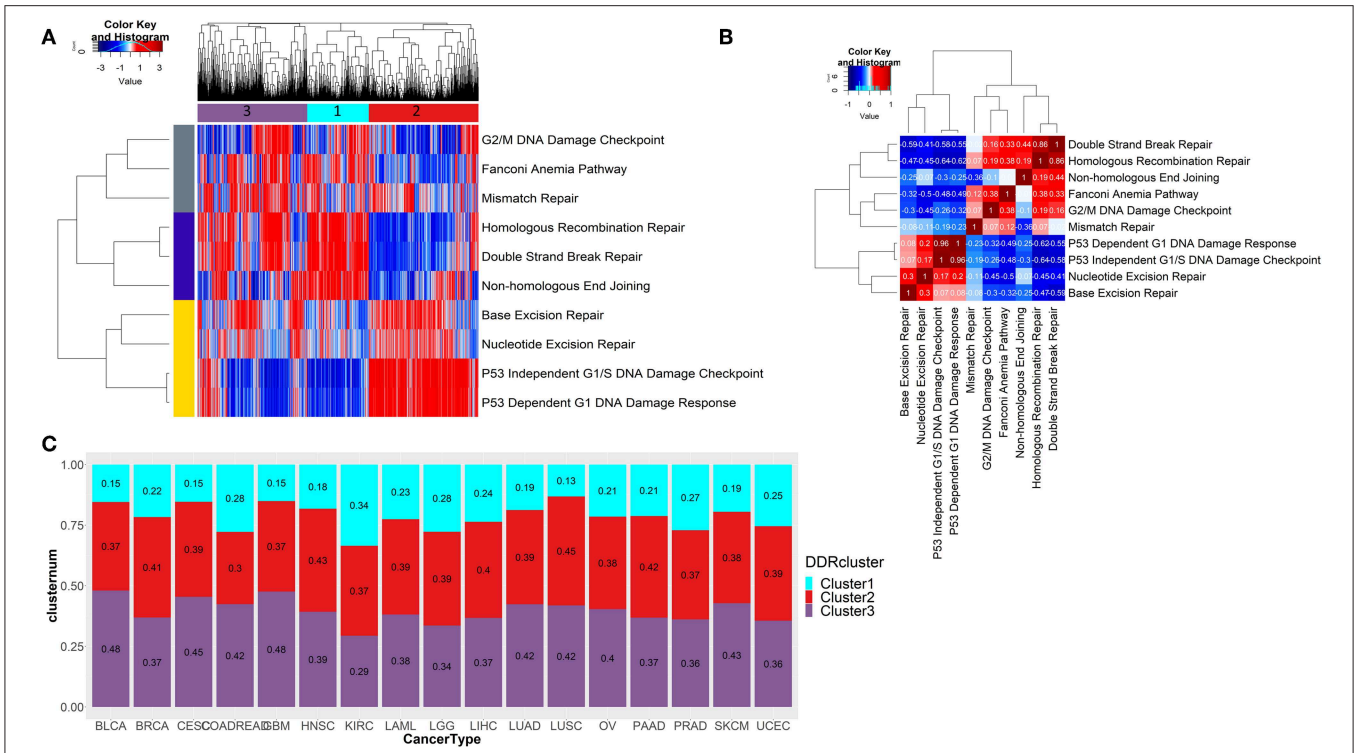

FIGURE 2 | (A) Unsupervised clustering of ssGSEA scores of 10 DDR pathways across 7,272 tumor samples reveals three distinct clusters of tumors. A mutually exclusive enrichment pattern can be seen between these DDR pathways: P53 dependent or independent G1 DNA damage response and double strand break repair, homologous recombination repair, and non-homologous end joining. **(B)** Correlation plot showing the correlation of ssGSEA enrichments of 10 DDR pathways. **(C)** Stacked barplot shows the fraction of samples belonging to each of the three DDR clusters identified from **(A)** in each of the 17 tumor types from TCGA.

S phase (28). Among the pathways in group 3, nucleotide and base excision repair had weak positive correlation with *p53* mediated DNA damage checkpoints. All pathways from group 3 had negative correlations with the pathways from group 1 and group 2. *P53* dependent or independent DNA damage response showed strongest negative correlation with homologous recombination repair ($r < -0.6$). From published literature we see that *p53* has direct role in suppressing homologous recombination repair of DNA double strand breaks (29). Thus, tumors may undergo DNA double strand break repair through activated homologous recombination repair in the absence of *p53* mediated apoptosis, while tumors are most likely to undergo cell cycle arrest at G1 phase by intervention of *p53*. We checked the distribution the samples assigned to these three clusters in each of the 17 cancer types (shown in **Figure 2C**). Though there was some variability in distribution of three clusters in different cancer types, cluster 1 had the lowest frequency of samples in almost all cancer types (only kidney renal cell carcinoma KIRC had almost equal frequency of all 3 clusters).

Underlying Gene Mutation Signatures of the Three Major DDR Clusters

To compare the somatic mutations among DDR pathway genes between the 3 clusters (obtained from the ssGSEA analysis, see **Figure 2A**), we performed a statistical test for mutual co-occurrence of the somatic mutations of the 221 genes among the three DDR clusters. **Figure 3A**, represents 40 genes (hypergeometric test, FDR corrected $p < 0.3$) showing higher occurrence of somatic mutations. These genes formed mutually exclusive pattern between the DDR clusters. The mutated genes representing cluster 1 were mostly associated with nucleotide excision repair (*POLR2A, POLR2B, ERCC4, POLD1*), mismatch repair (*RFC1, MLH1*), base excision repair (*POLD1, PARP1*), and Fanconi anemia (*FANCM, FANCA*). The mutated genes in tumors from cluster 2 were mostly associated with homologous recombination repair (*BRCA2, RAD50, RAD54B, BLM, MDC1, LIG1*), non-homologous end joining (*RAD50, XRCC4*), *ATM* pathway (*TP53*), Fanconi anemia (*BRCA2, USP1*), meiotic recombination (*MLH3, RAD50, BLM*) and also mismatch repair (*EXO1, MSH6, MLH3*), base excision repair (*LIG1, LIG3*), and nucleotide excision repair (*ERCC5, DDB1, ERCC2, CUL4B, LIG1*). The genes mutated in cluster 3 were mainly associated with cell cycle checkpoints (*CHEK2, ATR, CDKN1A, POLE, PSME4, PSMC2, PRKDC*), and additionally with Fanconi anemia (*FANCE, PALB2*), and non-homologous end joining (*LIG4, PRKDC*). Moreover, in all cancer types, we observed mutually exclusive pattern of mutations between the clusters, but not within the same cluster (**Figures 3B–E**, **Supplementary Figure 1**;

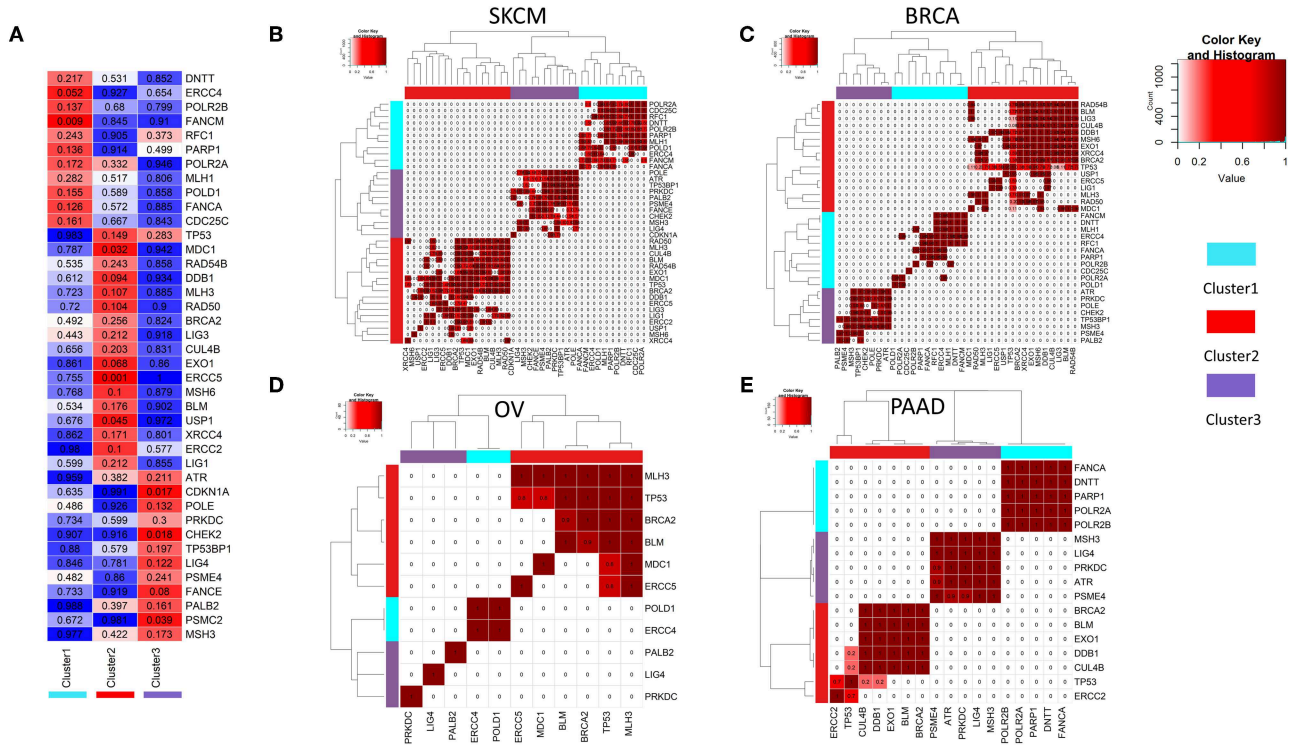

FIGURE 3 | (A) Mutual co-occurrence of certain DDR genes was observed with each of the three DDR clusters identified in 2b. In the matrix, the color key blue to red denotes the tendency from mutual exclusivity to mutual co-occurrence of the corresponding gene mutation (y-axis) and the corresponding DDR cluster (x-axis). The *p*-values for co-occurrence of DDR gene mutations and DDR clusters calculated using hypergeometric test are shown in each cell. **(B–E)** Mutually exclusive mutations of DDR genes representing three different DDR clusters (from 3a) is shown for tumor types **(B)** SKCM **(C)** BRCA **(D)** OV **(E)** PAAD.

p-value calculated using hypergeometric test followed by FDR correction).

Analysis of Transcriptome-Wide Synthetic Lethal Candidates Identifies Common and Exclusive Targets for Different DDR Clusters

We looked for potential synthetic lethal partners of the cluster specific 40 significant DDR genes (see **Figure 3A**) using two approaches: (1) from published synthetic lethal screens in human cell lines (14, 25) and (2) using our previously published machine-learning based algorithm DiscoverSL (13). To shortlist the most probable SL candidates from the DiscoverSL predictions, we applied two *in-silico* validation approach. First, we calculated the conditional essentiality of the SL interaction, i.e., the statistical significance of difference between the shRNA scores (targeting the synthetic lethal gene) for human cell lines with or without mutation in the primary gene; and second, we performed Kaplan-Meier analysis on TCGA clinical data to check if the primary gene is mutated, the differences in disease-free survival between patients when the SL interactor gene downregulated (expression < median) compared to samples where the gene is upregulated (expression > median). The SL pairs which showed significant effects of co-inactivation from both validation methods were chosen as the final list of most probable SL interactors for DDR genes. **Figure 4A** shows a representation of selected SL interactors for genes from the three DDR clusters. A subset of genes was shown to be exclusively associated with each cluster (shown as colored boxes in **Figure 4A**). We checked the functional enrichments of the common and exclusive SL interactors of these DDR genes. The common SL interactors for all three clusters were enriched for *MAPK* pathway, *ERBB* pathway, *GAP* junction, and proteasomes (**Figure 4B**). Functional enrichment analysis exclusive to the three DDR clusters (**Figures 4C–E**) showed that, cluster 1 is associated with *NGF* signaling, *ERBB* signaling, integrin pathway, retinoic acid pathway, Fc gamma mediated phagocytosis; cluster 2 is found to be enriched with cell cycle and immune system associated pathways were enriched, and cluster 3 had mostly immune response related pathways.

DDR Genes Having Distinct Alteration Patterns Between Different DDR Clusters Are Potentially Synthetic Lethal

Having observed mutually exclusive mutation pattern of 40 DDR genes associated with different clusters (shown in selected cancers in **Figures 3B–E**), we wanted to see if these genes also exhibit synthetic lethality. To test this hypothesis, we

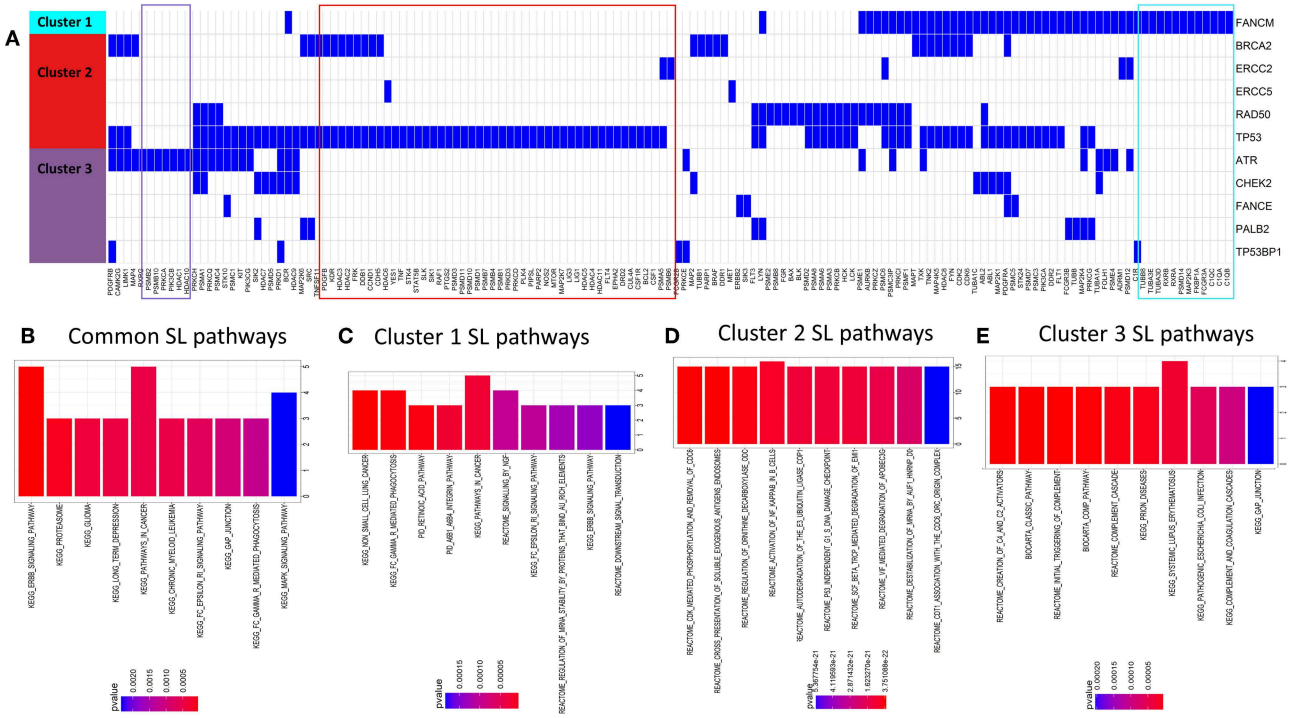

FIGURE 4 | (A) Predicted SL interactors of genes mutated in cluster 1, cluster 2, or cluster 3. Blue denotes an SL interaction and white denotes no SL interaction between the corresponding SL gene (columns) and DDR cluster (row). We can see there is some overlap and some exclusivity between SL partners for DDR genes from different DDR clusters. **(B–E)** Barcharts show pathways enriched for predicted synthetic lethal partners **(B)** common for all clusters **(C–E)**, unique for gene mutations specific to DDR clusters 1, 2 and 3, respectively.

searched for synthetic lethal interactions between DDR genes from published synthetic lethal screens in human cell lines. We identified SL interactions between multiple DDR genes that supported our postulation (**Supplementary Table 1**). Further, from the predicted SL interactions from DiscoverSL we found many potential SL relationships that fulfilled the 2 *in silico* validation criteria mentioned above (**Supplementary Table 1**). A representation of 3 SL pairs one from each cluster, that passed our rigorous filter criteria were shown in **Figure 5**. The filtered SL pairs are validated *in-silico* at shRNA level (**Figure 5A**), and by Kaplan Meier analysis showing the clinical relevance of the same pairs as disease-free survival when ± mutation in one gene had a significant association of over (>median) or under (<median) expression of SL partner gene (**Figure 5B**). As shown from the figure, *PARP1* (cluster 1) was found to have conditional essentiality with cell lines having mutation in *CHEK2* (cluster 3) and a survival advantage of down regulation of *PARP1* in prostate cancer patients when *CHEK2* was mutated. Similarly, *TP53BP1* (cluster 3) has conditional essentiality in cell lines having mutation in *TP53* (cluster 2) with survival advantage in lung cancer patients, and *POLD1* (cluster 3) has conditional essentiality in cell lines having mutation in *BRCA2* (cluster 1) and survival advantage shown in skin cancer patients. A complete list of SL interactions (previously reported or novel prediction) is shown in **Supplementary Table 1**.

Analysis of Drug Sensitivity Associated With Mutations in DDR Genes From Different Clusters

To find potential drugs for targeting the SL interactors of DDR genes from different clusters, we combined the drug-target information from the databases DrugBank (21) and DGIdb (22), and the drug sensitivity data in cell lines from GDSC portal (23). We limited our drug search to only the drugs approved by FDA for treating cancers, as per the National Cancer Institute resource (https://www.cancer.gov/about-cancer/treatment/drugs). For the drugs targeting SL interactors of the DDR genes from each cluster, we calculated the relative drug sensitivity in presence of mutations in the primary gene. **Figure 6A** shows the drugs targeting potential SL interactors for the mutations in the primary DDR genes from different clusters. Drugs showing significantly increased sensitivity for specific DDR gene mutations highlighted with green ($p < 0.1$, one-sided t-test). Combining the drug sensitivity results with the information on the potential SL interactions from literature and computer predictions, we generated a network of the DDR gene alterations, SL interactions and drugs (**Figure 6B**). The SL interactions are restricted to only those showing significant clinical benefit from the disease-free survival analysis (described in the previous section). The drug Gefitinib (targeting *EGFR* signaling) was only seen to have sensitivity for the gene *FANCE* from DDR

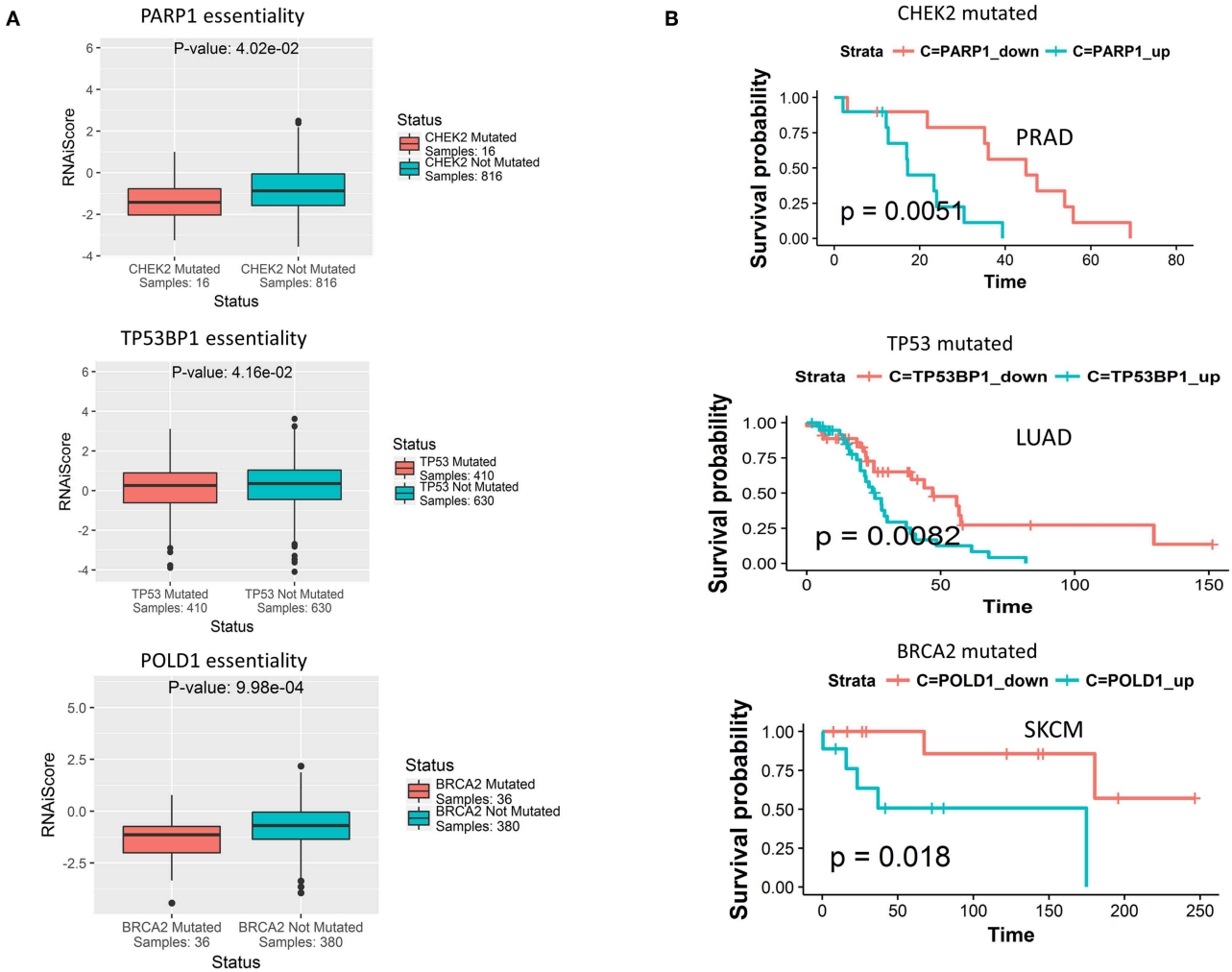

FIGURE 5 | (A) Predicted synthetic lethal partners for gene mutations specific to each DDR cluster, that have conditional essentiality in presence of the corresponding gene mutations as observed from cancer cell line RNAi screening data from Achilles portal. The term RNAiScore in y-axis is used to represent the essentiality score of genes in shRNA screenings processed by ATARiS algorithm, as collected from the Achilles project v 2.4.3 (described in the data collection section in Methods). The more negative RNAiScore, the more essential the corresponding gene. **(B)** From TCGA genomic and clinical data, certain predicted synthetic lethal genes of the primary genes from each of the three DDR cluster show survival advantage in terms of increased disease-free survival when down-regulated compared to when up-regulated (down<median, up>median) in certain cancer types in presence of somatic mutations in that DDR gene.

cluster 3 (**Figure 6C**). The drug Bleomycin (targeting DNA replication, **Figure 6D**) showed sensitivity to only TP53 mutation. The drugs Olaparib (*PARP*-inhibitor, **Figure 6E**), Nilotinib (targeting *ABL* signaling, **Figure 6F**), Lenalidomide targeting protein stability, and Alectinib targeting *RTK* signaling was only seen to have sensitivity for genes from DDR cluster 2 (*BRCA2, TP53,* or *ERCC5*). The drugs Vorinostat, Trametinib, Idelalisib, Docetaxel, Bortezomib, Dasatinib, and Midostaurin, targeting histone acetylation, *PI3K/MTOR* signaling, *ERK/MAPK* signaling, mitosis, proteasome and kinases, respectively, showed sensitivity for DDR genes from all three clusters (**Figures 6A,F**).

DISCUSSION

DNA damage response alterations are vital to the transformed cells to evade senescence. But at the same time, these alterations which are common in cancers are also supposed as "Achilles heel" of the cancer that makes them vulnerable to certain cytotoxic or targeted therapies (30). In order to get an understanding of potential targets specific to different DDR alterations, we performed an analysis of multi-cancer study on the patterns of alteration in 10 DDR pathways across 7,272 tumors from 17 tumor histology in TCGA. We identified distinct sample clusters based on defect in DDR mechanism rather than by

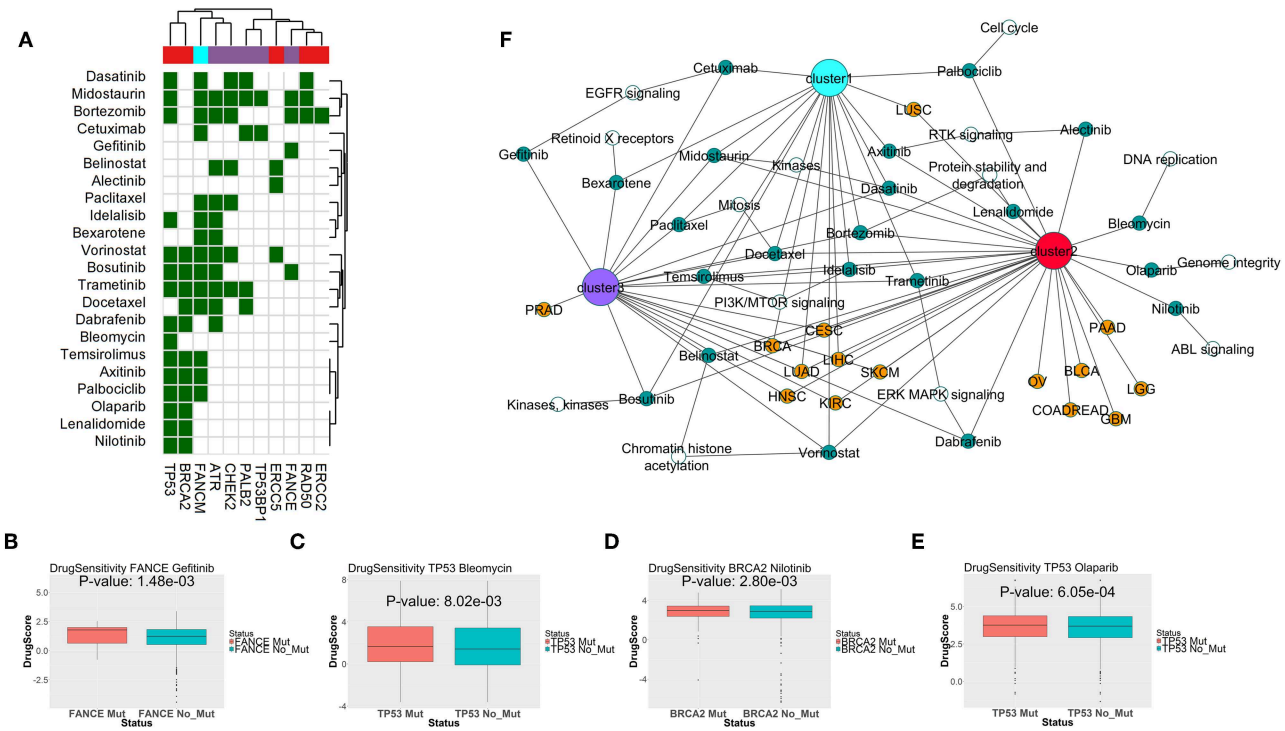

FIGURE 6 | (A) Drugs targeting predicted synthetic lethal partners for gene mutations specific to each DDR cluster, that have conditional sensitivity in presence of the corresponding gene mutations as observed from cancer cell line drug screening data from GDSC portal. In the matrix, color coding of each cell denotes whether the corresponding drug (in y-axis) is sensitive to mutations in the corresponding DDR gene (in x-axis). The column color labels annotate the DDR clusters where mutations in the corresponding DDR gene is prevalent. **(B–E)** Sensitivities of Gefitinib in presence of FANCE mutation, Bleomycin in presence of TP53 mutation, Nilotinib in presence of BRCA2 mutation, and Olaparib in presence of TP53 mutation; as seen from cancer cell lines in GDSC portal. The DrugScore in the y-axis represents LN IC50 values of the drugs in the cell lines with/without mutation in the corresponding DDR genes. **(F)** Association network of predicted synthetic lethal genes of gene mutations specific to each DDR cluster across TCGA tumor types, and potential drugs targeting the synthetic lethal genes which are also sensitive to mutations in the primary DDR gene. The following color coding is applied; tumor types: red, DDR gene mutations specific to DDR cluster 1: cyan, DDR gene mutations specific to DDR cluster 2: pink, DDR gene mutations specific to DDR cluster 3: purple, synthetic lethal genes: white and drugs: green.

histology. This pattern of exclusive enrichment of certain DDR pathways and depletion of others is expected as tumors with defects in certain DDR pathways tend to rely on the residual DDR pathways to evade apoptosis resulting from genotoxic stress (7). Cancer type-specific distribution of the number of tumor samples belonging to these three clusters showed that all cancer types had a higher fraction belonging to defects in double strand break repair pathways, such as homologous recombination, which is consistent with the observations from a previous pan-cancer study (6).

Notably, looking at the underlying genomic signatures of the DDR clusters, we found that the somatic mutation patterns of genes from different clusters showed a clear mutually exclusive signature in all cancers (see **Figure 3A**). Association of the genes representing the three clusters indicates that these genes were involved in complementary DDR pathways; cluster 1 has genetic alterations related to single strand break repair pathways like base excision and nucleotide excision repair. Cluster 2 has genetic alterations related to homologous recombination, non-homologous end joining repair, and nucleotide excision repair. Cluster 3 has genetic alterations mostly related to cell cycle checkpoints. In support of our findings, a considerable crosstalk among the single- and double-strand lesion repair pathways and replication fork restart pathways has been reported by several studies. A functional crosstalk was shown in which overexpression of a DNA repair component in one pathway compensates for a repair defect in another, conferring therapeutic resistance (31). A signaling crosstalk between the homologous recombination and canonical non-homologous end joining pathways through *ATR*, *ATM*, and *DNA-PK* has been reported (32, 33). Finally, a direct crosstalk when specific components are shared among pathways, for example, *PARP1* functions in base excision repair and in alternative non-homologous end joining (34). These findings suggest that simultaneous alterations in these pathways will be potentially detrimental to the tumor cells. Identifying cancers that are functionally defective in specific repair pathways could benefit DNA-repair targeted therapies (35). From our findings, we showed that there are indeed potential SL relationships between genes from different clusters, and their co-inactivation can be lethal to the tumor cells (as seen in **Figure 5**, from RNAi screening data, e.g., *CHEK2* and *PARP1*, *TP53* and *TP53BP1*, *BRCA2* and *POLD1*).

As many of the SL interactions found from the essentiality screens do not translate into clinically beneficial targets, we also checked from TCGA clinical data, whether co-inactivation of the potential SL candidates show a significant increase in disease-free survival time. Among the potential SL interactors from different clusters, *BRCA2* (cluster 2) and *PARP1* (cluster 1) have been reported in literature as SL partners (26). Additionally, we found potential SL relationships between *TP53* (cluster 2) and *TP53BP1* (cluster 3), and *CHEK2* (cluster 3) with *PARP1* (cluster 1) that has not been reported previously but show clinical benefits upon co-inactivation in lung adenocarcinoma (LUAD) and prostate adenocarcinoma (PRAD), respectively. We observed that co-inactivation of potential SL partners does not always show significant clinical benefit (in increased survival time) in all tumor types. The varying sensitivity to co-inactivation of same SL partners in different tumor types may be linked to the underlying heterogeneity of different tumor histology.

Given the importance of DDR pathways in cancer, we hypothesize the occurrence of common SL mechanisms between cancer types. We identified SL genes common to all clusters, that are associated with *MAPK*, *ERBB*, proteasome pathways. From the drug sensitivity data, the cancer drugs targeting kinases (Dasatinib, Bosutinib, Axitinib, Alectinib), *PI3K/MTOR* pathway (Idelalisib, Temsirolimus), *MEK* pathway (Trametinib, Dabrafenib), *EGFR* signaling (Cetuximab, Gefitinib), proteasome (Bortezomib), *HDAC*s (Vorinostat, Belinostat), cell cycle (Paclitaxel, Docetaxel, Palbociclib), Retinoid receptors (Bexarotene) were found to be sensitive to mutations in genes from multiple DDR clusters. The importance of the receptor tyrosine kinase signaling (*EGFR/MEK/ERK/PI3K*) in regulation of DDR pathways and mediating radiation or chemo resistance is well-known, and many ongoing clinical trials are investigating the potential of combination therapies involving DDR inhibitors and tyrosine kinase inhibitors in cancers [reviewed by (36)]. Also, there is evidence of *HDAC* inhibitors triggering DNA damage in cancer cells which further attenuates by DNA-damaging chemotherapy or radiation (37). So, inactivation of DDR proteins may sensitize cancer cells to *HDAC* inhibitors, as we see from our analysis. There are reports connecting proteasomes to DDR pathways and proteasome inhibitors are shown to enhance sensitization of cancer cells to DNA damaging agents (38). Consistently, our analysis indicates that co-inactivation of DDR genes combined with proteasome inhibitors may be lethal to cancer cells.

Among the SL interactor pathways exclusive to DDR cluster 1, there were pathways associated with efficient DNA double strand break repair, e.g., integrin, *ERBB* pathways. It has been previously shown that activated *ERBB* pathway can trigger DNA double strand break repair (39) and disabling the *ERBB* pathway resulted in genotoxic cell death induced by radiation (40). Similarly, it has been shown that beta integrins can positively regulate components of homologous recombination repair of DNA double strand breaks, facilitating resistance to radiation-induced cell death (41). Thus, co-inactivation of single strand break repair (which is predominantly associated with DDR cluster 1) with *ERBB* or integrin pathway can be lethal to cancer cells. This observation is further supported by our drug sensitivity analysis, as we observed sensitivity of *EGFR* signaling inhibitor drug cetuximab to be sensitive to alterations in cluster 1 (**Figure 6F**).

The SL interaction of cluster 2 with cell cycle related pathways was also expected from our analysis, as the gene alterations specific to cluster 3 were mostly associated with cell cycle checkpoints. Consistently, from the drug sensitivity analysis, we found sensitivity of the drug Palbociclib (targets cell cycle) in presence of alterations in cluster 2. Besides them, some drugs were only sensitive to mutations in cluster 2 which was mostly associated with double strand break repair; e.g., Olaparib (*PARP* inhibitor), Nilotinib (*ABL* inhibitor), and Bleomycin (DNA ligase inhibitor). *PARP* inhibitor drugs are the first ever FDA-approved therapies for treating tumors deficient in homologous recombination repair (42). In case of Bleomycin, we found literature reports supporting the sensitivity to Bleomycin by impairing *p53* function in transgenic mice (43).

Interestingly, the SL interactors of gene alterations specific to cluster 3 were mostly enriched for immune system mediated cell killing, e.g., complement cascade associated with innate immunity. As stated earlier, the DDR cluster 3 was mostly associated with alterations in cell cycle checkpoint genes, e.g., *CHEK2*, *ATR*, *PRKDC*. It was reported that inhibition of cell cycle components (*CDK4/6*) can trigger anti-tumor immune response (44). Also, DDR signaling is involved in innate immune response, and currently DDR inhibitors (*ATR* or *PARP1* inhibitors) combined with immune checkpoint inhibitors are undergoing clinical trials (45–47).

In summary, DNA and DNA damage response proteins have incredible potential as next generation therapeutic targets for the treatment of multiple cancers. While long term effects of DDR inhibition have yet to be understood in patients, and the potential for the emergence of secondary cancers exists, there is significant evidence at both the preclinical and early clinical stage that this specific targeting strategy will be the next breakthrough in cancer therapy. Our systematic analysis of multi-cancer SL targets and drug sensitivity revealed many potential drug targets for treating cancers deficient in DNA damage response in addition to *PARP* inhibitors and established a framework to explore and prioritize the potential targeted therapies for certain DDR alterations in cancer.

DATA AVAILABILITY STATEMENT

The datasets generated for this study can be found in the http://cancergenome.nih.gov/abouttcga/overview/howitworks/datasharingmanagement.

AUTHOR CONTRIBUTIONS

SD and US conceived and designed the study. SD developed the computational algorithms and implementations under the supervision of KC and US. Result interpretations done by SD, US, and KC.

FUNDING

This research was supported by the Intramural Research Program of the National Institutes of Health, National Cancer Institute.

SUPPLEMENTARY MATERIAL

The Supplementary Material for this article can be found online at: https://www.frontiersin.org/articles/10.3389/fonc.2019.01136/full#supplementary-material

Supplementary Figure 1 | Mutually exclusive mutations of DDR genes representing three different DDR clusters (from **Figure 3A**) is shown for 15 tumor types.

Supplementary Table 1 | This table contains a filtered list of the literature reported and predicted synthetic lethal interactions of DDR genes from 3 clusters in TCGA tumor types. The synthetic lethal interactions presented in this table has the following filters: (1) the primary gene (Gene1) has mutation in at-least 5 tumor samples from the corresponding TCGA tumor type (2) the primary gene (Gene1) and the synthetic lethal gene (Gene2) has significant conditional essentiality from the Achilles shRNA screening data ($p < 0.1$) (3) there is significant difference in survival between patients having high or low expression of the synthetic lethal gene (Gene2) in presence of mutation in Gene1 ($p < 0.1$) (4) there is significant difference in drug sensitivity for drugs targeting Gene2 in cell lines with or without mutation in Gene1 ($p < 0.1$).

REFERENCES

1. d'Adda di Fagagna F, Reaper PM, Clay-Farrace L, Fiegler H, Carr P, Von Zglinicki T, et al. A DNA damage checkpoint response in telomere-initiated senescence. *Nature.* (2003) 426:194–8. doi: 10.1038/nature02118
2. Jackson SP, Bartek J. The DNA-damage response in human biology and disease. *Nature.* (2009) 461:1071–8. doi: 10.1038/nature08467
3. Negrini S, Gorgoulis VG, Halazonetis TD. Genomic instability–an evolving hallmark of cancer. *Nat Rev Mol Cell Biol.* (2010) 11:220–8. doi: 10.1038/nrm2858
4. Goldstein M, Kastan MB. The DNA damage response: implications for tumor responses to radiation and chemotherapy. *Annu Rev Med.* (2015) 66:129–43. doi: 10.1146/annurev-med-081313-121208
5. Hoeijmakers JH. Genome maintenance mechanisms for preventing cancer. *Nature.* (2001) 411:366–74. doi: 10.1038/35077232
6. Knijnenburg TA, Wang L, Zimmermann MT, Chambwe N, Gao GF, Cherniack AD, et al. Genomic and molecular landscape of DNA damage repair deficiency across the cancer genome atlas. *Cell Rep.* (2018) 23:239–54.e6. doi: 10.1016/j.celrep.2018.03.076
7. Dietlein F, Thelen L, Reinhardt HC. Cancer-specific defects in DNA repair pathways as targets for personalized therapeutic approaches. *Trends Genet.* (2014) 30:326–39. doi: 10.1016/j.tig.2014.06.003
8. Lord CJ, Ashworth A. PARP inhibitors: synthetic lethality in the clinic. *Science.* (2017) 355:1152–8. doi: 10.1126/science.aam7344
9. Luo J, Emanuele MJ, Li D, Creighton CJ, Schlabach MR, Westbrook TF, et al. A genome-wide RNAi screen identifies multiple synthetic lethal interactions with the Ras oncogene. *Cell.* (2009) 137:835–48. doi: 10.1016/j.cell.2009.05.006
10. Turner NC, Lord CJ, Iorns E, Brough R, Swift S, Elliott R, et al. A synthetic lethal siRNA screen identifying genes mediating sensitivity to a PARP inhibitor. *EMBO J.* (2008) 27:1368–77. doi: 10.1038/emboj.2008.61
11. Jerby-Arnon L, Pfetzer N, Waldman YY, McGarry L, James D, Shanks E, et al. Predicting cancer-specific vulnerability via data-driven detection of synthetic lethality. *Cell.* (2014) 158:1199–209. doi: 10.1016/j.cell.2014.07.027
12. Lu X, Megchelenbrink W, Notebaart RA, Huynen MA. Predicting human genetic interactions from cancer genome evolution. *PLoS ONE.* (2015) 10:e0125795. doi: 10.1371/journal.pone.0125795
13. Das S, Deng X, Camphausen K, Shankavaram U. DiscoverSL: an R package for multi-omic data driven prediction of synthetic lethality in cancers. *Bioinformatics.* (2019) 35:701–2. doi: 10.1093/bioinformatics/bty673
14. Lee JS, Das A, Jerby-Arnon L, Arafeh R, Auslander N, Davidson M, et al. Harnessing synthetic lethality to predict the response to cancer treatment. *Nat Commun.* (2018) 9:2546. doi: 10.1038/s41467-018-04647-1
15. Cancer Genome Atlas Research, Weinstein JN, Collisson EA, Mills GB, Shaw RMK, Ozenberger BA, et al. The Cancer Genome Atlas Pan-Cancer analysis project. *Nat Genet.* (2013) 45:1113–20. doi: 10.1038/ng.2764
16. Cerami E, Gao J, Dogrusoz U, Gross BE, Sumer SO, Aksoy BA, et al. The cBio cancer genomics portal: an open platform for exploring multidimensional cancer genomics data. *Cancer Discov.* (2012) 2:401–4. doi: 10.1158/2159-8290.CD-12-0095
17. Rahman M, Jackson LK, Johnson WE, Li DY, Bild AH, Piccolo SR. Alternative preprocessing of RNA-Sequencing data in The Cancer Genome Atlas leads to improved analysis results. *Bioinformatics.* (2015) 31:3666–72. doi: 10.1093/bioinformatics/btv377
18. Liberzon A, Subramanian A, Pinchback R, Thorvaldsdottir H, Tamayo P, Mesirov JP. Molecular signatures database (MSigDB) 3.0. *Bioinformatics.* (2011) 27:1739–40. doi: 10.1093/bioinformatics/btr260
19. Cowley GS, Weir BA, Vazquez F, Tamayo P, Scott JA, Rusin S, et al. Parallel genome-scale loss of function screens in 216 cancer cell lines for the identification of context-specific genetic dependencies. *Sci Data.* (2014) 1:140035. doi: 10.1038/sdata.2014.35
20. Barretina J, Caponigro G, Stransky N, Venkatesan K, Margolin AA, Kim S, et al. The Cancer Cell Line Encyclopedia enables predictive modelling of anticancer drug sensitivity. *Nature.* (2012) 483:603–7. doi: 10.1038/nature11003
21. Wishart DS, Feunang YD, Guo AC, Lo EJ, Marcu A, Grant JR, et al. DrugBank 5.0: a major update to the DrugBank database for 2018. *Nucleic Acids Res.* (2018) 46:D1074–82. doi: 10.1093/nar/gkx1037
22. Cotto KC, Wagner AH, Feng YY, Kiwala S, Coffman AC, Spies G, et al. DGIdb 3.0: a redesign and expansion of the drug-gene interaction database. *Nucleic Acids Res.* (2018) 46:D1068–73. doi: 10.1093/nar/gkx1143
23. Yang W, Soares J, Greninger P, Edelman EJ, Lightfoot H, Forbes S, et al. Genomics of Drug Sensitivity in Cancer (GDSC): a resource for therapeutic biomarker discovery in cancer cells. *Nucleic Acids Res.* (2013) 41:D955–61. doi: 10.1093/nar/gks1111
24. Hanzelmann S, Castelo R, Guinney J. GSVA: gene set variation analysis for microarray and RNA-seq data. *BMC Bioinformatics.* (2013) 14:7. doi: 10.1186/1471-2105-14-7
25. Guo J, Liu H, Zheng J. SynLethDB: synthetic lethality database toward discovery of selective and sensitive anticancer drug targets. *Nucleic Acids Res.* (2016) 44:D1011–7. doi: 10.1093/nar/gkv1108
26. Benjamini Y, Hochberg Y. Controlling the false discovery rate: a practical and powerful approach to multiple testing. *J R Stat Soc.* (1995) 57:289–300. doi: 10.1111/j.2517-6161.1995.tb02031.x
27. Peng M, Xie J, Ucher A, Stavnezer J, Cantor SB. Crosstalk between BRCA-Fanconi anemia and mismatch repair pathways prevents MSH2-dependent aberrant DNA damage responses. *Embo J.* (2014) 33:1698–712. doi: 10.15252/embj.201387530
28. Moynahan ME, Jasin M. Mitotic homologous recombination maintains genomic stability and suppresses tumorigenesis. *Nat Rev Mol Cell Biol.* (2010) 11:196–207. doi: 10.1038/nrm2851
29. Linke SP, Sengupta S, Khabie N, Jeffries BA, Buchhop S, Miska S, et al. p53 interacts with hRAD51 and hRAD54, and directly modulates homologous recombination. *Cancer Res.* (2003) 63:2596–605.
30. O'Connor MJ. Targeting the DNA Damage Response in Cancer. *Mol Cell.* (2015) 60:547–60. doi: 10.1016/j.molcel.2015.10.040

31. Kelley MR, Logsdon D, Fishel ML. Targeting DNA repair pathways for cancer treatment: what's new? *Future Oncol.* (2014) 10:1215–37. doi: 10.2217/fon.14.60
32. Ashley AK, Shrivastav M, Nie J, Amerin C, Troksa K, Glanzer JG, et al. DNA-PK phosphorylation of RPA32 Ser4/Ser8 regulates replication stress checkpoint activation, fork restart, homologous recombination and mitotic catastrophe. *DNA Repair.* (2014) 21:131–9. doi: 10.1016/j.dnarep.2014.04.008
33. Liu S, Opiyo SO, Manthey K, Glanzer JG, Ashley AK, Amerin C, et al. Distinct roles for DNA-PK, ATM and ATR in RPA phosphorylation and checkpoint activation in response to replication stress. *Nucleic Acids Res.* (2012) 40:10780–94. doi: 10.1093/nar/gks849
34. Wang M, Wu W, Wu W, Rosidi B, Zhang L, Wang H, et al. PARP-1 and Ku compete for repair of DNA double strand breaks by distinct NHEJ pathways. *Nucleic Acids Res.* (2006) 34:6170–82. doi: 10.1093/nar/gkl840
35. Mirza MR, Monk BJ, Herrstedt J, Oza AM, Mahner S, Redondo A, et al. Niraparib maintenance therapy in platinum-sensitive, recurrent ovarian cancer. *N Engl J Med.* (2016) 375:2154–64. doi: 10.1056/NEJMoa1611310
36. Mahajan K, Mahajan NP. Cross talk of tyrosine kinases with the DNA damage signaling pathways. *Nucleic Acids Res.* (2015) 43:10588–601. doi: 10.1093/nar/gkv1166
37. Robert C, Rassool FV. HDAC inhibitors: roles of DNA damage and repair. *Adv Cancer Res.* (2012) 116:87–129. doi: 10.1016/B978-0-12-394387-3.00003-3
38. Jacquemont C, Taniguchi T. Proteasome function is required for DNA damage response and fanconi anemia pathway activation. *Cancer Res.* (2007) 67:7395–405. doi: 10.1158/0008-5472.CAN-07-1015
39. Mukherjee B, McEllin B, Camacho CV, Tomimatsu N, Sirasanagandala S, Nannepaga S, et al. EGFRvIII and DNA double-strand break repair: a molecular mechanism for radioresistance in glioblastoma. *Cancer Res.* (2009) 69:4252–9. doi: 10.1158/0008-5472.CAN-08-4853
40. O'Rourke DM, Kao GD, Singh N, Park BW, Muschel RJ, Wu CJ, et al. Conversion of a radioresistant phenotype to a more sensitive one by disabling erbB receptor signaling in human cancer cells. *Proc Natl Acad Sci USA.* (1998) 95:10842–7. doi: 10.1073/pnas.95.18.10842
41. Ahmed KM, Pandita RK, Singh DK, Hunt CR, Pandita TK. beta1-integrin impacts Rad51 Stability and DNA double-strand break repair by homologous recombination. *Mol Cell Biol.* (2018) 38:e00672–17. doi: 10.1128/MCB.00672-17
42. Farmer H, McCabe N, Lord CJ, Tutt NJA, Johnson DA, Richardson TB, et al. Targeting the DNA repair defect in BRCA mutant cells as a therapeutic strategy. *Nature.* (2005) 434:917–21. doi: 10.1038/nature 03445
43. Ghosh S, Mendoza T, Ortiz LA, Hoyle GW, Fermin CD, Brody AR, et al. Bleomycin sensitivity of mice expressing dominant-negative p53 in the lung epithelium. *Am J Respir Crit Care Med.* (2002) 166:890–7. doi: 10.1164/rccm.2109094
44. Chaikovsky AC, Sage J. Beyond the cell cycle: enhancing the immune surveillance of tumors via CDK4/6 inhibition. *Mol Cancer Res.* (2018) 16:1454–7. doi: 10.1158/1541-7786.MCR-18-0201
45. Higuchi T, Flies DB, Marjon NA, Mantia-Smaldone G, Ronner L, Gimotty PA, et al. CTLA-4 blockade synergizes therapeutically with PARP inhibition in BRCA1-deficient ovarian cancer. *Cancer Immunol Res.* (2015) 3:1257–68. doi: 10.1158/2326-6066.CIR-15-0044
46. Sato H, Niimi A, Yasuhara T, Permata BMT, Hagiwara Y, Isono M, et al. DNA double-strand break repair pathway regulates PD-L1 expression in cancer cells. *Nat Commun.* (2017) 8:1751. doi: 10.1038/s41467-017-01883-9
47. Le DT, Uram JN, Wang H, Bartlett BR, Kemberling H, Eyring AD, et al. PD-1 blockade in tumors with mismatch-repair deficiency. *N Engl J Med.* (2015) 372:2509–20. doi: 10.1056/NEJMoa1500596

Conflict of Interest: The authors declare that the research was conducted in the absence of any commercial or financial relationships that could be construed as a potential conflict of interest.

frontiers in Oncology

MINI REVIEW
published: 10 December 2019
doi: 10.3389/fonc.2019.01388

Harnessing DNA Double-Strand Break Repair for Cancer Treatment

*Anika Trenner and Alessandro A. Sartori**

Institute of Molecular Cancer Research, University of Zurich, Zurich, Switzerland

DNA double-strand breaks (DSBs) are highly deleterious, with a single unrepaired DSB being sufficient to trigger cell death. Compared to healthy cells, cancer cells have a higher DSB burden due to oncogene-induced replication stress and acquired defects in DNA damage response (DDR) mechanisms. Consequently, hyperproliferating cancer cells rely on efficient DSB repair for their survival. Moreover, augmented DSB repair capacity is a major cause of radio- and chemoresistance and, ultimately, cancer recurrence. Although inherited DDR defects can predispose individuals to develop certain cancers, the very same vulnerability may be therapeutically exploited to preferentially kill tumor cells. A paradigm for DNA repair targeted therapy has emerged in cancers that exhibit mutations in *BRCA1* or *BRCA2* tumor suppressor genes, conferring a strong defect in homologous recombination, a major and error-free DSB repair pathway. Clinical validation of such approaches, commonly described as synthetic lethality (SL), has been provided by the regulatory approval of poly(ADP-ribose) polymerase 1 inhibitors (PARPi) as monotherapy for *BRCA1/2*-mutated breast and ovarian tumors. In this review, we will describe the different DSB repair mechanisms and discuss how their specific features could be exploited for cancer therapy. A major emphasis is put on advances in combinatorial treatment modalities and SL approaches arising from DSB repair pathway interdependencies.

Keywords: DSB repair, homologous recombination (HR), BRCA, alternative end joining (a-EJ), PARP inhibition (PARPi), DNA polymerase theta, synthetic lethality, cancer therapy

OPEN ACCESS

Edited by:
Yitzhak Zimmer,
University Hospital Bern, Switzerland

Reviewed by:
Souparno Bhattacharya,
AstraZeneca, United States
Shao-Chun Wang,
China Medical University, Taiwan

***Correspondence:**
Alessandro A. Sartori
sartori@imcr.uzh.ch

Specialty section:
This article was submitted to Molecular and Cellular Oncology, a section of the journal Frontiers in Oncology

Received: *27 September 2019*
Accepted: *25 November 2019*
Published: *10 December 2019*

Citation:
Trenner A and Sartori AA (2019) Harnessing DNA Double-Strand Break Repair for Cancer Treatment. Front. Oncol. 9:1388. doi: 10.3389/fonc.2019.01388

INTRODUCTION

The integrity of our genome is constantly challenged by endogenous and exogenous insults that can induce DNA damage. To counteract genotoxic threats, cells are equipped with a diverse set of DNA damage signaling and repair mechanisms, collectively known as the DNA damage response (DDR) (1). During tumorigenesis, however, precancerous cells frequently acquire loss-of-function alterations in DDR genes, including core components of selected DNA repair pathways, to accelerate mutagenesis and become malignant (2). While healthy cells have to deal with a minor amount of damage and take advantage of the full DNA repair capacity, malignant cells are frequently equipped with reduced DNA repair functionality to cope with increased replication stress and elevated levels of endogenous DNA damage (3). Consequently, cancer cells become even more dependent on DNA repair mechanisms to survive and proliferate. Conventional treatment modalities such as radiation therapy and certain forms of chemotherapy have been built on the premise to force DNA damage-induced cell death. In summary, cancer cells are often compromised in their ability to adequately process DNA damage, which exerts selective pressure to sustain DNA repair through upregulation of mutagenic pathways, ultimately promoting disease progression and therapy resistance (4, 5).

DNA double-strand breaks (DSBs) are considered the most lethal of all DNA lesions, eliciting the majority of the cytotoxic effects induced by ionizing radiation (IR) and certain anti-cancer drugs. Therefore, DSB repair represents a potent and targetable vulnerability in cancer cells. In healthy somatic cells two-ended DSBs are mainly repaired by two pathways: classical non-homologous end joining (c-NHEJ) and homologous recombination (HR) (**Figure 1**). Auxiliary mechanisms of DSB repair include single-strand annealing (SSA) and alternative end joining (a-EJ) that rely on the presence of larger repeat sequences and microhomologies at the breakpoint, respectively [(6, 7); **Figure 1**]. Importantly, functional interdependencies between different DNA repair pathways and within compensatory DSB repair mechanisms offer therapeutic opportunities to selectively treat DDR-deficient tumors based on the concept of synthetic lethality (SL) (3, 5, 8, 9).

DSB REPAIR PATHWAYS

The decision as to whether a given DSB is processed by c-NHEJ, HR, or alternative repair pathways is determined by several factors, including genetic and genomic background, DSB complexity, chromatin state, and cell cycle phase. For instance, c-NHEJ operates throughout the cell cycle, whereas HR relies on the presence of an undamaged sister chromatid and is therefore restricted to late S/G2 (7, 10). Therefore, HR activation requires high cyclin-dependent kinase (CDK) activity (11). In addition, numerous HR genes are found upregulated in S/G2 phase of the cell cycle (7). At the chromatin level, the appropriate equilibrium between HR and c-NHEJ is mainly established by BRCA1 and 53BP1, large DDR adaptor proteins that are enriched at DSB sites (12, 13). Whereas, 53BP1 mediates c-NHEJ events and is pivotal in repairing programmed DSBs (e.g., during class-switch recombination), BRCA1 antagonizes 53BP1 to promote DSB resection and HR [(14, 15); **Figure 1**]. Importantly, one-ended DSBs, predominantly induced by fork breakage or collapse due to high replication stress, lack an adjacent second DNA end for rejoining and can only be repaired by HR-related mechanisms (7).

C-NHEJ

C-NHEJ is accountable for the repair of most two-ended DSBs in mammalian cells (**Figure 1**). Rapid and high-affinity binding of the Ku70-Ku80 heterodimer (Ku) to DNA ends is followed by the recruitment of DNA-dependent protein kinase catalytic subunit (DNA-PKcs), forming the active DNA-PK holoenzyme. Key functions of DNA-PK in c-NHEJ are (i) promoting synapsis of the broken ends, (ii) coordinating necessary processing of incompatible ends by DNA nucleases (e.g., Artemis) and polymerases, and (iii) engaging the DNA ligase complex composed of DNA ligase IV, XRCC4, XLF, and PAXX (7, 16). Despite rejoining DSBs without the use of extensive sequence homology, c-NHEJ is often highly accurate and its core factors therefore considered as genome "caretakers" (10, 17, 18).

HR

In case c-NHEJ fails or is inappropriate, DSBs are subjected to extensive 5′-end resection, generating 3′-single-stranded (ss) DNA overhangs that interfere with Ku loading and promote high-fidelity repair by HR [(7, 19); **Figure 1**]. In a first step, the MRE11-RAD50-NBS1 (MRN) complex in conjunction with CtIP, also known as RBBP8, coordinates tethering and short-range nucleolytic degradation of DSB ends (20, 21). MRE11 exhibits a dual endo- and exonuclease activity that is critical for DNA end resection (22). Following long-range resection carried out by EXO1 or the BLM-DNA2 ensemble, the 3′ ssDNA tails are coated by the RPA heterotrimer. In the central step of HR, BRCA2 with the help of BRCA1 and PALB2 delivers RAD51 monomers to ssDNA, resulting in RPA removal and RAD51 presynaptic filament formation required for strand invasion and homology search. Interestingly, in G1 phase, BRCA1-PALB2-BRCA2-RAD51 complex formation is impaired by proteasome-mediated degradation of PALB2 (7). Mechanistically, PALB2-interacting protein KEAP1 in complex with cullin-3-RBX1 ubiquitylate PALB2, thereby suppressing PALB2-BRCA1 (23). HR in somatic cells is mostly completed by synthesis-dependent strand annealing (SDSA), generating non-crossovers, although other outcomes are possible (24).

Alternative DSB Repair Pathways

A-EJ is genetically distinct from Ku-dependent c-NHEJ and RAD51-dependent HR and requires the presence of microhomology (MH) regions (2–20 bp), which are exposed following MRN-CtIP-mediated resection [(25, 26); **Figure 1**]. Importantly, long-range resection impedes a-EJ and favors HR or SSA (27, 28). DNA polymerase theta (Polθ), a low-fidelity DNA polymerase-helicase, has been recently identified as key factor driving a-EJ by limiting RAD51 nucleation onto ssDNA (29–31). The Polθ-helicase domain displaces RPA from ssDNA tails, whereas the Polθ-polymerase domain promotes their synapsis, thereby facilitating MH-mediated annealing and subsequent gap filling (32, 33). The essential ligation step during a-EJ is performed by the DNA ligase IIIα-XRCC1 complex (26). Contrary to a-EJ, SSA requires more extensive DNA end resection followed by RAD52-mediated annealing of homologous tandem repeat sequences (>20 bp) [(34); **Figure 1**]. Whether a-EJ and SSA serve primarily as backup pathways in mammalian cells deficient in either c-NHEJ or HR, or are favored at specific genomic loci still remains to be established (35).

DSB REPAIR PROTEIN DYSFUNCTION IN CANCER

Only a minor number of human cancers are associated with downregulation or alterations of core c-NHEJ genes (36). Rare mutations in *LIG4* (encoding DNA ligase IV), *XLF*, *DCLRE1C* (encoding Artemis) or *PRKDC* (encoding DNA-PKcs) have been identified in a radiosensitive sub-class of patients with severe combined immunodeficiency (SCID) and can predispose to cancer (37, 38). As c-NHEJ is the predominant DSB repair pathway in human cells, complete loss-of-function is likely to

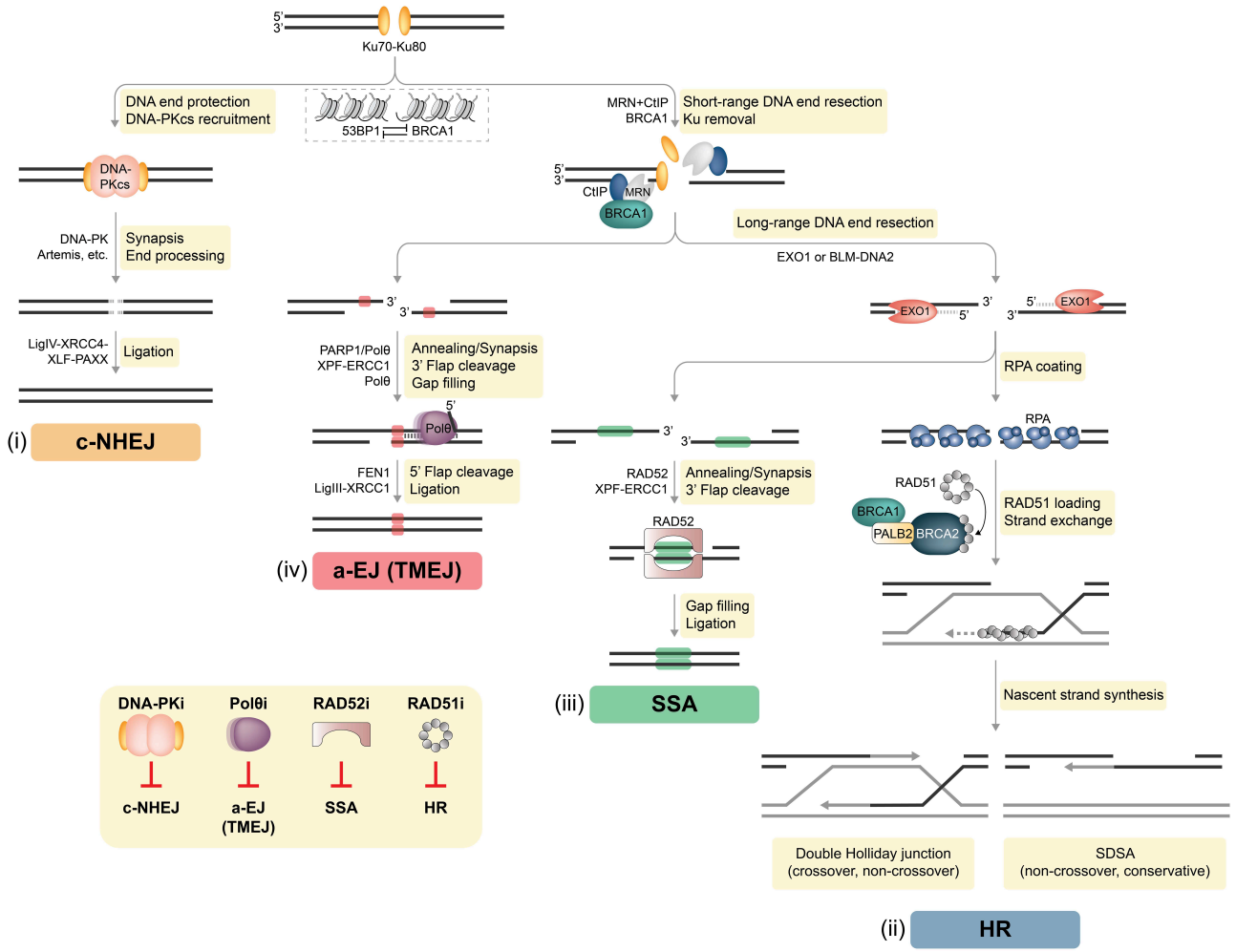

FIGURE 1 | DSB repair pathways in mammalian cells. Two-ended DSBs are preferably repaired by two major competing pathways: classical non-homologous end joining (c-NHEJ) and homologous recombination (HR). In addition, DSBs can be subjected to alternative end joining [a-EJ, also referred to as DNA polymerase theta-mediated end joining (TMEJ)] or single-strand annealing (SSA). BRCA1 and 53BP1 are placed at the center of DSB repair pathway choice. Whereas, chromatin recruitment of 53BP1 drives c-NHEJ, BRCA1 antagonizes 53BP1 to channel DSB repair into HR. **(i)** C-NHEJ begins with Ku70-Ku80 (Ku) binding to DSB ends, followed by the recruitment of DNA-dependent protein kinase catalytic subunit (DNA-PKcs), forming the DNA-PK holoenzyme implicated in DNA synapsis. If necessary, DNA-PK coordinates limited processing of incompatible or chemically modified DNA ends by nucleases (e.g., Artemis) and other enzymes. The DNA ligase IV (LigIV)-XRCC4-XLF-PAXX complex executes the final ligation step. DNA end resection interferes with the default engagement of c-NHEJ by removing Ku from DNA ends, which is a critical step for initiating HR **(ii)**. First, the MRE11-RAD50-NBS1 (MRN) complex senses the DSB and with the help of BRCA1 and CtIP promotes limited resection of the 5′ strand. Next, more extensive 5′-3′ resection by exonuclease 1 (EXO1), or by the Bloom's syndrome (BLM) helicase together with the DNA2 nuclease, generates long 3′ ssDNA overhangs that become rapidly coated with the RPA heterotrimer. The BRCA1-PALB2-BRCA2 complex disassembles RAD51 heptamers and loads monomeric RAD51 onto ssDNA, promoting RAD51 filament assembly. Template-dependent strand extension is followed by "synthesis-dependent strand annealing" (SDSA), resulting in a non-crossover gene conversion. Alternatively, capture of the second ssDNA by the D-loop forms a double Holliday junction intermediate, which can be resolved either as a non-crossover or as a crossover. **(iii)** SSA requires at least 20–25 base pairs (bp) of DNA sequence homology, which are typically found between repetitive elements (indicated as green boxes) in the genome. Subsequently, RAD52 promotes annealing of complementary ssDNA and leftover non-homologous flaps of the 3′ overhangs are cleaved by XPF-ERCC1. The factors that promote gap filling and ligation during SSA remain largely elusive. **(iv)** In contrast to SSA, a-EJ (or TMEJ) utilizes short microhomologies (MHs) of 2–20 bp (indicated as red boxes) to join the two DNA strands. PARP1 has been implicated in promoting DNA end synapsis and recruiting the specialized DNA polymerase θ (Polθ) to DSBs. Polθ stabilizes MH-mediated joints between the two DNA ends serving as primers for fill-in synthesis. 3′ flaps extending from the joints are removed by XPF/ERCC1. Flap endonuclease 1 (FEN1) has recently been implicated in the removal of 5′ flaps generated by Polθ-mediated strand displacement, while the DNA Ligase III (LigIII)-XRCC1 complex is essential for the final ligation step. *Inset, bottom left:* DSB repair pathway-specific inhibitors. Inhibition of c-NHEJ has so far been mainly achieved by targeting DNA-PK using different small molecule inhibitors. Strategies to inhibit a-EJ and SSA focus on targeting their respective DNA annealing factors Polθ and RAD52, while the primary target to disrupt HR is RAD51 (see text for more details).

drive cell death due to an unreasonably high DSB burden (36). Elevated DNA-PKcs levels were implicated in the progression of various types of tumors such as prostate cancer and melanoma (36). Noteworthy, *PRKDC* is with 2.1% the sixth most frequently mutated DNA repair gene in all cancers and considered a potential oncogene, exhibiting frequent copy number gains (39).

A comprehensive analysis of somatic DDR gene alterations delineates HR as the most frequently altered DNA repair pathway across 33 cancer types, most notably ovarian cancer (40). Mutational signatures associated with robust HR deficiency (HRD) primarily included alterations affecting *BRCA1*, *BRCA2*, two canonical RAD51 paralog genes (*RAD51B*, *RAD51C*), *BLM,* and *RAD50* (40). Large-scale molecular profiling of solid tumor samples across 21 cancer lineages detected pathogenic HR gene mutations with an overall frequency of 17.4%. Here, again, *BRCA2* (3%) and *BRCA1* (2.8%) were the most commonly mutated bona fide HR genes and predominantly seen in ovarian and breast cancers (41). Heterozygous germline mutations in *BRCA1* and *BRCA2* are responsible for the majority of hereditary breast and ovarian cancer (HBOC) syndrome patients. However, only ∼20–25% of HBOC families have *BRCA* mutations and other low-to-moderate penetrance HBOC susceptibility genes involved in HR have been identified, including *BRIP1*, *RAD51C,* and *PALB2* (42). Moreover, revisiting whole-exome sequencing datasets of non-BRCA1/2 familial breast cancer patients confirmed the existence of likely pathogenic germline variants in *MRE11A, RAD50,* and *NBN*, encoding components of the MRN complex (43, 44). Lord and Ashworth have coined the term "BRCAness" to denote HRD tumors that share molecular features of *BRCA1/2*-mutant tumors and are therefore expected to effectively respond to the same treatment modalities (45). Remarkably, however, a recent study indicated that most somatic *BRCA1/2* alterations in non-BRCA associated cancer types may be incidental findings unrelated to tumor pathogenesis, rendering them therapeutically irrelevant (46). In contrast to the situation encountered for *BRCA1/2*, no inactivating mutations of *RAD51* have been reported in tumors. Paradoxically, *RAD51* is frequently found overexpressed and has been associated with poor prognosis in patients with solid malignancies, thus potentially acting as a driver of aberrant HR (47).

Similarly, elevated MRN expression has been correlated with tumor progression and poor survival in patients with rectal and gastric carcinomas and prostate cancer (48–50). However, with the exception of a positive relationship between MRN deficiency and microsatellite instable (MSI) colorectal cancers, large scale studies will be required to substantiate its relevance in clinical settings (51). Like MRN, CtIP also has rather oncogenic potential at the cellular level, most likely by facilitating a-EJ-dependent chromosomal instability (52–54). Accordingly, mice heterozygous for a null *Ctip* allele did not display increased tumor susceptibility, meanwhile CtIP inactivation suppressed mammary tumorigenesis caused by p53 deficiency (55). Although still far from being fully characterized, a-EJ is intrinsically mutagenic, typically generating deletions at the repair junction, and suggested to be a major driving force of genomic instability in human cancers (56–58). In particular, a-EJ reliant on Polθ, also referred to as theta mediated end joining (TMEJ, see **Figure 1**), has emerged as a distinct DSB repair pathway acting predominantly in HRD tumors or on breaks incompatible with c-NHEJ and HR (59). Consistently, depletion of BRCA1/2 resulted in increased usage of TMEJ using reporter assays in human cells (25). Elevated *POLQ* (encoding for Polθ) expression has been described in numerous cancer types, including breast and ovarian cancer (29, 59–61). Overall, CtIP and Polθ may drive tumorigenesis through a-EJ in defined biological contexts and therefore represent promising therapeutic targets.

DSB REPAIR PROTEINS AS DRUG TARGETS

As outlined above, DSB repair constitutes an Achilles' heel of cancer cells and there is a continuous search for compounds specifically targeting DSB repair components to exploit this key vulnerability.

Combinatorial Treatment Regimens Involving DSB Repair Inhibitors

DNA repair targeted therapy was first considered most beneficial in combination with conventional DNA-damaging agents (62, 63). In recent years, mainly thanks to the development of PARPi, additional treatment strategies including DDR inhibitor combinations have been implemented in clinical trials (3, 64, 65). Furthermore, DDR-targeting drugs were found to enhance the effectiveness of immunotherapy by fostering increased immunogenic surveillance and restricted tumor growth (66, 67). An elevated mutation load was shown to increase neoantigen levels in cancer cells thereby promoting tumor immunogenicity (68). Here, we will mainly focus on available DSB repair pathway inhibitors and their synergistic effect in combination with standard chemo- or radiotherapy. Moreover, existing PARPi-based combination strategies will also be highlighted.

Pharmacological Targeting of c-NHEJ

Restraining c-NHEJ capacity has been primarily achieved by targeting DNA-PK (**Figure 1**). Conceptually, compounds blocking c-NHEJ are thought of as being most effective when used in combination with radiation therapy, as c-NHEJ is taking care of roughly 80% of IR-induced DSBs (69). Whereas, numerous DNA-PKcs small-molecule inhibitors (DNA-PKi) have been developed over the last 20 years, only one specific agent is known to target the Ku heterodimer (70). Weterings et al. identified a compound interfering with the binding of Ku to DNA and sensitizing human cell lines to IR (71). Similarly, the majority of DNA-PKi displayed synergistic effects with IR and chemotherapeutics including etoposide and cisplatin (72). For example, VX-984 induced radiosensitivity of glioblastoma cells grown as orthotopic xenografts (73), whereas combination of the DNA-PKi KU-0060648 with ATR inhibitor AZD6738 potentiated radiosensitization of head and neck squamous cell carcinoma cell lines (74). The most potent DNA-PKi (M3814, CC-115 and CC-122) are currently being investigated in several clinical trials (72). Of particular interest, a dose escalation phase I clinical trial combines M3814 with Avelumab (NCT03724890), a human monoclonal antibody targeting the protein programmed death-ligand 1 (PD-L1). Remarkably, CC-115, a dual inhibitor targeting DNA-PK and the structurally related mammalian target

of rapamycin kinase (TORK), was shown to induce caspase-dependent cell death in primary chronic lymphocytic leukemia (CLL) cells and to be clinically effective in CLL patients with an *ATM* mutation (75, 76). However, it remains an open question of whether DNA-PKi act solely by impairing DSB repair, as other cellular functions of DNA-PKcs have been reported, including cell cycle progression, transcription and telomere maintenance (70).

Pharmacological Targeting of HR

MRE11 harbors endo- and exonuclease activity essential for DNA end resection, thereby channeling DSBs into homology-directed repair pathways (22). A forward chemical genetic screen identified mirin as the first MRE11 inhibitor targeting its exonuclease activity and preventing ATM activation (77). In addition, structure-guided nuclease-specific MRE11 inhibitors revealed that endonuclease inhibition promotes c-NHEJ in lieu of HR, whereas exonuclease inhibition caused a more profound DSB repair defect (78, 79). CtIP's role in DSB resection has been mostly attributed to its interaction with and stimulation of MRE11, although intrinsic CtIP endonuclease activities have also been demonstrated (80–83). Intriguingly, CtIP-specific inhibitors have not been reported yet. However, inhibition of Bromodomain-containing protein 4 (BRD4) was found to induce an HRD signature by decreasing transcriptional activity of the *CtIP* promoter and enhancer (84). Reduced CtIP protein levels correlated with increased PARPi sensitivity, potentially qualifying CtIP as a predictive marker for PARPi response. Consistently, different BRD4 inhibitors (e.g., JQ1 and AZD5153) sensitized a broad range of tumor types to PARPi in multiple *in vitro* and *in vivo* models (85).

BRCA1 and BRCA2 represent challenging targets for structure-based drug discovery, as they are both large proteins made up of short, functional domains, serving as hubs for multiple protein-protein interactions, interspersed by long, intrinsically disordered linkers (86). In this regard, Pessetto et al. identified a cell permeable peptide ablating phosphoprotein binding by the BRCA1 tandem BRCT domains and enhancing PARPi sensitivity of cancer cells (87). Similarly, a BRCA2-mimetic cell-penetrating peptide disrupting BRCA2-RAD51 interaction conferred PARPi sensitivity in cancer cell lines (88). Small molecules selectively targeting BRCA1's ubiquitin ligase activity, which is mediated by the N-terminal RING domain and required for efficient DSB resection (89), might also offer a valid alternative to inhibit HR.

Chemical inhibitors of RAD51 (e.g., B02, IBR2, RI-1/2) have been reported to either interfere with RAD51 oligomerization, filament formation or DNA binding, and, ultimately, to induce HR deficiency [(78, 90–94); **Figure 1**]. Triple combination of B02, the PARPi veliparib and a p38 MAPkinase inhibitor (LY2228820) significantly reduced primary tumor growth in an orthotopic triple negative breast cancer (TNBC) mammary xenograft model (95). Similarly, cancer cell proliferation in a breast cancer xenograft model and in a chronic myelogenous leukemia model bearing the BCR-ABL^{T315I} mutation was significantly slowed upon IBR2 treatment (94). RI-1 potentiated the effect of the alkylating agent Iomustine on a glioma xenograft model, reduced growth of cervical cancer xenografts and hindered TNBC growth *in vivo* when combined with veliparib (96–98). Based on these preclinical findings, RAD51i were proposed as potential candidates for a novel class of broad-spectrum therapeutics for difficult-to-treat cancers. Interestingly, Cyteir Therapeutics is currently recruiting patients for a phase 1/2 study with CYT-0851, an oral RAD51i designed to reduce the ability of RAD51 to migrate to and from sites of excessive DNA damage (NCT03997968). In addition to direct RAD51 inhibition, inactivation of RAD51 can also be achieved by indirect mechanisms, including tyrosine kinase inhibitors (93). For example, it was recently reported that cediranib (AZD-2171), a potent inhibitor of vascular endothelial growth factor (VEGF) tyrosine kinases, constrains HR through transcriptional repression of *RAD51* and *BRCA1/2* (99). Accordingly, combination of the PARPi olaparib with cediranib showed superior progression-free and overall survival outcomes in relapsed ovarian cancer patients without documented *BRCA1/2* mutations (100).

Even though drugs inhibiting c-NHEJ or HR have proven highly effective in combinatorial treatment strategies, they usually lack tumor specificity and receiving patients often suffer from toxic side effects, resulting in a narrow therapeutic window. Nowadays, SL-based strategies provide a more promising approach for therapeutic interventions, particularly in patients with HRD.

Exploiting Synthetic Lethality in HR-Defective Tumors

The most popular synthetic lethal interaction (SLI) exploited in cancer therapy is the one between *BRCA* and *PARP1* genes (101, 102). Catalytic inhibition of PARP1 "traps" PARP1 molecules on damaged DNA, resulting in replication fork collapse and DSB formation. In combination with HRD, due to *BRCA1/2* loss, PARP trapping leads to persistent accumulation of DSBs, inducing cell cycle arrest and apoptosis (**Figure 2A**). In two landmark studies, pharmacological targeting of PARP1 with the orally active PARPi olaparib showed a favorable therapeutic index in homozygous BRCA-mutated breast or ovarian cancer (103, 104). There are currently six small-molecule PARPi available in the clinic, four of them (olaparib, rucaparib, niraparib and talazoparib) have already obtained approval in different therapeutic settings (65). Despite this remarkable success story, resistance to PARPi remains a major problem in the clinic and an active area of research (105). Nonetheless, the identification of additional, cancer-specific SL gene pairs holds great promise in developing effective monotherapy regimens, as exemplified below (**Figure 2B**).

Two seminal studies from the Sfeir and D'Andrea laboratories established that HRD cancers display a pronounced dependency on TMEJ to limit the toxicity of DSBs [(29, 30); **Figure 2B**]. Moreover, the fact that Polθ is generally absent in normal cells but upregulated in many cancers makes it a highly desirable drug target (29). Consequently, two established precision oncology companies, Artios Pharma and Repare

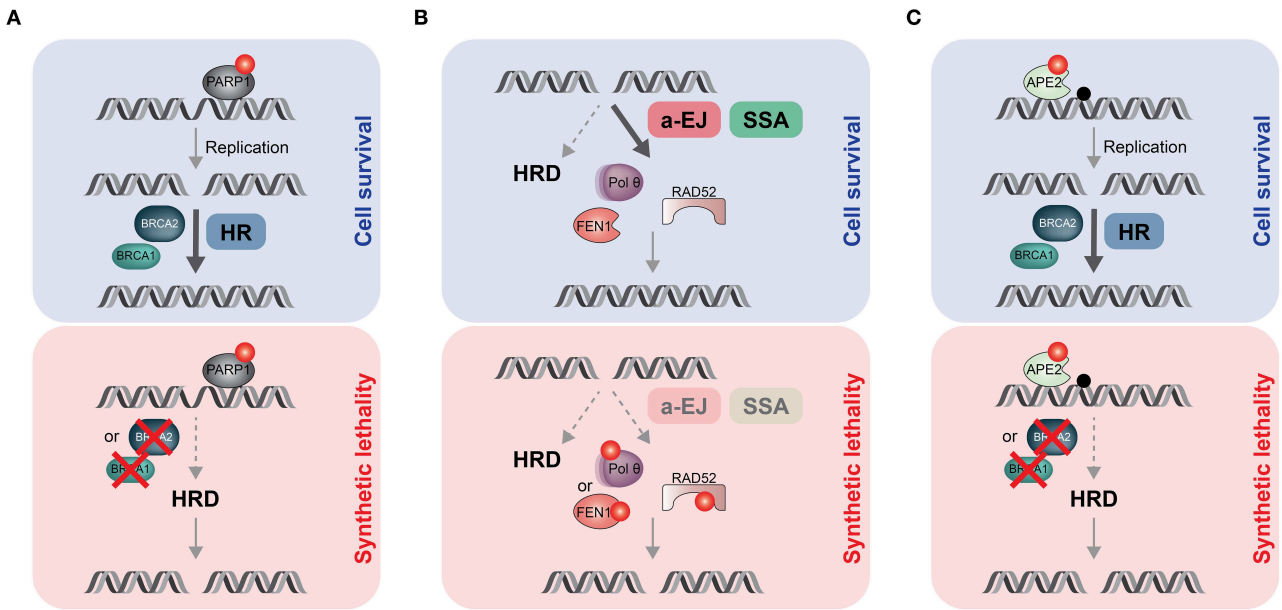

FIGURE 2 | Synthetic lethal (SL) strategies to target HR-deficient (HRD) tumors. **(A)** PARPi (red dot) trap PARP1 proteins on endogenous DNA lesions, including single-strand breaks or gaps. If not removed timely, trapped PARP1 blocks the replication machinery, leading to one-ended DSBs that need to be repaired by HR. In HRD tumors such as *BRCA1*- or *BRCA2*-mutated cancers, DSBs persist and accumulate, ultimately causing cell death due to SL. **(B)** HRD tumors are addicted to alternative, mutagenic DSB repair process (a-EJ and SSA) to sustain proliferation. Targeting Polθ (or FEN1) or RAD52 by small molecule inhibitors (red dots) would eliminate a-EJ or SSA, respectively, resulting in SL. **(C)** Apurinic/apyrimidinic (AP) sites (black dot) are one of the most frequent spontaneous lesions in DNA. If not timely removed by APE2, they have the potential to block DNA replication. Consequently, APE2 inhibition (red dot) would lead to massive accumulation of AP sites associated with increased rates of fork collapse and DSB formation. In healthy cells, HR can deal with those DSBs, promoting cell survival. In contrast, treating HRD tumors with APE2i would cause DSB-induced cell death due to SL.

Therapeutics, have launched Polθ inhibitor programs with first-in-human clinical studies due to start soon. Furthermore, CRISPR-based genetic screens targeting 309 murine DDR genes identified 140 *Polq* SL genes, including many HR mediators, several c-NHEJ genes and key components of the 53BP1 anti-resection pathway (106). Notably, 30% of human breast cancers in the TCGA cohort were found to be likely deficient in one or more of the 140 *Polq* SL genes, significantly broadening the number of patients that may benefit from Polθ inhibition (106).

Another interesting SLI was repeatedly reported between *RAD52* and *BRCA1/2* [(107–111); **Figure 2B**]. Due to the multiple roles of RAD52 in genome maintenance pathways, the exact mechanism underlying the RAD52-BRCA SL remains to be fully understood (112). However, it has been reported that RAD52-dependent SSA acts as an important backup when direct protein-protein interactions in the BRCA1-PALB2-BRCA2 complex, required to channel resected DSBs down the HR path, are disrupted (113). In large agreement with this notion, RAD52 inhibitors exerted synergistic activity with PARPi against BRCA1-deficient tumor cells (114). Remarkably, combined disruption of *RAD52* and *POLQ* caused additive hypersensitivity to cisplatin, indicating distinct back-up roles in DSB repair and a potentially effective approach for SL therapeutic strategies (115). Several small-molecule RAD52 inhibitors have been developed, but none of them have been subjected to clinical trials (78).

Last but not least, genetic screens by the Elledge laboratory uncovered *FEN1* (encoding Flap endonuclease 1) and *APEX2* (encoding AP endonuclease 2, APE2) as SL genes in *BRCA1/2*-deficient backgrounds (116). They proposed that in the context of HRD, FEN1 may be responsible for the removal of Polθ-dependent 5′ flaps during TMEJ (**Figures 1**, **2B**), while APE2 is mainly processing abasic sites at replication forks to avoid fork collapse and DSB formation [(116); **Figure 2C**].

Notably, acquired genomic instability due to HRD facilitates acquisition of mutations that could trigger therapy resistance (4). For instance, PARPi resistance mechanisms have mostly been linked to either reactivating *BRCA* mutations or DDR rewiring, thereby functionally restoring HR. In these cases, chemical inhibition of the reactivated HR pathway has been proposed to overcome PARPi resistance (117). Interestingly, numerous studies revealed that reversion mutations of *BRCA* genes display MH signatures that likely originate from error-prone DSB repair mechanisms such as a-EJ and SSA (118). Consequently, combined inhibition of PARP1 and Polθ (or RAD52) should prolong drug responses and prevent resistance acquisition (118). In addition, targeting alternative SLIs with HRD (**Figure 2C**) could be beneficial when PARPi resistance arises due to loss of PARP1 expression or activation (117).

Finally, it remains to be said that only few robust SLIs have been identified since the discovery of the SL between PARP inhibition and *BRCA1/2* loss of function in 2005 (119). Moreover,

it has been argued that most SLIs display incomplete penetrance due to extensive molecular heterogeneity seen in tumors (120). Therefore, assessing the penetrance of SLIs will become an important aspect of future research.

CONCLUSIONS

It has become increasingly evident that targeted inhibition of DSB repair proteins offers a wide range of possible applications in cancer treatment. Initially, combinatorial therapy of DSB repair inhibitors with DNA-damaging agents (e.g., IR or cisplatin) were considered most effective. Given that DSB repair deficiency results in increased tumor immunogenicity, the combination of selected DSB repair inhibitors with immunotherapy will very likely find its way into the clinic. In addition, the emerging concept of exploiting SL as anti-cancer therapy is expected to allow more selective and efficient tumor killing without the side-effects of conventional drugs. Importantly, sequential therapy with DNA repair inhibitors was found to be less toxic compared to simultaneous drug administration meanwhile retaining treatment efficacy (121, 122). Consequently, detailed evaluation of the drug administration timing is of vital interest to reduce cytotoxicity. In addition, the stratification of robust biomarkers and detection of mutational signatures will be highly critical to the implementation of SL but also combinatorial therapy regimens (123). Finally, DSBs are repaired by multifactorial pathways that are heavily connected. These interdependencies generate potentially druggable vulnerabilities but also opportunities for tumors to develop drug resistance. Thus, establishing potent inhibitors for each DSB repair pathway will create new treatment opportunities for a wide range of tumors.

AUTHOR CONTRIBUTIONS

All authors listed have made a substantial, direct and intellectual contribution to the work, and approved it for publication.

FUNDING

Our research was supported by the Swiss National Science Foundation (grant number: 31003A_176161, to AS), the Swiss Cancer League (grant numbers: KFS-3845-02-2016-R and KFS-4702-02-2019, to AS), and the Forschungskredit of the University of Zurich (grant number: FK-19-037, to AT).

ACKNOWLEDGMENTS

We apologize to authors whose work could not be cited due to space limitations.

REFERENCES

1. Ciccia A, Elledge SJ. The DNA damage response: making it safe to play with knives. *Mol Cell*. (2010) 40:179–204. doi: 10.1016/j.molcel.2010.09.019
2. Dietlein F, Thelen L, Reinhardt HC. Cancer-specific defects in DNA repair pathways as targets for personalized therapeutic approaches. *Trends Genet*. (2014) 30:326–39. doi: 10.1016/j.tig.2014.06.003
3. O'Connor MJ. Targeting the DNA damage response in cancer. *Mol Cell*. (2015) 60:547–60. doi: 10.1016/j.molcel.2015.10.040
4. Bouwman P, Jonkers J. The effects of deregulated DNA damage signalling on cancer chemotherapy response and resistance. *Nat Rev Cancer*. (2012) 12:587–98. doi: 10.1038/nrc3342
5. Curtin NJ. DNA repair dysregulation from cancer driver to therapeutic target. *Nat Rev Cancer*. (2012) 12:801–17. doi: 10.1038/nrc3399
6. Ceccaldi R, Rondinelli B, D'Andrea AD. Repair pathway choices and consequences at the double-strand break. *Trends Cell Biol*. (2016) 26:52–64. doi: 10.1016/j.tcb.2015.07.009
7. Scully R, Panday A, Elango R, Willis NA. DNA double-strand break repair-pathway choice in somatic mammalian cells. *Nat Rev Mol Cell Biol*. (2019) 1–17. doi: 10.1038/s41580-019-0152-0
8. Kantidze OL, Velichko AK, Luzhin AV, Petrova NV, Razin SV. Synthetically lethal interactions of ATM, ATR, and DNA-PKcs. *Trends Cancer*. (2018) 4:755–68. doi: 10.1016/j.trecan.2018.09.007
9. Motegi A, Masutani M, Yoshioka K-I, Bessho T. Aberrations in DNA repair pathways in cancer and therapeutic significances. *Semin Cancer Biol*. (2019) 58:29–46. doi: 10.1016/j.semcancer.2019.02.005
10. Lieber MR. Mechanisms of human lymphoid chromosomal translocations. *Nat Rev Cancer*. (2016) 16:387–98. doi: 10.1038/nrc.2016.40
11. Krenning L, van den Berg J, Medema RH. Life or death after a break: what determines the choice? *Mol Cell*. (2019) 76:346–58. doi: 10.1016/j.molcel.2019.08.023
12. Chapman JR, Taylor MRG, Boulton SJ. Playing the end game: DNA double-strand break repair pathway choice. *Mol Cell*. (2012) 47:497–510. doi: 10.1016/j.molcel.2012.07.029
13. Densham RM, Morris JR. Moving mountains—the BRCA1 promotion of DNA resection. *Front Mol Biosci*. (2019) 6:836–14. doi: 10.3389/fmolb.2019.00079
14. Bunting SF, Callen E, Wong N, Chen H-T, Polato F, Gunn A, et al. 53BP1 inhibits homologous recombination in Brca1-deficient cells by blocking resection of DNA breaks. *Cell*. (2010) 141:243–54. doi: 10.1016/j.cell.2010.03.012
15. Daley JM, Sung P. 53BP1, BRCA1, and the choice between recombination and end joining at DNA double-strand breaks. *Mol Cell Biol*. (2014) 34:1380–8. doi: 10.1128/MCB.01639-13
16. Pannunzio NR, Watanabe G, Lieber MR. Nonhomologous DNA end-joining for repair of DNA double-strand breaks. *J Biol Chem*. (2018) 293:10512–23. doi: 10.1074/jbc.TM117.000374
17. Difilippantonio MJ, Zhu J, Chen HT, Meffre E, Nussenzweig MC, Max EE, et al. DNA repair protein Ku80 suppresses chromosomal aberrations and malignant transformation. *Nature*. (2000) 404:510–4. doi: 10.1038/35006670
18. Roth DB, Gellert M. New guardians of the genome. *Nature*. (2000) 404:823–5. doi: 10.1038/35009180
19. Zhao W, Wiese C, Kwon Y, Hromas R, Sung P. The BRCA tumor suppressor network in chromosome damage repair by homologous recombination. *Annu Rev Biochem*. (2019) 88:221–45. doi: 10.1146/annurev-biochem-013118-111058
20. Andres SN, Williams RS. CtIP/Ctp1/Sae2, molecular form fit for function. *DNA Repair*. (2017) 56:109–17. doi: 10.1016/j.dnarep.2017.06.013
21. Marini F, Rawal CC, Liberi G, Pellicioli A. Regulation of DNA double strand breaks processing: focus on barriers. *Front Mol Biosci*. (2019) 6:836–8. doi: 10.3389/fmolb.2019.00055
22. Syed A, Tainer JA. The MRE11–RAD50–NBS1 complex conducts the orchestration of damage signaling and outcomes to stress in DNA replication and repair. *Annu Rev Biochem*. (2018) 87:263–94. doi: 10.1146/annurev-biochem-062917-012415
23. Orthwein A, Noordermeer SM, Wilson MD, Landry S, Enchev RI, Sherker A, et al. A mechanism for the suppression of homologous recombination in G1 cells. *Nature*. (2015) 528:422–6. doi: 10.1038/nature16142

24. Wright WD, Shah SS, Heyer W-D. Homologous recombination and the repair of DNA double-strand breaks. *J Biol Chem*. (2018) 293:10524–35. doi: 10.1074/jbc.TM118.000372
25. Ahrabi S, Sarkar S, Pfister SX, Pirovano G, Higgins GS, Porter ACG, et al. A role for human homologous recombination factors in suppressing microhomology-mediated end joining. *Nucleic Acids Res*. (2016) 44:5743–57. doi: 10.1093/nar/gkw326
26. Sallmyr A, Tomkinson AE. Repair of DNA double-strand breaks by mammalian alternative end-joining pathways. *J Biol Chem*. (2018) 293:10536–46. doi: 10.1074/jbc.TM117.000375
27. Deng SK, Gibb B, de Almeida MJ, Greene EC, Symington LS. RPA antagonizes microhomology-mediated repair of DNA double-strand breaks. *Nat Struct Mol Biol*. (2014) 21:405–12. doi: 10.1038/nsmb.2786
28. Truong LN, Li Y, Shi LZ, Hwang PYH, He J, Wang H, et al. Microhomology-mediated end joining and homologous recombination share the initial end resection step to repair DNA double-strand breaks in mammalian cells. *Proc Natl Acad Sci USA*. (2013) 110:7720–5. doi: 10.1073/pnas.1213431110
29. Ceccaldi R, Liu JC, Amunugama R, Hajdu I, Primack B, Petalcorin MIR, et al. Homologous-recombination-deficient tumours are dependent on Polθ-mediated repair. *Nature*. (2015) 518:258–62. doi: 10.1038/nature14184
30. Mateos-Gomez PA, Gong F, Nair N, Miller KM, Lazzerini-Denchi E, Sfeir A. Mammalian polymerase θ promotes alternative NHEJ and suppresses recombination. *Nature*. (2015) 518:254–7. doi: 10.1038/nature14157
31. Wood RD, Doublié S. DNA polymerase θ (POLQ), double-strand break repair, and cancer. *DNA Repair*. (2016) 44:22–32. doi: 10.1016/j.dnarep.2016.05.003
32. Kent T, Chandramouly G, McDevitt SM, Ozdemir AY, Pomerantz RT. Mechanism of microhomology-mediated end-joining promoted by human DNA polymerase θ. *Nat Struct Mol Biol*. (2015) 22:230–7. doi: 10.1038/nsmb.2961
33. Mateos-Gomez PA, Kent T, Deng SK, McDevitt S, Kashkina E, Hoang TM, et al. The helicase domain of Polθ counteracts RPA to promote alt-NHEJ. *Nat Struct Mol Biol*. (2017) 24:1116–23. doi: 10.1038/nsmb.3494
34. Bhargava R, Onyango DO, Stark JM. Regulation of single-strand annealing and its role in genome maintenance. *Trends Genet*. (2016) 32:566–75. doi: 10.1016/j.tig.2016.06.007
35. Seol J-H, Shim EY, Lee SE. Microhomology-mediated end joining: good, bad and ugly. *Mutat Res Fund Mol Mech Mutagen*. (2018) 809:81–7. doi: 10.1016/j.mrfmmm.2017.07.002
36. Sishc BJ, Davis AJ. The role of the core non-homologous end joining factors in carcinogenesis and cancer. *Cancers*. (2017) 9:81–30. doi: 10.3390/cancers9070081
37. Srivastava M, Raghavan SC. DNA double-strand break repair inhibitors as cancer therapeutics. *Chem Biol*. (2015) 22:17–29. doi: 10.1016/j.chembiol.2014.11.013
38. Woodbine L, Gennery AR, Jeggo PA. The clinical impact of deficiency in DNA non-homologous end-joining. *DNA Repair*. (2014) 16:84–96. doi: 10.1016/j.dnarep.2014.02.011
39. Chae YK, Anker JF, Carneiro BA, Chandra S, Kaplan J, Kalyan A, et al. Genomic landscape of DNA repair genes in cancer. *Oncotarget*. (2016) 7:23312–21. doi: 10.18632/oncotarget.8196
40. Knijnenburg TA, Wang L, Zimmermann MT, Chambwe N, Gao GF, Cherniack AD, et al. Genomic and molecular landscape of DNA damage repair deficiency across the cancer genome atlas. *Cell Reports*. (2018) 23:239–54.e6. doi: 10.1016/j.celrep.2018.03.076
41. Heeke AL, Pishvaian MJ, Lynce F, Xiu J, Brody JR, Chen WJ, et al. Prevalence of homologous recombination–related gene mutations across multiple cancer types. *JCO Precis Oncol*. (2018) 2018:1–13. doi: 10.1200/PO.17.00286
42. Nielsen FC, van Overeem Hansen T, Sørensen CS. Hereditary breast and ovarian cancer: new genes in confined pathways. *Nat Rev Cancer*. (2016) 16:599–612. doi: 10.1038/nrc.2016.72
43. Bartkova J, Tommiska J, Oplustilova L, Aaltonen K, Tamminen A, Heikkinen T, et al. Aberrations of the MRE11-RAD50-NBS1 DNA damage sensor complex in human breast cancer: MRE11 as a candidate familial cancer-predisposing gene. *Mol Oncol*. (2008) 2:296–316. doi: 10.1016/j.molonc.2008.09.007
44. Yin J, Wu K, Ma Q, Dong H, Zhu Y, Hu L, et al. Revisiting non-BRCA1/2 familial whole exome sequencing datasets implicates NCK1 as a cancer gene. *Front Genet*. (2019) 10:527. doi: 10.3389/fgene.2019.00527
45. Lord CJ, Ashworth A. BRCAness revisited. *Nat Rev*. (2016) 16:110–20. doi: 10.1038/nrc.2015.21
46. Jonsson P, Bandlamudi C, Cheng ML, Srinivasan P, Chavan SS, Friedman ND, et al. Tumour lineage shapes BRCA-mediated phenotypes. *Nature*. (2019) 571:576–9. doi: 10.1038/s41586-019-1382-1
47. Gachechiladze M, Škarda J, Soltermann A, Joerger M. RAD51 as a potential surrogate marker for DNA repair capacity in solid malignancies. *Int J Cancer*. (2017) 141:1286–94. doi: 10.1002/ijc.30764
48. Ho V, Chung L, Singh A, Lea V, Abubakar A, Lim SH, et al. Overexpression of the MRE11-RAD50-NBS1 (MRN) complex in rectal cancer correlates with poor response to neoadjuvant radiotherapy and prognosis. *BMC Cancer*. (2018) 18:177–111. doi: 10.1186/s12885-018-4776-9
49. Li J, Su T, Yang L, Zhang C, He Y. High expression of MRE11 correlates with poor prognosis in gastric carcinoma. *Diagn Pathol*. (2019) 14:87–9. doi: 10.1186/s13000-019-0844-y
50. Wang J, Xu W-H, Wei Y, Zhu Y, Qin X-J, Zhang H-L, et al. Elevated MRE11 expression associated with progression and poor outcome in prostate cancer. *J Cancer*. (2019) 10:4333–40. doi: 10.7150/jca.31454
51. Situ Y, Chung L, Lee C, Ho V. MRN (MRE11-RAD50-NBS1) Complex in human cancer and prognostic implications in colorectal cancer. *IJMS*. (2019) 20:816–11. doi: 10.3390/ijms20040816
52. Bennardo N, Cheng A, Huang N, Stark JM. Alternative-NHEJ is a mechanistically distinct pathway of mammalian chromosome break repair. *PLoS Genet*. (2008) 4:e1000110. doi: 10.1371/journal.pgen.1000110
53. Yu X, Wu LC, Bowcock AM, Aronheim A, Baer R. The C-terminal (BRCT) domains of BRCA1 interact *in vivo* with CtIP, a protein implicated in the CtBP pathway of transcriptional repression. *J Biol Chem*. (1998) 273:25388–92. doi: 10.1074/jbc.273.39.25388
54. Zhang Y, Jasin M. An essential role for CtIP in chromosomal translocation formation through an alternative end-joining pathway. *Nat Struct Mol Biol*. (2010) 18:80–4. doi: 10.1038/nsmb.1940
55. Reczek CR, Shakya R, Miteva Y, Szabolcs M, Ludwig T, Baer R. The DNA resection protein CtIP promotes mammary tumorigenesis. *Oncotarget*. (2016) 7(22):32172–83. doi: 10.18632/oncotarget.8605
56. Bétermier M, Bertrand P, Lopez BS. Is non-homologous end-joining really an inherently error-prone process? *PLoS Genet*. (2014) 10:e1004086. doi: 10.1371/journal.pgen.1004086
57. Stephens PJ, McBride DJ, Lin M-L, Varela I, Pleasance ED, Simpson JT, et al. Complex landscapes of somatic rearrangement in human breast cancer genomes. *Nature*. (2009) 462:1005–10. doi: 10.1038/nature08645
58. Stephens PJ, Greenman CD, Fu B, Yang F, Bignell GR, Mudie LJ, et al. Massive genomic rearrangement acquired in a single catastrophic event during cancer development. *Cell*. (2011) 144:27–40. doi: 10.1016/j.cell.2010.11.055
59. Schimmel J, van Schendel R, den Dunnen JT, Tijsterman M. Templated insertions: a smoking gun for polymerase theta-mediated end joining. *Trends Genet*. (2019) 35:632–44. doi: 10.1016/j.tig.2019.06.001
60. Higgins GS, Harris AL, Prevo R, Helleday T, McKenna WG, Buffa FM. Overexpression of *POLQ* confers a poor prognosis in early breast cancer patients. *Oncotarget*. (2010) 1:175–84. doi: 10.18632/oncotarget.124
61. Lemee F, Bergoglio V, Fernandez-Vidal A, Machado-Silva A, Pillaire MJ, Bieth A, et al. DNA polymerase θ up-regulation is associated with poor survival in breast cancer, perturbs DNA replication, and promotes genetic instability. *Proc Natl Acad Sci USA*. (2010) 107:13390–5. doi: 10.1073/pnas.0910759107
62. Gavande NS, VanderVere-Carozza PS, Hinshaw HD, Jalal SI, Sears CR, Pawelczak KS, et al. DNA repair targeted therapy: the past or future of cancer treatment? *Pharmacol Ther*. (2016) 160:65–83. doi: 10.1016/j.pharmthera.2016.02.003
63. Toulany M. Targeting DNA double-strand break repair pathways to improve radiotherapy response. *Genes*. (2019) 10:25–20. doi: 10.3390/genes10010025
64. Minchom A, Aversa C, Lopez J. Dancing with the DNA damage response: next-generation anti-cancer therapeutic strategies. *Ther Adv Med Oncol*. (2018) 10:1758835918786658. doi: 10.1177/1758835918786658

65. Pilié PG, Gay CM, Byers LA, O'Connor MJ, Yap TA. PARP inhibitors: extending benefit beyond BRCA-mutant cancers. *Clin Cancer Res*. (2019) 25:3759–71. doi: 10.1158/1078-0432.CCR-18-0968
66. Brown JS, Sundar R, Lopez J. Combining DNA damaging therapeutics with immunotherapy: more haste, less speed. *Br J Cancer*. (2017) 118:312–24. doi: 10.1038/bjc.2017.376
67. Truini A, Germano G, Bardelli A. Inactivation of DNA repair—prospects for boosting cancer immune surveillance. *Genome Med*. (2018) 10:124–123. doi: 10.1186/s13073-018-0603-9
68. Pilié PG, Tang C, Mills GB, Yap TA. State-of-the-art strategies for targeting the DNA damage response in cancer. *Nat Rev Clin Oncol*. (2019) 16:81–104. doi: 10.1038/s41571-018-0114-z
69. Shibata A, Jeggo P. A historical reflection on our understanding of radiation-induced DNA double strand break repair in somatic mammalian cells; interfacing the past with the present. *Int J Radiat Biol*. (2019) 95:945–56. doi: 10.1080/09553002.2018.1564083
70. Mohiuddin IS, Kang MH. DNA-PK as an emerging therapeutic target in cancer. *Front Oncol*. (2019) 9:635. doi: 10.3389/fonc.2019.00635
71. Weterings E, Gallegos AC, Dominick LN, Cooke LS, Bartels TN, Vagner J, et al. A novel small molecule inhibitor of the DNA repair protein Ku70/80. *DNA Repair*. (2016) 43:98–106. doi: 10.1016/j.dnarep.2016.03.014
72. Harnor SJ, Brennan A, Cano C. Targeting DNA-dependent protein kinase for cancer therapy. *ChemMedChem*. (2017) 12:895–900. doi: 10.1002/cmdc.201700143
73. Timme CR, Rath BH, O'Neill JW, Camphausen K, Tofilon PJ. The DNA-PK inhibitor VX-984 enhances the radiosensitivity of glioblastoma cells grown *in vitro* and as orthotopic xenografts. *Mol Cancer Ther*. (2018) 17:1207–16. doi: 10.1158/1535-7163.MCT-17-1267
74. Hafsi H, Dillon MT, Barker HE, Kyula JN, Schick U, Paget JT, et al. Combined ATR and DNA-PK inhibition radiosensitizes tumor cells independently of their p53 status. *Front Oncol*. (2018) 8:245. doi: 10.3389/fonc.2018.00245
75. Mortensen DS, Perrin-Ninkovic SM, Shevlin G, Elsner J, Zhao J, Whitefield B, et al. Optimization of a series of triazole containing mammalian target of rapamycin (mTOR) kinase inhibitors and the discovery of CC-115. *J Med Chem*. (2015) 58:5599–608. doi: 10.1021/acs.jmedchem.5b00627
76. Thijssen R, ter Burg J, Garrick B, van Bochove GGW, Brown JR, Fernandes SM, et al. Dual TORK/DNA-PK inhibition blocks critical signaling pathways in chronic lymphocytic leukemia. *Blood*. (2016) 128:574–83. doi: 10.1182/blood-2016-02-700328
77. Dupré A, Boyer-Chatenet L, Sattler RM, Modi AP, Lee JH, Nicolette ML, et al. A forward chemical genetic screen reveals an inhibitor of the Mre11–Rad50–Nbs1 complex. *Nat Chem Biol*. (2008) 4:119–25. doi: 10.1038/nchembio.63
78. Hengel SR, Spies MA, Spies M. Small-molecule inhibitors targeting DNA repair and DNA repair deficiency in research and cancer therapy. *Cell Chem Biol*. (2017) 24:1101–19. doi: 10.1016/j.chembiol.2017.08.027
79. Shibata A, Moiani D, Arvai AS, Perry J, Harding SM, Genois M-M, et al. DNA double-strand break repair pathway choice is directed by distinct MRE11 nuclease activities. *Mol Cell*. (2014) 53:7–18. doi: 10.1016/j.molcel.2013.11.003
80. Anand R, Ranjha L, Cannavo E, Cejka P. Phosphorylated CtIP functions as a co-factor of the MRE11-RAD50-NBS1 endonuclease in DNA end resection. *Mol Cell*. (2016) 64:940–50. doi: 10.1016/j.molcel.2016.10.017
81. Anand R, Jasrotia A, Bundschuh D, Howard SM, Ranjha L, Stucki M, et al. NBS1 promotes the endonuclease activity of the MRE11-RAD50 complex by sensing CtIP phosphorylation. *EMBO J*. (2019) 38:2585–2516. doi: 10.15252/embj.2018101005
82. Makharashvili N, Tubbs AT, Yang SH, Wang H, Barton O, Zhou Y, et al. Catalytic and noncatalytic roles of the CtIP endonuclease in double-strand break end resection. *Mol Cell*. (2014) 54:1022–33. doi: 10.1016/j.molcel.2014.04.011
83. Wang H, Li Y, Truong LN, Shi LZ, Hwang PY-H, He J, et al. CtIP maintains stability at common fragile sites and inverted repeats by end resection-independent endonuclease activity. *Mol Cell*. (2014) 54:1012–21. doi: 10.1016/j.molcel.2014.04.012
84. Sun C, Yin J, Fang Y, Chen J, Jeong KJ, Chen X, et al. BRD4 inhibition is synthetic lethal with PARP inhibitors through the induction of homologous recombination deficiency. *Cancer Cell*. (2018) 33:401–16.e8. doi: 10.1016/j.ccell.2018.01.019
85. Duan Y, Guan Y, Qin W, Zhai X, Yu B, Liu H. Targeting Brd4 for cancer therapy: inhibitors and degraders. *Med Chem Commun*. (2018) 9:1779–802. doi: 10.1039/C8MD00198G
86. Chen C-C, Feng W, Lim PX, Kass EM, Jasin M. Homology-directed repair and the role of BRCA1, BRCA2, and related proteins in genome integrity and cancer. *Ann Rev Cancer Biol*. (2018) 2:313–36. doi: 10.1146/annurev-cancerbio-030617-050502
87. Pessetto ZY, Yan Y, Bessho T, Natarajan A. Inhibition of BRCT(BRCA1)-phosphoprotein interaction enhances the cytotoxic effect of olaparib in breast cancer cells: a proof of concept study for synthetic lethal therapeutic option. *Breast Cancer Res Treat*. (2012) 134:511–7. doi: 10.1007/s10549-012-2079-4
88. Trenner A, Godau J, Sartori AA. A short BRCA2-derived cell-penetrating peptide targets RAD51 function and confers hypersensitivity toward PARP inhibition. *Mol Cancer Ther*. (2018) 17:1392–1404. doi: 10.1158/1535-7163.MCT-17-1156
89. Densham RM, Morris JR. The BRCA1 Ubiquitin ligase function sets a new trend for remodelling in DNA repair. *Nucleus*. (2017) 8:116–25. doi: 10.1080/19491034.2016.1267092
90. Budke B, Kalin JH, Pawlowski M, Zelivianskaia AS, Wu M, Kozikowski AP, et al. An optimized RAD51 inhibitor that disrupts homologous recombination without requiring michael acceptor reactivity. *J Med Chem*. (2012) 56:254–63. doi: 10.1021/jm301565b
91. Budke B, Logan HL, Kalin JH, Zelivianskaia AS, Cameron McGuire W, Miller LL, et al. RI-1: a chemical inhibitor of RAD51 that disrupts homologous recombination in human cells. *Nucleic Acids Res*. (2012) 40:7347–57. doi: 10.1093/nar/gks353
92. Huang F, Motlekar NA, Burgwin CM, Napper AD, Diamond SL, Mazin AV. Identification of specific inhibitors of human RAD51 recombinase using high-throughput screening. *ACS Chem Biol*. (2011) 6:628–35. doi: 10.1021/cb100428c
93. Ward A, Khanna KK, Wiegmans AP. Targeting homologous recombination, new pre-clinical and clinical therapeutic combinations inhibiting RAD51. *Cancer Treat Rev*. (2015) 41:35–45. doi: 10.1016/j.ctrv.2014.10.006
94. Zhu J, Zhou L, Wu G, Konig H, Lin X, Li G, et al. A novel small molecule RAD51 inactivator overcomes imatinib-resistance in chronic myeloid leukaemia. *EMBO Mol Med*. (2013) 5:353–65. doi: 10.1002/emmm.201201760
95. Wiegmans AP, Miranda M, Wen SW, Al-Ejeh F, Möller A. RAD51 inhibition in triple negative breast cancer cells is challenged by compensatory survival signaling and requires rational combination therapy. *Oncotarget*. (2016) 7:60087–100. doi: 10.18632/oncotarget.11065
96. Berte N, Piee-Staffa A, Piecha N, Wang M, Borgmann K, Kaina B, et al. Targeting homologous recombination by pharmacological inhibitors enhances the killing response of glioblastoma cells treated with alkylating drugs. *Mol Cancer Ther*. (2016) 15:2665–78. doi: 10.1158/1535-7163.MCT-16-0176
97. Chen Q, Cai D, Li M, Wu X. The homologous recombination protein RAD51 is a promising therapeutic target for cervical carcinoma. *Oncol Rep*. (2017) 38:767–74. doi: 10.3892/or.2017.5724
98. Shi Y, Jin J, Wang X, Ji W, Guan X. DAXX, as a tumor suppressor, impacts DNA damage repair and sensitizes BRCA-proficient TNBC cells to PARP inhibitors. *Neoplasia*. (2019) 21:533–44. doi: 10.1016/j.neo.2019.04.001
99. Kaplan AR, Gueble SE, Liu Y, Oeck S, Kim H, Yun Z, et al. Cediranib suppresses homology-directed DNA repair through down-regulation of BRCA1/2 and RAD51. *Sci Transl Med*. (2019) 11:eaav4508. doi: 10.1126/scitranslmed.aav4508
100. Liu JF, Barry WT, Birrer M, Lee JM, Buckanovich RJ, Fleming GF, et al. Overall survival and updated progression-free survival outcomes in a randomized phase II study of combination cediranib and olaparib versus olaparib in relapsed platinum-sensitive ovarian cancer. *Ann Oncol*. (2019) 30:551–7. doi: 10.1093/annonc/mdz018
101. Bryant HE, Schultz N, Thomas HD, Parker KM, Flower D, Lopez E, et al. Specific killing of BRCA2-deficient tumours with inhibitors of poly(ADP-ribose) polymerase. *Nature*. (2005) 434:913–7. doi: 10.1038/nature03443
102. Farmer H, McCabe N, Lord CJ, Tutt ANJ, Johnson DA, Richardson TB, et al. Targeting the DNA repair defect in BRCA mutant cells as a therapeutic strategy. *Nature*. (2005) 434:917–20. doi: 10.1038/nature03445

103. Audeh MW, Carmichael J, Penson RT, Friedlander M, Powell B, Bell-McGuinn K, et al. Oral poly(ADP-ribose) polymerase inhibitor olaparib in patients with BRCA1 or BRCA2 mutations and recurrent ovarian cancer: a proof-of-concept trial. *Lancet*. (2010) 376:245–51. doi: 10.1016/S0140-6736(10)60893-8
104. Tutt A, Robson M, Audeh MW, Weitzerl JN, Friedlander M, Arun B, et al. Oral poly(ADP-ribose) polymerase inhibitor olaparib in patients with BRCA1 or BRCA2 mutations and advanced breast cancer: a proof-of-concept trial. *Lancet*. (2010) 376:235–44. doi: 10.1016/S0140-6736(10)60892-6
105. Noordermeer SM, van Attikum H. PARP inhibitor resistance: a Tug-of-war in BRCA-mutated cells. *Trends Cell Biol*. (2019) 29:820–34. doi: 10.1016/j.tcb.2019.07.008
106. Feng W, Simpson DA, Carvajal-Garcia J, Price BA, Kumar RJ, Mose LE, et al. Genetic determinants of cellular addiction to DNA polymerase theta. *Nat Commun*. (2019) 10:22–13. doi: 10.1038/s41467-019-12234-1
107. Cramer-Morales K, Nieborowska-Skorska M, Scheibner K, Padget M, Irvine DA, Sliwinski T, et al. Personalized synthetic lethality induced by targeting RAD52 in leukemias identified by gene mutation and expression profile. *Blood*. (2013) 122:1293–304. doi: 10.1182/blood-2013-05-501072
108. Feng Z, Scott SP, Bussen W, Sharma GG, Guo G, Pandita TK, et al. Rad52 inactivation is synthetically lethal with BRCA2 deficiency. *Proc Natl Acad Sci USA*. (2011) 108:686–91. doi: 10.1073/pnas.1010959107
109. Hengel SR, Malacaria E, Folly da Silva Constantino L, Bain FE, Diaz A, Koch BG, et al. Small-molecule inhibitors identify the RAD52-ssDNA interaction as critical for recovery from replication stress and for survival of BRCA2 deficient cells. *Elife*. (2016) 5:e14740. doi: 10.7554/eLife.14740
110. Huang F, Goyal N, Sullivan K, Hanamshet K, Patel M, Mazina OM, et al. Targeting BRCA1- and BRCA2-deficient cells with RAD52 small molecule inhibitors. *Nucleic Acids Res*. (2016) 44:4189–99. doi: 10.1093/nar/gkw087
111. Lok BH, Carley AC, Tchang B, Powell SN. RAD52 inactivation is synthetically lethal with deficiencies in BRCA1 and PALB2 in addition to BRCA2 through RAD51-mediated homologous recombination. *Oncogene*. (2012) 32:3552–8. doi: 10.1038/onc.2012.391
112. Jalan M, Olsen KS, Powell SN. Emerging roles of RAD52 in genome maintenance. *Cancers*. (2019) 11:1038–1013. doi: 10.3390/cancers11071038
113. Anantha RW, Simhadri S, Foo TK, Maio S, Liu J, Shen Z, et al. Functional and mutational landscapes of BRCA1 for homology-directed repair and therapy resistance. *Elife*. (2017) 6:e21350. doi: 10.7554/eLife.21350
114. Sullivan-Reed K, Bolton-Gillespie E, Dasgupta Y, Langer S, Siciliano M, Nieborowska-Skorska M, et al. Simultaneous targeting of PARP1 and RAD52 triggers dual synthetic lethality in BRCA-deficient tumor cells. *Cell Rep*. (2018) 23:3127–36. doi: 10.1016/j.celrep.2018.05.034
115. Kelso AA, Lopezcolorado FW, Bhargava R, Stark JM. Distinct roles of RAD52 and POLQ in chromosomal break repair and replication stress response. *PLoS Genet*. (2019) 15:e1008319. doi: 10.1371/journal.pgen.1008319
116. Mengwasser KE, Adeyemi RO, Leng Y, Choi MY, Clairmont C, D'Andrea AD, et al. Genetic screens reveal FEN1 and APEX2 as BRCA2 synthetic lethal targets. *Mol Cell*. (2019) 73:885–99.e6. doi: 10.1016/j.molcel.2018.12.008
117. D'Andrea AD. Mechanisms of PARP inhibitor sensitivity and resistance. *DNA Repair*. (2018) 71:172–6. doi: 10.1016/j.dnarep.2018.08.021
118. Gogola E, Rottenberg S, Jonkers J. Resistance to PARP inhibitors: lessons from preclinical models of BRCA-associated cancer. *Ann Rev Cancer Biol*. (2019) 3:235–54. doi: 10.1146/annurev-cancerbio-030617-050232
119. Ashworth A, Lord CJ. Synthetic lethal therapies for cancer: what's next after PARP inhibitors? *Nat Rev Clin Oncol*. (2018) 15:564–76. doi: 10.1038/s41571-018-0055-6
120. Ryan CJ, Bajrami I, Lord CJ. Synthetic lethality and cancer – penetrance as the major barrier. *Trends Cancer*. (2018) 4:671–83. doi: 10.1016/j.trecan.2018.08.003
121. Benada J, Ejlertsen B, Sørensen CS. Overcoming treatment toxicity through sequential therapy. *Cancer Cell*. (2019) 35:821–2. doi: 10.1016/j.ccell.2019.05.006
122. Fang Y, McGrail DJ, Sun C, Labrie M, Chen X, Zhang D, et al. Sequential therapy with PARP and WEE1 inhibitors minimizes toxicity while maintaining efficacy. *Cancer Cell*. (2019) 35:851–67.e7. doi: 10.1016/j.ccell.2019.05.001
123. Ma J, Setton J, Lee NY, Riaz N, Powell SN. The therapeutic significance of mutational signatures from DNA repair deficiency in cancer. *Nat Commun*. (2018) 9:3292. doi: 10.1038/s41467-018-05228-y

Conflict of Interest: The authors declare that the research was conducted in the absence of any commercial or financial relationships that could be construed as a potential conflict of interest.

frontiers in Oncology

ORIGINAL RESEARCH
published: 17 December 2019
doi: 10.3389/fonc.2019.01416

Nanoformulation of Talazoparib Increases Maximum Tolerated Doses in Combination With Temozolomide for Treatment of Ewing Sarcoma

Paige Baldwin[1], Rostislav Likhotvorik[2], Nabeela Baig[2], Jodie Cropper[2], Ruth Carlson[2], Raushan Kurmasheva[2,3†] and Srinivas Sridhar[1,4,5*†]*

[1] Department of Bioengineering, Northeastern University, Boston, MA, United States, [2] Greehey Children's Cancer Research Institute, San Antonio, TX, United States, [3] Department of Molecular Medicine, The University of Texas Health Science Center at San Antonio, San Antonio, TX, United States, [4] Department of Physics, Northeastern University, Boston, MA, United States, [5] Division of Radiation Oncology, Harvard Medical School, Boston, MA, United States

OPEN ACCESS

Edited by:
Michaela Medová,
University Hospital Bern, Switzerland

Reviewed by:
Alvaro Galli,
Pisa Research Area (CNR), Italy
Bernd E. R. Nuernberg,
University of Tübingen, Germany

***Correspondence:**
Raushan Kurmasheva
Kurmasheva@uthscsa.edu
Srinivas Sridhar
s.sridhar@northeastern.edu

[†] These authors have contributed equally to this work and share senior authorship

Specialty section:
This article was submitted to Molecular and Cellular Oncology, a section of the journal Frontiers in Oncology

Received: 10 September 2019
Accepted: 28 November 2019
Published: 17 December 2019

Citation:
Baldwin P, Likhotvorik R, Baig N, Cropper J, Carlson R, Kurmasheva R and Sridhar S (2019) Nanoformulation of Talazoparib Increases Maximum Tolerated Doses in Combination With Temozolomide for Treatment of Ewing Sarcoma. Front. Oncol. 9:1416. doi: 10.3389/fonc.2019.01416

The Pediatric Preclinical Testing Program previously identified the PARP inhibitor talazoparib (TLZ) as a means to potentiate temozolomide (TMZ) activity for the treatment of Ewing sarcoma. However, the combination of TLZ and TMZ has been toxic in both preclinical and clinical testing, necessitating TMZ dose reduction to ∼15% of the single agent maximum tolerated dose. We have synthesized a nanoparticle formulation of talazoparib (NanoTLZ) to be administered intravenously in an effort to modulate the toxicity profile of this combination treatment. Results in Ewing sarcoma xenograft models are presented to demonstrate the utility of this delivery method both alone and in combination with TMZ. NanoTLZ reduced gross toxicity and had a higher maximum tolerated dose than oral TLZ. The dose of TMZ did not have to be reduced when combined with NanoTLZ as was required when combined with oral TLZ. This indicated the NanoTLZ delivery system may be advantageous in decreasing the systemic toxicity associated with the combination of oral TLZ and TMZ.

Keywords: talazoparib, temozolomide, nanoparticle, combination therapy, Ewing sarcoma

INTRODUCTION

Ewing sarcoma (ES) comprises the fourth most common highly malignant childhood solid tumor (1, 2). Most patients are diagnosed between 10 and 20 years old and 70% of patients will be cured with intensive chemotherapy regimens (3). However, 25% of patients present with metastatic disease at the time of diagnosis and the prognosis for these cases is unfavorable with 5-year survival rates around 30% (1). Advances in chemotherapy regimens, radiotherapy, and surgery have shown dramatic improvements in the management of local tumors. These advances have come in the form of dose intensification and compression, with few advances in identifying new compounds for treating these tumors. However, very little progress has been made in the treatment of advanced or metastatic disease.

ES is defined by a tumor-specific chromosomal translocation (4–6). In approximately 85% of all tumors, the EWSR1 gene on chromosome 22 is fused to FLI1, a member of E26 transformation-specific sequence (ETS) family of transcription factors, on chromosome 11. In the remaining 15% of ES tumors, the EWSR1 is fused to other members of the ETS family, mostly

the ERG gene on chromosome 21 (7, 8). It has been shown recently, that ETS transcription factors interact with Poly-ADP ribose polymerase 1 (PARP1), the founding member of the DNA damage repair superfamily of enzymes (9, 10). It is postulated that PARP1 is a direct transcriptional target of EWSR1-FLI1, and it interacts with EWSR1-FLI1 or EWSR1-ERG fusion proteins in a feed-forward loop to enhance oncogenic transcription factor function (9). Further, ETS gene fusions induce DNA double-strand breaks (9, 11). Thus, it is postulated that inhibiting PARP activity has a selective effect on ES cells through downregulating the activity of the oncogenic EWSR1-FLI1 fusion protein, leading to selective hypersensitivity of ES cell lines to PARP inhibitors as was identified using a genomic screen (12). However, despite the promising activity of PARP inhibitors as single agents *in vitro*, they have shown only modest activity in *in vivo* models without defects in homologous recombination (10).

Talazoparib (TLZ), a potent PARP inhibitor, was evaluated as a single agent in 44 xenograft models representing childhood solid tumors, but only two models demonstrated regression (10). There was no activity in ES xenografts, which appears to be reflective of clinical activity, since a phase II clinical trial of the PARP inhibitor olaparib showed no activity in ES tumors (13). Preclinical studies indicate the combination of PARP inhibitors with chemotherapy agents that damage DNA induces synergy *in vitro* and promising activity in xenograft models (9, 10, 14–16). It has been shown *in vitro* that the potency of temozolomide (TMZ) can be potentiated up to 40-fold through inhibition of PARP by TLZ, not only in ES cells (17). In our previous study, neither TLZ nor TMZ as single agents yielded biologically significant anti-tumor activity against ES xenografts, while the combination of the two agents led to dramatic regression in 5 of the 10 ES xenograft models (17). However, this combination was toxic, necessitating a reduction of TMZ to ∼15% of its single agent maximum tolerated dose (MTD). Results of a recent phase I/II clinical trial to assess the combination of TMZ and TLZ in pediatric patients with recurrent disease (NCT02116777) suggests a similar TMZ dose reduction is required to make this combination tolerable.

Nanoparticles have been widely studied as drug delivery systems due to their inherent ability to reduce toxicity while maintaining therapeutic efficacy (18, 19). Nanoparticles can be administered intravenously meaning the drug is 100% available in the vasculature. In contrast, oral drugs must cross the gastro-intestinal barrier, a rate limiting step for drug absorption, and subsequently undergo first-pass metabolism. Tumors are known to rapidly induce blood vessel growth to supply them with nutrients, resulting in a highly disorganized vascular network with compromised lymphatic draining. This leaky vasculature, and poor lymphatic drainage, aids in the enhanced permeability and retention (EPR) effect, whereby nanoparticles are more likely to extravasate and remain in tumor tissue instead of healthy tissues (20). A nanoformulation of TLZ (NanoTLZ) has been developed and shown to be more effective than oral TLZ at delaying ascites formation in a disseminated ovarian cancer model (21). Additionally, NanoTLZ induced greater regression than both oral and intravenous (IV) TLZ in a *BRCA1* deficient model of breast cancer without any signs of toxicity (22). Therefore, we sought to utilize NanoTLZ in combination with TMZ to more effectively treat ES. We hypothesized that NanoTLZ would be less toxic than oral TLZ, consequently allowing for combination with TMZ at doses closer to the single agent MTD. Lowering the toxicity of the combination is expected to provide more effective treatment for these tumors.

MATERIALS AND METHODS

Synthesis and Characterization of NanoTLZ

Formulation and characterization of NanoTLZ have been previously reported (21, 22). Briefly, fixed ratios of 1, 2-dipalmitoyl-sn-glycero-3-phosphocholine (DPPC), 1,2-dioleoyl-3-tri methyl-ammonium-propane (chloride salt) (DOTAP), cholesterol, and 1,2-distearoyl-sn-glycero-3 phosphoethanolamine-N-[methoxy(polyethyleneglycol)-2000 (DSPE-PEG2000), and TLZ were mixed in chloroform and evaporated to form a thin film. The film was hydrated with phosphate buffered saline (PBS) at 50°C and sized using bath sonication for 20 min. Nanoparticles were dialyzed against PBS and additional non-encapsulated drug which is insoluble in aqueous media was removed via syringe filter (23). Vehicle nanoparticles were prepared following the same protocol without the addition of TLZ. Fluorescently labeled nanoparticles were prepared by including Cyanine 5 (Cy5) in the lipid mixture.

Each batch was characterized in regards to size and zeta potential using a Brookhaven 90Plus analyzer equipped with ZetaPALS. The concentration of encapsulated TLZ was measured by lysing nanoparticles with methanol for analysis via high performance liquid chromatography as previously described.

In vitro Assessment of NanoTLZ

ES-6, ES-7, EW-8 ES cells have been previously determined to be sensitive to single agent TLZ and therefore, were utilized to ensure NanoTLZ was as effective as free TLZ *in vitro* (10). TC-71 cell line is not sensitive to single agent TLZ but has been previously shown that treatment with a low dose of TLZ can potentiate killing by TMZ, therefore, TC-71 was further used to assess the ability of NanoTLZ to potentiate the effect of TMZ by treating cells with the IC_{10} of either TLZ or NanoTLZ and assessing dose response to TMZ. The Alamar Blue® assay was used to assess cell viability (*BioRad*). Cells were seeded to reach 20–40% confluency. TLZ, NanoTLZ, or TMZ were added to wells 24 h after cell seeding, and incubated for 96 h. Following the 96 h incubation of cells in 24-well plates, 10% v/v of Alamar Blue was added and fluorescence was measured after 4 h (excitation 530 nm, emission 590 nm). Wells containing RPMI 1640 (*Hyclone*), 10%FBS (*Sigma*) and untreated cells, 10% v/v Alamar blue, were used as positive controls. Wells with culture medium without cells containing 10% v/v Alamar Blue were assays as negative controls. Fluorescence was recorded on the Spectra Max plate reader, with the Alamar Blue protocol provided by *Softmax Software*. All experiments were performed in triplicate. Statistical analysis and curve plotting (3-parameter polynomial analysis) were performed using standard equations

included in the GraphPad Prism 7.0c package (*GraphPad Software Inc., USA*).

Immunoblotting

Mice harboring KT-10 xenografts were treated with 0.165 mg/kg TLZ BID x5 PO or 0.33 mg/kg NanoTLZ SID, IV, on days 1, 3, and 5. Tumors were collected from 3 mice/group for immunoblotting. Cells were lysed using RIPA buffer (*89900, Pierce*) according to standard protocols. Samples were separated on a 4–12% gradient gel (*NP0321, Invitrogen*) and then transferred onto a PVDF or nitrocellulose membrane. Membranes were blocked with 3% BSA in TBS-T for 1 h at room temperature, then incubated with primary PARP1/cleaved PARP1 or GAPDH antibodies overnight (*Cell Signaling Technology*). After secondary antibody incubation and washing, membranes were developed using enhanced chemiluminescence (*NEL103001EA, PerkinElmer*).

MTD of NanoTLZ

All animal studies and procedures, unless otherwise stated, were conducted in accordance with the Institutional Animal Care and Use Committee (IACUC) reviewed and approved at the University of Texas Health San Antonio.

For evaluation of toxicity, non-tumored C.B.17SC *scid-/-* female mice (*Taconic Farms, NY*) were administered 0.125, 0.25, 0.5, or 1 mg/kg NanoTLZ IV either on days 1, 3, and 5 or daily for 5 days to assess the single agent MTD ($n = 3$/group). To assess the combination MTD, mice were treated with 0.5 mg/kg NanoTLZ IV daily for 5 days combined with 5, 10, 20, 30, or 40 mg/kg TMZ oral gavage daily for 5 days. A second combination assessed 1.0 mg/kg NanoTLZ IV on days 1, 3, and 5 combined with 50 mg/kg TMZ oral gavage for 5 days. Body weight was measured daily for 21 days. Loss of more than 20% of the initial body weight was considered toxic and the next lower dose would be considered the MTD.

In vivo Localization

This animal study was performed in accordance with protocols approved by the IACUC at Northeastern University. NCr-nu/nu mice were implanted with 10^6 MDA-MB-231-D3H2LN cells in matrigel. When tumors reached ∼100 mm^3 a single dose of NanoTLZ-Cy5 IV was administered ($n = 3$). Twenty-four hours after administration fluorescent imaging was completed using an IVIS Lumina II. The primary image was collected at an excitation wavelength of 640 nm, the background image was excited at 570 nm and the collected emission was 695–770 nm.

Efficacy of NanoTLZ Monotherapy

The KT-10 Wilms tumor PDX model was used to assess the activity of NanoTLZ. This model has a PALB2 mutation, hence is defective in homologous recombination and is sensitive to TLZ (10). The PPTP previously identified relevant doses of free TLZ for this model which were used in this study (10). MTD testing in non-tumored mice as mentioned in section MTD of NanoTLZ was used to identify the NanoTLZ dose. C.B.17SC *scid-/-* mice implanted with KT-10 xenografts were treated with 1 mg/kg NanoTLZ or vehicle (empty nanoparticles) IV on days 1, 3, and 5; or with 0.1625 or 0.33 mg/kg free TLZ by oral gavage daily for 5 days ($n =$ 8–10/group). Tumor diameters were measured weekly using digital calipers, and body weights were measured. Animals were euthanized when tumor volume reached 400% of the volume at start of treatment. Tumor responses were classified into 5 categories: progressive disease (PD), >25% increase in tumor volume; stable disease (SD), <25% increase in tumor volume and <50% regression; partial response (PR), regression ≥50% for at least one time point; complete response (CR), no measurable tumor (<0.04 cm^3); and maintained complete response (MCR), tumor volume <0.1 cm^3 at the end of the study (17).

NanoTLZ in Combination With TMZ

C.B.17SC *scid-/-* mice implanted with TC-71 ES xenografts were utilized to assess efficacy of NanoTLZ in combination with TMZ. The TC-71 model was selected as it does not respond to either TLZ or TMZ as a single agent but is responsive to the combination (17). Mice were treated with 1 mg/kg NanoTLZ IV on days 1, 3, and 5 combined with TMZ 50 mg/kg oral gavage (PO) daily for 5 days ($n = 10$/group). Tumor dimensions and body weight were measured twice weekly. Animals were euthanized when tumor volume reached 400% of the volume at start of treatment. Tumor responses were as described above.

Statistical Analysis

All *in vitro* data were plotted as mean ± SD. The statistical significance of *in vitro* data was determined by using Student's *t*-tests with $\alpha = 0.05$ for significance. *In vivo* efficacy data were plotted individually or as median relative tumor volume. Toxicity data were plotted as mean ± SEM. The log-rank test with the Bonferroni correction for multiple comparisons was used to assess family-wise significance of survival curves. All statistical testing computed with Prism 7.

RESULTS

Validation of NanoTLZ

NanoTLZ has been previously optimized and found to have stable physicochemical properties which impart advantages for nanoparticle mediated delivery of TLZ (21, 22). In order to validate NanoTLZ efficacy *in vitro*, ES-6, ES-7, and EW-8 ES cells were treated with either TLZ or NanoTLZ. All cell lines were found to have lower IC_{50} values in response to NanoTLZ (**Figure 1A**). Both NanoTLZ and TLZ were also found to potentiate the effect of TMZ in TC-71 cells (**Figure 1B**).

The PARP1 total and cleaved protein levels were evaluated in KT-10 xenograft model. This Wilms tumor model has shown previously to be sensitive to the free TLZ treatment, hence, it was used here to determine the effect of NanoTLZ on the target protein (10). As shown on **Figure 1C**, PARP1 levels were significantly reduced in tumor cells treated with TLZ or NanoTLZ compared to control or empty nanoparticle. The levels of cleaved PARP1 remained low overall in all treatment groups with slight increases of cleaved

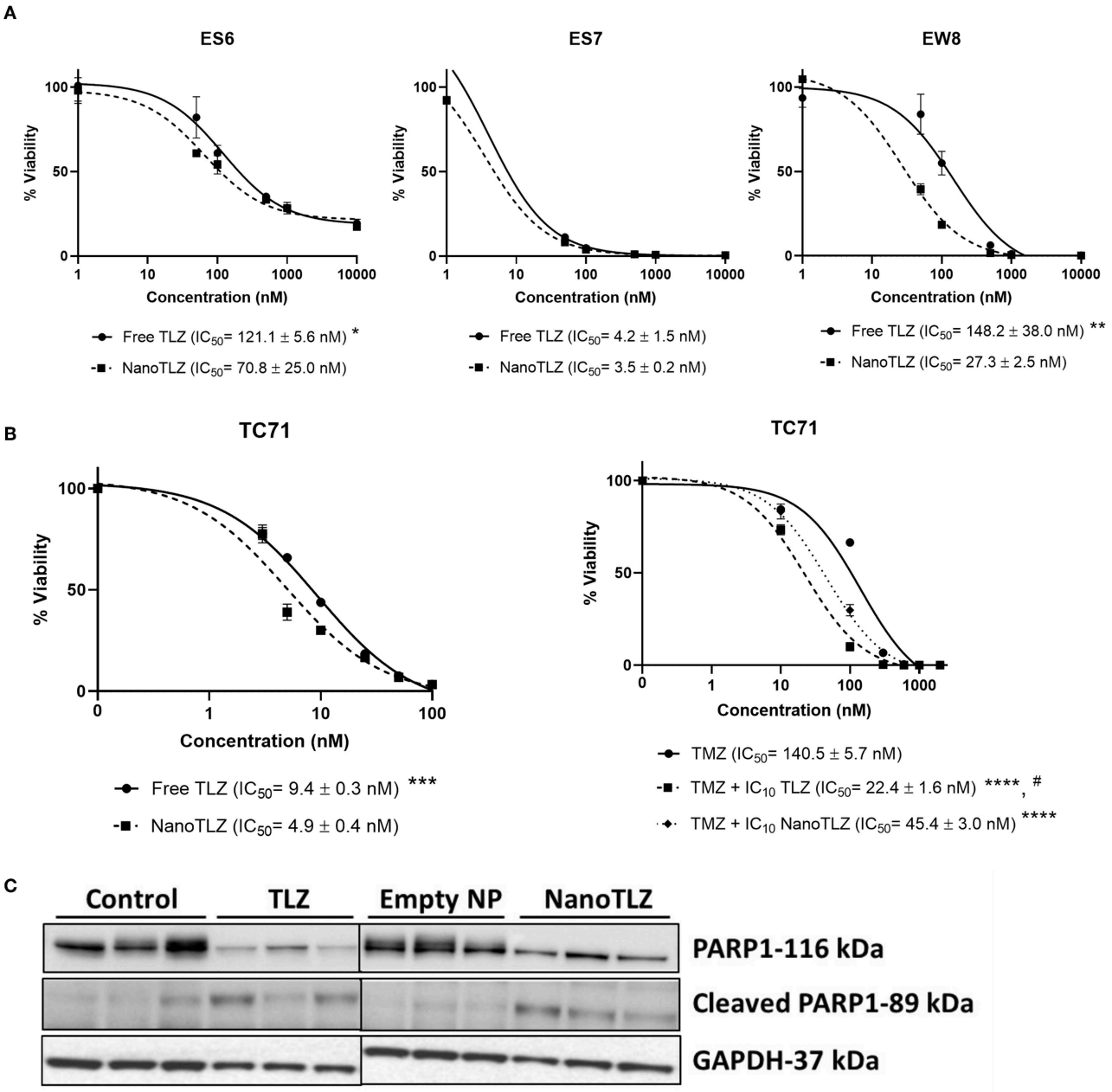

FIGURE 1 | NanoTLZ is as efficacious at free TLZ *in vitro.* ES-6, ES-7, and EW-8 cell lines were treated with TLZ or NanoTLZ for 72 h and viability was assessed by Alamar Blue ($n = 3$/line). IC_{50} plots for TLZ and NanoTLZ in ES-6, ES-7, and EW-8 cell lines **(A)**. Statistical significance of TLZ and NanoTLZ IC_{50} values were assessed for each cell line by Student's *t*-tests with $\alpha = 0.05$ for significance; $^{*}p < 0.05$ vs. NanoTLZ; $^{**}p < 0.01$ vs. NanoTLZ.TC-71 cells were treated with the IC_{10} of TLZ or NanoTLZ and dose response to TMZ was measured using Alamar Blue. Potentiation of TMZ activity in TC-71 cells combined with TLZ or NanoTLZ **(B)**. Statistical significance of TMZ, TLZ, and NanoTLZ combination IC_{50} values were assessed by one way ANOVA followed by Tukey's test for multiple comparisons; $^{***}p < 0.001$ vs. NanoTLZ; $^{****}p < 0.0001$ vs. TMZ; $^{\#}p < 0.001$ vs. TMZ + NanoTLZ. Mice harboring KT-10 xenografts were treated with 0.165 mg/kg TLZ BID x5 PO or 0.33 mg/kg NanoTLZ SID, IV, on days 1, 3, and 5. NanoTLZ and TLZ demonstrate inhibitory effect on total PARP1 protein levels in KT-10 tumor xenograft ($n = 3$/group) **(C)**.

PARP1 in TLZ and NanoTLZ treated cells indicating that neither of the drugs had strong apoptotic effect at the clinically relevant doses used before (0.165 mg/kg TLZ BID x5 PO and 0.33 mg/kg NanoTLZ SID, days 1, 3, and 5, IV) (17).

The efficacy of NanoTLZ relies on the EPR effect; therefore, it was crucial to ensure the particles accumulate at the tumor. NanoTLZ was fluorescently labeled *via* the encapsulation of Cyanine 5 (Cy5) dye. The addition of Cy5 did not significantly alter the diameter, polydispersity, or zeta potential

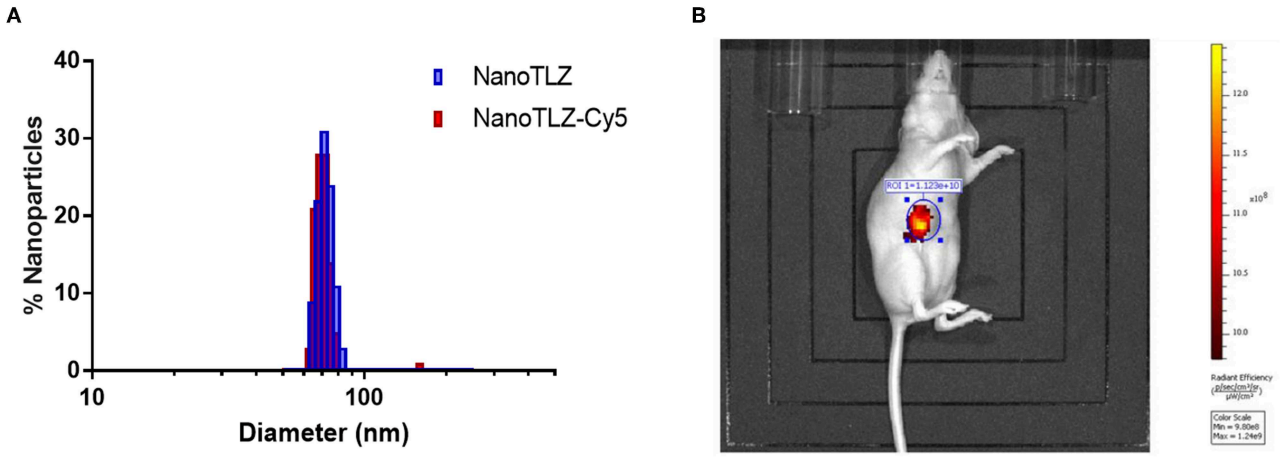

FIGURE 2 | NanoTLZ preferentially accumulates within tumors. The size distribution of NanoTLZ as measured by DLS does not change with the addition of Cy5 dye **(A)**. Live animal fluorescent imaging demonstrated NanoTLZ-Cy5 accumulates in the tumor 24 h after injection ($n = 3$) **(B)**.

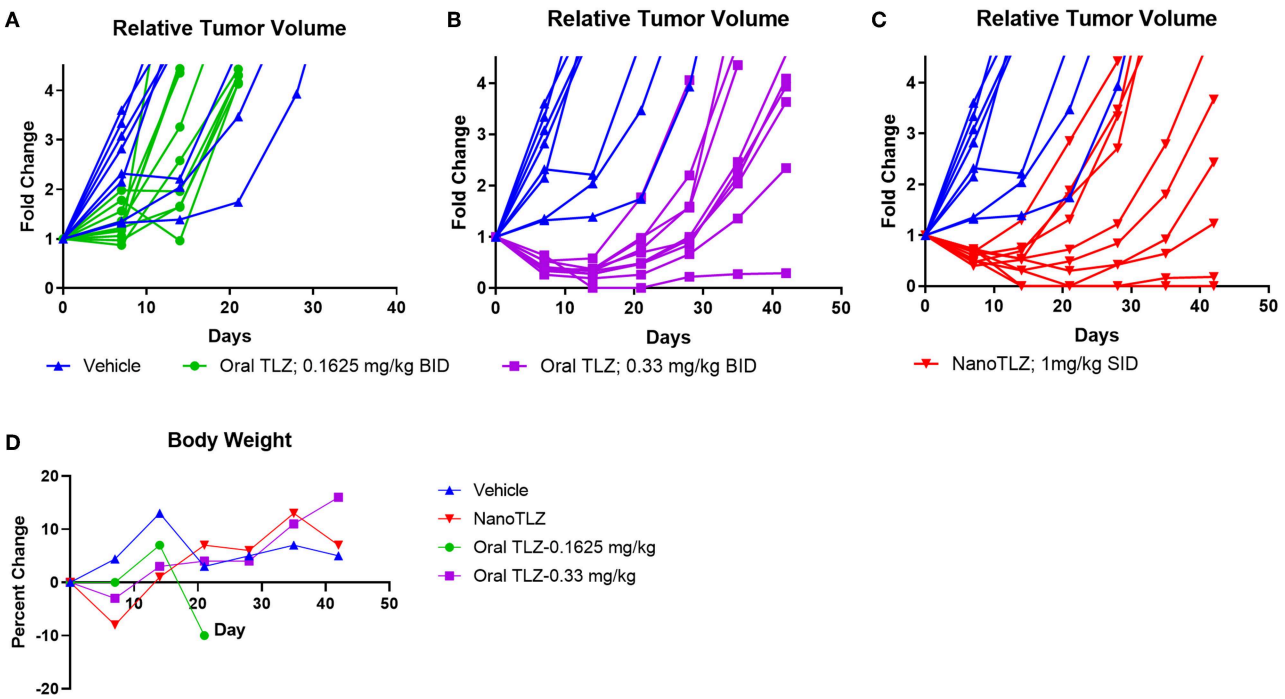

FIGURE 3 | KT-10 xenografts exhibit a dose dependent response to TLZ. Animals bearing KT-10 xenografts were treated with either 0.1625 mg/kg **(A)**, 0.33 mg/kg oral TLZ BID x 5 **(B)**, or 1.0 mg/kg NanoTLZ (IV) SID x 5 **(C)** and relative tumor volume was plotted for each animal ($n = 8$–10/group). Percent change in weight during and after treatment **(D)**.

of NanoTLZ, and therefore was optimal to assess tumor accumulation (**Figure 2A**). Twenty-four hours after a single dose of NanoTLZ-Cy5 was administered, fluorescence was observed localized to the tumor via live animal imaging (**Figure 2B**).

NanoTLZ Monotherapy

Toxicity testing was conducted to assess the MTD of single agent NanoTLZ. Doses of up to 1 mg/kg NanoTLZ (IV) administered daily (SID) on days 1, 3, and 5 and for 5 consecutive days were tolerated with no appreciable weight loss (data not shown). Therefore, 1 mg/kg on days 1, 3, and 5 was chosen to compare to oral TLZ therapy since the nanoformulation was expected to have a longer circulation time, and not require daily dosing.

As mentioned earlier, the KT-10 Wilms tumor PDX model has a PALB2 mutation, hence is defective in homologous recombination and is sensitive to TLZ (10). Animals bearing KT-10 xenografts were treated with either 0.1625 mg/kg or 0.33

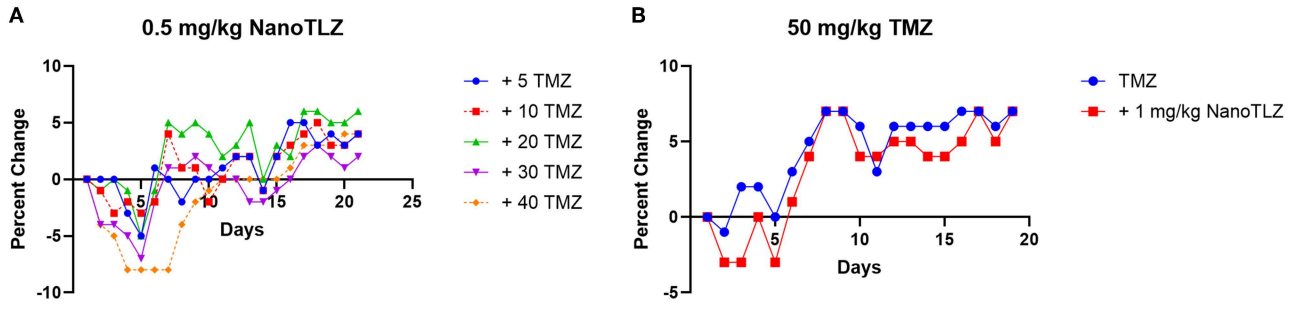

FIGURE 4 | NanoTLZ and TMZ are tolerable at higher doses than previously established with TLZ and TMZ. Tumor free mice ($n = 3$/group) were treated with 0.5 mg/kg NanoTLZ SID x5 in combination with increasing doses of TMZ and body weight was measured daily for 21 days **(A)**. An alternative schedule assessed weight change during treatment with 50 mg/kg TMZ for 5 days and 1.0 mg/kg NanoTLZ on days 1, 3, and 5 **(B)**.

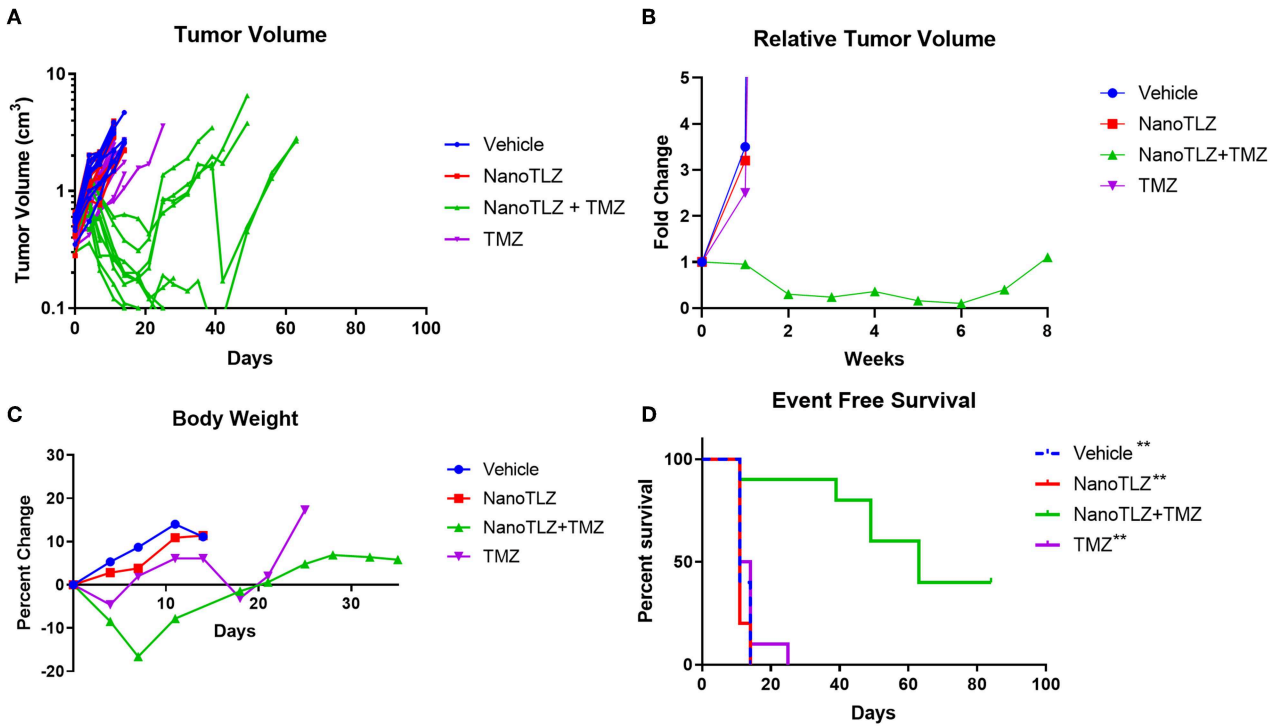

FIGURE 5 | TC-71 xenografts are responsive to the combination of NanoTLZ + TMZ. Mice bearing TC-71 xenografts ($n = 10$/group) were treated with 1 mg/kg vehicle or NanoTLZ (IV) on days 1, 3, and 5, 50 mg/kg TMZ (PO) on days 1–5, or the combination of the two and tumor volume was monitored twice weekly **(A)**. Median relative tumor volume during 8 weeks of treatment **(B)**. Change in body weight during and up to 30 days after treatment **(C)**. Kaplan-Meier survival of TC-71 xenografts for 12 weeks after treatment initiation **(D)**. Statistical significance assessed via the log-rank test followed by the Bonferroni correction for multiple comparisons, $^{**}p < 0.01$ vs. NanoTLZ+TMZ.

mg/kg free TLZ (PO) administered twice daily (BID) for 5 days. These doses were selected based on our previous testing of free TLZ (10). KT-10 tumors responded to TLZ treatment in a dose-dependent manner (**Figures 3A,B**). All tumors responded to oral TLZ and NanoTLZ therapy (**Figures 3B,C**). Most tumors in both treatment groups exhibited a partial response (PR) to therapy. However, 2/10 (20%) of tumors treated with NanoTLZ exhibited a complete response (CR), and 1/10 (10%) maintained complete response (MCR) over the course of the study. In contrast, only 10% of tumors treated with oral TLZ exhibited a CR to treatment. None of the treatments elicited significant weight loss throughout the course of the study (**Figure 3D**).

NanoTLZ Combined With TMZ

We previously established TC-71 xenografts are sensitive to the combination of TLZ and TMZ and therefore sought to explore the effect of utilizing NanoTLZ in combination with TMZ. Toxicity testing demonstrated the combination of NanoTLZ and TMZ daily for 5 days resulted in an average loss of ∼8% body weight at the highest dose of each drug (**Figure 4A**). The

combination of 1 mg/kg NanoTLZ on days 1, 3, and 5 and 50 mg/kg TMZ daily for 5 days resulted in an average loss of 3% body weight, therefore, this regimen was chosen for efficacy testing (**Figure 4B**). Treatment with 1 mg/kg NanoTLZ or empty nanoparticles IV on days 1, 3, and 5 did not yield any antitumor response (**Figures 5A,B**). Single agent TMZ, 50 mg/kg PO daily for 5 days, also was not active in this model as evidenced by the median fold change in tumor volume (**Figure 5B**). The combination of NanoTLZ+TMZ was active with all tumors initially responding to the treatment (**Figure 5A**). Progressive disease (PR) was observed in both single agent control arms, while 4/10 (40%) of tumors exhibited a PR to the combination and an additional 40% of tumors maintained a CR.

The combination therapy did elicit acute weight loss of 16.6% during the treatment cycle, but animals recovered after the treatment period (**Figure 5C**). Twenty percent weight loss is considered to be acceptable per the Pediatric Preclinical Testing Program (PPTP) protocol used in this study (10, 17). One animal treated with the combination therapy did not tolerate the treatment and was found dead the week after completing treatment. TMZ at the same dose only resulted in a loss of 4.6% body weight during the treatment period, while NanoTLZ elicited no weight loss throughout the study.

The combination of NanoTLZ and TMZ significantly extended the overall survival compared to the vehicle control and single agent groups (**Figure 5D**). The median survival time was 11–14 days in the control groups compared to 63 days in the combination group ($^{**}p < 0.01$). At the end of the observation period 4/10 mice treated with NanoTLZ and TMZ had no palpable tumors.

DISCUSSION

The combination of TLZ and TMZ has demonstrated substantial activity in a number of ES models, however, toxicity necessitated TMZ dose reduction. In order to bypass some of the limitations associated with oral drug delivery a nanoformulation of TLZ, NanoTLZ, was assessed in two different xenograft models. *In vitro* comparison of TLZ and NanoTLZ demonstrated NanoTLZ was as potent if not more potent than TLZ, as evidenced by the IC_{50} values. Both TLZ and NanoTLZ potentiated the effect of TMZ in TC71 cells, though TLZ was more efficient than NanoTLZ. Together, these results indicated NanoTLZ is of similar potency to free TLZ and should be assessed *in vivo*. *In vivo* imaging demonstrated that NanoTLZ preferentially accumulates in tumors, likely through the EPR effect, and presents a pronounced target inhibition effect. This suggests that more drug may be delivered to the tumor resulting in less drug accumulation in other organs. It was expected this would decrease the systemic toxicity observed with oral TLZ delivery.

KT-10 xenografts have demonstrated dose dependent response to single agent TLZ and therefore, this model was utilized in order to ensure NanoTLZ maintained efficacy *in vivo*. Both NanoTLZ at 1 mg/kg SID and oral TLZ at 0.33 mg/kg BID induced similar responses. However, 3/10 of animals treated with NanoTLZ exhibited a CR with 1/3 MCR until the end of the study, while only 1/10 of animals treated with oral TLZ exhibited a CR. It is important to note that animals receiving NanoTLZ treatment received 33% more drug daily than those on oral TLZ treatment because NanoTLZ was found to be more tolerable than oral TLZ. This higher dose is likely one factor contributing to the enhanced response rate. PARP inhibitors have been shown to exhibit a better anti-tumor effect when PARP is at least 90% inhibited (24, 25). One strategy for achieving long-term inhibition is twice daily administration, as was done with the oral treatment. Previous studies have demonstrated plasma drug concentrations after a single dose of NanoTLZ can be fit with a two compartment model yielding a terminal half-life of 37.5 h (22). The extended half-life of the nanoformulation lead to a similar antitumor effect with only a single injection daily, compared to the twice daily oral administration.

Although ES cell lines were found to be sensitive to PARP inhibitors *in vitro*, the lack of *in vivo* translation necessitated the need to develop rational combinations. The PPTP previously demonstrated 6/10 ES xenografts were sensitive to the combination of TLZ and TMZ (17). Two different combination doses were found to be tolerable when combining the two oral drugs, but both required substantial dose reduction of either TLZ or TMZ. Previous tolerable doses were 30 mg/kg TMZ SID x 5 + 0.1 mg/kg TLZ BID x5, or 12 mg/kg TMZ SID x 5 + 0.25 mg/kg TLZ BID x5 (17). Toxicity testing with NanoTLZ in combination with oral TMZ indicated the combination was better tolerated than the combination of the two free drugs, allowing each drug to be delivered at a higher dose than in the previous study. The combination of 1 mg/kg NanoTLZ administered on days 1, 3, and 5, with 50 mg/kg TMZ SID x5 induced a response in all tumors with a PR in 4/10 and MCR in 4/10 tumors 12 weeks post treatment initiation. Although little weight loss was observed during the MTD testing this treatment regimen did induce acute weight loss (<20%) during the treatment period in the efficacy study, but this was reversed when the treatment ended. The MTD testing was conducted in tumor-free mice and differences in weight loss may be attributed to the shrinking tumors or the presence of the tumors themselves, both of which may affect body weight. The combination of NanoTLZ and oral TMZ significantly extended overall survival compared to each of the single agent controls.

The data presented here demonstrates that changing the delivery system from oral TLZ to NanoTLZ provides an opportunity to modify the dosing required for combination therapy. NanoTLZ was tolerated at a higher total dose compared with free TLZ, and allowed combination with higher doses of TMZ. The KT-10 data demonstrated NanoTLZ administered once daily at a high dose achieved a similar response to twice daily lower dosing, indicating the pharmacokinetics had been altered. The combination of NanoTLZ and TMZ in TC-71 xenografts was promising, but perhaps a better response could be elicited with a lower dose of NanoTLZ administered daily.

NanoTLZ demonstrates similar activity *in vivo* as oral TLZ, but only requires once daily dosing rather than twice daily. It is better tolerated than the oral formulation, which allows for higher doses to be administered. NanoTLZ administered every other day for 5 days effectively potentiated

the effect of daily TMZ treatment with 40% of animals being tumor free after 12 weeks. The combination of oral TLZ and TMZ has previously demonstrated both preclinical and clinical toxicity; therefore, NanoTLZ can provide greater versatility in further exploring the best way to limit systemic toxicity while maximizing the effect of this combination.

DATA AVAILABILITY STATEMENT

The datasets generated for this study are available on request to the corresponding author.

ETHICS STATEMENT

The animal study was reviewed and approved by the Institutional Animal Care and Use Committee (IACUC) reviewed and approved at the University of Texas Health at San Antonio or Northeastern University.

AUTHOR CONTRIBUTIONS

PB, RK, and SS designed the research. PB, RC, NB, JC, and RL performed the research. PB and RK analyzed the data. PB wrote the manuscript. RK and SS edited the manuscript.

FUNDING

This work was partially supported with funding from the Greehey Children's Cancer Research Institute at The University of Texas Health at San Antonio (RK) and partially funded by the Nanomedicine Innovation Center at Northeastern University (SS).

ACKNOWLEDGMENTS

We would like to thank personnel in the GCCRI Xenograft Core, particularly Mr. Edward Favours and Dr. Abhik Bandyopadhyay, for their excellent technical support.

REFERENCES

1. Esiashvili N, Goodman M, Marcus RB. Changes in incidence and survival of ewing sarcoma patients over the past 3 decades. *J Pediatr Hematol Oncol.* (2008) 30:425–30. doi: 10.1097/MPH.0b013e31816e22f3
2. Rodriguez-Galindo C. Pharmacological management of Ewing sarcoma family of tumours. *Expert Opin Pharmacother.* (2004) 5:1257–70. doi: 10.1517/14656566.5.6.1257
3. Kushner BH, Qin J, LaQuaglia MP, Gorlick R, Kolb EA, Meyers PA, et al. Long-term event-free survival after intensive chemotherapy for Ewing's family of tumors in children and young adults. *J Clin Oncol.* (2003) 21:3423–30. doi: 10.1200/JCO.2003.10.033
4. Aurias A, Rimbaut C, Buffe D, Zucker JM, Mazabraud A. Translocation involving chromosome 22 in Ewing's sarcoma. A cytogenetic study of four fresh tumors. *Cancer Genet Cytogenet.* (1984) 12:21–5. doi: 10.1016/0165-4608(84)90003-7
5. Turc-Carel C, Aurias A, Mugneret F, Lizard S, Sidaner I, Volk C, et al. Chromosomes in Ewing's sarcoma. I. An evaluation of 85 cases of remarkable consistency of t(11;22)(q24;q12). *Cancer Genet Cytogenet.* (1988) 32:229–38. doi: 10.1016/0165-4608(88)90285-3
6. Delattre O, Zucman J, Plougastel B, Desmaze C, Melot T, Peter M, et al. Gene fusion with an ETS DNA-binding domain caused by chromosome translocation in human tumours. *Nature.* (1992) 359:162–5. doi: 10.1038/359162a0
7. Sorensen PHB, Lessnick SL, Lopez-Terrada D, Liu XF, Triche TJ, Denny CT. A second Ewing's sarcoma translocation, t(21;22), fuses the EWS gene to another ETS–family transcription factor, ERG. *Nat Genet.* (1994) 6:146–51. doi: 10.1038/ng0294-146
8. Potratz J, Dirksen U, Jürgens H, Craft A. Ewing sarcoma: clinical state-of-the-art. *Pediatr Hematol Oncol.* (2012) 29:1–1. doi: 10.3109/08880018.2011.622034
9. Goyal SV, Feng FY, Tomlins SA, Prensner JR, Patel S, Liu M, et al. PARP-1 inhibition as a targeted strategy to treat Ewing's sarcoma. *Cancer Res.* (2012) 72:1608–13. doi: 10.1158/0008-5472.CAN-11-3648
10. Smith MA, Hampton OA, Reynolds CP, Kang MH, Maris JM, Gorlick R, et al. Initial testing (stage 1) of the PARP inhibitor BMN 673 by the pediatric preclinical testing program: PALB2 mutation predicts exceptional *in vivo* response to BMN 673. *Pediatr Blood Cancer.* (2015) 62:91–8. doi: 10.1002/pbc.25201
11. Brenner JC, Ateeq B, Li Y, Yocum AK, Cao Q, Asangani IA, et al. Mechanistic rationale for inhibition of Poly(ADP-Ribose) polymerase in ETS gene fusion-positive prostate cancer. *Cancer Cell.* (2011) 19:664–78. doi: 10.1016/j.ccr.2011.04.010
12. Garnett MJ, Edelman EJ, Heidorn SJ, Greenman CD, Dastur A, Lau KW, et al. Systematic identification of genomic markers of drug sensitivity in cancer cells. *Nature.* (2012) 483:570–5. doi: 10.1038/nature11005
13. Choy E, Butrynski JE, Harmon DC, Morgan JA, George S, Wagner AJ, et al. Phase II study of olaparib in patients with refractory Ewing sarcoma following failure of standard chemotherapy. *BMC Cancer.* (2014) 14:813. doi: 10.1186/1471-2407-14-813
14. Vormoor B, Curtin NJ. Poly(ADP-ribose) polymerase inhibitors in Ewing sarcoma. *Curr Opin Oncol.* (2014) 26:428–33. doi: 10.1097/CCO.0000000000000091
15. Shen Y, Rehman FL, Feng Y, Boshuizen J, Bajrami I, Elliott R, et al. BMN 673, a novel and highly potent PARP1/2 inhibitor for the treatment of human cancers with DNA repair deficiency. *Clin Cancer Res.* (2013) 19:5003–15. doi: 10.1158/1078-0432.CCR-13-1391
16. Liu X, Shi Y, Guan R, Donawho C, Luo Y, Palma J, et al. Potentiation of temozolomide cytotoxicity by Poly(ADP)Ribose polymerase inhibitor ABT-888 requires a conversion of single-stranded DNA damages to double-stranded DNA breaks. *Mol Cancer Res.* (2008) 6:1621–9. doi: 10.1158/1541-7786.MCR-08-0240
17. Smith MA, Reynolds CP, Kang MH, Kolb EA, Gorlick R, Carol H, et al. Synergistic activity of PARP inhibition by talazoparib (BMN 673) with temozolomide in pediatric cancer models in the pediatric preclinical testing program. *Clin Cancer Res.* (2015) 21:819–32. doi: 10.1158/1078-0432.CCR-14-2572
18. Park J, Fong PM, Lu J, Russell KS, Booth CJ, Saltzman WM, et al. PEGylated PLGA nanoparticles for the improved delivery of doxorubicin. *Nanomedicine.* (2009) 5:410–8. doi: 10.1016/j.nano.2009.02.002
19. Zhang L, Gu F, Chan J, Wang A, Langer R, Farokhzad O. Nanoparticles in medicine: therapeutic applications and developments. *Clin Pharmacol Ther.* (2008) 83:761–9. doi: 10.1038/sj.clpt.6100400
20. Maeda H. The enhanced permeability and retention (EPR) effect in tumor vasculature: the key role of tumor-selective macromolecular drug targeting. *Adv Enzyme Regul.* (2001) 41:189–207. doi: 10.1016/S0065-2571(00)00013-3
21. Baldwin P, Ohman A, Medina J, McCarthy E, Dinulescu D, Sridhar S. Nanoformulation of talazoparib delays tumor progression and ascites formation in a late stage cancer model. *Front Oncol.* (2019) 9:353. doi: 10.3389/fonc.2019.00353
22. Zhang D, Baldwin P, Leal AS, Carapellucci S, Sridhar S, Liby KT. A nano-liposome formulation of the PARP inhibitor Talazoparib enhances

treatment efficacy and modulates immune cell populations in mammary tumors of BRCA-deficient mice. *Theranostics.* (2019); 9:6224–38. doi: 10.7150/thno.36281

23. Zhang Y, Sriraman SK, Kenny HA, Luther E, Torchilin V, Lengyel E. Reversal of chemoresistance in ovarian cancer by co-delivery of a P-glycoprotein inhibitor and paclitaxel in a liposomal platform. *Mol Cancer Ther*. (2016) 15:2282–93. doi: 10.1158/1535-7163.MCT-15-0986
24. Kim G, Ison G, McKee AE, Zhang H, Tang S, Gwise T, et al. FDA approval summary: olaparib monotherapy in patients with deleterious germline BRCA-mutated advanced ovarian cancer treated with three or more lines of chemotherapy. *Clin Cancer Res.* (2015) 21:4257–61. doi: 10.1158/1078-0432.CCR-15-0887
25. CDER Pharmacology, Clinical Evaluation CFDR. *Center for Drug Evaluation and Clinical Pharmacology and Biopharmaceutics Review*. Olaparib (2013).

Conflict of Interest: The authors declare that the research was conducted in the absence of any commercial or financial relationships that could be construed as a potential conflict of interest.

frontiers in Oncology

REVIEW
published: 17 January 2020
doi: 10.3389/fonc.2019.01538

The Interplay Between the DNA Damage Response, RNA Processing and Extracellular Vesicles

Xiangbing Meng[1,2]*, *Shujie Yang*[1,2]* and *Vanessa J. A. Camp*[1]

[1] Department of Pathology, Carver College of Medicine, University of Iowa, Iowa City, IA, United States, [2] Holden Comprehensive Cancer Center, Carver College of Medicine, University of Iowa, Iowa City, IA, United States

RNA processing was recently found to affect DNA damage response. The RNA processing factors THRAP3 and BCLAF1 play critical role in keeping DNA genomic stability by regulating the transcription, mRNA splicing and export of DNA repair proteins BRCA2, PALB2, Rad51, FANCD2, and FANCL in response to DNA damage. RNA processing factors THRAP3 and BCLAF1 play critical roles in maintaining DNA genomic stability. These factors regulate transcription, mRNA splicing and nuclear RNA export of DNA repair proteins BRCA2, PALB2, Rad51, FANCD2, and FANCL in response to DNA damage. Splicing factors SRSF10 and Sam68 were found to control the DNA damage agent-induced mRNA splicing of transcripts including BCLAF1, BRCA1, BCL2L1, CASP8, CHK2, and RBBP8 to regulate apoptosis, cell-cycle transition and DNA repair. Splicing factors and RNA binding proteins (RBPs) were also found to play a critical role in DNA/RNA hybrids (R-loops) formed during transcription and RNA processing to prevent RNA-induced genome instability. At the same time, DNA repair proteins FANCI and FANCD2 were found to regulate the nuclear localization of splicing factors SF3B1 in the DNA damage response. In addition, tumor-derived extracellular vesicles (Evs) enhanced by chemotherapeutic agents in cancer were found to promote cancer metastasis and drug resistance. Inhibiting Evs from cancer cells significantly reduced cancer metastasis and drug resistance. Furthermore, cross-talk between the DNA damage response and the immune response was observed including the enhancement of the efficacy of immune checkpoint blockade by PARP inhibitors and the effect of PD-L1 on mRNA stability of various mRNAs involved in DNA damage response by acting as a novel RNA binding protein to increase drug resistance in cancer cells. This review will introduce recent progress on the interplay of the DNA damage response, the RNA processing and the extracellular vesicles mediated metastasis.

Keywords: THRAP3, BCLAF1, RNA processing, extracellular vesicles, R-loops, RBPs, PD-L1

OPEN ACCESS

Edited by:
Michaela Medová,
University Hospital Bern, Switzerland

Reviewed by:
Souparno Bhattacharya,
AstraZeneca, United States
Vandna Kukshal,
Washington University School of Medicine in St. Louis, United States

***Correspondence:**
Xiangbing Meng
xiangbing-meng@uiowa.edu
Shujie Yang
shujie-yang@uiowa.edu

Specialty section:
This article was submitted to Molecular and Cellular Oncology, a section of the journal Frontiers in Oncology

Received: *19 September 2019*
Accepted: *19 December 2019*
Published: *17 January 2020*

Citation:
Meng X, Yang S and Camp VJA (2020) The Interplay Between the DNA Damage Response, RNA Processing and Extracellular Vesicles. Front. Oncol. 9:1538. doi: 10.3389/fonc.2019.01538

INTRODUCTION

Generally, RNA processing is not included in DNA damage response network, which is mainly consisted of DNA repair proteins, cell cycle checkpoint regulators, PI3K-like kinases ATM, ATR, or DNA-PK and downstream kinases Chk1 and Chk2. However, recent studies indicate RNA processing directly involves in traditional DNA damage repair mediated by BRCA1 (1) and BRCA2

(2, 3). Many observations indicate that there are connections between DNA damage and immune system activation. Intracellular immune checkpoint protein PD-L1 was fond to regulate DNA damage response by acting as RNA binding proteins to regulate many DNA repair proteins (4). DNA damage also can activate immune system (5–7). In this review, we will introduce recent progression on how RNA processing cross-talk with cellular response to DNA damage and the connections between immune system with cellular response to DNA damage including how immune checkpoint protein PD-L1 regulates cellular response to DNA damage and how DNA damage can active immune system.

RNA Processing Factors Also Function in Maintaining DNA Genomic Stability

RNA-processing factors function in the maintenance of genome stability; they regulate mRNAs encoding for DNA repair proteins or directly involve in DNA damage responses by interacting with DNA repair proteins. For example, RBM14 is an RNAbp and joins the PARP-dependent DSB repair by interacting with PARP1 (8). Other RNA-binding proteins including FUS/TLS, EWS, TARF15, and some hnRNPs also play important roles in the PARP-dependent DSB repair process (8, 9). mRNA splicing factor hnRNP C is another example required for PALB2/BRCA2 nucleoprotein complex function in DNA repair (3). Knockdown of hnRNP C caused the expression reduction of DNA repair proteins including BRCA1, BRCA2, RAD51, and BRIP1 at both the mRNA level and the protein level (10). BCLAF1 (1) is a BRCA1 binding partner at the BRCA1-mRNA splicing complex induced by DNA damage, which was named as a Bcl2-associated transcription factor to promote apoptosis. BRCA1/BCLAF1 target genes include *ATRIP*, *BACH1*, and *EXO1* (1). Besides BCLAF1, the DNA damage-induced BRCA1 protein complex includes BRCA1, Prp8, U2AF65, U2AF35, and SF3B1 (1). Depletion of BRCA1, BCLAF1, and U2AF65 increases sensitivity to DNA damage and causes defective DNA repair. A high incidence of somatic mutations of BCLAF1, U2AF65, U2AF35, SRSF2, SF3A1, SF3B1, and PRPF40B at the BRCA1/BCLAF1 mRNA splicing complex was reported in various cancer types (1). Most transcription and pre-mRNA splicing processes are inhibited in response to DNA damage. However, transcription, pre-mRNA splicing and mRNA exportation from the nucleus are active in response to DNA damage for DNA damage response (DDR) genes including BRCA2, PALB2, Rad51, FANCD2, and FANCL (11). These genes are required for DNA damage repair to maintain genomic stability and are regulated by RNAbps THRAP3 and BCLAF1 in response to DNA damage. Depletion of both BCLAF1 and THRAP3 leads to the reduction of mRNA splicing, downregulation of the export of BCLAF1/THRAP3 target genes, and the loss of their encoded proteins compared to mild effects by depletion of THRAP3 or BCLAF1 alone (**Figure 1**) (11).

Splicing Factors and RNA Helicases Are Involved in Cellular Responses DNA Damage

During the DNA damage response, splicing factors and RNA helicases play integral roles in gene expression. mRNA interactome capture was utilized to identify proteins that were highly enriched in mRNA metabolic processes and components of the nucleolar proteome, including several RNA helicases DDX5/p68, DDX1, SLFN11, and DDX3X (9). DDX54 is one of the 266 RBPs in the DDR proteins with increased binding to poly (A)+ RNA upon IR exposure (9). The interaction of DDX54 with specific proteins of core spliceosomal complexes B (CDC40), C(DDX41), and U2 snRNP including SF3B1, DDX42, U2AF1, and DHX8 was increased upon IR exposure (9). Another example of RNAbp in cellular responses to DNA damage is MFAP1 (microfibrillar-associated protein 1), a spliceosome-associated factor. MFAP1 depletion induced the increase of γH2AX foci and DNA breaks by causing alterations of mRNA splicing and gene expression of target genes involved in cellular responses to DNA damage (12).

DNA Damage Induces the Alterations of RNA Splicing of Many Transcripts Involved in Genomic Stability Maintenance

DNA damage induced by oxaliplatin was found to change the binding and activity of several regulatory RNA binding proteins including SRSF10, hnRNP A1/A2, and Sam68 on the Bcl-x pre-mRNA to alter splice site selection and to increase the level of pro-apoptotic Bcl-xS (13, 14). These RNA binding proteins also collaborate to drive the DNA damage-induced splicing alteration of several transcripts involved in cellular response to DNA damage including BCLAF1, BRCA1, BCL2L1, CASP8, and CHK2 (**Figure 1**) (13, 14). Mutations of the RNA processing factors result in the increase of spicing isoforms of DNA repair proteins including BARD1β, FANCEΔ4, and BRCA1-Δ11q in cancers. BRCA1-associated RING domain protein 1 (BARD1) splice variant (SV), BARD1β, can sensitize colon cancer cells to poly ADP ribose polymerase 1 (PARP-1) inhibition by impairing BRCA1 mediated DNA homologous recombination repair (15). FANCE splice isoform (FANCEΔ4) impaired mono-ubiquitination of FANCD2 and FANCI, which inhibits the FA-BRCA pathway (16). A BRCA1-Δ11q splice variant lacking part of exon 11 still contributes to drug resistance to PARP inhibitors and cisplatin. Spliceosome inhibitors can reduce BRCA1-Δ11q levels and increase sensitivity to PARP inhibitors and cisplatin in cancer cells carrying exon 11 mutations of BRCA1 (17).

DNA Repair Proteins Function to Prevent Co-transcriptional R-loop-Associated DNA Damage

RNA–DNA hybrids (R-loops) have been associated with genomic instability in human diseases including cancer and neurological diseases. RNases H are a family of endonucleases that hydrolyze RNA residues in RNA/DNA hybrids to prevent the accumulation

Abbreviations: FUS/TLS, fused in sarcoma/translocated in sarcoma; EWS, Ewing sarcoma; TARF15, TATA box-binding protein-associated factor 68 kDa; hnRNPs, heterogeneous nuclear ribonucleoproteins; MFAP1, microfibrillar-associated protein 1; IRF3, interferon regulatory factor 3; STING, STimulator of Interferon Genes; TBK1, TANK binding kinase 1; IRF3, interferon regulatory factor 3; Evs, extracellular vesicles; RNAbps, RNA binding proteins; R-loops, DNA/RNA hybrids.

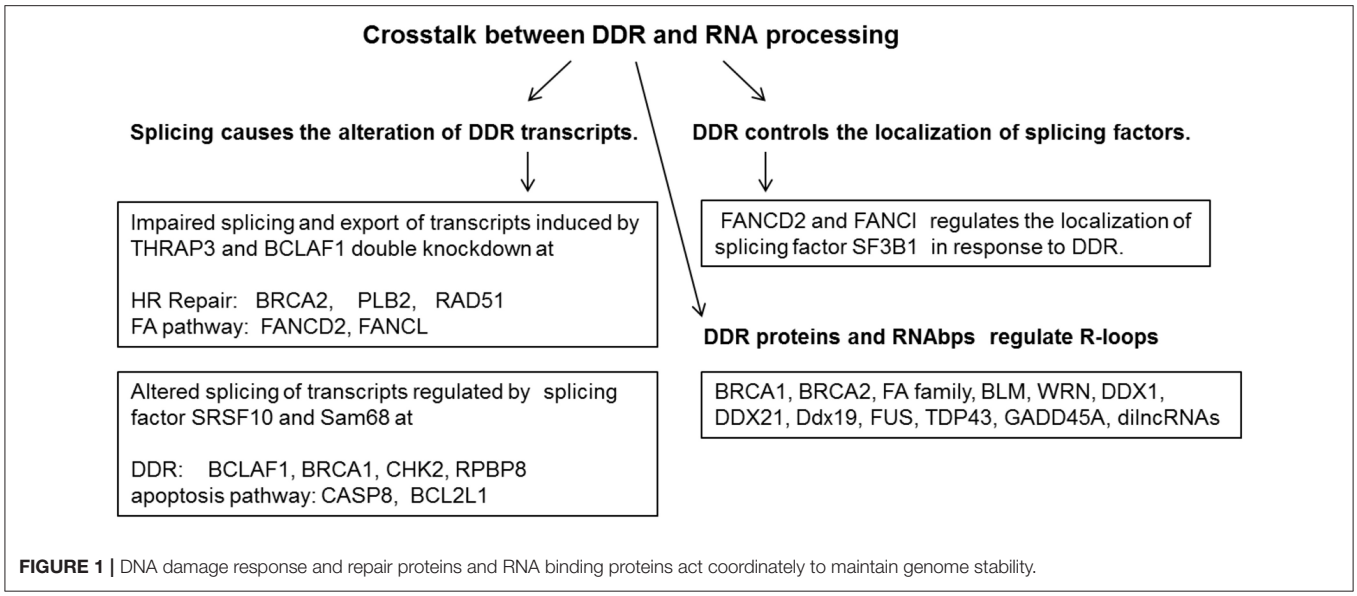

FIGURE 1 | DNA damage response and repair proteins and RNA binding proteins act coordinately to maintain genome stability.

of R-loops for the maintenance of genome stability (18). The ssDNA-binding protein replication protein A (RPA) interacts with RNaseH1 at R loops in cells. RPA acts as a sensor of R loops and a regulator of RNaseH1 in suppression of genomic instability (19). Genome-wide RNA-loops are studied by S9.6 antibody CHIP against RNA–DNA hybrids and RNAse H1 R-ChIP. A catalytically inactive RNASEH1 that can bind RNA–DNA hybrids but not resolve them is used in RNAse H1 R-ChIP (18). In contrast to the S9.6 antibody, RNASEH1 has a higher affinity for RNA-DNA hydrids (20). Using S9.6 antibody coupled to mass spectrometry, SRSF1, FACT, and Top1, were identified as R-loop-associated factors. DHX9 helicase promotes R-loop suppression and transcriptional termination. Endonuclease RNase H and helicases DHX9 (20) and SETX are known to resolve the R-loop (21). The RNA/DNA hybrid interactome is a useful resource to study R-loop biology (22). R-loops at CTG.CAG tracts are vulnerable to cause DNA instability (22–25). Enhanced R-loops formation are observed at gene-specific repeat expansions in many genetic disorders such as Huntington's disease [CAG repeats], and fragile X mental retardation or fragile X syndrome (FXS). These well-known neurological diseases are associated with abnormal R-loops accumulation at trinucleotide repeat (22–25). Splicing factors and RNA binding proteins (RBPs) play critical role in DNA/RNA hybrids (R-loops) to prevent RNA-induced genome instability (26). Although no clear mechanisms have been identified, many DNA repair proteins, RNA binding proteins and long non-coding RNAs are involved in suppression R-loops formation as shown in **Table 1**.

TABLE 1 | Known factors involved in R-loops.

Factors	Function
BRCA1 and SETX complex	Suppresses R-loop associated DNA damage
BRCA2 and PAF1	Prevent R-loops accumulation
FA pathway	Prevent R-loops accumulation
RECQ like helicases Sgs1and BLM	Regulate R-loop-associated genome instability
WRN	Prevents R-loop-associated genomic instability
RNA helicases DDX1, DDX21, and Ddx19	Reduce R·loops formation
RNA processing proteins FUS and TDP43	Inhibit R loops-associated DNA damage
GA0045A	R-loops dependent TET1 binding CpG islands at promoters
Long non-coding RNAs (dilncRNAs)	Required for R-loop-driven DNA damage repair

The BRCA1 and SETX Complex Suppresses R-loop-Associated DNA Damage

Senataxin (SETX) is a RNA/DNA helicase and a BRCA1 interacting protein identified by yeast two hybrid assays and MS-based BRCA1/protein interaction screens (21). Knockout SETX gene leads to a defect in reproduction in male mice. Mutations of SETX is found in two distinct neurological disorders including ataxia with oculomotor apraxia type 2 (26) and a juvenile form of ALS (27). BRCA1 and SETX complex is recruited to suppress co-transcriptional R-loop-associated DNA damage (21). A deficiency in BRCA1/SETX complex results in unrepaired ssDNA breaks and increases of γ-H2Ax signal.

Inactivated BRCA2 and Depleted PAF1 Cause the R-loops Accumulation

R-loops are frequently found in BRCA2-deficient cancer cells. BRCA2 is involved in the release of RNA polymerase II (RNAPII) from promoter-proximal pausing (PPP) sites. BRCA2 inactivation decreases RNAPII-associated factor 1 (PAF1) recruitment and impedes nascent RNA synthesis. PAF1 depletion also causes the R-loop accumulation (2, 3).

The FA Pathway Plays a Role in Preventing R-loop Accumulation

The FA pathway prevents R loop accumulation that hinders replication fork (RF) progression and results in DNA breaks.

FANCD2 foci increase in untreated and MMC-treated cells defective in FANCD2 or FANCA indicates that the FA functions at R loop. FANCD2 was found to interact and recruit RNA processing (28–30) enzymes hnRNPU and DDX47 to R-loops during mild replication stress (33). BRCA2/FANCD1 and FANCD2/FANCI were found to protect stalled replication forks, indicating that the Fanconi Anemia (FA) pathway may take a role in preventing R loop-dependent genome instability. The Fanconi anemia (FA) pathway is critical to repair inter-strand DNA cross-links (ICLs). However, a 5′ exonuclease, SAN1, is involved in ICLs independent of the FA pathway. Knockout of SAN1 increases sensitivity to ICLs. SAN1 was found to interact with senataxin (SETX) to resolve R-loops to prevent cross-link sensitivity (28–30).

R-loop-Associated Genome Instability Is Regulated by RECQ-Like Helicases Sgs1 and BLM

Sgs1 is the ortholog of human Bloom's syndrome helicase BLM in yeast. The loss of *SGS1* increases R-loop accumulation. BLM has been confirmed in suppressing R-loop in Bloom's syndrome fibroblasts or by depletion of BLM in human cancer cells (31).

WRN Is a Regulator for R-loop-Associated Genomic Instability

Werner syndrome (WS) is a rare, autosomal recessive disorder characterized by the appearance of premature aging caused by deficiency of Werner protein (WRN). WRN deficiency sensitizes cells to replication- transcription collisions and promotes accumulation of R-loops. WS cells show impaired ATR-mediated CHK1 activation to mild replication stress. WS cells prevent chromosomal instability by ATM mediated activation of CHK1 (32).

RNA Helicases DDX1, DDX21, and Ddx19 Are Involved in Reducing R-loops

RNA helicase DDX1 is necessary to maintain the single-stranded DNA generated by end resection. DDX1 plays a role in resolving RNA-DNA structures accumulated at sites of active transcription with DSBs (33). Knockdown of SIRT7 as well as depletion of DDX21 leads to the increased formation of R loops and DNA double-strand breaks, indicating that DDX21 and SIRT7 mediated deacetylation of DDX21 cooperate to prevent R-loop accumulation (34). The nucleopore- associated mRNA export factor Ddx19 was activated by ATR/Chk1 and re-localized to the nucleus to remove nuclear R-loops upon replication stress or DNA damage. Ddx19 resolves R-loops *in vitro* via its helicase activity (35).

RNA Processing Proteins FUS and TDP43 Are Involved in R-loop-Associated DNA Damage

FUS and TDP43 are linked to Amyotrophic lateral sclerosis (ALS), a progressive motor neuron dysfunction disease. FUS or TDP43 depletion leads to an accumulation of transcription- associated DNA damage and increased sensitivity to a transcription-arresting agent. FUS or TDP43 normally contribute to the prevention of transcription-associated DNA damage (36).

GADD45A Is Involved in R-loops Dependent TET1 Binding CpG Islands at Promoters

R-loops are enriched at CpG islands (CGIs) to regulate chromatin states. GADD45A (growth arrest and DNA damage protein 45A) is an epigenetic R-loop reader to recruit the demethylation machinery at promoter CGIs. GADD45A binds to R-loops and recruits TET1 (ten-eleven translocation 1) to promote DNA demethylation at the promoter of tumor suppressor TCF21. The antisense long non-coding (lncRNA) TARID (TCF21 antisense RNA inducing promoter demethylation) forms an R-loop at the TCF21 promoter and the binding of GADD45A to the R-loop triggers local DNA demethylation and TCF21 expression. Thousands of R-loop-dependent TET1 binding sites at CGIs is identified in embryonic stem cells by genomic profiling (37).

Long Non-coding RNAs (dilncRNAs) Are Required for R-loop-Driven DNA Damage Repair

Damage-induced long non-coding RNAs (dilncRNAs) are transcribed from broken DNA ends to pair with the resected DNA ends, form DNA:RNA hybrids and promote homologous recombination (HR) repair by contributing to the recruitment of the HR proteins BRCA1, BRCA2, RNase H2, and RAD51. BRCA2 mediates the localization of RNase H2 to DSBs by directly interacting with RNase H2 (38).

DNA Repair Proteins Control the Nuclear Distribution of Splicing Factors in Replication Stress

Both FANCD2 and FANCI were co-purified with SF3B1 and yielded strong signals of interaction with SF3B1 in the nucleus in proximity ligation assay (PLA) (39). FANCI and SF3B1 yielded strong PLA signals throughout the cell cycle, whereas PLA signals between FANCD2 and SF3B1 were restricted to the chromatin of interphase cells (39). Therefore, it is hypothesized that FANCI associates with and regulates the dynamics of the nucleoplasmic pool of SF3B1, whereas FANCD2 associates with the chromatin-bound pool of SFs.

TUMOR-DERIVED EXTRACELLULAR VESICLES AFFECT BYSTANDER CELLS IN TUMOR MICRO-ENVIRONMENT

Tumor-derived Evs secreted from cancer cells treated with chemotherapy carry distinct type of damage-associated molecular patterns (DAMPs) that activate innate immune cells including natural killer (NK) cells. Stress-induced ligands from tumor-derived Evs bind with activating receptor NKG2D to activate NK cells in the tumor microenvironment (40). Activated NK cells promote the clearance of drug-treated tumor cells (40). The Evs is necessary for the RNA clearance step in homologous recombination repair of DNA double-strand

breaks (DSBs). Chemotherapy stress promotes extracellular vesicles (Evs) secretion from tumor cells. The released Evs from cells treated with cisplatin were found to induce invasion and increased resistance to cisplatin via p38 and JNK signaling when taken up by bystander cells in tumor microenvironment. Evs uptake inhibitors heparin, amiloride, and dynasore were shown to prevent Evs-mediated adaptive response and sensitize cells to cisplatin (41). MiR-21 in the exosomes released from cisplatin- resistant oral cavity squamous cell carcinoma (OSCC) cells was reported to decrease the DNA damage signaling in response to cisplatin and increase drug resistance to cisplatin by targeting PTEN and PDCD4 (42). Annexin A6 enriched tumor-derived Evs secreted from cancer cells treated with chemotherapeutic compounds taxanes and anthracyclines were found to promote cancer metastasis to lung by inducing the activation of NFκB and CCL2. Inhibiting annexin A6 in Evs from cancer cells significantly reduced cancer metastasis (43). Exosomes generated from breast cancer cells lead to the generation of reactive oxygen species, DNA damage response, and the stabilization of p53 and autophagy in primary mammary epithelial cells (44). Exosomes released by ovarian cancer regulate intercellular communication between tumor cells and local immune cells, cancer-associated fibroblasts and normal stroma, within the tumor microenvironment to accelerate pre-metastatic niche formation and metastatic invasion (45). Preoperative administrations of the non-steroidal antiinflammatory drug ketorolac and/or resolvins induced T cell responses and eliminated micrometastases in multiple tumor-resection models. Ketorolac and resolvins exhibited synergistic antitumor activity (46). A similar observation was also found in leukemia. Exosomes secreted from acute myeloid leukemia (AML) cells create a leukemic niche at the bone marrow (BM) to promote leukemic cell proliferation by inducing DKK1 and suppress normal hematopoiesis through exosome secretion. Disruption of exosome secretion delayed leukemia development by targeting the exosome release regulator Rab27a in AML cells (47).

CROSSTALK BETWEEN THE DNA DAMAGE RESPONSE AND IMMUNE CHECKPOINT INHIBITION

PD-L1 (B7-H1) Regulates the DNA Damage Response

PD-L1 has been well-known as immune checkpoint inhibition to the activation of T cells by interacting with PD1. PD-L1 was recently found as a novel RNA binding protein to increase drug resistance in cancer cells by increasing mRNA stability of various mRNAs encoding for proteins involved in DDR and repair (4). Luo lab reported that PD-L1 acts as an RNA binding protein to protect target RNAs from degradation by interacting with EXOSC10 and EXOSC4, which are key components of the RNA exosome (4). Knockdown of PD-L1 by small hairpin RNAs (shRNAs) increases sensitivity to the chemotherapy agent, cisplatin. Knockdown of PD-L1 also increases sensitivity to ionizing radiation (IR) (4). Genome-wide RNA transcripts interacting with PD-L1 were identified by the crosslinked RIP sequencing (RIP-seq) by PD-L1 antibody. PD-L1 knockdown on the alteration of gene expression in genome wide was identified by comparing control and PD-L1 knockdown cells by RNA sequencing (RNA- seq). About 135 genes were found to be enriched in both datasets of the RNA-seq analysis and RIP-seq analysis, including ATM, BRCA1, and FANCL and other genes involved in cellular responses to DNA damage metabolic, transcriptional, and protein modification pathways (4). A PD-L1 antibody, H1A, was developed to destabilize PD-L1 by disrupting the PD-L1 stabilizer CMTM6. This disruption resulted in PD-L1 degradation through the lysosome and increased sensitivity to radiotherapy and cisplatin (4). These studies indicate that targeting intracellular PDL1 may enhance the efficacy of chemotherapy or radiotherapy by overcoming PDL1 mediated drug resistance (**Figure 2**).

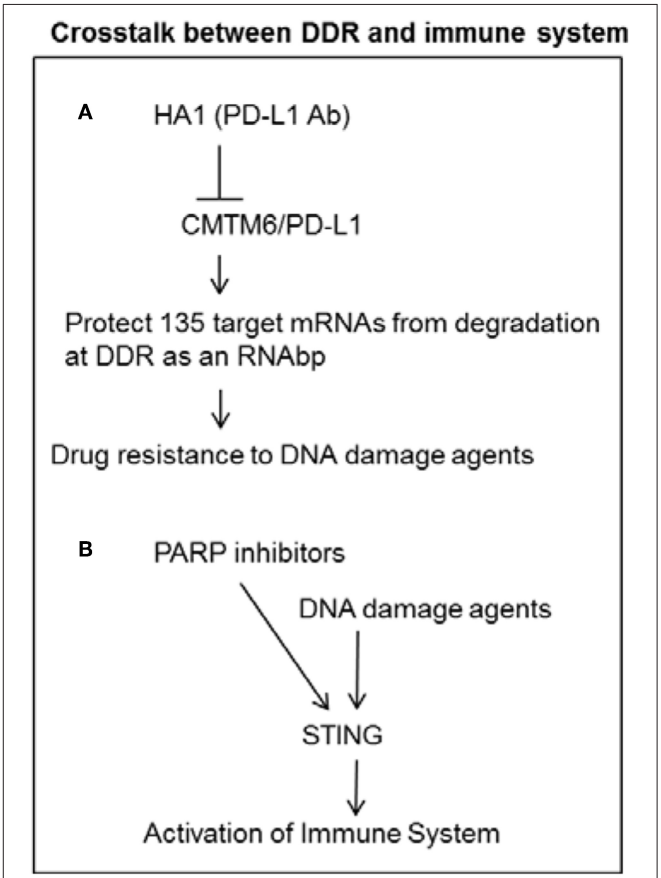

FIGURE 2 | Crosstalk between DDR and immune system. **(A)** PD-L1 can increase mRNA stability of DNA damage response genes as a RNA binding protein in cancer cells. PD-L1 antibody H1A can increase sensitivity to DNA damage agents by reducing PD-L1 mediated stability of DDR transcripts. **(B)** DNA damage agents and PARP inhibitors can induce STING pathway to activate immune system.

Activation of Immune System by DNA Damage Response

Immune System Is Activated by PARP Inhibitors

Recent studies show that PARP inhibitor or Chk1 inhibitor promotes antitumor immunity of PD-L1 blockade in NSCLC. PARP inhibitor selectively triggers anti-tumor immunity in ERCC1- or BRCA-defective contexts, indicating that PARP inhibitors might promote therapeutic effects by inhibiting DNA damage repair and activating anti-tumor effect in populations with DNA repair defect (**Figure 2**) (48, 49). PARP inhibitor was also found to trigger the STING-dependent immune response independent of BRCAness (50).

Activation of Immune System by DNA Damage Activated STING

In addition to causing the activation of cell cycle checkpoint and DNA repair and the induction of cell death, DNA damage response network induced by chemotherapy and radiotherapy can also activate the immune system. Damaged cancer cells secrete type I interferons and proinflammatory cytokines transcriptionally activated by IRF3 or NFB. The cytosolic damaged DNA from micronuclei can be recognized by the DNA sensor cGAS (cyclic guanosine monophosphate adenosine monophosphate synthase) to activate type I interferons by STING/TBK1/IRF3 pathway (5–7). Homologous recombination repair protein RAD51 also plays a role in initiating immune signaling by preventing the fragmented nascent DNA accumulates in the cytoplasm and initiation of the STING-induced innate immune response (51). Etoposide-induced DNA damage can induce the activation of NF-κB by an alternative STING- dependent and cGAS-independent pathway. The alternative STING signaling pathway includes the DNA damage response proteins ATM (ataxia telangiectasia mutated), PARP1 (poly-ADP-ribose polymerase 1), DNA sensor IFI16 (interferon-inducible protein 16), Tp53, and the E3 ubiquitin LIGASE TRAF6 (52). The efficacy of immune checkpoint blockade (ICB) is enhanced by ATM inhibition and further potentiated by radiation in pancreatic cancer (52).

CONCLUSION

In summary, there are cross-talks between cellular responses to DNA damage, RNA processing, and the extracellular vesicles related to immune checkpoint inhibition. RNAbps involved in RNA processing play critical roles in maintaining DNA genomic stability by regulating the transcription, mRNA splicing, and export of DNA repair proteins. On the other hand, DNA repair proteins can regulate the nuclear distribution of splicing factors in response to DNA damage. Splicing factors, RNAbps, and DNA repair proteins also work coordinately to prevent RNA-induced genome instability by resolving R-loops formed during transcription and RNA processing. Cross-talk between the immune response and cellular responses to DNA damage includes the enhancement of the effect of immune checkpoint inhibitors by PARP inhibitors or STING pathway. Tumor-derived Evs enhance cancer metastasis and drug resistance partially due to PD-L1 delivered from tumor-derived Evs, which acts as a novel RNA binding protein to increase drug resistance in cancer cells by affecting mRNA stability of various mRNAs involved in cellular response to DNA damage.

AUTHOR CONTRIBUTIONS

XM, SY, and VC wrote the manuscript.

FUNDING

This manuscript was supported by NIH grants R01CA184101 (XM) and R37CA238274 (SY). XM was also supported by an Oberley award from HCCC. HCCC at The University of Iowa was supported by National Cancer Institute Award P30CA086862.

REFERENCES

1. Savage KI, Gorski JJ, Barros EM, Irwin GW, Manti L, Powell AJ, et al. Identification of a BRCA1-mRNA splicing complex required for efficient DNA repair and maintenance of genomic stability. *Mol Cell.* (2014) 54:445–59. doi: 10.1016/j.molcel.2014.03.021
2. Shivji MKK, Renaudin X, Williams CH, Venkitaraman AR. BRCA2 regulates transcription elongation by RNA polymerase II to prevent R-loop accumulation. *Cell Rep.* (2018) 22:1031–9. doi: 10.1016/j.celrep.2017.12.086
3. Bhatia V, Barroso SI, Garcia-Rubio ML, Tumini E, Herrera-Moyano E, Aguilera A. BRCA2 prevents R-loop accumulation and associates with TREX-2 mRNA export factor PCID2. *Nature.* (2014) 511:362–5. doi: 10.1038/nature13374
4. Tu X, Qin B, Zhang Y, Zhang C, Kahila M, Nowsheen S, et al. PD-L1 (B7-H1) competes with the RNA exosome to regulate the DNA damage response and can be targeted to sensitize to radiation or chemotherapy. *Mol Cell.* (2019) 74:1215–26.e1214. doi: 10.1016/j.molcel.2019.04.005
5. Harding SM, Benci JL, Irianto J, Discher DE, Minn AJ, Greenberg RA. Mitotic progression following DNA damage enables pattern recognition within micronuclei. *Nature.* (2017) 548:466–0. doi: 10.1038/nature23470
6. Mackenzie KJ, Carroll P, Martin CA, Murina O, Fluteau A, Simpson DJ, et al. cGAS surveillance of micronuclei links genome instability to innate immunity. *Nature.* (2017)548:461–5. doi: 10.1038/nature23449
7. Chen Q, Sun L, Chen ZJ. Regulation and function of the cGAS-STING pathway of cytosolic DNA sensing. *Nat Immunol.* (2016)17:1142–9. doi: 10.1038/ni.3558
8. Kai M. Roles of RNA-binding proteins in DNA damage response. *Int J Mol Sci.* (2016) 17:310. doi: 10.3390/ijms17030310
9. Milek M, Imami K, Mukherjee N, Bortoli F, Zinnall U, Hazapis O, et al. DDX54 regulates transcriptome dynamics during DNA damage response. *Genome Res.* (2017) 27:1344–59. doi: 10.1101/gr.218438.116
10. Anantha RW, Alcivar AL, Ma J, Cai H, Simhadri S, Ule J, et al. Requirement of heterogeneous nuclear ribonucleoprotein C for BRCA gene expression and homologous recombination. *PLoS ONE.* (2013) 8:e61368. doi: 10.1371/journal.pone.0061368
11. Vohhodina J, Barros EM, Savage AL, Liberante FG, Manti L, Bankhead P, et al. The RNA processing factors THRAP3 and BCLAF1 promote the DNA damage response through selective mRNA splicing and

nuclear export. *Nucleic Acids Res.* (2017) 45:12816–33. doi: 10.1093/nar/gkx1046
12. Salas-Armenteros I, Barroso SI, Rondon AG, Perez M, Andujar E, Luna R, et al. Depletion of the MFAP1/SPP381 splicing factor causes R-loop-independent genome instability. *Cell Rep.* (2019) 28:1551–63.e1557. doi: 10.1016/j.celrep.2019.07.010
13. Cloutier A, Shkreta L, Toutant J, Durand M, Thibault P, Chabot B. hnRNP A1/A2 and Sam68 collaborate with SRSF10 to control the alternative splicing response to oxaliplatin-mediated DNA damage. *Sci Rep.* (2018) 8:2206. doi: 10.1038/s41598-018-20360-x
14. Shkreta L, Toutant J, Durand M, Manley JL, Chabot B. SRSF10 connects DNA damage to the alternative splicing of transcripts encoding apoptosis, cell-cycle control, and DNA repair factors. *Cell Rep.* (2016) 17:1990–2003. doi: 10.1016/j.celrep.2016.10.071
15. Ozden O, Bishehsari F, Bauer J, Park SH, Jana A, Baik SH, et al. Expression of an oncogenic BARD1 splice variant impairs homologous recombination and predicts response to PARP-1 inhibitor therapy in colon cancer. *Sci Rep.* (2016)6:26273. doi: 10.1038/srep26273
16. Bouffard F, Plourde K, Belanger S, Ouellette G, Labrie Y, Durocher F. Analysis of a FANCE splice isoform in regard to DNA repair. *J Mol Biol.* (2015) 427:3056–73. doi: 10.1016/j.jmb.2015.08.004
17. Wang Y, Bernhardy AJ, Cruz C, Krais JJ, Nacson J, Nicolas E, et al. The BRCA1-Delta11q alternative splice isoform bypasses germline mutations and promotes therapeutic resistance to PARP inhibition and cisplatin. *Cancer Res.* (2016) 76:2778–90. doi: 10.1158/0008-5472.CAN-16-0186
18. Chen JY, Zhang X, Fu XD, Chen L. R-ChIP for genome-wide mapping of R-loops by using catalytically inactive RNASEH1. *Nat Protoc.* (2019) 14:1661–85. doi: 10.1038/s41596-019-0154-6
19. Nguyen HD, Yadav T, Giri S, Saez B, Graubert TA, Zou L. Functions of replication protein A as a sensor of R loops and a regulator of RNaseH1. *Mol Cell.* (2017) 65:832–47.e834. doi: 10.1016/j.molcel.2017.01.029
20. Cristini A, Groh M, Kristiansen MS, Gromak N. RNA/DNA hybrid interactome identifies DXH9 as a molecular player in transcriptional termination and R-loop-associated DNA damage. *Cell Rep.* (2018) 23:1891–905. doi: 10.1016/j.celrep.2018.04.025
21. Hatchi E, Skourti-Stathaki K, Ventz S, Pinello L, Yen A, Kamieniarz-Gdula K, et al. BRCA1 recruitment to transcriptional pause sites is required for R-loop-driven DNA damage repair. *Mol Cell.* (2015) 57:636–47. doi: 10.1016/j.molcel.2015.01.011
22. Lopez Castel A, Cleary JD, Pearson CE. Repeat instability as the basis for human diseases and as a potential target for therapy. *Nat Rev Mol Cell Biol.* (2010) 11:165–70. doi: 10.1038/nrm2854
23. Richard P, Manley JL. R loops and links to human disease. *J Mol Biol.* (2017) 429:3168–80. doi: 10.1016/j.jmb.2016.08.031
24. Zanzoni A, Spinelli L, Ribeiro DM, Tartaglia GG, Brun C. Post-transcriptional regulatory patterns revealed by protein-RNA interactions. *Sci Rep.* (2019) 9:4302. doi: 10.1038/s41598-019-40939-2
25. Skourti-Stathaki K, Proudfoot NJ, Gromak N. Human senataxin resolves RNA/DNA hybrids formed at transcriptional pause sites to promote Xrn2-dependent termination. *Mol Cell.* (2011) 42:794–805. doi: 10.1016/j.molcel.2011.04.026
26. Moreira MC, Klur S, Watanabe M, Nemeth AH, Le Ber I, Moniz JC, et al. Senataxin, the ortholog of a yeast RNA helicase, is mutant in ataxia-ocular apraxia 2. *Nat Genet.* (2004) 36:225–7. doi: 10.1038/ng1303
27. Chen YZ, Bennett CL, Huynh HM, Blair IP, Puls I, Irobi J, et al. DNA/RNA helicase gene mutations in a form of juvenile amyotrophic lateral sclerosis (ALS4). *Am J Hum Genet.* (2004) 74:1128–35. doi: 10.1086/421054
28. Okamoto Y, Hejna J, Takata M. Regulation of R-loops and genome instability in Fanconi anemia. *J Biochem.* (2019)165:465–70. doi: 10.1093/jb/mvz019
29. Garcia-Rubio ML, Perez-Calero C, Barroso SI, Tumini E, Herrera-Moyano E, Rosado IV, et al. The fanconi anemia pathway protects genome integrity from R-loops. *PLoS Genet.* (2015) 11:e1005674. doi: 10.1371/journal.pgen.1005674
30. Okamoto Y, Abe M, Itaya A, Tomida J, Ishiai M, Takaori-Kondo A, et al. FANCD2 protects genome stability by recruiting RNA processing enzymes to resolve R-loops during mild replication stress. *FEBS J.* (2019) 286:139–50. doi: 10.1111/febs.14700
31. Chang EY, Novoa CA, Aristizabal MJ, Coulombe Y, Segovia R, Chaturvedi R, et al. RECQ-like helicases Sgs1 and BLM regulate R-loop-associated genome instability. *J Cell Biol.* (2017) 216:3991–4005. doi: 10.1083/jcb.201703168
32. Marabitti V, Lillo G, Malacaria E, Palermo V, Sanchez M, Pichierri P, et al. ATM pathway activation limits R-loop-associated genomic instability in Werner syndrome cells. *Nucleic Acids Res.* (2019) 47:3485–502. doi: 10.1093/nar/gkz025
33. Li L, Germain DR, Poon HY, Hildebrandt MR, Monckton EA, McDonald D, et al. DEAD box 1 facilitates removal of RNA and homologous recombination at DNA double-strand breaks. *Mol Cell Biol.* (2016) 36:2794–810. doi: 10.1128/MCB.00415-16
34. Song C, Hotz-Wagenblatt A, Voit R, Grummt I. SIRT7 and the DEAD-box helicase DDX21 cooperate to resolve genomic R loops and safeguard genome stability. *Genes Dev.* (2017) 31:1370–81. doi: 10.1101/gad.300624.117
35. Hodroj D, Recolin B, Serhal K, Martinez S, Tsanov N, Abou Merhi R, et al. An ATR-dependent function for the Ddx19 RNA helicase in nuclear R-loop metabolism. *EMBO J.* (2017) 36:1182–98. doi: 10.15252/embj.201695131
36. Hill SJ, Mordes DA, Cameron LA, Neuberg DS, Landini S, Eggan K, et al. Two familial ALS proteins function in prevention/repair of transcription-associated DNA damage. *Proc. Natl Acad Sci USA.* (2016) 113:E7701–9. doi: 10.1073/pnas.1611673113
37. Arab K, Karaulanov E, Musheev M, Trnka P, Schafer A, Grummt I, et al. GADD45A binds R-loops and recruits TET1 to CpG island promoters. *Nat Genet.* (2019)51:217–23. doi: 10.1038/s41588-018-0306-6
38. D'Alessandro G, Whelan DR, Howard SM, Vitelli V, Renaudin X, Adamowicz M, et al. BRCA2 controls DNA:RNA hybrid level at DSBs by mediating RNase H2 recruitment. *Nat Commun.* (2018) 9:5376. doi: 10.1038/s41467-018-07799-2
39. Moriel-Carretero M, Ovejero S, Gerus-Durand M, Vryzas D, Constantinou A. Fanconi anemia FANCD2 and FANCI proteins regulate the nuclear dynamics of splicing factors. *J Cell Biol.* (2017) 216:4007–26. doi: 10.1083/jcb.201702136
40. Vulpis E, Soriani A, Cerboni C, Santoni A, Zingoni A. Cancer exosomes as conveyors of stress- induced molecules: new players in the modulation of NK cell response. *Int J Mol Sci.* (2019) 20:E611. doi: 10.3390/ijms20030611
41. Samuel P, Mulcahy LA, Furlong F, McCarthy HO, Brooks SA, Fabbri M, et al. Cisplatin induces the release of extracellular vesicles from ovarian cancer cells that can induce invasiveness and drug resistance in bystander cells. *Philos Trans R Soc Lond B Biol Sci.* (2018) 373:65. doi: 10.1098/rstb.2017.0065
42. Liu T, Chen G, Sun D, Lei M, Li Y, Zhou C, et al. Exosomes containing miR-21 transfer the characteristic of cisplatin resistance by targeting PTEN and PDCD4 in oral squamous cell carcinoma. *Acta Biochim Biophys Sin.* (2017) 49:808–16. doi: 10.1093/abbs/gmx078
43. Keklikoglou I, Cianciaruso C, Guc E, Squadrito ML, Spring LM, Tazzyman S, et al. Chemotherapy elicits pro-metastatic extracellular vesicles in breast cancer models. *Nat Cell Biol.* (2019) 21:190–202. doi: 10.1038/s41556-018-0256-3
44. Dutta S, Warshall C, Bandyopadhyay C, Dutta D, Chandran B. Interactions between exosomes from breast cancer cells and primary mammary epithelial cells leads to generation of reactive oxygen species which induce DNA damage response, stabilization of p53 and autophagy in epithelial cells. *PLoS ONE.* (2014) 9:e97580. doi: 10.1371/journal.pone.0097580
45. Feng W, Dean DC, Hornicek FJ, Shi H, Duan Z. Exosomes promote pre-metastatic niche formation in ovarian cancer. *Mol Cancer.* (2019) 18:124. doi: 10.1186/s12943-019-1049-4
46. Panigrahy D, Gartung A, Yang J, Yang H, Gilligan MM, Sulciner ML, et al. Preoperative stimulation of resolution and inflammation blockade eradicates micrometastases. *J Clin Invest.* (2019) 129:2964-79. doi: 10.1172/JCI127282
47. Kumar B, Garcia M, Weng L, Jung X, Murakami JL, Hu X, et al. Acute myeloid leukemia transforms the bone marrow niche into a leukemia-permissive microenvironment through exosome secretion. *Leukemia.* (2018) 32:575–87. doi: 10.1038/leu.2017.259

48. Chabanon RM, Soria JC, Lord CJ, Postel-Vinay S. Beyond DNA repair: the novel immunological potential of PARP inhibitors. *Mol Cell Oncol.* (2019) 6:1585170. doi: 10.1080/23723556.2019.1585170
49. Sen T, Rodriguez BL, Chen L, Corte CMD, Morikawa N, Fujimoto J, et al. Targeting DNA damage response promotes antitumor immunity through STING-mediated T-cell activation in small cell lung cancer. *Cancer Disc.* (2019) 9:646–61. doi: 10.1158/2159-8290.CD-18-1020
50. Shen J, Zhao W, Ju Z, Wang L, Peng Y, Labrie M, et al. PARPi triggers the STING-dependent immune response and enhances the therapeutic efficacy of immune checkpoint blockade independent of BRCAness. *Cancer Res.* (2019) 79:311–9. doi: 10.1158/0008-5472.CAN-18-1003
51. Bhattacharya S, Srinivasan K, Abdisalaam S, Su F, Raj P, Dozmorov I, et al. RAD51 interconnects between DNA replication, DNA repair and immunity. *Nucleic Acids Res.* (2017) 45:4590–605. doi: 10.1093/nar/gkx126
52. Dunphy G, Flannery SM, Almine JF, Connolly DJ, Paulus C, Jonsson KL, et al. Non-canonical activation of the DNA sensing adaptor STING by ATM and IFI16 mediates NF-κB signaling after nuclear DNA damage. *Mol Cell.* (2018) 71:745–60.e745. doi: 10.1016/j.molcel.2018.07.034

Conflict of Interest: The authors declare that the research was conducted in the absence of any commercial or financial relationships that could be construed as a potential conflict of interest.

frontiers in Oncology

ORIGINAL RESEARCH
published: 13 February 2020
doi: 10.3389/fonc.2020.00127

DNA-PK Inhibitor, M3814, as a New Combination Partner of Mylotarg in the Treatment of Acute Myeloid Leukemia

*Michael I. Carr[1], Astrid Zimmermann[2], Li-Ya Chiu[1], Frank T. Zenke[2], Andree Blaukat[2] and Lyubomir T. Vassilev[1]**

[1] Translational Innovation Platform Oncology, EMD Serono Research and Development Institute, Inc., Billerica, MA, United States, [2] Translational Innovation Platform Oncology, Merck KGaA, Darmstadt, Germany

Despite significant advances in the treatment of acute myeloid leukemia (AML) the long-term prognosis remains relatively poor and there is an urgent need for improved therapies with increased potency and tumor selectivity. Mylotarg is the first AML-targeting drug from a new generation of antibody drug conjugate (ADC) therapies aiming at the acute leukemia cell compartment with increased specificity. This agent targets leukemia cells for apoptosis with a cytotoxic payload, calicheamicin, carried by a CD33-specific antibody. Calicheamicin induces DNA double strand breaks (DSB) which, if left unrepaired, lead to cell cycle arrest and apoptosis in cancer cells. However, repair of DSB by the non-homologous end joining pathway driven by DNA-dependent protein kinase (DNA-PK) can reduce the efficacy of calicheamicin. M3814 is a novel, potent and selective inhibitor of DNA-PK. This compound effectively blocks DSB repair, strongly potentiates the antitumor activity of ionizing radiation and DSB-inducing chemotherapeutics and is currently under clinical investigation. Suppressing DSB repair with M3814 synergistically enhanced the apoptotic activity of calicheamicin in cultured AML cells. Combination of M3814 with Mylotarg in two AML xenograft models, MV4-11 and HL-60, demonstrated increased efficacy and significantly improved survival benefit without elevated body weight loss. Our results support a new application for pharmacological DNA-PK inhibitors as enhancers of Mylotarg and a potential new combination treatment option for AML patients.

Keywords: DNA-PK, ADC-antibody drug conjugate, AML-acute myeloid leukemia, therapy, DSB-double-strand break

OPEN ACCESS

Edited by:
Michaela Medová, Department of Radiation Oncology, University Hospital Bern, Switzerland

Reviewed by:
Benjamin P. C. Chen, UT Southwestern Medical Center, United States
Souparno Bhattacharya, AstraZeneca, United States

***Correspondence:**
Lyubomir T. Vassilev
lubo.vassilev@emdserono.com

Specialty section:
This article was submitted to Molecular and Cellular Oncology, a section of the journal Frontiers in Oncology

Received: *09 September 2019*
Accepted: *24 January 2020*
Published: *13 February 2020*

Citation:
Carr MI, Zimmermann A, Chiu L-Y, Zenke FT, Blaukat A and Vassilev LT (2020) DNA-PK Inhibitor, M3814, as a New Combination Partner of Mylotarg in the Treatment of Acute Myeloid Leukemia. Front. Oncol. 10:127. doi: 10.3389/fonc.2020.00127

INTRODUCTION

It is estimated that over 20,000 people in the U.S. will be diagnosed with AML in 2019 (1). Despite established standards of induction and consolidation therapies, the overall 5 years survival rate is ∼30%, and U.S. statistics show few changes in per capita AML deaths in the last two decades (1). Strong chemotherapeutic regimens remain the standard approaches to AML treatment, and patient mortality is often linked to treatment-related toxicities or ablated normal hematopoiesis (2). Further limitations arise when considering the advanced median age of diagnosis (68 years), and associated health-liabilities, when facing broadly cytotoxic treatments. Accordingly, death rates from AML are higher in patients over 65 years of age (1). Therefore, there is a clear need for novel,

targeted therapeutic strategies for AML. Such therapies would ideally display high potency toward the leukemic burden and improved tolerability in normal tissues.

Antibody drug conjugates (ADCs) are targeted therapeutics with broad potential for anti-cancer efficacy through their diverse target antigens and drug payloads. ADCs consist of recombinant monoclonal antibodies (mAbs) that are covalently bound to cytotoxic chemical agents (commonly referred to as warheads) via synthetic linkers. These conjugates facilitate the delivery of highly cytotoxic small-molecule drugs with the high selectivity, stability and pharmacokinetic profile of mAbs (3). The first ADC to receive FDA approval, gemtuzumab ozogamicin (Mylotarg^{TM}), leverages the selectivity of an anti-CD33 antibody to target AML cells. The transmembrane glycoprotein CD33 is expressed on the surface of leukemia blasts in most patients with AML, but not on normal hematopoietic stem cells (4). Mylotarg consists of a humanized IgG_4 anti-CD33 antibody conjugated to the calicheamicin derivative N-acetyl-γ-calicheamicin dimethyl hydrazide (4). Its anti-leukemic activity is derived from the internalization and lysosomal localization of CD33/Mylotarg complexes, wherein the acidic environment facilitates linker hydrolysis and release of the cytotoxic calicheamicin moiety (4–6).

Calicheamicin is a member of the enediyne family of antibiotics, which binds the minor groove of DNA in a sequence-specific manner and is reduced to form a reactive intermediate that triggers the formation of DNA double strand breaks (DSB) and single strand breaks (SSB) (7–10). Calicheamicin-induced DNA damage leads to cell cycle arrest to assist DNA repair machinery or, if damage is unrepairable, apoptosis and cell death (11). DNA repair and/or the associated cell fate decisions occur through activation of the ataxia telangiectasia mutated (ATM), ataxia telangiectasia and rad3-related (ATR) and DNA-dependent protein kinase (DNA-PK)-driven pathways (12, 13). Accordingly, cells defective for ATM or DNA-PK are hypersensitive to calicheamicin (9, 14). Given the apparent impact of DNA-PK activity on cells sensitivity to calicheamicin-induced DNA damage, we hypothesized that pharmacological inhibition of DNA-PK catalytic activity may enhance the anti-leukemic effects of Mylotarg by potentiation of the cytotoxicity of its warhead, calicheamicin. M3814 belongs to a new generation of potent and selective inhibitors of DNA-PK protein kinase (15, 16). It effectively blocks DSB repair driven by DNA-PK via the non-homologous end joining (NHEJ) mechanism and strongly potentiates the antitumor activity of ionizing radiation and DSB-inducing chemotherapy agents (15). M3814 has completed Phase 1 evaluation as a single agent and currently undergoing clinical investigation in combination with radiotherapy and/or immunotherapy in solid tumors.

The guardian of the genome, p53, is a central regulatory node in DNA damage response shown to be a key player in protecting or destroying cells with damaged DNA to suppress tumor formation (17, 18). Recently, we reported that p53 plays a critical role in determining cell fate in the response of irradiated cancer cells to DNA-PK inhibitor, M3814 (16). Blocking DSB repair in cancer cells expressing wild-type p53 causes overactivation of the ATM signaling axis with a substantial boost of p53 activity and reinforcement of ATM/p53-controlled cell cycle checkpoints, leading to a complete cell cycle arrest and premature cell senescence. Cancer cells with dysfunctional p53 were not protected from entry into mitosis with unrepaired DSBs, causing severe chromosomal aberrations, mitotic errors and apoptotic cell death. This new mechanistic model for response to combined treatment with DSB-inducing agents and a DNA-PK inhibitor was derived from solid tumor cell lines which have been shown to retain their p53-dependent cell cycle arrest but frequently lose their p53 apoptotic activity (19). Acute leukemia cells, however, are known to preserve their ability to undergo effective apoptosis and cell death in response to p53 pathway activation (20). Therefore, the M3814-induced p53 activity boost in response to DSBs could further potentiate the activity of calicheamicin in AML cells, the majority of which express wild-type and functional p53. Here, we show that suppressing DSB repair with M3814 synergistically enhances the anti-leukemic activity of calicheamicin in cultured AML cells through p53 dependent and independent mechanisms. Combination of the selective DNA-PK inhibitor with Mylotarg in two AML xenograft models is well-tolerated, provides significant efficacy and survival benefit compared to Mylotarg alone and could offer a new combination approach to AML therapy.

MATERIALS AND METHODS

Cell Lines and Reagents

All cell lines were obtained, mycoplasma free, from the Merck Tissue Culture Bank (Merck KGaA, Darmstadt, Germany). Cells were originally purchased from ATCC (Manassas, Virginia), or DSMZ (Braunschweig, Germany) and kept in liquid nitrogen at low passage until use. Cell line identity was confirmed by short tandem repeats (STRs) analyses and mycoplasma infection was excluded by PCR-based testing. Molm-13, MV4-11, and HL-60 cells were maintained in RPMI 1640 media (GIBCO, Gaithersburg, MD) supplemented with 20% heat-inactivated fetal bovine serum (FBS). AML cell lines were cultured at low confluency and no longer than 20 passages to avoid cell differentiation. Culture medium was supplemented with 10% fetal bovine serum (FBS) (Corning Life Science, Tewksbury, MA, USA). M3814 and M3814R were synthesized at Merck KGaA, Darmstadt, Germany. Calicheamicin was purchased from MedChemExpress (Monmouth Junction, NJ, USA). All compounds were dissolved in DMSO to prepare stock solutions and kept frozen at −20°C until use. The final concentration of DMSO in media did not exceed 0.1% (vol/vol). Mylotarg (gentusumab ozogamicin for injection, Pfizer, 5 mg/vial) was purchased from Asaman, Inc. (Avon, MA, USA).

Cell Growth and Viability Assays

For drug combination matrix cell growth/viability testing, cells were plated at 2×10^4 cells/ml overnight in 96-well plates. The next day, cells were treated with the indicated concentrations of M3814 and calicheamicin. Drugs were added using D300e digital dispenser (Tecan) in DMSO with diluent normalization (DMSO 0.1%). Effect on cell growth/viability was assessed at 48, 72 or 144 h using the CellTiterGlo 2.0 Cell Assay (Promega, Madison, WI, USA) according to manufacturer's protocol. Luminescence

was detected using an EnVision plate reader (Perkin Elmer, Waltham, MA, USA). Calicheamicin dose-response curves and IC50 values for fixed M3814 doses were generated by graphing relative viability and curve fitting using GraphPad Prism (v8.0.1). Synergism between M3814 and calicheamicin was calculated and graphed according to Bliss and Loewe models using Combenefit software (v. 2.021) (21). Cell counting assays were performed by plating 2×10^5 cells/well in 6-well plates and treating in triplicate with the indicated drugs. Viable cells were counted at specified timepoints using trypan exclusion and a Cellometer Mini automated cell counter (v1.2.3.3) (Nexcelom Bioscience, Lawrence, MA, USA).

Live-Cell Imaging

Live-cell imaging was performed using an IncuCyte ZOOM live cell analysis system (Essen BioScience, Ann Arbor, MI, USA). 2,000 cells/well were plated in poly-d-lysine coated, black walled 96-well plates (Becton Dickinson, Bedford, MA, USA). Incucyte Annexin V Green reagent was added to media as per manufacturer's instructions (Essen BioScience, Ann Arbor, MI, USA). Cells were treated with the indicated concentrations of M3814 and calicheamicin and imaged using a 10x objective at 2 h intervals for 5 days. Relative apoptosis was calculated as Annexin V-positive events per mm^2 normalized to percent confluence.

Western Blot Analyses

MV4-11 cells plated at $1–5 \times 10^5$ cells/ml in T75 flasks were treated with the indicated drugs. Lysates were prepared at 6, 24, 48, or 96 h using RIPA lysis buffer (Cell Signaling Technology, Danvers, MA) supplemented with protease and phosphatase inhibitors (Roche Diagnostics, Indianapolis, IN, USA). Lysates were resolved using NuPAGE 4–12% Bis-Tris, or 3–8% Tris-Acetate gels (Thermo Fisher Scientific, Waltham, MA, USA), and transferred to Nitrocellulose membranes with an iBlot 2 Gel Transfer Device (Thermo Fisher Scientific, Waltham, MA, USA). Membranes were treated and imaged with a LI-COR Odyssey CLx imaging system in accordance with the LI-COR Near-Infrared (NIR) Western Blot Detection Protocol (LI-COR, Lincoln, NE, USA). Primary antibodies were as follows: p-ATM (S1981) (#ab81292, Abcam Biotechnology, Cambridge, MA, USA); ATM (#MA1-23152, Thermo Fisher Scientific, Waltham, MA, USA); p-CHK2 (T68) (#2197, Cell Signaling Technology, Danvers, MA, USA); CHK2 (#6334, Cell Signaling Technology, Danvers, MA, USA); p-p53 (S15) (#9284, Cell Signaling Technology, Danvers, MA, USA); p53 (#48818, Cell Signaling Technology, Danvers, MA, USA); p21 (#2947, Cell Signaling Technology, Danvers, MA, USA); MDM2 (#sc-965, Santa Cruz Biotechnology, Dallas, TX, USA); Puma (#12450, Cell Signaling Technology, Danvers, MA, USA); Cleaved PARP (#5625, Cell Signaling Technology, Danvers, MA, USA); Cleaved Caspase 3 (#9664, Cell Signaling Technology, Danvers, MA, USA), and Vinculin (#V9131, Sigma-Aldrich, St. Louis, MO, USA).

Gene Expression Analysis

RNA was isolated using RNeasy Mini Kit with on column DNase digestion (Qiagen, Germantown, MD, USA). RNA purity and concentration were determined using a Nanodrop spectrophotometer (Thermo Fisher Scientific). cDNA was synthesized using Superscript IV Vilo Master Mix (Thermo Fisher Scientific) as described by manufacturer. Quantitative PCR was performed using TaqMan Fast Advanced Master Mix and a 7500 Fast Dx Real-Time PCR Instrument (Applied Biosystems). TaqMan probes used were CDKN1A (Hs00355782_m1), MDM2 (Hs01066930_m1), BBC3 (Hs00248075_m1) and GAPDH (Hs02758991_g1). Relative fold-change gene expression was normalized to GAPDH.

Cell Cycle and Apoptosis

For cell cycle and apoptosis analyses, $0.4–2 \times 10^6$ cells/well were plated in 6-well plates and treated in triplicate with the indicated drugs. At specified timepoints, 1×10^6 cells were either fixed in 70% ethanol and stained with 7-AAD (7-amino-actinomycin D) (BD Biosciences, San Jose, CA, USA) for cell cycle analysis, or stained with phycoerythrin (PE) conjugated Annexin V and 7-AAD for apoptosis analysis, using the PE Annexin V Apoptosis Detection Kit I (BD Biosciences, San Jose, CA, USA). Samples were analyzed using a BD FACSCanto flow cytometer (BD Bioscience, San Jose, CA) and data was processed using FlowJo software (v10.6.1) (FlowJo, LLC).

Animal Studies

Study designs and animal usage were approved by local animal welfare authorities (Regierungspräsidium Darmstadt, Hesse, Germany). For MV4-11 xenograft studies, female, 8–10 weeks old H2d Rag2 [C;129P2-H2^{d}-TgH(II2rg)^{tm1Brn}-TgH(Rag2)^{tm1Alt}N4] mice (Taconic Biosciences, Denmark) were used. 2.5×10^6 tumor cells were injected subcutaneously in the flank, in 100 µl of 1:1 (v:v) Dulbecco's phosphate-buffered saline (calcium- and magnesium-free)/ Matrigel^{TM} Basement Membrane Matrix (BD Biosciences). Tumors were left to reach 65–180 mm^3 and mice were randomized into groups of equal mean tumor volume (170 mm^3) prior to treatment. For HL-60 xenograft studies, female, 6–8 weeks old Hsd:Athymic Nude-Foxn1^{nu} mice (Envigo, France) were used. 2×10^6 tumor cells were injected subcutaneously in the flank, in 100 µl of 1:1 (v:v) Dulbecco's phosphate-buffered saline (calcium and magnesium free)/Matrigel^{TM} Basement Membrane Matrix (BD Biosciences). Tumors were left to reach 94–284 mm^3 and mice were randomized into groups of equal mean tumor volume (170 mm^3) prior to treatment. M3814 was suspended for oral administration in a vehicle of 0.5% Methocel/0.25% Tween20 in 300 mM citrate buffer, pH 2.5. Mylotarg was formulated for intravenous administration according to the package insert by reconstituting the lyophilizate to a concentration of 1 mg/ml in water for injection and diluting to final concentration using 0.9% saline.

Statistical Analyses

All statistical tests were performed with GraphPad PRISM version 7.0 (GraphPad Software Inc.). The data were analyzed with Student *t*-tests. $P \leq 0.05$ were considered statistically significant. All assays were conducted independently three times, unless indicated otherwise, and representative data is shown as

mean ± SD. Significance values are $^{*}p < 0.05$, $^{**}p < 0.01$, and $^{***}p < 0.001$. NS stands for non-significant ($p > 0.05$).

RESULTS

M3814 Potentiates the Antitumor Activity of Calicheamicin in AML Cells

We have previously shown that the DNA-PK inhibitor M3814 can effectively enhance the antitumor effect of ionizing radiation (IR) by inhibiting NHEJ repair of IR-induced DSBs in solid tumor cells (15, 16). In cancer cells expressing wild-type p53, this effect is largely due to overactivation of the ATM/p53 signaling axis boosting p53 to levels much higher than the levels induced by radiation alone. This is leading to a complete cell cycle arrest and premature cell senescence but not apoptosis (16). We hypothesized that p53 wild-type acute leukemia cells, known to be highly sensitive to p53-induced apoptosis (22), will be more effectively killed by the M3814 mediated p53 boost in response to calicheamicin-induced DSBs.

To this aim, we first examined whether M3814 potentiates the cytotoxicity of calicheamicin in p53 wild-type AML cells *in vitro*. Exponentially proliferating MV4-11 and Molm-13 cells (both expressing wild-type p53) were exposed to concentration ranges of calicheamicin and M3814, alone and in combination, and the effect on cell growth/viability was determined after 48 h by the CellTiter-Glo assay. Cell viability was reduced across a range of calicheamicin concentrations when combined with increasing doses of M3814 (100, 300, and 900 nM). These concentrations are within the previously defined selectivity range (16). The curve shift and the corresponding IC50 values suggested a combination effect (**Figure 1A**). Analysis of cell viability across the full range of calicheamicin and M3814 concentrations by two different methods (Loewe and Bliss excess) using Combenefit software (21) revealed similar regions of synergy in the dose matrices for both cell lines (**Figure 1B**). The concentration ranges at which synergy was observed at this timepoint was 0.2–4 pM calicheamicin for MV4-11 and 0.4–10 pM for the Molm-13 cells. To confirm that the observed synergism between M3814 and calicheamicin is indeed due to inhibition of DNA-PK catalytic activity, we tested the effect of the DNA-PK inhibitor on cell growth/viability of MV4-11 and Molm-13 cells using the pharmacologically active M3814 eutomer (**Figure 1C**, upper panel) and its distomer, M3814R (**Figure 1C**, lower panel), shown to be over 20-fold less potent in inhibiting DNA-PK enzymatic activity (16). As expected, synergy was observed in both cell lines exposed to the combination of M3814 and calicheamicin but not in cells treated with M3814R and calicheamicin, indicating that the inhibition of DNA-PK kinase activity underlies the observed synergistic relationship (**Figure 1C**).

M3814 Overactivates p53 in Response to Calicheamicin in AML Cells

We investigated the effect of the combination treatment with calicheamicin and M3814 on p53 activity in the p53 wild-type MV4-11 cell line. Cells were treated with solvent (DMSO) or calicheamicin (0.5 or 1 pM) and M3814 (300 or 1,000 nM) alone and in combination. These M3814 concentrations were shown to be within the activity range (over 80% DNA-PK inhibition) in most tested cancer cell lines, while remaining selective to its target (16). Gene expression analysis of three key p53 transcriptional targets, responsible for p53 protein stability (Mdm2), p53-dependent cell cycle arrest (p21) and p53-dependent apoptosis induction (Puma), showed a dose-dependent upregulation in response to calicheamicin after 24 and 48 h exposure to the indicated concentrations of single agents or drug combinations (**Figure 2A**). While M3814 treatment did not affect p53 target gene expression in the absence of calicheamicin-induced DNA damage, combined M3814 and calicheamicin treatment resulted in a dose-dependent 2- to 5-fold increase in expression (**Figure 2A**). These results indicated that the combination treatment enhances p53 pathway activation in the response to calicheamicin in agreement with our findings in solid tumor cellular models (16).

We then examined the status of ATM/p53 signaling in MV4-11 cells. Exponentially growing cells were exposed to the solvent (DMSO), calicheamicin (1 pM), M3814 (1 μM), and their combination (1 μM M3814 plus 1 pM calicheamicin) and the levels of key proteins from the ATM (p-ATM, p-CHK2) and p53 pathways (p-p53^{Ser15}, p21, Mdm2, Puma) were analyzed by Western blotting at 6, 24, 48, and 96 h (**Figure 2B**). At a concentration of 1 pM, calicheamicin increased slightly the levels of p-ATM^{Ser1981} and its direct phosphorylation target p-CHK2^{Thr68}, most notably between 6 and 48 h. The effect on p53 signaling was more pronounced with p-p53^{Ser15} and total p53 levels following the pattern of p-CHK2 activation. The p53 transcriptional targets, p21, Mdm2, and Puma, all had elevated, if slightly different patterns. Cell cycle checkpoint protein p21 was upregulated quickly but its level decreased after 24 h while the apoptosis regulator Puma reached highest levels at 48 h and remained elevated until 96 h post treatment. Mdm2 was elevated more uniformly within the studied period. As seen previously in epithelial cancer cells (16), DNA-PK inhibitor did not show significant effect on all tested proteins except for Puma levels that were slightly higher than the levels in the DMSO control also found to be somewhat elevated at 48 and 96 h. These increases in the control treatments are likely caused by apoptosis in a small fraction of cells due to population overgrowth. The combination of calicheamicin and M3814 induced the expression levels of all tested proteins compared to calicheamicin or M3814 alone at as early as 6 h and caused a pronounced upregulation at 24 h, when p-ATM^{Ser1981} was most elevated. The cell cycle inhibitor, p21, was highest at 24 h and remained elevated until 96 h while calicheamicin-induced p21 was down to basal levels at 96 h. Mdm2 levels were more uniform and higher than in the treatment with calicheamicin alone. The apoptosis inducer, Puma, was also elevated compared to calicheamicin alone and strongest at 48 h. Two markers of apoptosis, cleaved Caspase 3 and cleaved PARP, were also tested. Cleaved caspase 3 was mildly elevated by calicheamicin alone, most notably at 96 h, but significantly stronger in the combination treatment peaking at 96 h. Cleaved PARP elevation was only detected in the combination treatment and was highest at 96 h. These Western blot analyses revealed that M3814 can

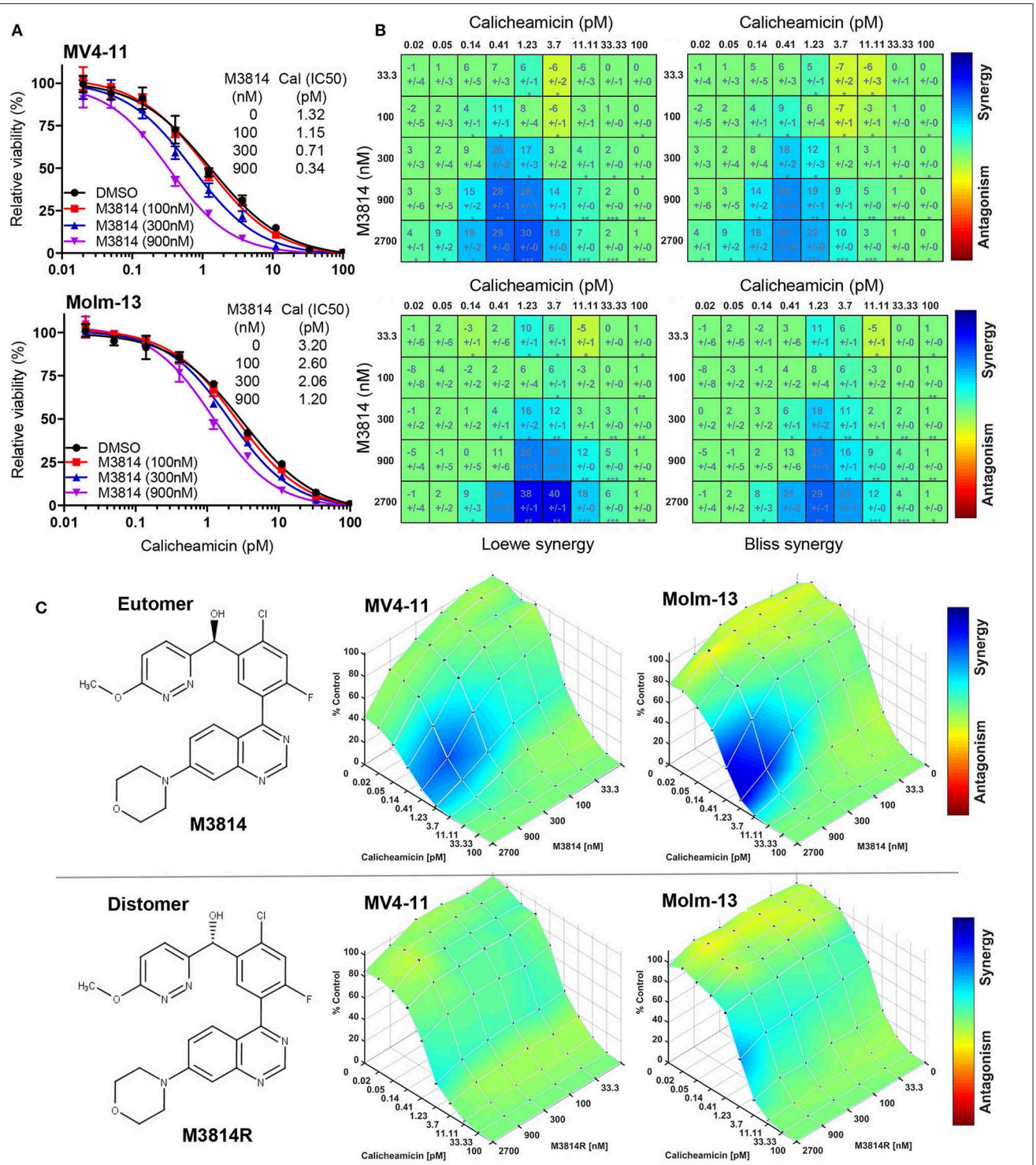

FIGURE 1 | M3814 synergizes with calicheamicin in killing AML cells. **(A)** Proliferating MV4-11 and Molm-13 cells were exposed to increasing concentrations of calicheamicin alone or in combination with three fixed concentrations of M3814 and their viability was measured after 48 h by CellTiter-Glo assay. Relative viability was graphed for fixed M3814 doses and curve fitting performed to generate IC50 values. **(B)** Loewe and Bliss synergy score matrices for MV4-11 and Molm-13 cells treated with combinations of calicheamicin and M3814. Relative viability by CellTiter-Glo assay was processed using Combenefit software to generate synergy score matrices. Boxes/cells include synergy scores above standard deviations and significance indicators. $^{*}P < 0.05$, $^{**}P < 0.01$, $^{***}P < 0.001$. **(C)** The structure of the pharmacologically active enantiomer (eutomer) M3814 and overlays of Bliss synergy matrices on combination dose response surfaces for MV4-11 and Molm-13 cells treated with calicheamicin and M3814 for 48 h (top). The structure of the pharmacologically inactive enantiomer (distomer) M3814R and overlays of Bliss synergy matrices on combination dose response surfaces for MV4-11 and Molm-13 cells treated with calicheamicin and M3814R for 48 h (bottom). Results were analyzed and graphed using Combenefit software.

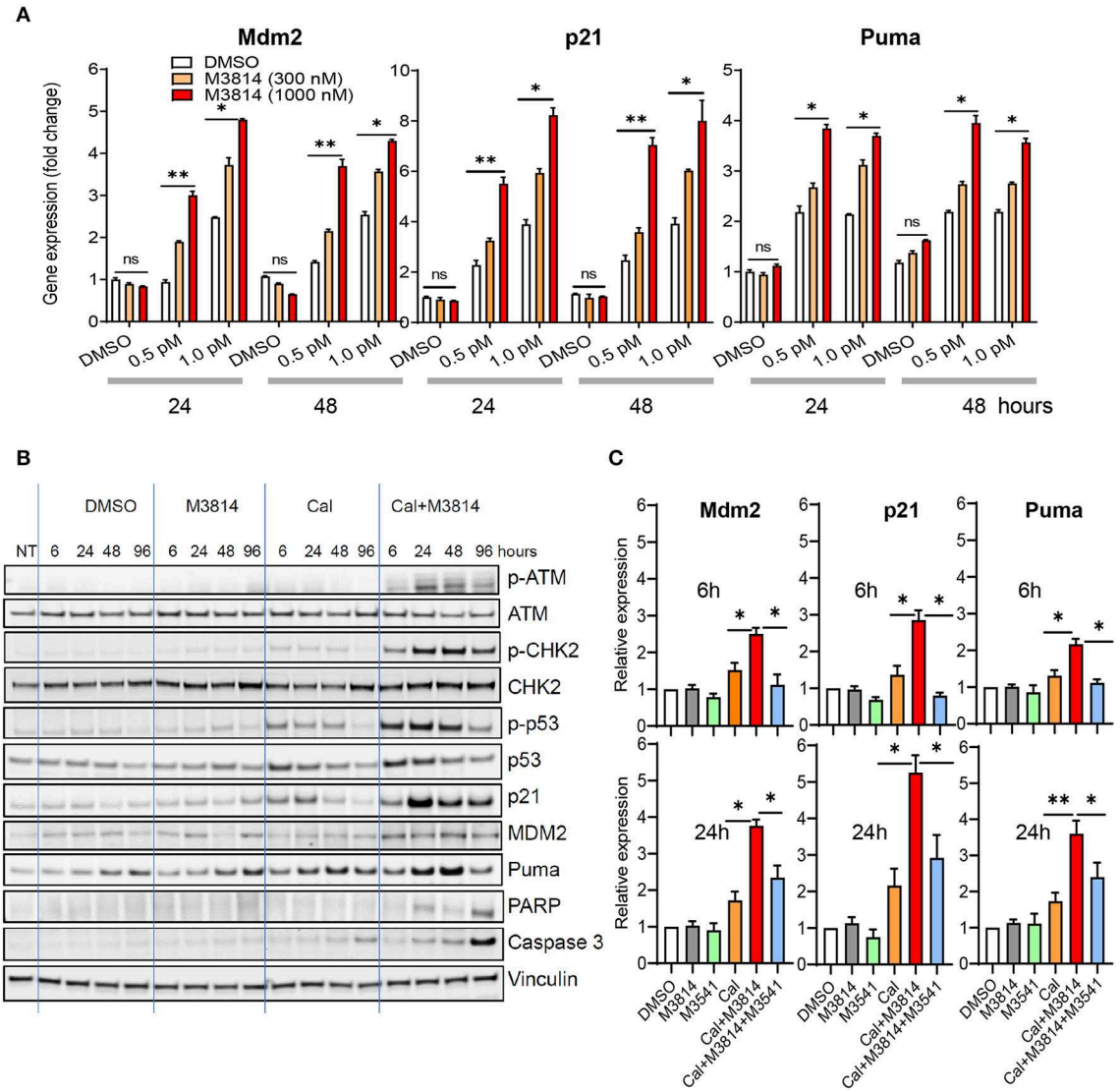

FIGURE 2 | M3814 overactivates p53 in response to calicheamicin in AML cells. **(A)** Relative gene expression analysis of key p53 transcriptional targets, Mdm2, p21 and Puma, in MV4-11 (p53 wild-type) cells treated with DMSO, calicheamicin (0.5 or 1.0 pM), or M3814 (300 or 1,000 nM) alone or in combination. Relative expression determined by the $2^{(-\Delta\Delta Ct)}$ method with GAPDH reference. **(B)** Western blot analysis of ATM and p53 pathway proteins as well as apoptotic indicators at 6, 24, 48, and 96 h in lysates of MV4-11 cells treated with vehicle, M3814 (1 μM), calicheamicin (1pM), or the combination of calicheamicin (1 pM), and M3814 (1 μM). **(C)** Relative gene expression analysis at 6 and 24 h of key p53 transcriptional targets, Mdm2, p21, and Puma, in MV4-11 (p53 wild-type) cells treated with DMSO, M3814 (1 μM), M3541 (1 μM), calicheamicin (1.0 pM), calicheamicin (1 pM) + M3814 (1 μM), or calicheamicin (1 pM) + M3814 (1 μM) + M3541 (1 μM). *$P < 0.05$, **$P < 0.01$, ***$P < 0.001$.

enhance ATM/p53 signaling in the AML cell line MV4-11 in agreement with our findings in epithelial cancer cell lines (16). The overactivation of the ATM and p53 pathways resulted in significantly higher levels of the p53-dependent controllers of cell cycle and apoptosis, p21 and Puma, predicting stronger cell cycle arrest and/or apoptotic activity.

To confirm the role of ATM activation in the elevated p53 response we used the novel, potent and selective inhibitor of ATM catalytic activity, M3541 (23). Adding 1 μM M3541, a concentration previously shown to inhibit over 80% of ATM autophosphorylation in response to ionizing radiation in multiple cancer cell lines (16, 23), to the combination of calicheamicin and M3814 in MV4-11 cells abrogated the enhancing effect of M3814 on p53 targets, p21, Mdm2, and Puma, bringing them close to untreated levels at 6 h and still significantly reduced relative to the calicheamicin/M3814 combination at 24 h (**Figure 2C**). ATM inhibitors have limitations as a cellular probe for DSB-induced p53 activation because they simultaneously inhibit its main function as a driver of DSB repair via the homologous recombination pathway (24). Continuous ATM inhibition has been shown to suppress the repair of DSBs and potentiate DSB-inducing agents (23) that may lead to a secondary

ATM-independent activation of p53 at later time points. This may explain the incomplete inhibition of the p53 response at 24 h. However, the observed suppression of p53 activation in the early stages of the calicheamicin/M3814 combination treatment is in agreement with our data with solid tumor cell lines (16) and support the hypothesis that p53 activity boost is downstream of M3814-induced ATM overactivation.

ATM/p53 Pathway Boost by M3814 Contributes to the Antitumor Activity of Calicheamicin in MV4-11 Cells

When activated by genotoxic stress, the p53 pathway can exert two major functions, cell cycle arrest and/or apoptosis to aid in the repair of DNA damage or eliminate damaged cells and suppress tumorigenesis (25). Both functions are activated by many genotoxic chemotherapeutics in p53 wild-type cancer cells and contribute to the antitumor activity of these agents (26). The p53-dependent apoptotic response plays a major role in the therapy of AML which is predominantly p53 wild-type (22). We assessed if the enhanced activation of the p53 pathway by M3814 contributes to potentiation of calicheamicin antitumor activity.

Firstly, we examined the cell cycle effect of the combined treatment. MV4-11 cells were exposed to calicheamicin (1.0 pM) and M3814 (1 μM) alone and in combination as in **Figure 2** for 24 h and subjected to cell cycle analyses (**Figure 3A**). M3814 treatment slightly slowed down cell cycle progression as revealed by mild growth delay (**Figure 3B**). Calicheamicin alone partially arrested MV4-11 cells in G1 phase primarily reducing the S phase population. The combination treatment led to nearly complete cell cycle block in G1 and G2/M phase with only 5% of the cells remaining in S phase, typical for p53-dependent, p21-mediated cell cycle arrest (19, 27) that effectively halted cell growth (**Figure 3B**). These experiments suggested that the M3814 mediated ATM-dependent p53 boost could contribute to the antitumor effect by strengthening the calicheamicin-induced cell cycle arrest.

Next, we asked if the DNA-PK inhibitor can enhance calicheamicin-induced apoptosis in MV4-11 cells *in vitro*. Again, cells were exposed to calicheamicin (1.0 pM) and M3814 (1 μM) alone and in combination, and the cell population undergoing apoptosis was identified and quantified by staining with phycoerythrin (PE) conjugated Annexin V and 7-amino-actinomycin D (7-AAD) at 24, 48, 72, and 96 h (**Figure 3C**). The changes in apoptotic cell fraction (combined early and late apoptosis) are summarized in **Figure 3D**. A time-dependent increase in the fraction of MV4-11 cells undergoing early and late apoptosis was observed in response to calicheamicin alone. The combined treatment resulted in a consistent increase in the fraction of apoptotic cells relative to calicheamicin alone. These results support the hypothesis that by overactivation of the ATM signaling axis M3814 increased calicheamicin-induced p53 transcriptional activity, reinforced p53-dependent cell cycle arrest and apoptosis thus extending the validity of our mechanistic model (16) to acute leukemia cells. In contrast to irradiated solid tumor cells, which acquired p53-dependent premature senescence in the presence of M3814, this boost in p53 activity led to increased calicheamicin-induced apoptosis and cell death in MV4-11 cells. Therefore, M3814-induced p53 overactivation could offer a new approach to enhancing the activity of Mylotarg's warhead calicheamicin in AML cells.

M3814 Potentiates Calicheamicin Cytotoxicity Independent of p53 in HL-60 Cells

Most AML patients express wild-type p53 in their blasts at diagnosis (22). However, ∼10% carry disabling p53 mutants and represent a significant treatment challenge with the established AML therapies (28). The mechanistic model for potentiation of DSB-inducing agents by M3814 in solid tumors cells (16) predicted enhancement of p53-dependent response in p53 wild-type AML cells, but also suggested potentiation of DSB-inducing therapies in p53 dysfunctional cells. These p53-mutant or null cells lack p53-dependent cell cycle arrest and effective protection from mitotic entry with unrepaired DSBs that could lead to mitotic catastrophe (16, 29). In epithelial cancer cells, such outcome was delayed until chromosomal damage accumulates over one or more subsequent cell cycles (16).

We examined the mechanism of response to the calicheamicin/M3814 combination in the p53-null AML line HL-60. Firstly, we compared the relative viability of the combined treatment in the p53 wild-type MV4-11 and the p53-deficient HL-60 cell line. Exponentially growing cells were exposed to a combination matrix of a range of M3814 and calicheamicin concentrations, and their relative growth/viability was determined at 48, 72, and 144 h. Dose-response curves generated for three fixed M3814 concentrations (100, 300, and 900 nM) indicated a delayed onset of cytotoxicity for the combination in HL-60 cells compared to MV4-11 (**Figure 4A**). Our data revealed that M3814 could synergistically enhance the activity of calicheamicin in HL-60 cells but with delayed kinetics.

These findings were supported by live-cell imaging of MV4-11 and HL-60 cells continuously monitoring calicheamicin/M3814 induced changes in cell growth and viability. IncuCyte Annexin V reagent was used to assess real-time apoptosis induction. Annexin V positive cell events were recorded over a period of 5 days and normalized to cell confluence (**Figure 4B**). Comparison of the curves of relative apoptotic events showed that while M3814 potentiated calicheamicin apoptotic activity in MV4-11 cell continuously, it provided insignificant enhancement in HL-60 cells up to 50 h which was substantially accelerated over the later part of drug exposure. These results are consistent with the hypothesis that p53-dependent apoptosis of AML cells known to occur with rapid onset (22) is the primary driver of the early response to the calicheamicin/M3814 combination in MV4-11 cells. The delayed cell killing of the p53-null HL-60 cells resembled the delayed response of p53 dysfunctional epithelial tumor cells to ionizing radiation and M3814 (16) and suggested that mitotic catastrophe might be involved.

Next, we analyzed the effect of calicheamicin/M3814 treatment on cell cycle progression and viability. HL-60 cells were exposed to calicheamicin (5 pM), M3814 (1 μM) or the combination and their cell cycle distribution was analyzed at

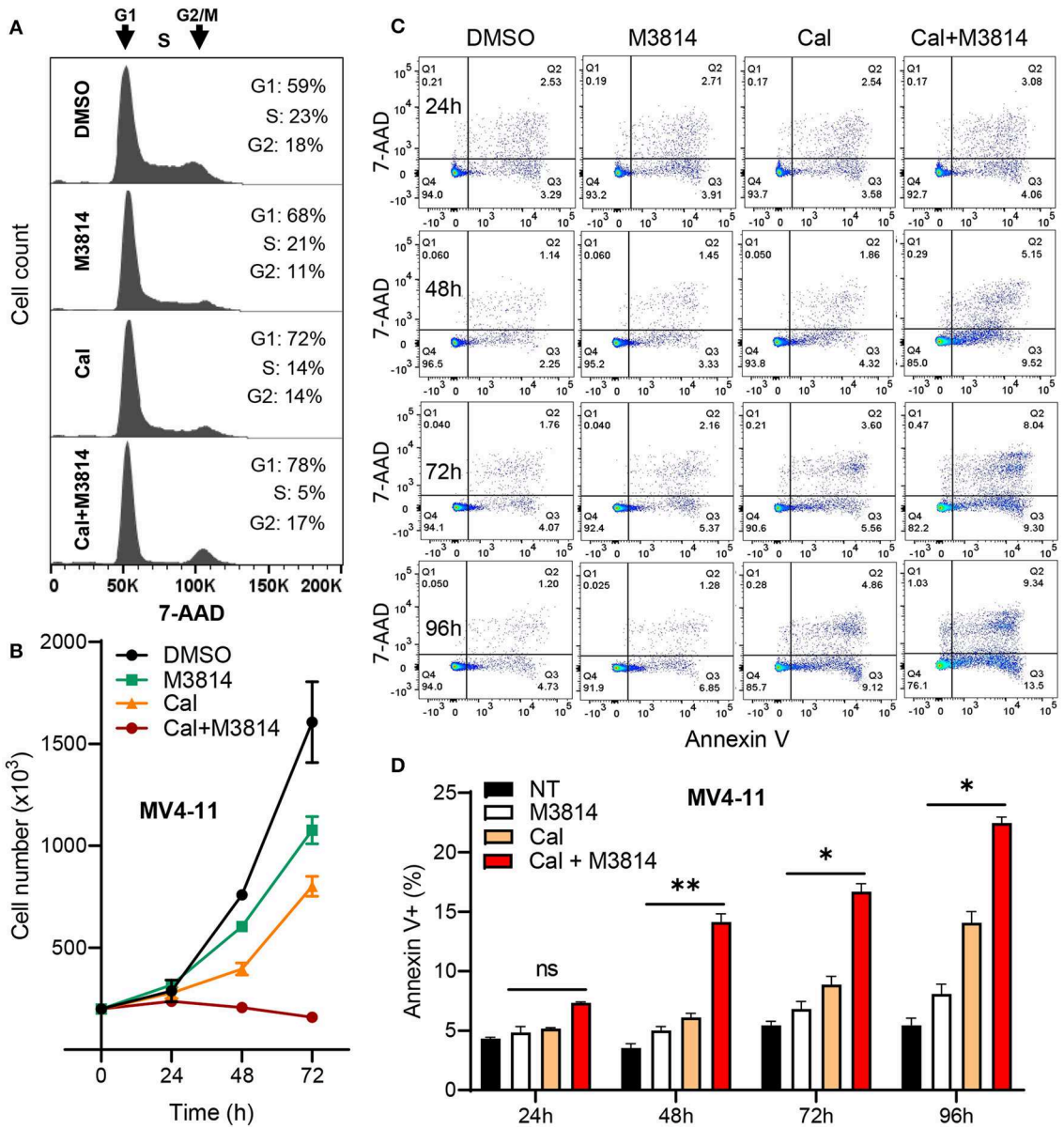

FIGURE 3 | M3814 enhances antitumor activity of calicheamicin in AML cells by a p53-dependent mechanism. **(A)** Cell cycle analysis of 7-AAD stained MV4-11 cells treated with DMSO, M3814 (1 μM), calicheamicin (1 pM), or calicheamicin (1pM) + M3814 (1 μM). **(B)** Cell number as assessed by trypan exclusion at 0, 24, 48, and 72 h for MV4-11 cells treated in triplicate with DMSO, M3814 (1 μM), calicheamicin (1 pM) or the combination of calicheamicin (1pM) + M3814 (1 μM). **(C)** Representative images from flow cytometry analysis of apoptosis at 24, 48, 72, and 96 h in MV4-11 cells treated in triplicate with DMSO, M3814 (1 μM), calicheamicin (1 pM) or the combination of calicheamicin (1 pM) and M3814 (1 μM). **(D)** Average percentage of Annexin V-positive cells (early and late apoptotic) from flow cytometry analysis of cells treated in triplicate as in (c) and analyzed at 24, 48, 72, and 96 h. $^{*}P < 0.05$, $^{**}P < 0.01$, $^{***}P < 0.001$.

48, 72, and 96 h (**Figure 4C**). The DMSO control and M3814 treatment exhibited a normal cell cycle profile with traces of apoptotic (sub-G1) population remaining practically unchanged. Cells treated with calicheamicin showed a slight G2/M arrest and increased apoptotic (sub-G1) fraction little changed over the next 2 days. HL-60 cells exposed to the combination were arrested predominantly in G2/M (57%) and had 22% apoptotic (sub-G1) fraction at 48 h. At 72 h, the G2/M peak diminished dramatically giving rise to an increasing (39%) apoptotic (sub-G1) population. At 96 h, most of the cells (63%) were in the sub-G1 population. The remaining 37% of the cell population displayed a profile indicative of ongoing cell death. These results demonstrated that M3814 can substantially enhance the killing potential of calicheamicin in the p53-defficient AML cell line HL-60. Altogether, our experiments revealed that the DNA-PK inhibitor M3814 synergizes with and effectively potentiates the activity of calicheamicin in proliferating AML cells *in vitro*.

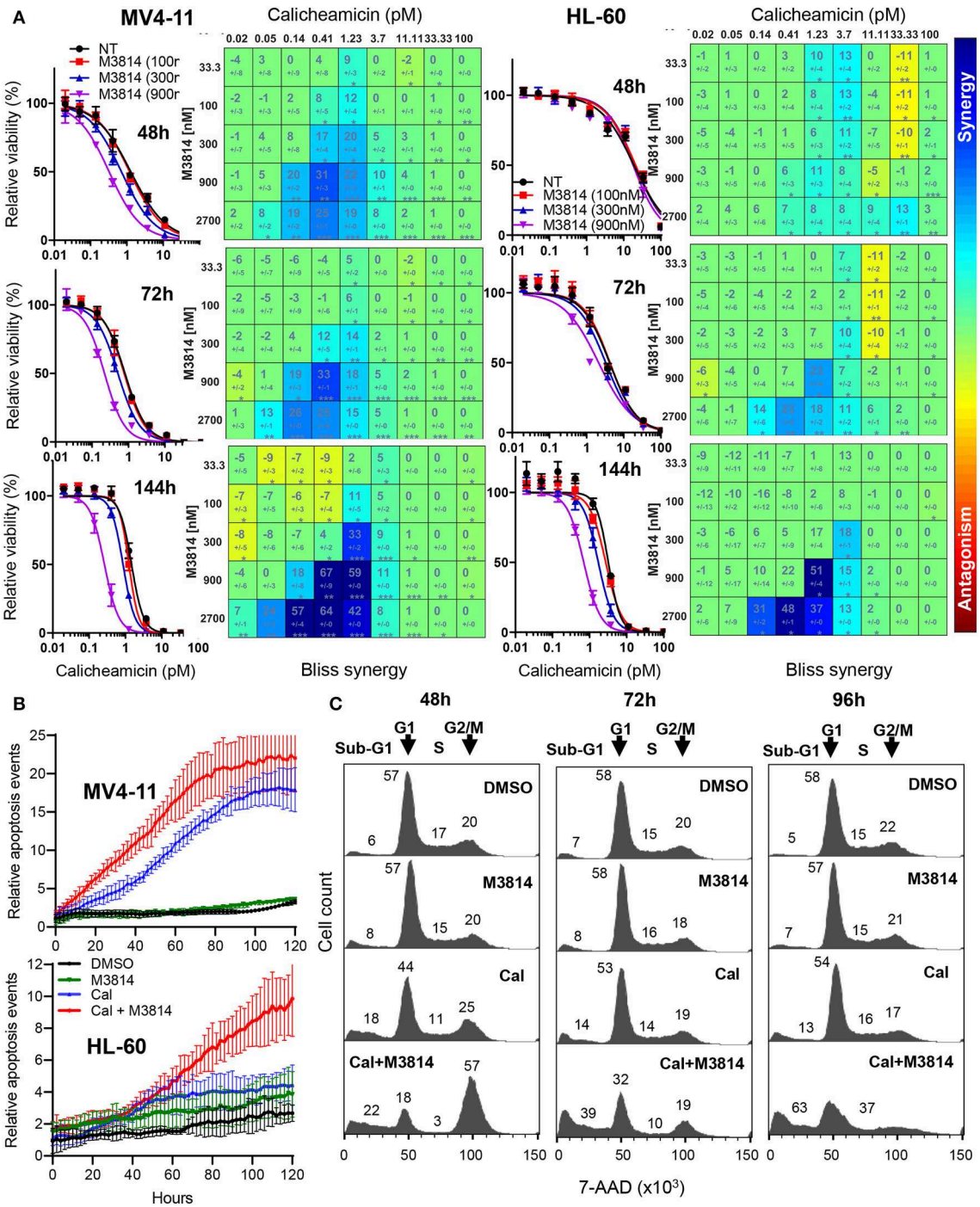

FIGURE 4 | M3814 potentiates calicheamicin cytotoxicity independent of p53 in HL-60 cells. **(A)** Calicheamicin dose-response curves for fixed M3814 concentrations and Bliss synergy matrices for MV4-11 cells (left) and HL-60 cells (right) treated with calicheamicin and M3814 as in **Figure 1** and assayed for relative viability using CellTiter-Glo assay at 48, 72, and 144 h. Synergy results were analyzed and graphed using Combenefit software. **(B)** MV4-11 cells (top) and HL-60 cells (bottom) were seeded in 96-well plates and exposed to vehicle (DMSO), M3814 (900 nM), calicheamicin (1.2 pM) or combination of M3814 (900 nM) + calicheamicin (1.2 pM) in the presence of IncuCyte Annexin V reagent and their growth and apoptosis was monitored by live time-lapse imaging by IncuCyte at 10x magnification. Relative apoptosis events were determined from imaging data and calculated as Annexin V-positive events normalized to percent confluence, averaged from eight fields of view across duplicate wells. **(C)** Cell cycle analysis of 7-AAD stained HL-60 cells treated with DMSO, M3814 (1 μM), calicheamicin (5 pM) or the combination of calicheamicin (5 pM) + M3814 (1 μM) for 48, 72, and 96 h. Cells in each phase (sub-G1, G1, S, G2/M) were calculated as a percentage of total cell count (100%) and corresponding numbers positioned in close proximity to the phase they represent.

M3814 Shows Strong Combination Benefit With Mylotarg in AML Xenograft Models

We sought to determine whether the potentiation of free calicheamicin by M3814 *in vitro* could translate to an *in vivo* combination setting with Mylotarg using mouse xenograft models of AML. MV4-11 and HL-60 tumor xenografts were established subcutaneously in immunodeficient mice and treated intravenously with vehicle, a single dose of Mylotarg (0.1 mg/kg in MV4-11 and 1.0 mg/kg in HL-60) and daily oral doses of M3814 (100 mg/kg), alone and in combination. Animals were monitored over time for tumor volume and body weight changes. M3814 treatment alone did not show a significant effect on MV4-11 tumor volumes as compared to vehicle (**Figure 5**). Mylotarg treatment led to an initial reduction in tumor volume, and while *3* xenografts had a complete response, tumor outgrowth was observed in *7* animals. Combined treatment with M3814 and Mylotarg, however, resulted in complete responses in 7 of 10 tumor xenografts. Similar results were seen in HL-60 xenografts where no significant activity of M3814 alone on tumor volumes was detected (**Figure 5**). At the used dose, Mylotarg treatment did not produce a substantial reduction in tumor volume across the treatment group, 3 xenografts had a complete response and tumor outgrowth was observed in *6* animals. Combined treatment with M3814 and Mylotarg, increased the number of complete responses, with no measurable tumor volume in eight of nine treated animals at the termination of the study on day 45. Thus, there was a clear combination effect of M3814 and Mylotarg *in vivo* in both MV4-11 and HL-60 tumor xenografts. Furthermore, this combination had minimal effects on body weight in both MV4-11 and HL-60 studies, indicating potential favorable tolerability (**Figure 5**).

DISCUSSION

Using molecular tools and early chemical inhibitors, DNA-PK inhibition has been shown to enhance the antitumor effect of ionizing radiation and DSB-inducing chemotherapeutics and was proposed as a new combination strategy for cancer therapy (30, 31). M3814 is the first potent and selective inhibitor of DNA-PK catalytic activity that has undergone Phase 1 clinical evaluation and is currently being tested in proof-of-concept clinical studies in combination with DSB-inducing therapies. Due to its target selectivity, M3814 offers an excellent molecular probe for mechanistic studies and therapeutic intervention in DSB repair. Recently, we showed that inhibition of radiation-induced DSB-repair by M3814

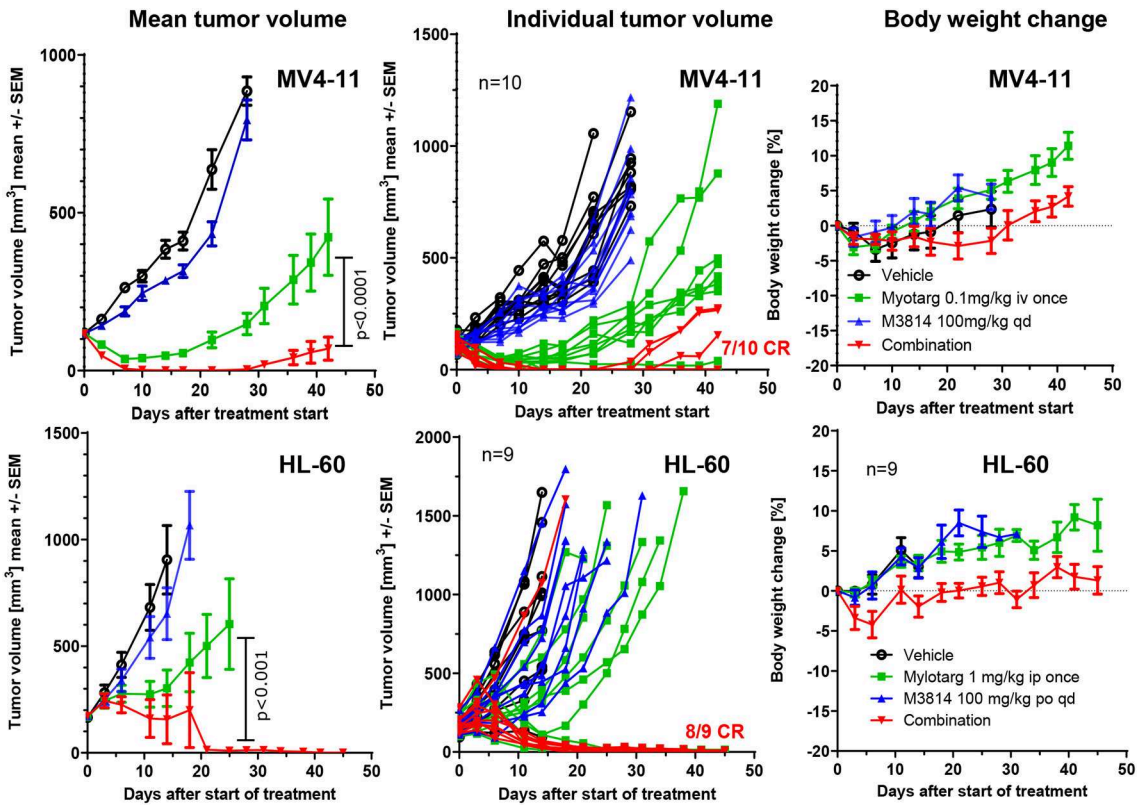

FIGURE 5 | M3814 shows a strong combination benefit with Mylotarg in AML xenograft models. Established subcutaneous MV4-11(group size: 10 mice) and HL-60 (group size: 9 mice) xenograft tumors in immunodeficient mice were treated with Mylotarg (0.1 mg/kg in MV4-11 and 1.0 mg/kg in HL-60, single administration, intravenous injection), M3814 (100 mg/kg, daily, oral gavage), and the combination thereof as indicated. Statistical analysis was performed on log transformed tumor volume data applying a repeated measurement ANOVA with Bonferroni post-test for comparing the groups treated with Mylotarg + M3814 and Mylotarg alone using GraphPad Prism software. CR, complete response.

causes a unique reinforcement of ATM/p53 regulated cell cycle checkpoints and two district cellular responses that are under p53 control: p53 dependent complete proliferation block and premature senescence that protect cells from death or mitotic catastrophe and apoptotic death in the absence of p53 functionality (16). While an enhanced p53 response protects irradiated solid tumor cells from the lethal consequences of radiation-induced DNA damage, the same response in acute leukemia cells may offer a new way for enhanced cell killing via p53-dependent apoptosis. This difference in p53 dependent apoptotic response has been attributed to the fact that that majority of solid tumors expressing wild-type p53 acquire defects in the p53-dependent apoptotic signaling (19, 32) while most acute leukemias are known to preserve p53 wild-type status and apoptotic function (22).

Here, we investigate the applicability of this approach to combination therapy of DNA-PK inhibitor M3814 with Mylotarg, an ADC armed with a potent DSB-inducing warhead, calicheamicin. Our results demonstrate that calicheamicin activity is synergistically potentiated by M3814 in p53 wild-type MV4-11 and MOLM-13 cells *in vitro*. The significant overactivation of the p53 pathway and induction of cell cycle arrest and apoptosis in MV4-11 cells suggests that p53-dependent cell cycle arrest and apoptosis is an important contributor to the potentiation of calicheamicin in the p53 wild-type setting. Our results do not exclude p53-independent killing of p53 wild-type AML cells. Indeed, it has been shown that calicheamicin can induce apoptosis in p53-null clone of the p53 wild-type HCT116 cancer cell line but did not investigate the possibility for involvement of different mechanisms (11). Engaging the p53-dependent apoptotic signaling has been established as an important component of current AML therapies with proven clinical success and its synergistic enhancement by a DNA-PK inhibitor offers a new approach for potential therapeutic intervention.

A different mechanism is likely behind the enhanced activity of calicheamicin/M3814 combination in the p53 null HL-60 cell line. In the absence of functional p53, a weakened checkpoint control allows a larger number of cells to enter mitosis with unrepaired DSBs, frequently leading to mitotic catastrophe (29). The slower onset of cell death in HL-60 cells during calicheamicin/M3814 treatment and the predominant G2/M arrest giving rise to an increasing apoptotic (sub-G1) population remarkably resembling the fate of irradiated HeLa cell under M3814 treatment (16) hint to involvement of mitotic catastrophe (33). However, apoptotic or necrotic cell death independent of mitotic catastrophe in p53-deficient cells cannot be excluded as a contributor to the overall enhanced AML cell killing in response to the calicheamicin/M3814 combination. Future focused studies in panels of p53-deficient cell lines are needed to establish the predominant mechanism of M3814 enhanced calicheamicin-induced cell death in AML.

The results described in this manuscript suggest that regardless of the p53 status of AML cells and the mechanisms of response, DNA-PK inhibition effectively sensitizes AML cells to Mylotarg *in vitro* and *in vivo*. Thus, M3814 could offer a new combination approach to AML therapy with a potentially improved treatment outcome. Selectively targeting the CD33-positive AML cells may spare normal bone marrow cells from enhanced p53-dependent toxicity. Indeed, our mouse models revealed a minimal increase of body weight loss which was fully reversible. However, the true safety window of such a combination strategy could be determined only in the proper clinical setting.

Antibody drug conjugates with several deferent DNA damaging payloads have been reported and are at different stages of preclinical and clinical evaluation (34). They may offer interesting new opportunities for combination with inhibitors of DNA repair pathways, such as M3814.

DATA AVAILABILITY STATEMENT

The datasets generated for this study are available on request to the corresponding author.

ETHICS STATEMENT

The animal study was reviewed and approved by Animal Welfare Committee, Merck KGaA, Darmstadt, Germany.

AUTHOR CONTRIBUTIONS

MC, AZ, L-YC, and LV designed the experiments. MC, AZ, and L-YC performed experiments, analyzed and graphed data. LV, MC, and AZ wrote the manuscript. LV, AZ, MC, FZ, and AB discussed experimental data, revised and edited the full content of the manuscript. All authors have read, revised critically and approved the final version of the manuscript.

FUNDING

This study was funded by Merck KGaA, Darmstadt, Germany.

REFERENCES

1. Howlader N, Noone AM, Krapcho M, Miller D, Brest A, Yu M, et al. *Cancer Statistics Review, 1975–2016*. Bethesda, MD: NCI (2019). Available online at: https://seer.cancer.gov/csr/1975_2016/ (accessed December 11, 2019).
2. Cowan AJ, Laszlo GS, Estey EH, Walter RB. Antibody-based therapy of acute myeloid leukemia with gemtuzumab ozogamicin. *Front Biosci*. (2013) 18:1311–34. doi: 10.2741/4181
3. Beck A, Goetsch L, Dumontet C, Corvaïa N. Strategies and challenges for the next generation of antibody-drug conjugates. *Nat Rev Drug Dis*. (2017) 16:315–37. doi: 10.1038/nrd.2016.268
4. Hamann PR, Hinman LM, Hollander I, Beyer CF, Lindh D, Holcomb R, et al. Gemtuzumab ozogamicin, a potent and selective anti-CD33 antibody-calicheamicin conjugate for treatment of acute myeloid leukemia. *Bioconjugate Chem*. (2002) 13:47–58. doi: 10.1021/bc010021y

5. van der Jagt RH, Badger CC, Appelbaum FR, Press OW, Matthews DC, Eary J, et al. Localization or radiolabeled antimyeloid antibodies in a human acute leukemia xenograft tumor model. *Cancer Res*. (1992) 52:89–94.
6. Press OW, Shan D, Howell-Clark J, Eary J, Appelbaum FR, Matthews D, et al. Comparative metabolism and retention of iodine-125, Yttrium-90, and Indium-111 radioimmunoconjugates by cancer cells. *Cancer Res*. (1996) 56:2123–9.
7. Long BH, Golik J, Forenza S, Ward B, Rehfuss R, Dabrowiak JC, et al. Esperamicins, a class of potent antitumor antibiotics: mechanism of action. *Proc Natl Acad Sci USA*. (1989) 86:2–6. doi: 10.1073/pnas.86.1.2
8. Sugiura Y, Uesawa Y, Takahashi Y, Kuwahara J, Golik J, Doyle TW. Nucleotide-specific cleavage and minor-groove interaction of DNA with esperamicin antitumor antibiotics. *Proc Natl Acad Sci USA*. (1989) 86:7672–6. doi: 10.1073/pnas.86.20.7672
9. Elmroth K, Nygren J, Mårtensson S, Ismail IH, Hammarsten O. Cleavage of cellular DNA by calicheamicin γ1. *DNA Repair*. (2003) 2:363–74. doi: 10.1016/S1568-786400235-5
10. Zein N, Sinha AM, McGahren WJ, Ellestad GA. Calicheamicin gamma 1I: an antitumor antibiotic that cleaves double-stranded DNA site specifically. *Science*. (1989) 240:1198–201. doi: 10.1126/science.3240341
11. Prokop A, Wrasidlo W, Lode H, Herold R, Lang F, Henze G, et al. Induction of apoptosis by enediyne antibiotic calicheamicin II proceeds through a caspase-mediated mitochondrial amplification loop in an entirely Bax-dependent manner. *Oncogene*. (2003) 22:9107–20. doi: 10.1038/sj.onc.1207196
12. Amico D, Barbiu AM, Erba E, Rambaldi A, Introna M, Golay J. Differential response of human acute myeloid leukemia cells to gemtuzumab ozogamicin *in vitro*: role of Chk1 and Chk2 phosphorylation and caspase 3. *Blood*. (2003) 101:4589–97. doi: 10.1182/blood-2002-07-2311
13. Mårtensson S, Nygren J, Osheroff N, Hammarsten O. Activation of the DNA-dependent protein kinase by drug-induced and radiation-induced DNA strand breaks. *Radiat. Res*. (2003) 160:291–301. doi: 10.1667/0033-75871600291:AOTDPK2.0.CO;2
14. Sullivan N, Lyne L. Sensitivity of fibroblasts derived from ataxia-telangiectasia patients to calicheamicin gamma 1l. *Mutat. Res*. (1990) 245:171–5. doi: 10.1016/0165-799290046-M
15. Zenke FTZA, Sirrenberg C, Dahmen H, Vassilev L, Pehl U, Fuchss T, et al. M3814, a novel investigational DNA-PK inhibitor: enhancing the effect of fractionated radiotherapy leading to complete regression of tumors in mice. *Cancer Res.* (2016) 76(Suppl.):1658. doi: 10.1158/1538-7445.AM2016-1658
16. Sun Q, Guo Y, Liu X, Czauderna F, Carr MI, Zenke FT, et al. Therapeutic implications of p53 status on cancer cell fate following exposure to ionizing radiation and the DNA-PK inhibitor M3814. *Mol Cancer Res*. (2019) 17:2457–68. doi: 10.1158/1541-7786.MCR-19-0362
17. Ciccia A, Elledge SJ. The DNA damage response: making it safe to play with knives. *Mol Cell*. (2010) 40:179–204 doi: 10.1016/j.molcel.2010.09.019
18. Reinhardt HC, Schumacher B. The p53 network: cellular and systemic DNA damage responses in aging and cancer. *Trends Genetics*. (2012) 28:128–36. doi: 10.1016/j.tig.2011.12.002
19. Tovar C, Rosinski J, Filipovic Z, Higgins B, Kolinsky K, Hilton H, et al. Small-molecule MDM2 antagonists reveal aberrant p53 signaling in cancer: implications for therapy. *Proc Natl Acad Sci USA*. (2006) 103:1888–93. doi: 10.1073/pnas.0507493103
20. Kojima K, Konopleva M, Samudio IJ, Shikami M, Cabreira-Hansen M, McQueen T, et al. MDM2 antagonists induce p53-dependent apoptosis in AML: implications for leukemia therapy. *Blood*. (2005) 106:3150–9. doi: 10.1182/blood-2005-02-0553
21. DiVeroli GY, Fornani C, Wang D, Mollard S, Bramhall JL, Richards FM, et al. Combenefit: an interactive platform for the analysis and visualization of drug combinations. *Bioinformatics*. (2016) 32:2866–8. doi: 10.1093/bioinformatics/btw230
22. Kojima K, Ishizawa J, Andreeff M. Pharmacological activation of wild-type p53 in the therapy of leukemia. *Exp Hematol*. (2016) 44:791–8. doi: 10.1016/j.exphem.2016.05.014
23. Fuchss T, Mederski WW, Zenke FT, Dahmen H, Zimmermann A, Blaukat A. Highly potent and selective ATM kinase inhibitor M3541: a clinical candidate drug with strong antitumor activity in combination with radiotherapy. *Cancer Res*. (2018) 78(Suppl.):329–9. doi: 10.1158/1538-7445.AM2018-329
24. Shiloh Y, Ziv Y. The ATM protein kinase: regulating the cellular response to genotoxic stress, and more. *Nat Rev Mol Cell Biol*. (2013) 14:197–210. doi: 10.1038/nrm3546
25. Rashi-Elkeles S, Elkon R, Shavit S, Lerenthal Y, Linhart C, Kupershtein A, et al. Transcriptional modulation induced by ionizing radiation: p53 remains a central player. *Mol Oncol*. (2011) 5:336–48. doi: 10.1016/j.molonc.2011.06.004
26. Cheok CF, Lane DP. Exploiting the p53 pathway for therapy. *Cold Spring Harb Perspect Med*. (2017) 7:a026310. doi: 10.1101/cshperspect.a026310
27. Bunz F, Dutriaux A, Lengauer C, Waldman T, Zhou S, Brown JP, et al. Requirement for p53 and p21 to sustain G2 arrest after DNA damage. *Science*. (1998) 282:1497–501. doi: 10.1126/science.282.5393.1497
28. Kadia TM, Jain P, Ravandi F, Garcia-Manero G, Andreeff M, Takahashi K, et al. TP53 mutations in newly diagnosed Acute Myeloid Leukemia -Clinico-molecular characteristics, response to therapy, and outcomes. *Cancer*. (2016) 122:3484–91. doi: 10.1002/cncr.30203
29. Castedo M, Perfettini JL, Roumier T, Andreau K, Medema R, Kroemer G. Cell death by mitotic catastrophe: a molecular definition. *Oncogene*. (2004) 23:2825–37. doi: 10.1038/sj.onc.1207528
30. Curtin NJ. DNA repair dysregulation from cancer driver to therapeutic target. *Nat Rev Cancer*. (2012) 12:801–17. doi: 10.1038/nrc3399
31. Furgason JM, Bahassi el M. Targeting DNA repair mechanisms in cancer. *Pharmacol Ther*. (2013) 137:298–308. doi: 10.1016/j.pharmthera.2012.10.009
32. Toledo F, Wahl GM. Regulating the p53 pathway: *in vitro* hypotheses, *in vivo* veritas. *Nat Rev Cancer*. (2006) 6:909–23. doi: 10.1038/nrc2012
33. Vitale I, Galluzzi L, Castedo M, Kroemer G. Mitotic catastrophe: a mechanism for avoiding genomic instability. *Nat Rev Mol Cell Biol*. (2011) 12:385–92. doi: 10.1038/nrm3115
34. Fu Y, Ho M. DNA and damaging agent-based antibody-drug conjugates for cancer therapy. *Antibody Ther*. (2018) 1:243–53. doi: 10.1093/abt/tby007

Conflict of Interest: All authors are employees of Merck KGaA or its subsidiary EMD Serono, Inc.

frontiers in Oncology

REVIEW
published: 05 May 2020
doi: 10.3389/fonc.2020.00670

Replication Fork Remodeling and Therapy Escape in DNA Damage Response-Deficient Cancers

Martin Liptay[1†], *Joana S. Barbosa*[1†] *and Sven Rottenberg*[1,2*]

[1] *Institute of Animal Pathology, Vetsuisse Faculty, University of Bern, Bern, Switzerland,* [2] *Bern Center for Precision Medicine, University of Bern, Bern, Switzerland*

Most cancers have lost a critical DNA damage response (DDR) pathway during tumor evolution. These alterations provide a useful explanation for the initial sensitivity of tumors to DNA-targeting chemotherapy. A striking example is dysfunctional homology-directed repair (HDR), e.g., due to inactivating mutations in *BRCA1* and *BRCA2* genes. Extensive efforts are being made to develop novel targeted therapies exploiting such an HDR defect. Inhibitors of poly(ADP-ribose) polymerase (PARP) are an instructive example of this approach. Despite the success of PARP inhibitors, the presence of primary or acquired therapy resistance remains a major challenge in clinical oncology. To move the field of precision medicine forward, we need to understand the precise mechanisms causing therapy resistance. Using preclinical models, various mechanisms underlying chemotherapy resistance have been identified. Restoration of HDR seems to be a prevalent mechanism but this does not explain resistance in all cases. Interestingly, some factors involved in DNA damage response (DDR) have independent functions in replication fork (RF) biology and their loss causes RF instability and therapy sensitivity. However, in BRCA-deficient tumors, loss of these factors leads to restored stability of RFs and acquired drug resistance. In this review we discuss the recent advances in the field of RF biology and its potential implications for chemotherapy response in DDR-defective cancers. Additionally, we review the role of DNA damage tolerance (DDT) pathways in maintenance of genome integrity and their alterations in cancer. Furthermore, we refer to novel tools that, combined with a better understanding of drug resistance mechanisms, may constitute a great advance in personalized diagnosis and therapeutic strategies for patients with HDR-deficient tumors.

Keywords: DNA replication, replication fork, chemotherapy, drug resistance, DNA damage response, DNA damage tolerance, PARP inhibitors, BRCA1/2

OPEN ACCESS

Edited by:
Christian Reinhardt,
University of Cologne, Germany

Reviewed by:
Zhi-Xiang Xu,
University of Alabama at Birmingham, United States
Alvaro Galli,
Italian National Research Council, Italy

***Correspondence:**
Sven Rottenberg
sven.rottenberg@vetsuisse.unibe.ch

[†] *These authors have contributed equally to this work*

Specialty section:
This article was submitted to Molecular and Cellular Oncology, a section of the journal Frontiers in Oncology

Received: *07 February 2020*
Accepted: *09 April 2020*
Published: *05 May 2020*

Citation:
Liptay M, Barbosa JS and Rottenberg S (2020) Replication Fork Remodeling and Therapy Escape in DNA Damage Response-Deficient Cancers. Front. Oncol. 10:670. doi: 10.3389/fonc.2020.00670

DNA DAMAGE RESPONSE-TARGETED CANCER THERAPY AND RESISTANCE

Damage to DNA occurs naturally in cells during cellular metabolism, or after exposure to external agents such as ultraviolet light, ionizing irradiation (IR), or genotoxic chemicals (1). While healthy cells are able to repair the DNA lesions, cells that have defects in the DNA damage response (DDR) pathway do not repair the lesions as efficiently, resulting in genome instability and potentially the development of cancer (2). Instructive examples of malignancies with defects

in the DDR are ovarian and breast cancers with mutations in genes of the homologous recombination (HR) pathway, such as *BRCA1* and *BRCA2* (3–7). The HR pathway is one of the three major cellular pathways that repair DNA double strand breaks (DSBs) (8–10). Whereas, the other pathways, classical non-homologous end-joining (NHEJ) and theta-mediated end joining (TMEJ) do not require a template for repair and tend to be error-prone, HR occurs after DNA replication and uses the undamaged sister chromatid as a template for error-free repair of DSBs [reviewed in (9, 11)].

Although DDR alterations cause mutagenesis and malignant transformation, they also provide a therapeutic opportunity that can be explored by DNA damage-inducing therapies (12, 13). In fact, alterations in the DDR even provide a useful explanation for the initial drug sensitivity. Most cancers have lost a critical DDR pathway during cancer evolution (14, 15). Patients therefore respond to clinical interventions that cause DNA damage, e.g., chemotherapy using DNA crosslinkers and radiotherapy. Whereas, the normal cells of the body can still cope with the damage, the tumor cells that lack proper DNA repair cannot and die. Accordingly, HR-deficient cancers (e.g., due to *BRCA1/2* mutations) are often sensitive to classical DNA-crosslinking agents such as platinum-based drugs (13, 16). However, these agents are associated with significant side effects due to the damage of normal tissues (17).

An alternative to this conventional therapy is a more targeted type of treatment that is based on the synthetic lethality concept: the mutation in one of two genes is harmless for the cells but the simultaneous inactivation of those two genes is lethal (18, 19). Because tumors that have lost a certain DDR pathway rely more on other DNA repair mechanisms, selectively inhibiting these alternative pathways gives an opportunity to induce synthetic lethality in these tumor cells. In contrast, the normal cells still have all DDR pathways available and can cope with the damage induced by the treatment.

A successful example of this concept is the approval of poly(ADP)ribose polymerase (PARP) inhibitors (PARPi) to target BRCA1/2-deficient ovarian and breast cancers (20, 21), with relatively moderate side effects [reviewed in (22, 23)]. Several PARP enzymes, and in particular its founding member PARP1, are important in coordinating responses to DNA damage (24, 25). PARP1 is quickly recruited to single-stranded DNA (ssDNA) sites upon damage and catabolizes the formation of branched PAR polymers, which then serve as a scaffold for the recruitment of downstream repair factors (26). When the lesion is removed, poly(ADP-ribose) glycohydrolase (PARG) removes the PAR chains and PARP1 is released from DNA, together with the other involved proteins. PARPi inhibit the PARylation reaction and trap PARP to DNA, delaying the repair of the damage. It is thought that accumulation of SSBs in the absence of PAR synthesis and physical trapping of PARP1 on DNA eventually lead to RF collapse and DSBs (8, 27, 28). Since PARP1 also senses unligated Okazaki fragments during DNA replication and facilitates their repair, the synthetic lethality may also origin from replication-associated single-stranded DNA gaps (29). Recently, another model for PARPi-induced genotoxicity was presented, where PARPi deregulates restart of transiently stalled forks (see "Replication fork reversal and its players" below), elevating the fork progression rate above a tolerable threshold in the presence of DNA damage (30–32). However, the relevance of the mechanisms mentioned above in different model systems and different therapy contexts remains to be better understood. Importantly, since HR is required for error-free DSB repair following replication, BRCA1/2-deficient tumor cells lacking HR activity are not able to tolerate the damage induced by PARPi and they eventually die, whereas normal cells can cope with PARPi treatment (27).

Despite the clinical benefits of PARPi, most patients with disseminated BRCA1/2-mutated cancer still die because their tumors either show upfront resistance or develop secondary resistance (33). Thus, drug resistance remains a major challenge in targeting DDR pathways.

Mechanisms of resistance to PARPi in HR-deficient tumors have been studied extensively in preclinical models [reviewed in (34)]. Residual hypomorphic activity or reactivation of BRCA1/2 function by secondary mutations, is one of the major mechanisms found in patients (5, 35–39). Moreover, the restoration of HR independently of BRCA1 function (via the downregulation of factors involved in blocking DNA end resection and promoting NHEJ) is also prominent in animal models (40–54) and we expect that this also occurs in humans. Additional mechanisms discovered are related to the upregulation of the drug efflux transporter ABCB1/P-gp (55, 56), the loss of the drug target via downregulation of PARP1 in BRCA1/2-proficient cells (57), PARP1 point mutations that abrogate PARPi-induced trapping (58), or the partial restoration of PARylation activity via the loss of PARG, the functional antagonizer of PARP1 (59).

More recently, attention has been brought to the contribution of replication fork (RF) integrity to genome stability and drug response (60, 61). Interestingly, besides their role in DNA repair, BRCA1/2 are also important to protect stalled RFs, allowing the resolution of replication intermediates while preventing excessive nucleolytic degradation (62–64). This dual role of BRCA1/2 in DNA repair and RF protection makes BRCA1/2-deficient cells highly sensitive to DNA damaging agents and drugs affecting replication (see more details in the section "Fork stability as a resistance mechanism in BRCA-deficient tumors"). Besides BRCA1/2, other DNA repair factors such as RNF8, RNF168, 53BP1, and RAD51 are present at RFs and play a role in their dynamics (65–70). In agreement with this, several studies have demonstrated that restored stability of RF in BRCA1/2-deficient cells achieved via re-activation of BRCA1/2 or additional loss of other factors regulating RF processing, confers resistance to PARPi and platinum drugs (62, 63, 71–73) [reviewed in (60, 61)].

Hence, various well-known mediators of DSB repair have independent functions in RF biology. Since their defect is linked to increased anti-cancer therapy sensitivity, it raises the question whether the defective RF metabolism is the main determinant of anti-cancer therapy response or, at least, a major contributor.

Given the increasing implications of RF homeostasis for cancer therapy, we focus our attention in this review to RF remodeling and the different methods currently used to study RF constitution and dynamics. Next, we discuss crucial molecular

players of these processes and the relation of PARP and PARPi with the RF remodeling "metabolism." In addition, we discuss the role of fork stability and restart in cancer drug resistance and the biological role of DDT pathways in the maintenance of genome integrity and cancer. Moreover, we will suggest some practical applications of this knowledge in the clinic, in terms of diagnosis and prognosis, predicting personalized treatment responses, and for the development of new therapeutic strategies.

THE TOOL-BOX TO STUDY RF STRUCTURE, COMPOSITION AND DYNAMICS

To investigate RF biology, high-resolution, quantitative molecular tools are necessary, in particular for the study of protein interactions at RFs during unperturbed S-phase or replication stress. Because each method has it strengths and pitfalls, a combination of several methods is useful to obtain a complete picture of the hypothesis to be tested. Before focusing on the mechanisms of RF biology in the context of cancer therapy, we provide a brief outline of the most commonly used techniques.

Electron Microscopy (EM)

Electron microscopes use a beam of accelerated electrons as a source of illumination. Since the wavelength of electrons can be up to 100,000 times shorter than that of visible light photons, electron microscopes have a much higher resolution than light microscopes and are ideal to visualize small structures. Actually, EM is the only method that allows direct observation and quantification of DNA replication intermediates. Several structures, such as reversed forks, Holliday junctions and even the distinction between single-stranded DNA (ssDNA) and double-stranded DNA (dsDNA) have been observed using this method (74).

Briefly, living cells are exposed to tri-methyl-psoralen (TMP) and irradiated with 365–366 nm monochromatic light to cross-link DNA. This crosslinking step preserves DNA replication intermediate (RI) structures during the subsequent extraction and enrichment procedures. Genomic DNA is then extracted and, in an optional step, RI are enriched by binding, washing and elution in a benzoylated-naphthoylated DEAE (BND) cellulose column, since this resin has high affinity to ssDNA (which is always present at RFs). Afterwards, the DNA sample is concentrated in size-exclusion columns and spread in the presence of the cationic detergent benzyl-dimethyl-alkylammonium chloride (BAC). This monolayer of DNA is absorbed to carbon-coated grids and stained with uranyl acetate. Finally, the individual DNA molecules can be visualized after the grids undergo flat angle rotary shadowing with platinum (74) (**Figure 1A**).

The high resolving power of EM (in the range of 30–50 base-pairs) allows the visualization of the fine architecture of DNA structures, such as reversed forks, and, combined with drug treatment or genetic manipulations, can reveal any kind of DNA alterations caused by these perturbations. Moreover, because nucleosomal DNA is not accessible to the crosslinking reagent psoralen, the final, deproteinized DNA will appear as ssDNA bubbles that represent the nucleosome position *in vivo*, providing valuable information on the chromatin organization on replicating DNA (74) (**Figure 1A**). Despite the enormous benefits of EM, it is a relatively laborious technique, it requires specialized, expensive equipment and it is a static method that only provides a snapshot of the RIs at a given time-point (**Table 1**).

DNA Fiber Assay

In this procedure, ongoing replication events are sequentially labeled with two thymidine analogs [commonly iododeoxyuridine (IdU) and chlorodeoxyuridine (CldU)] and, after cell lysis, individual DNA molecules are stretched into fibers using the combing (75, 76) or the spreading technique (represented in **Figure 1B**) (77). The two modified nucleotides are then detected by two-color immunofluorescence and visualized in a fluorescence microscope (**Figure 1B**).

Unlike EM, the visualization of individual RFs using the DNA fiber assay provides a better understanding of the dynamic behavior of RFs, based on several parameters, such as: the speed of ongoing RFs, the number of newly initiated forks, the distance between replication origins, the frequency of fork stalling/collapse, for instance, upon induction of replication stress (78, 79). Therefore, the combination of different experimental variables, such as the duration of labeling with thymidine analogs, the existence (or not) and extent of chase after labeling, as well the exposure to different genotoxic agents, gives a global picture of the fluctuating alterations in RFs. Combinations of EM and DNA fiber methods offer optimized conditions to elucidate mechanistic aspects of the cellular responses to specific types of replication stress (80).

The scale of the detected DNA fibers is $1\,\mu m = 2–4$ Kb, which means that only RF degradation of at least 2 kb can be directly observed, whereas smaller losses are undetected, making this a technique relatively low in resolution, when compared to others (61) (**Table 1**). Even though the "simple" DNA fiber assay does not provide information on the location of the RFs in the genome, it can be combined with a DNA probe (Fluorescence *in situ* Hybridization-FISH) specific for a certain genomic region (81). Due to the limited sensitivity of immunofluorescence, the detection of proteins at RFs is not feasible with this method (**Table 1**).

Isolation of Proteins on Nascent DNA (iPOND)

As its name indicates, iPOND is an approach focused on the detection of proteins associated with nascent DNA. In this method, cells are incubated with the thymidine analog 5-Ethynyl-2′-deoxyuridine (EdU) to label newly replicated DNA. After cross-linking of proteins and DNA with formaldehyde, the click reaction in performed to link biotin to EdU (82). After cell lysis and sonication to shear chromatin, proteins in close proximity to biotin and EdU-labeled DNA are purified with streptavidin-coated agarose beads. These isolated proteins are then resolved by Western blotting or mass spectrometry

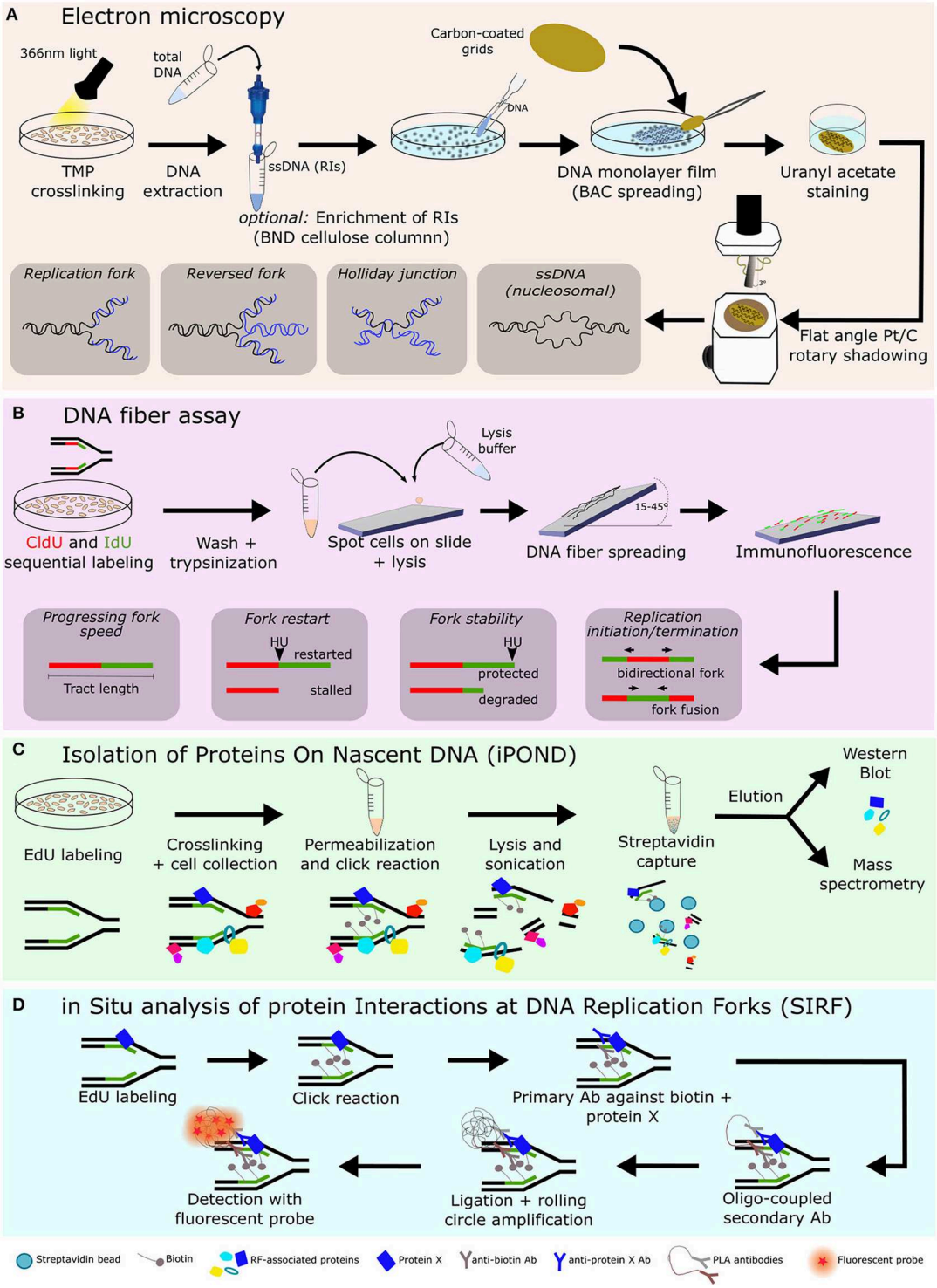

FIGURE 1 | Overview of techniques frequently used to study replication fork biology. Various methodologies, including electron microscopy **(A)**, single molecule DNA fiber assay, using the spreading technique **(B)**, iPOND **(C)**, and SIRF **(D)**, are being used to study replication fork-associated processes. Combining these techniques allowed many research groups to identify novel factors associated with replication forks and their role in replication fork dynamics and replication stress responses. Ab, antibody; BAC, benzyl-dimethyl- alkylammonium chloride; BND, benzoylated-naphthoylated DEAE; CldU, chlorodeoxyuridine; EdU, 5-Ethynyl-2′-deoxyuridine; IdU, iododeoxyuridine; iPOND, isolation of proteins on nascent DNA; PLA, proximity ligation assay; Pt/C, Platinum/carbon; RF, Replication fork; RIs, replication intermediates; SIRF, *in situ* analysis of protein interactions at DNA replication forks; TMP, tri-methyl-psoralen.

TABLE 1 | Summary of the advantages and disadvantages of the different techniques used to study replication fork biology.

Technique	Advantages	Disadvantages
Electron microscopy	○ Direct visualization and quantification of fork structures ○ High resolution: 30–50 base pairs	○ Static method ○ Laborious and requires specialized and expensive technique and equipment
DNA fiber assay	○ Single molecule resolution ○ Can measure several parameters: rate of fork elongation, inter-origin distances, frequency of origin firing, and frequency of fork collapse ○ Allows monitoring the dynamics of replication perturbation for a prolonged period of time	○ Relatively low resolution (only length differences corresponding to at least 2–4 Kb of DNA can be observed) ○ Inter-observer variability of the image analysis
iPOND	○ Improved sensitivity (compared to IF) ○ Combined with pulse-chase methods provides high spatial and temporal resolution of protein dynamics. ○ Allows analysis of posttranslational modifications ○ Compatible with unbiased screening approaches. ○ Coupling with SILAC/mass spectrometry: highly quantitative and unbiased	○ Laborious ○ Large amount of starting material required ○ Limited quantification potential ○ Does not consider heterogeneity of cell populations ○ SILAC/mass spectrometry: requires high-cost specialized equipment with limited access
SIRF	○ Single cell resolution ○ Allows analysis of heterogeneous cell populations (location and type) ○ Readily quantifiable ○ Sensitive (very little starting cell material) ○ Does not require special equipment	○ Not all epitopes at the forks may be accessible to antibodies ○ Limited to distances no >∼40 nm

IF, immunofluorescence; iPOND, Isolation of proteins on nascent DNA; SILAC, stable isotope labeling with amino acids in cell culture; SIRF, in situ analysis of protein interactions at DNA replication forks.

(69) (**Figure 1C**). Besides allowing the identification of proteins at active RFs, this technique also enables the investigation of proteins recruited to stalled and collapsed forks, depending on the addition of different replication stress-inducing agents to the cells (69).

Compared to immunofluorescence, iPOND is a more sensitive technique and also enables the analysis of posttranslational modifications. Additionally, combined with pulse-chase experiments, it offers a high spatial and temporal resolution of protein dynamics at replicating DNA. Another advantage of iPOND is the possibility to combine it with unbiased screening approaches by coupling iPOND to mass spectrometry (**Table 1**). Hence, this methodology is very useful to identify new proteins present at active and perturbed RFs (69).

Despite its relative high sensitivity, iPOND lacks an amplification step, which means that large amounts of starting material are needed to achieve sufficient protein for detection (82). It is also a laborious and not very trivial technique, requiring specialized technical skills. Other drawbacks of this tool are its limited quantitative potential and the fact that it analyses cells as a whole population, not considering individual cell heterogeneity (**Table 1**).

One extension of mass spectrometry-coupled iPOND is the combination with stable isotope labeling with amino acids in cell culture (SILAC). For this purpose, two different cell populations are grown in a medium containing either normal amino acids or amino acids labeled with stable non-radioactive heavy isotopes. This way, the abundance of specific proteins can be directly compared and quantified between the two samples (69).

An alternative protocol for iPOND, named aniPOND (accelerated native iPOND) has also been developed. The major advantages of aniPOND compared to the earlier described iPOND are the milder lysis conditions that preserve better the DNA-protein complexes, the absence of the formaldehyde crosslinking step that may interfere with downstream analysis, and an improved protein yield (83).

In situ Analysis of Protein Interactions at DNA Replication Forks (SIRF)

SIRF is a technology that fuses iPOND and a modified version of the proximity ligation assay (PLA), used to detect proteins in close proximity to others (84). In this method, like in iPOND, EdU is incorporated into replicating DNA and then biotinylated using the click chemistry (85). Afterwards cells are incubated with primary antibodies against biotin and the protein of interest and detection follows the principles of PLA: two secondary antibodies conjugated with oligonucleotides are added to the cells and bind to the primary antibodies. When the secondary antibodies (and consequently EdU-labeled DNA and the protein of interest) are in close proximity (<40 nm), the two oligonucleotides can anneal to each other and form a circular DNA structure that serves as a template for a PCR-based amplification reaction (rolling circle amplification). These amplified DNA circles are then

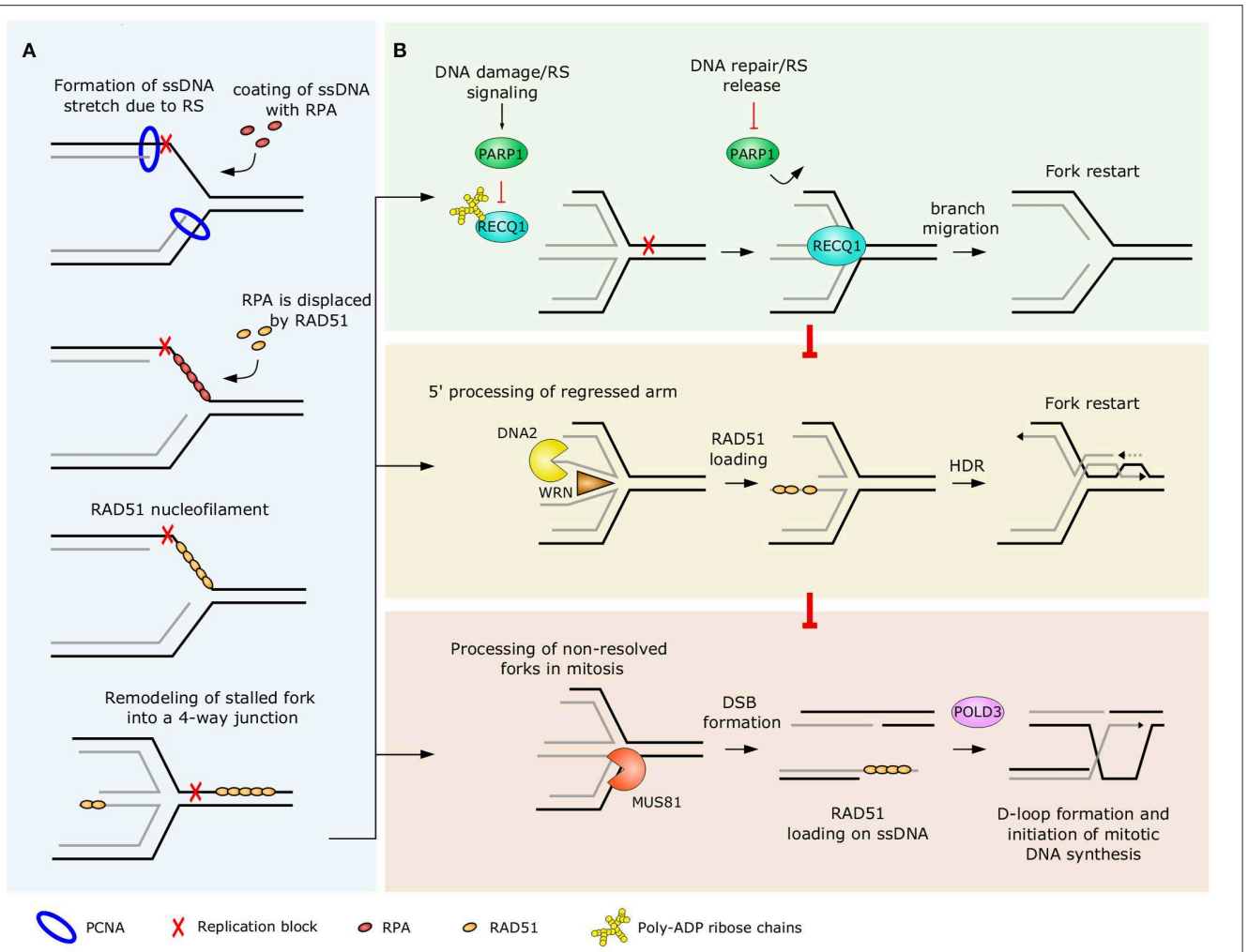

FIGURE 2 | RAD51-mediated RF reversal **(A)** and an overview of replication fork restart mechanisms **(B)**. **(A)** At stalled replication forks, ssDNA tracks are protected and coated with RPA. The DNA recombinase RAD51 replaces RPA and binds to DNA, contributing to the remodeling of the stalled fork into a reversed fork (4-way) structure. Besides RAD51, there are other replication fork remodelers, mentioned in the main text, but for simplicity only RAD51 is represented in this figure. **(B)** PARP1-mediated suppression of RECQ1 helicase is an important regulator of a premature restart of reversed forks (upper panel). Because of the least amount of processing involved, RECQ1-mediated pathway represents the first-choice restart mechanism of reversed forks. DNA2/WRN-driven restart involves regulated processing of the regressed arms and uses HDR to resolve the replication intermediate (middle panel). Reversed forks that could not be restarted in S phase are processed by MUS81 endonuclease later in mitosis and DSB break is formed in the process. The collapsed fork is then rescued by POLD3-driven D-loop formation and synthesis re-initiation (lower panel). PCNA, proliferating cell nuclear antigen; RPA, replication protein A.

detected by sequence-specific DNA fluorescent probes, allowing the visualization and quantification of signal that corresponds to the sites of interaction between active RFs and the protein of interest (85) (**Figure 1D**). Besides SIRF using EdU to label nascent DNA, mapping proteins at forks can also be assessed by the standard PLA method between any given protein and PCNA (or other fork components).

The combination of this efficient and sensitive tool with other immunofluorescence parameters, such as cell cycle or cell identity markers, enables the analysis of heterogeneous cell populations with a single cell resolution. Additionally, it can be performed in any standard molecular biology laboratory, as it does not require special equipment (85). Pitfalls of SIRF are the fact that only interactions closer than 40 nm can be visualized and that some epitopes at RFs may not be accessible to antibodies (85) (**Table 1**).

REPLICATION FORK REVERSAL AND ITS PLAYERS

Remodeling of RFs involves unwinding of newly synthesized strands and annealing of nascent and parental strands. In this process, the standard three-way junction forks are converted into four-way junction structures. Since annealing of nascent DNA strands form regressed arms at the fork, this remodeling event is called RF reversal (**Figure 2A**). This was shown to be an effective

mechanism allowing cells to cope with replication stress and to maintain genome integrity (70). Interestingly, recent work of Mutreja et al. (86) has demonstrated that replication fork reversal can be regulated globally and may represent a "safety brake" to prevent potential collisions of ongoing unaffected forks with DNA lesions ahead of them. The authors also demonstrated that this global fork slowing and reversal requires ATR-dependent signaling (86).

The initial step of fork reversal is associated with the accumulation of ssDNA at challenged RFs. This can occur either by physical uncoupling of the polymerase and replicative helicase or by controlled nucleolytic digestion of nascent DNA in certain contexts, such as in response to inter-strand crosslinks (ICLs) or increased torsional stress (70, 87). Uncovered ssDNA at the affected fork is promptly recognized by a highly abundant Replication protein A (RPA). The high affinity of RPA toward ssDNA allows a dynamic cellular response to a variety of replication stress-inducing agents of both endogenous and exogenous origin (88–90).

The interaction of RPA with ssDNA is highly dynamic and involves repeated dissociation and re-association of RPA subunits due to conformational changes. Dynamic interaction of RPA with both DNA and other proteins allows RPA to carry out various functions and is crucial for maintaining the stability of the fork affected by replication stress (**Figure 2A**). First, coating of ssDNA with RPA removes secondary structures (91, 92). RPA nucleofilaments then attract checkpoint signalization proteins such as ATR and its interactor ATRIP (ATR-interacting protein) to initiate a global cellular response to replication stress (89, 93). Furthermore, RPA nucleofilaments help recruit and regulate the activity of various DNA repair proteins required for stabilization and recovery of the challenged fork (94, 95). All these functions are essential for preventing RF collapse and maintenance of chromosomal integrity (91).

RAD51 recombinase is well-known for catalyzing strand-invasion in HR repair of DNA double-strand breaks. Loading to ssDNA at double-strand breaks is highly dependent on its interaction with BRCA2. However, RAD51 also plays an important role in regulating RF reversal (**Figure 2A**) (70). Interestingly, these two functions are genetically separated, since its recruitment to stalled forks and its enzymatic activity promoting fork reversal are BRCA2-independent (96, 97). Dungrawala et al. (98) identified a ssDNA-binding protein, RADX, to be enriched at RFs and to antagonize the accumulation of RAD51 and RF reversal. Nevertheless, how the recruitment of RAD51 to stalled forks is regulated remains largely elusive. Due to impaired fork reversal, cells depleted of RAD51 do not show reduced RF progression following genotoxic treatments, leading to hypersensitivity to a wide-range of genotoxic agents and increased frequency of chromosome breakage (70).

Several remodelers have been shown to associate with stalled RFs and drive their reversal, such as SMARCAL1, ZRANB3, and HLTF (94, 99, 100). Interestingly, a common feature of all three is the lack of a 3′-ssDNA unwinding activity typical for helicases. Instead, upon recruitment to stalled forks, their critical role in remodeling of challenged RFs is facilitated by their ATP-dependent dsDNA translocase activity, allowing the formation of regressed arms by unwinding of newly synthesized strands and annealing of nascent and parental strands (99, 101).

SMARCAL1 is a multi-domain protein of the SNF2 family of ATPases (102). It associates with the active replisome complex and drives the remodeling of stalled forks by branch migration and fork regression. SMARCAL1-mediated remodeling has been shown to prevent an alternative repair mechanism involving the initial formation of double-strand breaks by MUS81 cleavage of the stalled fork (94).

Another member of the SNF2 family of remodelers is the ZRANB3 translocase. Upon induction of replication stress, ZBRANB3 associates with polyubiquitinated PCNA to facilitate RF reversal and replication slowdown (100). Ciccia et al. (103) showed that ZRANB3 activity is also required for resolution of recombination intermediates and efficient restart of arrested forks. In mammalian cells, siRNA-mediated downregulation of ZRANB3 leads to increased frequency of sister chromatid exchange and sensitivity of the cells to treatments interfering with replication, such as hydroxyurea (HU), camptothecin (CPT), cisplatin, and UV irradiation (103).

HLTF, the last member of the SNF2-family known to be required for fork remodeling so far, was originally identified as a human homolog of the yeast template-switching protein Rad5 (104). The ancient and conserved HIRAN domain was shown to be crucial for the interaction of HLTF with 3′-ssDNA at RFs (105). Similar to Rad5 in yeast, HLTF also possesses a E3-ubiquitin ligase-containing RING domain, which facilitates the K-63-linked polyubiquitination of PCNA (104). HLTF RING mutants were shown to fail in promoting efficient fork reversal, likely due to impaired recruitment of the downstream remodeler ZBRANB3 and other factors that require polyubiquitinated PCNA for efficient association with stalled RFs (100, 106).

The interplay between various fork remodeling factors seems to be highly complex and is not fully understood yet.

Deficiencies in SMARCAL1, ZRANB3, or HLTF lead to enhanced replication stress, collapse of stalled RFs and chromosomal instability, which sensitizes these cells to a wide range of replication stress-inducing agents (99, 100, 107). Lower expression or truncating gene mutations of SMARCAL1, ZRANB3, and HLTF have also been linked to susceptibility to various types of cancer (108–113). Recently, Puccetti et al. (114) identified non-redundant functions of SMARCAL1 and ZRANB3 in alleviation of Myc oncogene-induced replication stress. The authors also showed that both alleles of SMARCAL1 and ZRANB3 are required for fork stabilization in Myc-overexpressing primary cells (114). However, SMARCAL1-, ZRANB3-, and HLTF-mediated fork remodeling also possess a threat to genome integrity in cells lacking functional BRCA1/2 by providing a substrate for unregulated extensive degradation of the regressed arms (72, 96, 97, 106). An overview of the factors described in this and the following chapters can be found in **Table 2**.

TABLE 2 | Overview of several key players involved in RF metabolism.

Factor	Enzymatic activity	Function in RF remodeling/ chemoresistance and clinical evidence	References
RAD51	Recombinase	RF reversal/depletion restores RF stability in BRCA-deficient cells *in vitro*.	(70)
RAD54	DNA translocase	Regulation of RF reversal and restoration through branch migration.	(115)
SMARCAL1 (SWI/SNF-related matrix-associated actin-dependent regulator of chromatin subfamily A-like protein 1)	ATP-dependent annealing helicase (translocase)	RF reversal/depletion restores RF stability and confers chemo-, PARPi-resistance in BRCA-deficient cells *in vitro*. Low mRNA associated with reduced survival in BRCA1-mutant breast cancer.	(96, 106)
ZRANB3 (Zinc finger Ran-binding domain-containing protein 3)	ATP-dependent annealing helicase and endonuclease (translocase)	RF reversal/depletion restores RF stability in BRCA1/2-deficient cells *in vitro*.	(97, 100, 106)
HLTF (Helicase-like transcription factor)	ATP-dependent annealing helicase (translocase)/E3 ubiquitin ligase	RF reversal/depletion restores RF stability in BRCA1/2-deficient cells *in vitro*.	(106)
FBH1 (F-box DNA helicase 1)	DNA helicase/translocase	RF reversal	(116)
BLM (Bloom syndrome protein)	ATP-dependent DNA helicase	RF reversal and restart	(117, 118)
RECQL5 (RecQ protein-like 5)	ATP-dependent DNA helicase	RF reversal	(119)
FANCM (Fanconi anemia group M protein)	ATP-dependent translocase	RF reversal, restart and protection of stalled forks	(120–122)
RADX (RPA-related, RAD51-antagonist on X-chromosome)	ssDNA-binding protein	Antagonizing RF reversal/depletion restores RF stability and confers chemo- and PARPi-resistance in BRCA2-deficient cells *in vitro*.	(98)
CtIP (CTBP-interacting protein)	5′ flap endonuclease	RF processing, restart of stalled forks	(72, 123)
MRE11 (Meiotic recombination 11)	3′->5′ exonuclease and endonuclease	RF processing/inhibition restores RF stability in BRCA1/2-deficient cells *in vitro*.	(63, 72, 97, 124)
RAD52		Recruitment of MRE11 to stalled RFs and fork degradation in BRCA2-deficient cells/depletion or inhibition restores RF stability in BRCA2-defective cells *in vitro*.	(97)
PTIP (PAXIP1—PAX-interacting protein 1)		RF processing via recruitment of MRE11/loss restores RF stability *in vitro*. Poor prognosis in BRCA1/2 mutant ovarian cancer.	(62)
PARP1 (Poly (ADP-ribose) polymerase 1)	Poly-ADP-ribosyltransferase	Recruitment of MRE11 to stalled RF, fork reversal, regulation of fork restart/deletion restores RF stability in BRCA1/2-deficient cells *in vitro*. Deficiency reduces tumor-free survival in Brca2$^{-/-}$ mouse model.	(62, 125)
EXO1 (Exonuclease 1)	5′->3′ exonuclease, 5′ structure specific DNA endonuclease, 5′->3′ RNase H	Further RF processing initiated by CtIP and MRE11/depletion restores RF stability in BRCA1/2-deficient cells *in vitro*.	(72)
RECQ1 (ATP-dependent DNA helicase Q1)	ATP-dependent DNA helicase	RF restart via branch migration	(30)
WRN (Werner syndrome ATP-dependent helicase)	ATP-dependent DNA helicase, 5′->3′ exonuclease	RF processing and HR-mediated restart of stalled forks	(126)
DNA2 (DNA replication ATP-dependent helicase/nuclease)	ssDNA-dependent ATPase, 5′->3′ helicase, 5′->3′ endonuclease	RF processing and HR-mediated restart of stalled forks	(127)
MUS81 (Methyl methanesulfonate and ultraviolet-sensitive gene clone 81)	Crossover junction endonuclease	RF fork processing and restart/Impaired recruitment via EZH2 inhibition or depletion restores RF stability in BRCA2-deficient cells *in vitro*. Low expression associated with poor prognosis in BRCA2-mutated tumors.	(73)
CHD4 (Chromodomain-helicase-DNA-binding protein 4)	Chromatin remodeler	RF processing via chromatin accessibility/depletion restores RF stability in BRCA-deficient cells and confers chemoresistance *in vitro*. Poor prognosis in BRCA2 mutant ovarian cancer.	(62, 71)
EZH2 (Enhancer of zeste homolog 2)	Chromatin modifier (Histone-lysine N-methyltransferase)	RF processing and restart via H3K27 trimethylation and MUS81 recruitment/depletion restores RF stability and confers chemoresistance in BRCA2-deficient cells. Low expression associated with poor prognosis in BRCA2-mutated tumors.	(73)

MECHANISMS OF FORK RESTART

The ability to restart stalled RFs is essential to avoid excessive accumulation of replication intermediates, which are prone to aberrant processing and if not resolved properly, may cause chromosome segregation defects later in mitosis (128–130). To carry out this task, eukaryotic cells have evolved various mechanisms to process stalled replication intermediates and to restart affected RFs (**Figure 2B**, **Table 2**). Conversion of reversed forks back to standard three-way DNA junctions is a process essential for restoration of replication and successful duplication of the genome. In eukaryotes, failure in restarting severely damaged forks can be, to a certain extent, buffered by firing of dormant replication origins. However, systemic dysregulation of the process e.g., by genetic alterations or drug interventions significantly elevates chromosomal instability (131, 132).

RECQ1 is the most abundant member of the RecQ family of helicases in human cells (133, 134). However, its specific role in replication was not known for a long time. Thangavel et al. (134) showed that RECQ1 associates with replication origins in a cell cycle-dependent manner and that depletion of RECQ1 suppresses the RF rate in unperturbed S phase. Berti et al. (30) provided a mechanistic explanation for this phenotype by identifying the role of RECQ1 in priming branch migration at reversed forks and driving their restart (**Figure 2B**). By combining electron microscopy with single-molecule DNA fiber assay, Berti at al. (30) demonstrated a critical function of the RECQ1 helicase in promoting RF restart following topoisomerase 1 inhibition. Furthermore, the authors showed that the activity of RECQ1 at the reversed RFs is negatively regulated by PARP1, demonstrating a major role of PARylation in preventing RECQ1-mediated restart of forks.

Germline mutations leading to loss of the helicase activity of RECQ1 have been associated with increased susceptibility to breast cancer (135, 136). Another study showed that embryonic fibroblasts from mice lacking RECQ1 activity display increased rates of spontaneous chromosomal breakage and aneuploidy (132). Importantly, while genetic alterations reducing the activity of RECQ1 have been shown to increase susceptibility to certain types of cancer, overexpression of RECQ1 has been associated with increased replication stress survival, drug resistance, and overall poor prognosis in patients with multiple myeloma. The authors also showed that reducing RECQ1 expression by DNA methyltransferase inhibition sensitized multiple myeloma cells to PARPi (137). Collectively, these findings highlight the importance of RECQ1 in DNA metabolism and maintenance of chromosomal integrity and may open opportunities for novel targeted therapies (135, 136).

Another mechanism by which reversed RFs can be restarted involves unwinding of nascent strands in regressed arms by the ATP-dependent helicase activity of Werner syndrome protein (WRN) and nucleolytic processing by DNA2 (**Figure 2B**). Compared to other factors acting at stalled RFs, the role of WRN is more complex due to its dual helicase and exonuclease activities (126). Recruitment of WRN to reversed RFs and its proper function is highly dependent on an orchestrated action of ATM and ATR kinases. Interestingly, phosphorylation mediated by ATM and ATR is required for different steps in the process of stalled fork recovery. While ATR-mediated phosphorylation of multiple residues at the C-terminus of WRN is required for proper nuclear foci formation and co-localization with RPA, ATM-mediated phosphorylation is essential for formation of RAD51 nuclear foci, enabling proper recovery of collapsed forks (138). Furthermore, both helicase and exonuclease activities are required to limit MUS81-dependent breakage of forks after HU-induced arrest (126). Rodriguez-Lopez et al. (139) showed that normal progression RFs is affected in cells lacking functional WRN protein. The authors observed asymmetric progression of bi-directional forks diverging from the majority of replication origins, suggesting an increased frequency of RF stalling. Based on these data, the authors concluded that WRN is either protecting RFs from collapse or promotes resolution of replication intermediates at collapsed forks (139).

DNA2, like WRN, possesses nucleolytic and helicase activities. Together with exonuclease 1 (EXO1), DNA2 has been known for its function in mediating processive DSB resection downstream of the MRN complex and CtIP in eukaryotic cells. By nucleolytic processing of 5′ ends and generating 3′ ssDNA overhangs at DSBs, EXO1 and DNA2 carry out the initial step essential for HR (140–142). Independently of its role in dsDNA break repair, DNA2 has also been shown to assist WRN in controlling HR-mediated restart of reversed RFs by resecting the regressed arm following nucleotide depletion by HU (127). Importantly, this function of DNA2 may play a major role in tolerance to chronic replication stress, induced e.g., by oncogene activation, commonly exhibited by cancer cells. Indeed, Peng et al. (143) demonstrated that normal pancreatic ductal cells that were transformed into cancer cells by activating K-RAS showed overexpression of DNA2 in early stages of transformation. Elevated levels of DNA2 mRNA were also found in a wide range of cancer types, further demonstrating the importance of DNA2-mediated recovery of stalled forks in replication stress tolerance (143, 144).

The restart of reversed RFs via RECQ1- and DNA2/WRN-dependent pathways allows the resolution of most of the reversed RFs in S phase and is essential for maintenance of chromosomal integrity in eukaryotic cells (30, 127). Nevertheless, more processing is required in certain situations to prevent potentially mutagenic genomic rearrangements arising from unresolved complex replication intermediates (145). MUS81 is a cell-cycle regulated, structure-specific endonuclease that preferentially cleaves branched DNA substrates, such as replication or recombination intermediates. Processing of the reversed forks by MUS81 leads to formation of DSBs and subsequent recovery of stalled forks via HR (**Figure 2B**). MUS81-dependent processing of stalled forks was initially implicated in the resolution of forks perturbed by nucleotide pool depletion (146). However, other groups showed that processing of unusual replication intermediates by MUS81 may also be responsible for oncogene-induced genotoxicity, since depletion of MUS81 alleviated chromosomal breakage and resulted in an increase of reversed forks in human U2OS cells overexpressing the oncogenes *Cyclin E* and *Cdc25A* (147). Therefore, the outcome of MUS81-mediated DNA processing and DSB induction at stalled forks is highly

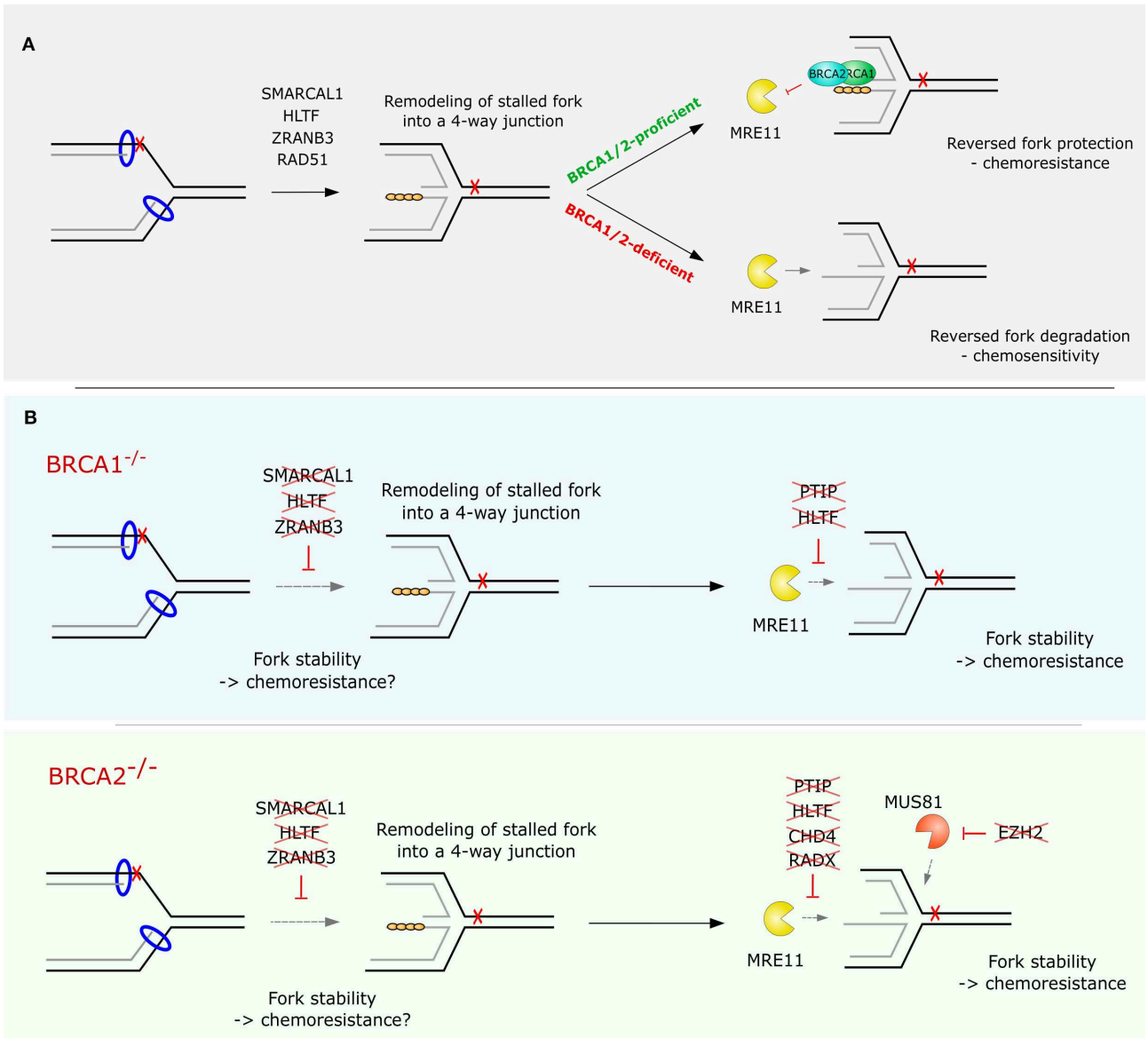

FIGURE 3 | Replication fork stability or degradation in BRCA1/2-proficient and -deficient cells. **(A)** Reversed replication fork arms are protected from degradation by RAD51 nucleofilaments stabilized by BRCA1 and BRCA2. In the absence of BRCA1/2 proteins RAD51 dissociates from ssDNA at the regressed arms, leaving the nascent DNA susceptible to nucleolytic resection by exonucleases such as MRE11. **(B)** Overview of the factors shown to restore RF stability and confer chemoresistance upon their loss in BRCA1- or BRCA2-deficient cells.

dependent on the genetic background and the context in which the replication intermediates are formed.

FORK STABILITY AS A RESISTANCE MECHANISM IN BRCA-DEFICIENT TUMORS

BRCA1 and BRCA2 have well-known roles in the repair of DNA DSBs by HR. BRCA1 is crucial for the resection of DNA at DBS sites, creating two regions of ssDNA on either side of the break. BRCA2, with the help of PALB2, localizes the DNA recombinase RAD51 to the exposed ssDNA regions, forming stable nucleoprotein filaments which invade the intact homologous DNA double helix (148). Besides these, BRCA1/2 have many other cellular functions independent of their role in HR. One of these is their function in the protection of RFs under replication stress conditions by stabilizing RAD51 nucleofilaments and preventing excessive processing of forks by nucleases (**Figure 3A**) (63, 64, 149). While RF reversal has been shown to alleviate chromosomal instability upon exposure to genotoxic treatments (70), it also provides an entry

point for nascent DNA degradation in cells lacking BRCA1 or BRCA2 (72, 96, 97, 106). Step-wise processing of nascent DNA at reversed forks by different nucleases has been shown to drive fork degradation. The MRE11-dependent resection is initiated by CtIP and then further extended by EXO1 (72). The enzymatic inhibition of MRE11 by mirin or siRNA-mediated depletion of EXO1 results in the protection of RFs in BRCA1/2-deficient cells treated with HU. Interestingly, the combination of MRE11 inhibition and EXO1 knockdown had a synergistic effect on the stability of stalled forks, indicating a potentially independent function of these nucleases in fork degradation (72). However, other groups have observed a full restoration of fork stability by MRE11 inhibition alone, pointing to MRE11 as the nuclease responsible for most of the processing of regressed arms in BRCA-deficient cells (62, 63). Furthermore, loss or down-regulation of factors involved in chromatin recruitment of MRE11 also restores fork stability and alleviates chromosome breakage in HU-treated BRCA-deficient cells (62).

Ray Chaudhuri et al. (62) showed that recruitment of MRE11 to stalled RFs is impaired upon loss of PTIP, a member of the MLL3/4 complex. The authors also demonstrated that *Ptip* deficiency rescues lethality in *Brca2*-deficient mouse embryonic stem cells. The restoration of RF stability promotes resistance of BRCA2-deficient tumors to cisplatin and PARPi independently of HR restoration. Interestingly, this function of PTIP at RFs is independent of its interaction with 53BP1 in the canonical DSB repair, since 53BP1/BRCA1-deficient B cells did not show any protection of forks upon nucleotide depletion (62). Similarly, loss of PARP1, which has been linked to regulation of MRE11-dependent restart and recombination at stalled forks (150), also restores RF stability and rescues lethality of *Brca2* null mouse embryonic stem cells (62). Another group demonstrated that depletion of RAD52, similarly to loss of PARP1 or PTIP, leads to reduced recruitment of MRE11 to chromatin and completely abolishes RF degradation in BRCA2-defective cells (97).

A genome-wide short hairpin RNA (shRNA) screen performed by Guillemente et al. (71) has identified the chromatin remodeling factor CHD4 to promote cisplatin resistance in *BRCA2*-mutated ovarian cancer cell line PEO-1 upon its downregulation. The depletion of CHD4 restored normal cell cycle progression and alleviated chromosomal aberrations upon cisplatin treatment (71). Mechanistically, similar to the situation in PTIP-,PARP1-, or RAD52-deficient cells, the phenotype of CHD4-depleted cells can be explained by the reduced chromatin recruitment of MRE11 and an increased RF stability in BRCA2-deficient cells upon replication stalling (62).

Various epigenetic modifications may also play an important role in RF remodeling and resolution of stalled RFs. Rondinelli et al. (73) performed a gene expression analysis of chromatin modifiers in HR-defective BRCA1/2-deficient tumors and found the enhancer of zeste homolog 2 (EZH2) to score as the top overexpressed chromatin modifier in various tumor types. The authors showed that EZH2 localizes to RFs stalled by HU and promotes recruitment of the MUS81 nuclease by mediating trimethylation of H3K27 (73). MUS81-dependent processing of stalled RFs has been shown to have a significant role in resolution of replication intermediates and replication restart (145, 151). Lai et al. proposed a new function of MUS81-dependent processing in replication stress tolerance and survival of BRCA2-deficient cells upon nucleotide depletion by HU. Lemacon et al. (72) then provided a mechanistic explanation for this phenotype by demonstrating that MUS81 resection at replication intermediates drives POLD3-dependent fork rescue upon HU-induced fork stalling. Interestingly, impaired MUS81 recruitment to RFs, e.g., by enzymatic inhibition or siRNA-mediated knockdown of EZH2, conferred RF stability and chemoresistance to PARPi and cisplatin in BRCA2-, but not in BRCA1-deficient cells (73). Consistent with these findings, low expression of EZH2/MUS81 have been found to correlate with chemoresistance and poor therapy outcome in patients with BRCA2-mutated tumors (73). However, it is not fully understood how MUS81 loss promotes PARPi resistance in BRCA2-deficient cells. The treatment-specific response of MUS81-depleted BRCA2-deficient cells to HU and PARPi may be explained by the importance of PARP1 in RF slowing and regulation of restart (30). Inhibition of PARP1 may promote RECQ1-dependent restart of reversed forks, therefore depriving cells of a substrate for MUS81 (30, 152, 153). However, more research has to be done to fully understand the context-specific synthetic lethal/viable interaction between BRCA2 and MUS81 deficiency.

Recently, the loss of RADX was identified as another mechanism protecting aberrant processing at stalled forks in BRCA2-deficient cells. RADX is an ssDNA binding protein that acts as a negative regulator of RAD51 (98). Dungrawala et al. (98) showed that inactivation of RADX enables excessive accumulation of RAD51 at RFs, leading to lower rate of replication elongation and formation of DSBs. However, in cells lacking BRCA2, depletion of RADX was sufficient to compensate for the decreased stability of RAD51 filaments and to rescue RF stability. This translated into reduced sensitivity to HU, cisplatin, CPT and PARPi.

Besides the proteins described above, several other factors have also been shown to promote RF remodeling such as DNA helicases FBH1, WRN, BLM, RECQL5, and DNA translocases RAD54 and FANCM (**Table 2**). However, the relevance of these proteins for replication fork metabolism in the context of BRCA1/2 deficiency and chemoresistance remains to be studied in more detail (115–117, 119, 120, 126). Collectively, genetic alterations resulting in rewired fork protection in BRCA1/2-deficient cells are highly complex and the interaction dynamics between various remodelers, processing factors, and other DNA repair factors remain to be further investigated. Furthermore, while loss of certain factors, such as PTIP, PARP1 (62), or fork remodelers SMARCAL1, HLTF, and ZRANB3 confer RF stability in both BRCA1- and BRCA2-deficient backgrounds (106), loss of CHD4, EZH2, and RADX only restore fork stability in cells lacking BRCA2 (**Figure 3B**) (71, 73, 98). These findings suggest that different pathways leading to restored fork stability may exist in mammalian cells, even though they all lead to the same endpoint: limited processing of stalled forks by nucleases (60). Importantly, while preventing reversed fork degradation by limiting nuclease access or activity (by loss of PTIP, CHD4, etc.) is likely to support therapy survival in the clinics, the possible

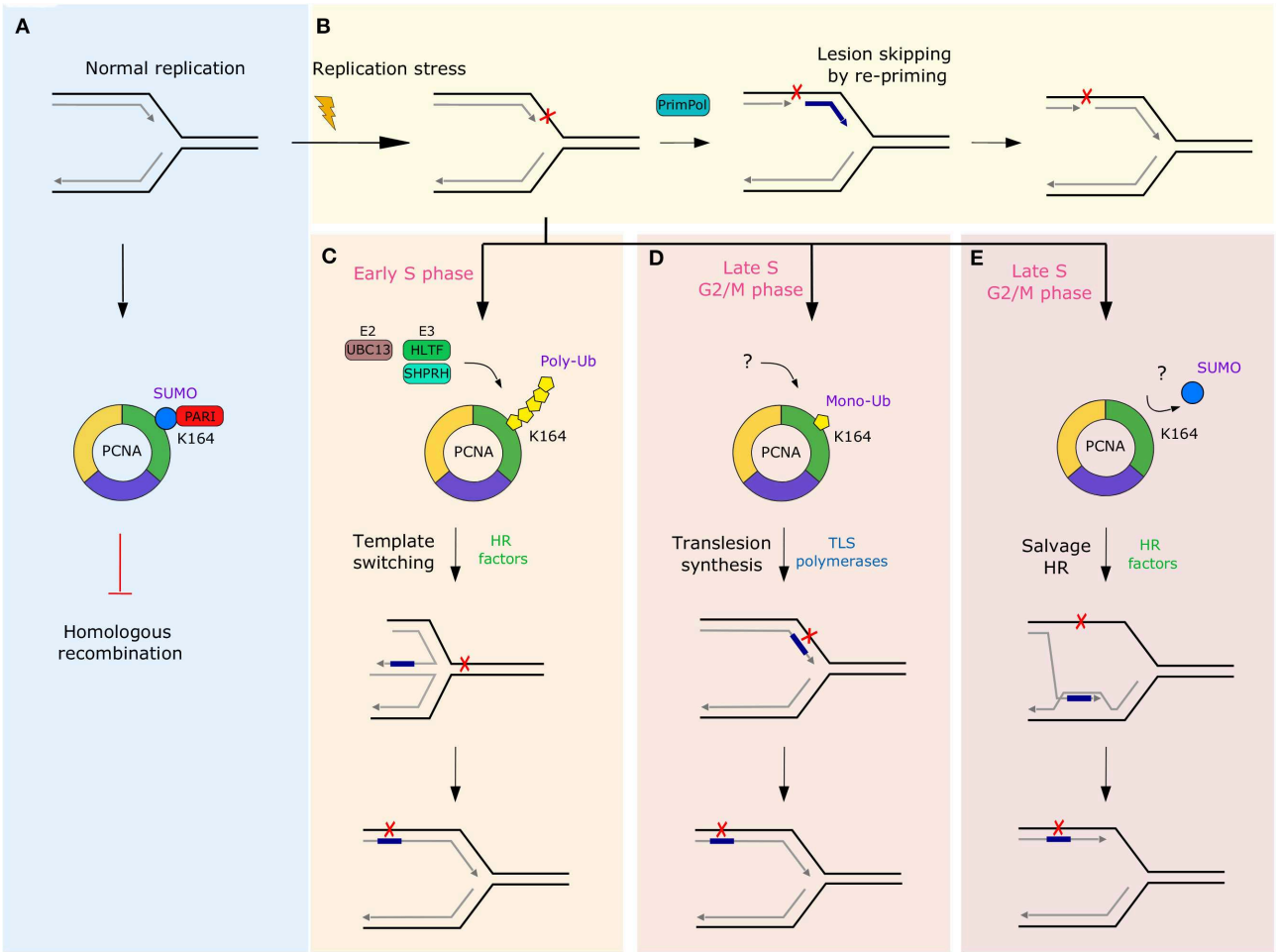

FIGURE 4 | Overview of the DDT pathways and their regulation by various post-translational modifications of PCNA. **(A)** During normal replication PCNA interacts with the anti-recombinase PARI through SUMO modification to prevent potentially mutagenic recombination events in the absence of replication stress. **(B)** In response to replication stress, PrimPol-mediated lesion skipping allows cells to re-initiate synthesis downstream of the lesion and prevent RF stalling, while leaving an ssDNA gap behind. Alternatively, cells can employ one of three DDT pathways regulated by various modifications at K164 of PCNA. **(C)** Poly-ubiquitination in early S-phase initiates a mechanistically complex, but error-free TS, which requires RAD51-mediated strand invasion and newly replicated sister chromatid for synthesis over the damaged template. In contrast, mono-ubiquitination leads to the frequently mutagenic TLS in late S or G2/M phase. This process requires a step-wise exchange of high-fidelity replicative polymerases for specialized low-fidelity non-processive polymerases to enable synthesis over the lesion **(D)**. **(E)** The last DDT mechanism is "salvage" HR repair which is commonly repressed by SUMOylation of PCNA and by the anti-recombinase PARI in order to prevent chromosome rearrangements caused by hyper-recombination. The question marks indicate that the factors involved in the processes in human cells are not clearly defined. HR, homologous recombination; PARI, PCNA-associated recombination inhibitor; SUMO, small ubiquitin-like modifier; TLS, translesion synthesis; Ub, ubiquitin.

impact of preventing formation of the reversed RF as a targeted structure for degradation is more debated.

DNA DAMAGE TOLERANCE PATHWAYS

Another group of mechanisms allowing maintenance of genome integrity, which can involve RF remodeling, are DDT pathways. While the highly complex DDR network is essential for ensuring genome integrity over generations, immediate activation of the repair machinery at the damaged DNA may not be beneficial in every scenario. Prolonged stalling of RFs induced by DNA damage significantly increases the risk of fork collapse and genome instability. To minimize the chances of increased rates of fork collapse and formation of highly cytotoxic DSBs, cells developed DDT pathways that enable DNA synthesis beyond the damaged template, thereby completing the DNA replication prior to damage repair. The bypassed lesion is then removed later on by the specialized DNA repair pathways in the process called post-replicative repair (154, 155). Four major DDT pathways enabling bypass of DNA lesions have been described thus far: translesion synthesis (TLS), DNA primase-polymerase (PrimPol) mediated re-priming, template switching (TS) and the HR-mediated "salvage" pathway (156, 157) (**Figure 4**).

TLS is a mechanistically straightforward pathway compared to the TS and HR salvage repair, and it only requires the replacement of high-fidelity replicative polymerases by specialized low-fidelity non-processive polymerases (158). Low-fidelity of the TLS polymerases can be attributed to the lack of proofreading activity and the more flexible structure of the active site, which is able to accommodate modified bases and allow base mismatches (159, 160). Exchange of a stalled replicative polymerase for a TLS polymerase is a stepwise process involving at least two switching events (161). In the first step, the replicative polymerase is replaced by one of the insertion TLS polymerases, such as POL κ, POL ι, POL η, or REV1 that enable DNA synthesis over the DNA lesion. Then, either the same or another extension TLS polymerase elongates the newly synthesized DNA fragment to prevent detection of the lesion by the proof-reading activity of the replicative DNA polymerase (162, 163). This step is facilitated by the POL ζ complex of B-family polymerases (REV3L, REV7, POLD2, POLD3 (164–167). The last switching event restores a replicative DNA polymerase on the DNA template and reinitiates normal DNA synthesis. However, while the TLS is an easy, straightforward mechanism allowing lesion bypass and preventing fork stalling, it is also intrinsically error-prone. This is due to the higher frequency of nucleotide misincorporation by the TLS polymerases on the undamaged template, and due to the fact that synthesis over certain lesions, such as abasic sites, is often mutagenic (159, 160).

Another DDT mechanism is facilitated by the TLS primase PrimPol. PrimPol is a member of the archeo-eukaryotic primase (AEP) superfamily and has been shown to enable the bypass of various types of DNA lesions, either via its TLS activity or by lesion skipping (157, 168–171). While TLS is characterized by continuous DNA synthesis over the damaged template, lesion skipping involves the re-initiation of DNA synthesis of the leading strand *de novo* downstream of the replication block on the undamaged template. Therefore, PrimPol-mediated re-priming also represents a powerful RF remodeling-independent restart mechanism for stalled forks (172–175). Unlike TLS, lesion skipping results in the formation of a ssDNA gap behind the site of re-initiation and it needs to be repaired post-replicatively (170). PrimPol shares several properties with other TLS polymerases; it lacks the 3′-5′ exonuclease proofreading activity and exhibits low-fidelity and low-processivity DNA synthesis (157, 176–178).

Interestingly, experimental data from yeast and human cells indicate that DNA re-priming and stalled RF reversal are mutually exclusive events (175, 179). Disturbing the balance between fork reversal and re-priming may have a significant impact on genome stability maintenance, especially in the context of anticancer therapy in *BRCA1/2*-mutated tumors. Recent work of Quinet et al. demonstrated that the ATR-mediated increase in expression of PrimPol and its recruitment to stalled RFs abolishes the nascent DNA degradation in BRCA1/2-deficient human cells treated with multiple doses of genotoxic agents, such as UVC, HU and cisplatin. The authors also showed that the PrimPol-mediated adaptive response is dependent on ATR signaling. However, while elevated levels of Prim Pol lead to stalled RF protection, it also resulted in accumulation of ssDNA gaps in the genome (175). More research is required to fully understand the dynamics between the two pathways and the biological consequences of preventing RF degradation in BRCA-mutated tumors at the expense of accumulation of ssDNA gaps resulting from discontinuous replication.

Another, genetically distinct DDT pathway, TS, is a mechanistically more complex pathway for lesion bypass. In contrast to TLS, it uses the homologous template for synthesis, and therefore, facilitates an error-free synthesis over the damage site. Similarly to HR DNA repair, the initial step requires the stalled nascent strand to invade the newly replicated sister chromatid and is facilitated by RAD51 (156, 180, 181). The structure formed when the stalled nascent strand invades the undamaged chromatid is called the sister chromatid junction (SCJ). The undamaged template is then used to replicate DNA over the lesion containing the parental strand. After the gap is filled, SCJ is resolved back into two duplex DNA strands and the lesion bypass process is completed (156).

The last known DDT mechanism called "salvage" HR pathway is an alternative to the TS pathway. Like TS, salvage HR repair also employs template switching to bypass the DNA lesion. However, the major difference between the two pathways is that salvage HR repair is hyper-recombinogenic and thus only serves as the last resort of cells to replicate DNA over lesion if TLS and TS fail (182–184).

A tight regulation of pathway choice between the DDT mechanisms is important to limit the accumulation of mutations in case of TLS. It also prevents aberrant recombination events leading to potential genomic rearrangements and genome instability in the case of the salvage HR pathway. The regulation of the TLS, TS, and salvage HR pathways is facilitated by post-translational modifications (PTM) of PCNA (see **Figure 4**), which act as a molecular switch regulating pathway choice (185). In contrast to other pathways, PrimPol-mediated lesion bypass is not stimulated by PCNA and its PTMs. Instead, human PrimPol may be directly recruited to the stalled RFs through its interaction with the ssDNA-binding protein RPA (176). The initial PCNA modification, which is induced upon contact of a RF with the DNA lesion, is mono-ubiquitination at K164. In yeast, this modification is carried out by the E2-E3 complex Rad6-Rad18. In humans, however, several proteins seem to be implicated and their dynamics is not fully understood yet (186). Preferentially, the mono-ubiquitin mark would be extended to a poly-ubiquitin chain in a UBC13-dependent manner to stimulate ZRANB3-driven RF reversal and the error-free TS pathway in early S-phase (100, 103, 187, 188). In human cells, at least two E3 ubiquitin ligases can cooperate with UBC13 in promoting PCNA polyubiquitination; HLTF and SHPRH (104). However, their relative contribution to extending the mono-ubiquitin mark on PCNA is not well-understood yet. The second DDT pathway choice is the mutagenic TLS that has been shown to occur in late S or G2/M phase of the cell cycle. This pathway is initiated if the K164 mono-ubiquitin mark on PCNA is not extended (156, 189). The last choice is the salvage HR pathway, which is ubiquitin-independent. In yeast, the pathway is actively suppressed during normal S phase by sumoylation of PCNA at K164 and by the activity of the Srs2 anti-recombinase

associated with SUMO-modified PCNA (190–192). In contrary to ubiquitination, sumoylation of PCNA is cell-cycle dependent and is strictly limited to S phase (193). Thus, HR-mediated lesion bypass is limited to late S and G2/M phases and serves only as the last resort for synthesis over the lesions that escaped the TS and TLS pathways (187). In humans, the Srs2 ortholog PARI (PCNA-associated recombination inhibitor) was shown to interact with PCNA and restrict unscheduled HR at RFs *in vitro* (194). However, the role of PCNA SUMOylation and its regulation in human cells is still debated (190).

ALTERATIONS OF DDT PATHWAYS IN CANCER

Defects in DNA replication or repair play a major role in genomic instability, one of the hallmarks of cancer. Given the importance of DDT pathways in the resolution of replication stress by preventing fork stalling and collapse, it is not surprising that alterations in genes encoding TLS polymerases and other DDT components have been associated with cancer development and drug resistance (195). When analyzing samples from various types of tumors, Albertella et al. found that about half of the tumor samples studied showed more than a 2-fold increase in expression of at least one specialized TLS DNA polymerase (196). On the one hand, increased activity of TLS polymerases may significantly contribute to mutagenicity and may increase the chances of oncogenic transformation (197). On the other hand, cancer cells with higher expression of these polymerases, such as Pol β, may escape the cytotoxic effect of various drugs, including alkylating agents, and hence significantly contribute to chemoresistance (198–200). Interestingly, different TLS polymerases were shown to be upregulated in different types of tumors; upregulation of Pol theta (Pol θ, POLQ) was shown to indicate poor outcome in breast cancer patients (201), while elevated expression of Pol eta (Pol η, POLH) correlates with decreased survival of patients with non-small cell lung cancer (202) or metastatic gastric adenocarcinoma treated with platinum drugs (203).

The ability of TLS polymerases to carry out replication over DNA lesions induced by anti-cancer treatments and therefore increase survival of cancer cells makes them attractive targets for improving the efficacy of currently used chemotherapeutics. Nevertheless, developing compounds highly selective toward TLS polymerases has been very challenging, mainly due to common substrates and some interaction partners shared by TLS and replicative polymerases (e.g., PCNA). Moreover, while several small molecule inhibitors of TLS components have been discovered, none of them were shown to have activity *in vivo* (204). Examples comprise previously described selective inhibitors of REV7 (205), oxetanocin derivatives inhibiting Pol η (206), or small molecule compounds blocking the interaction between components of the Pol ζ complex (207). One example of a small inhibitor shown to be active *in vivo* is a recently described molecule JH-RE-06. The compound prevents mutagenic TLS by blocking REV1-REV7 interaction and therefore, inhibiting the recruitment of polymerase POL ζ. This was shown to suppress TLS-mediated mutagenicity induced by cisplatin *in vitro* and to sensitize tumors to cisplatin treatment *in vivo* (204).

Moreover, suppression of various TLS components has been associated with an improved response to DNA damaging agents, such as cisplatin in certain types of tumors. siRNA-mediated knockdown of REV1 or REV3L (the essential subunit of POL ζ) was shown to sensitize intrinsically resistant tumors to chemotherapy or to reduce the frequency of acquired resistance in relapsed tumors (208). Doles et al. (209) showed that in addition to the pronounced sensitivity of REV3-deficient tumors to cisplatin and improved survival of treated mice, REV3-deficient cells also displayed lower amounts of cisplatin-induced mutations potentially decreasing a risk for secondary mutations leading to acquired resistance (209). Similarly, the suppression of Rev1 was shown to decrease cisplatin- and cyclophosphamide-induced mutagenesis in a mouse model for B-cell lymphoma and to limit acquired cyclophosphamide resistance *in vitro* (155). Moreover, DDT-defective $Pcna^{K164R}$ lymphoma and breast cancer lines were also hypersensitive to cisplatin (210).

In summary, both DNA repair and DDT pathways are important to prevent RF collapse and maintain genome integrity. Therefore, defects in proteins involved in these processes can lead to cancer and also affect the response of cells to different genotoxic agents, which reflects on drug sensitivity or resistance in the clinic. However, several aspects of the intricate relationship between DDR and DDT, as well as their interaction at the RF are still unclear and need to be further investigated.

FUTURE DIRECTIONS IN PREDICTING THERAPY RESPONSE

The understanding of resistance mechanisms involving known DDR factors and/or RF remodelers/processors, together with the advance in biological *in vitro* and *in vivo* models for studying cancer, should be implemented in the clinical practice in the future for personalized diagnosis and for selecting an effective treatment strategy. Classical clinical and histopathological staging/grading will remain an import source of information. Here, we expect that computational pathology and deep learning algorithms will have a major impact to overcome the problem of inter-observer variability. Recent studies in breast cancer suggest that quantitative image analysis of histomorphometric features of early stage ER+ breast cancer are useful to predict patient survival independently (211, 212). Moreover, there are great expectations that the multiomics analysis of tumor samples, including next generation DNA/RNA sequencing, epigenomics, proteomics, and metabolomics, will make a difference to predict therapy response (**Figure 5**) [reviewed in (213–215)]. Indeed, the combination of these approaches has already been useful in exploring several aspects of the biological complexity of cancer (216, 217). However, some challenges in this context include the computational integration of such heterogeneous data and the availability of adequate amounts of optimally collected tumor tissue both before and during therapy.

Some novel computer tools are available for this type of integrated analysis [reviewed in (214)] and include platforms

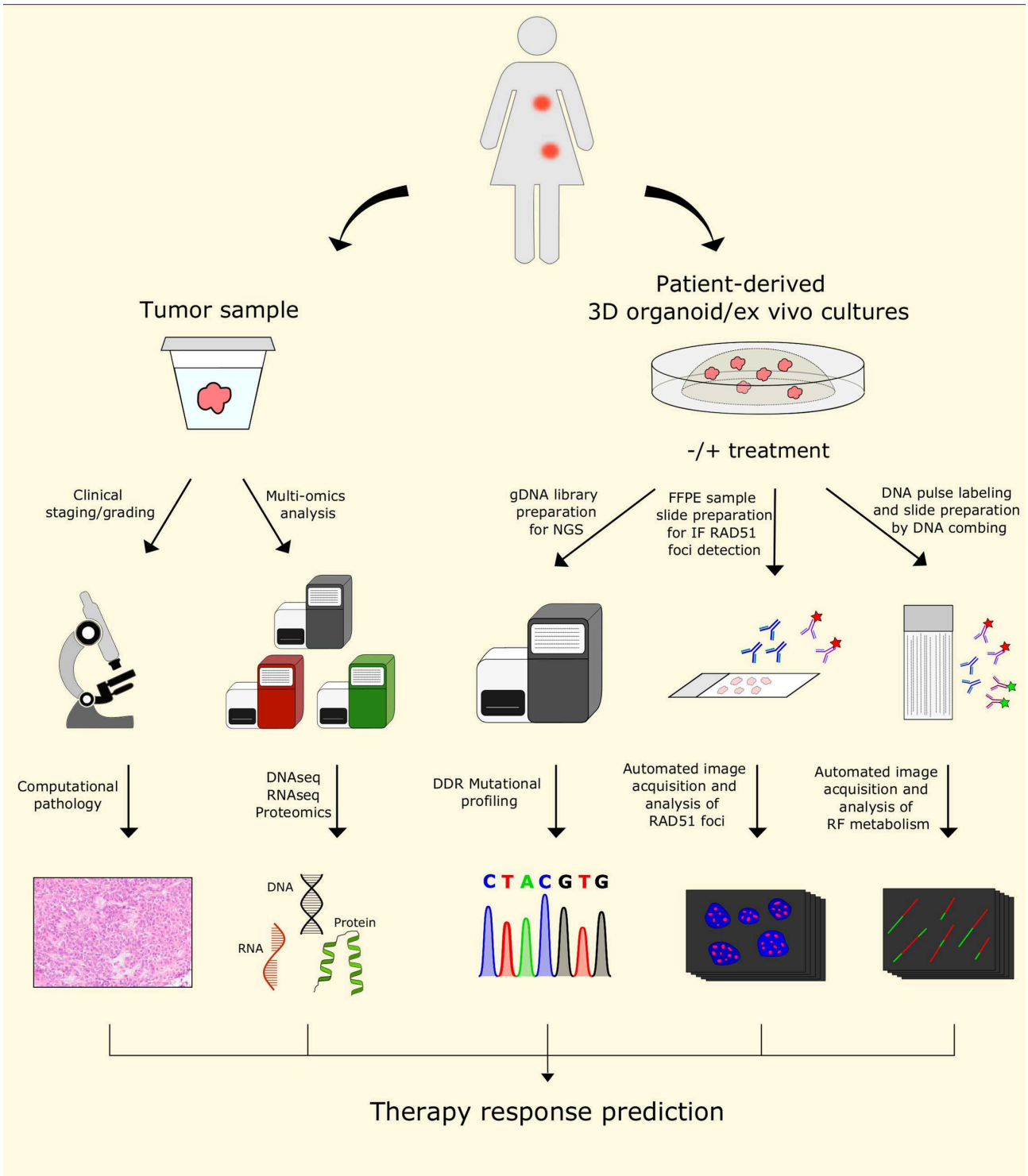

FIGURE 5 | Future perspectives for predicting personalized therapy outcome. The use of patient samples for histology and multi-omics analysis will remain valuable tools to characterize tumors. In addition, patient-derived 3D organoid/*ex vivo* cultures may provide additional material for functional testing, such as RAD51 foci detection upon ionizing radiation, or DNA fiber analysis to probe for replication fork speed and/or stability. Together with the increasing knowledge of the importance of DDT and RF remodeling in anticancer drug response, these additional tools may allow automated functional analyses coupled with NGS profiling of DDR genes in patient-derived samples, providing the potential for designing personalized therapy strategies and predicting their outcomes in the future. DDR, DNA damage response; FFPE, formalin-fixed, paraffin-embedded; gDNA, genomic DNA; IF, immunofluorescence; NGS, next-generation sequencing; RF, replication fork.

that analyse miRNA and mRNA expression (dChip-GemiNi, mirConnX, IntegraMiR), associate epigenomic with RNA expression and clinical data (such as MENT, MethHC, Wanderer, MethCNA) or integrate proteomic with several other types of data from multiple studies (XCMS Online, CancerSysDB) [reviewed in (214)].

The collection of data for multiomics analysis largely depends on the availability of patient samples. Moreover, the use of liquid biopsies and circulating tumor DNA for sequencing purposes would be complementary. Regarding the analysis at the protein level, the improvement in MS proteomics to reduce sample input and increase sensitivity for low abundance proteins would also help in this context.

The recent developments in the field of patient-derived 3D organoid cultures enable the expansion of tumor cells acquired by biopsy of different types of tumors (218–220). *In vitro*-cultured organoid lines often preserve morphological features, drug response profiles, as well as the heterogeneity of the original tumor (221). Therefore, 3D organoids could be another source of material for multi-omics approaches. However, it is important to keep in mind that the predictive power of tumor organoid cultures has clear limitations and is not 100% (222).

The ability to be rapidly expanded and genetically modified makes 3D organoids in principle a versatile tool for downstream functional testing of therapy response, including the study of RF biology (**Figure 5**) (62, 222). Nevertheless, the predictive power of 3D organoids has limitations that we still need to understand to make a significant step toward personalized medicine in clinical oncology (222). *Ex vivo* approaches to study living tumor fragments may be another direction in which RF biology in the context of anti-cancer therapy may be studied further.

Genetic testing for germline mutations in *BRCA1* and *BRCA2* has been available since the 1990s (223). Moreover, advances in next-generation sequencing (NGS) technology allowed for systematic investigation of the mutational landscape in *BRCA1*- and *BRCA2*-mutated tumors (224, 225). In addition, the identification of other DNA repair genes associated with HR deficiency opened the possibility for targeted therapy in those patients, including PARP inhibitors (226). Despite the undoubted significance of NGS data in predicting therapy success in patients with defects in the HR DNA repair pathway, this approach does not allow to study the role of epigenetics in modulating expression of HR genes, including *BRCA1* and *BRCA2*, nor functional testing for residual or restored HR repair or RF stability. Restoration of HR in BRCA1-deficient tumors by loss of 53BP1 is frequently found in tumors that acquire PARPi resistance (41, 50, 227). Similarly, loss of several other NHEJ and HR regulators, such as RIF1, REV7, and HELB have been shown to restore resection at DSB sites and promote HR repair, leading to improved DDT, chromosomal integrity, and consequently to acquired chemoresistance (44, 52, 53, 228). Restoration of damage-induced RAD51 foci formation is a well-established marker of DNA end processing and HR repair at DSBs. Therefore, implementing automated assays for RAD51 foci formation in patient samples would provide an important functional link to the complementary information acquired with next-generation sequencing on genetic alterations (**Figure 5**) (227).

As discussed above, the role of DDT pathways and DNA RF metabolism in the context of therapy response and resistance has gained a lot of attention in recent years. Various groups have identified novel factors implicated in the metabolism of DNA RFs and replication stress tolerance. Several of those factors, including DNA2, EZH2, and MUS81, showed the potential to be used as biomarkers for predicting response to DDR-targeting therapies in BRCA-deficient tumors (72, 137, 143). Nevertheless, similar to a functional HR restoration readout, functional assays for testing DDT, RF remodelers and fork stability would be needed to reliably phenotype tumor-derived samples and to predict therapy success. Recently, a novel system based on the formation of UVA-induced digoxygenin-tagged trimethylpsoralen ICLs was described by Mutreja et al. (86). Combined with the traditional DNA fiber spreading procedure, this technique allows the detection of individual ICL lesions and enables the study of cellular responses to ICL-inducing agents at the single-molecule resolution (86). One of the limitations of the DNA fiber technique currently used by many research groups is the time-consuming process of preparation of slides with the DNA spreads and the inter-observer variability of the image analysis (**Table 1**). Developing a pipeline for automated and standardized preparation of DNA fibers involving molecular combing and analysis of selected replication parameters, such as stability of stalled forks, rate of replication elongation, or lesion bypass, may enable a more precise prediction of therapy response in patients with DDR defects in their cancer. We hope that combining multiomics data with automated RAD51 foci formation and DNA RF analysis represents a powerful toolbox for predicting therapy outcome in patients with tumors defective in DDR pathways in the future (**Figure 5**).

AUTHOR CONTRIBUTIONS

ML and JB contributed equally to writting the manuscript and making the figures. SR contributed to writting and correcting the manuscript.

FUNDING

Our current research projects are supported by the Swiss National Science Foundation (310030_179360), the Swiss Cancer League (KLS-4282-08-2017), the European Union (ERC CoG-681572 to SR and MSCA-IF-743290 to JB), the Wilhelm Sander-Stiftung, the Novartis Stiftung für medizinisch-biologische Forschung, and the Boehringer Ingelheim Fonds (PhD fellowship to ML).

ACKNOWLEDGMENTS

We would like to thank Massimo Lopes, Marine Inglebert, Merve Mutlu, and Paola Francica for scientific discussions and critical reading of this manuscript.

REFERENCES

1. Jackson SP, Bartek J. The DNA-damage response in human biology and disease. *Nature.* (2009) 461:1071–8. doi: 10.1038/nature08467
2. Halazonetis TD, Gorgoulis VG, Bartek J. An oncogene-induced DNA damage model for cancer development. *Science.* (2008) 319:1352. doi: 10.1126/science.1140735
3. Cancer Genome Atlas Research Network. Integrated genomic analyses of ovarian carcinoma. *Nature.* (2011) 474:609–15. doi: 10.1038/nature10166
4. Nik-Zainal S, Davies H, Staaf J, Ramakrishna M, Glodzik D, Zou X, et al. Landscape of somatic mutations in 560 breast cancer whole-genome sequences. *Nature.* (2016) 534:47–54. doi: 10.1038/nature17676
5. Patch A-M, Christie EL, Etemadmoghadam D, Garsed DW, George J, Fereday S, et al. Whole-genome characterization of chemoresistant ovarian cancer. *Nature.* (2015) 521:489. doi: 10.1038/nature14410
6. Roy R, Chun J, Powell SN. BRCA1 and BRCA2: different roles in a common pathway of genome protection. *Nat Rev Cancer.* (2012) 12:68–78. doi: 10.1038/nrc3181
7. Scully R. Role of BRCA gene dysfunction in breast and ovarian cancer predisposition. *Breast Cancer Res.* (2000) 2:324–30. doi: 10.1186/bcr76
8. Cortez D. Preventing replication fork collapse to maintain genome integrity. *DNA Repair.* (2015) 32:149–57. doi: 10.1016/j.dnarep.2015.04.026
9. Schimmel J, van Schendel R, den Dunnen JT, Tijsterman M. Templated insertions: a smoking gun for polymerase theta-mediated end joining. *Trends Genet.* (2019) 35:632–44. doi: 10.1016/j.tig.2019.06.001
10. Shibata A. Regulation of repair pathway choice at two-ended DNA double-strand breaks. *Mutat Res.* (2017) 803–5:51–5. doi: 10.1016/j.mrfmmm.2017.07.011
11. Scully R, Panday A, Elango R, Willis NA. DNA double-strand break repair-pathway choice in somatic mammalian cells. *Nat Rev Mol Cell Biol.* (2019) 20:698–714. doi: 10.1038/s41580-019-0152-0
12. Forment JV, O'Connor MJ. Targeting the replication stress response in cancer. *Pharmacol Ther.* (2018) 188:155–67. doi: 10.1016/j.pharmthera.2018.03.005
13. O'Connor MJ. Targeting the DNA damage response in cancer. *Mol Cell.* (2015) 60:547–60. doi: 10.1016/j.molcel.2015.10.040
14. Lord CJ, Ashworth A. The DNA damage response and cancer therapy. *Nature.* (2012) 481:287–94. doi: 10.1038/nature10760
15. Nickoloff JA, Jones D, Lee S-H, Williamson EA, Hromas R. Drugging the cancers addicted to DNA repair. *JNCI.* (2017) 109:djx059. doi: 10.1093/jnci/djx059
16. Schouten PC, Gluz O, Harbeck N, Mohrmann S, Diallo-Danebrock R, Pelz E, et al. BRCA1-like profile predicts benefit of tandem high dose epirubicin-cyclophospamide-thiotepa in high risk breast cancer patients randomized in the WSG-AM01 trial. *Int J Cancer.* (2016) 139:882–9. doi: 10.1002/ijc.30078
17. Evans T, Matulonis U. PARP inhibitors in ovarian cancer: evidence, experience and clinical potential. *Ther Adv Med Oncol.* (2017) 9:253–67. doi: 10.1177/1758834016687254
18. Dobzhansky Th. Genetics of natural populations. Xiii. Recombination and variability in populations of drosophila pseudoobscura. *Genetics.* (1946) 31:269.
19. Huang A, Garraway LA, Ashworth A, Weber B. Synthetic lethality as an engine for cancer drug target discovery. *Nat Rev Drug Discov.* (2020) 19:23–38. doi: 10.1038/s41573-019-0046-z
20. Bryant HE, Schultz N, Thomas HD, Parker KM, Flower D, Lopez E, et al. Specific killing of BRCA2-deficient tumours with inhibitors of poly(ADP-ribose) polymerase. *Nature.* (2005) 434:913–7. doi: 10.1038/nature03443
21. Farmer H, McCabe N, Lord CJ, Tutt ANJ, Johnson DA, Richardson TB, et al. Targeting the DNA repair defect in BRCA mutant cells as a therapeutic strategy. *Nature.* (2005) 434:917–21. doi: 10.1038/nature03445
22. Bitler BG, Watson ZL, Wheeler LJ, Behbakht K. PARP inhibitors: clinical utility and possibilities of overcoming resistance. *Gynecol Oncol.* (2017) 147:695–704. doi: 10.1016/j.ygyno.2017.10.003
23. Geenen JJJ, Linn SC, Beijnen JH, Schellens JHM. PARP inhibitors in the treatment of triple-negative breast cancer. *Clin Pharmacokinet.* (2018) 57:427–37. doi: 10.1007/s40262-017-0587-4
24. Kim H, D'Andrea AD. Regulation of DNA cross-link repair by the Fanconi anemia/BRCA pathway. *Genes Dev.* (2012) 26:1393–408. doi: 10.1101/gad.195248.112
25. Pascal JM, Ellenberger T. The rise and fall of poly(ADP-ribose): an enzymatic perspective. *DNA Repair.* (2015) 32:10–6. doi: 10.1016/j.dnarep.2015.04.008
26. Leung AKL. Poly(ADP-ribose): an organizer of cellular architecture. *J Cell Biol.* (2014) 205:613. doi: 10.1083/jcb.201402114
27. Lupo B, Trusolino L. Inhibition of poly(ADP-ribosyl)ation in cancer: old and new paradigms revisited. *Biochim Biophys Acta.* (2014) 1846:201–15. doi: 10.1016/j.bbcan.2014.07.004
28. Murai J, Huang SY, Das BB, Renaud A, Zhang Y, Doroshow JH, et al. Trapping of PARP1 and PARP2 by clinical PARP inhibitors. *Cancer Res.* (2012) 72:5588–99. doi: 10.1158/0008-5472.CAN-12-2753
29. Hanzlikova H, Kalasova I, Demin AA, Pennicott LE, Cihlarova Z, Caldecott KW. The importance of Poly(ADP-Ribose) polymerase as a sensor of unligated okazaki fragments during DNA replication. *Mol Cell.* (2018) 71:319–31.e3. doi: 10.1016/j.molcel.2018.06.004
30. Berti M, Ray Chaudhuri A, Thangavel S, Gomathinayagam S, Kenig S, Vujanovic M, et al. Human RECQ1 promotes restart of replication forks reversed by DNA topoisomerase I inhibition. *Nat Struct Mol Biol.* (2013) 20:347–54. doi: 10.1038/nsmb.2501
31. Maya-Mendoza A, Moudry P, Merchut-Maya JM, Lee M, Strauss R, Bartek J. High speed of fork progression induces DNA replication stress and genomic instability. *Nature.* (2018) 559:279–84. doi: 10.1038/s41586-018-0261-5
32. Neelsen KJ, Lopes M. Replication fork reversal in eukaryotes: from dead end to dynamic response. *Nat Rev Mol Cell Biol.* (2015) 16:207–20. doi: 10.1038/nrm3935
33. Lord CJ, Ashworth A. PARP inhibitors: synthetic lethality in the clinic. *Science.* (2017) 355:1152. doi: 10.1126/science.aam7344
34. Gogola E, Rottenberg S, Jonkers J. Resistance to PARP inhibitors: lessons from preclinical models of BRCA-associated cancer. *Annu Rev Cancer Biol.* (2019) 3:235–54. doi: 10.1146/annurev-cancerbio-030617-050232
35. Afghahi A, Timms KM, Vinayak S, Jensen KC, Kurian AW, Carlson RW, et al. Tumor BRCA1 reversion mutation arising during neoadjuvant platinum-based chemotherapy in triple-negative breast cancer is associated with therapy resistance. *Clin Cancer Res.* (2017) 23:3365. doi: 10.1158/1078-0432.CCR-16-2174
36. Barber LJ, Sandhu S, Chen L, Campbell J, Kozarewa I, Fenwick K, et al. Secondary mutations in BRCA2 associated with clinical resistance to a PARP inhibitor. *J Pathol.* (2013) 229:422–9. doi: 10.1002/path.4140
37. Edwards SL, Brough R, Lord CJ, Natrajan R, Vatcheva R, Levine DA, et al. Resistance to therapy caused by intragenic deletion in BRCA2. *Nature.* (2008) 451:1111–5. doi: 10.1038/nature06548
38. Lheureux S, Bruce JP, Burnier JV, Karakasis K, Shaw PA, Clarke BA, et al. Somatic BRCA1/2 recovery as a resistance mechanism after exceptional response to poly (ADP-ribose) polymerase inhibition. *JCO.* (2017) 35:1240–9. doi: 10.1200/JCO.2016.71.3677
39. Norquist B, Wurz KA, Pennil CC, Garcia R, Gross J, Sakai W, et al. Secondary somatic mutations restoring BRCA1/2 predict chemotherapy resistance in hereditary ovarian carcinomas. *J Clin Oncol.* (2011) 29:3008–15. doi: 10.1200/JCO.2010.34.2980
40. Barazas M, Annunziato S, Pettitt SJ, de Krijger I, Ghezraoui H, Roobol SJ, et al. The CST complex mediates end protection at double-strand breaks and promotes PARP inhibitor sensitivity in BRCA1-deficient cells. *Cell Rep.* (2018) 23:2107–18. doi: 10.1016/j.celrep.2018.04.046
41. Bouwman P, Aly A, Escandell JM, Pieterse M, Bartkova J, van der Gulden H, et al. 53BP1 loss rescues BRCA1 deficiency and is associated with triple-negative and BRCA-mutated breast cancers. *Nat Struct Mol Biol.* (2010) 17:688–95. doi: 10.1038/nsmb.1831
42. Bunting SF, Callen E, Wong N, Chen H-T, Polato F, Gunn A, et al. 53BP1 inhibits homologous recombination in Brca1-deficient cells by blocking resection of DNA breaks. *Cell.* (2010) 141:243–54. doi: 10.1016/j.cell.2010.03.012
43. Callen E, Di Virgilio M, Kruhlak MJ, Nieto-Soler M, Wong N, Chen H-T, et al. 53BP1 mediates productive and mutagenic DNA repair through distinct phosphoprotein interactions. *Cell.* (2013) 153:1266–80. doi: 10.1016/j.cell.2013.05.023

44. Chapman JR, Barral P, Vannier J-B, Borel V, Steger M, Tomas-Loba A, et al. RIF1 is essential for 53BP1-dependent nonhomologous end joining and suppression of DNA double-strand break resection. *Mol Cell.* (2013) 49:858–71. doi: 10.1016/j.molcel.2013.01.002
45. Dev H, Chiang T-WW, Lescale C, de Krijger I, Martin AG, Pilger D, et al. Shieldin complex promotes DNA end-joining and counters homologous recombination in BRCA1-null cells. *Nat Cell Biol.* (2018) 20:954–65. doi: 10.1038/s41556-018-0140-1
46. Escribano-Díaz C, Orthwein A, Fradet-Turcotte A, Xing M, Young JTF, Tkáč J, et al. A cell cycle-dependent regulatory circuit composed of 53BP1-RIF1 and BRCA1-CtIP controls DNA repair pathway choice. *Mol Cell.* (2013) 49:872–83. doi: 10.1016/j.molcel.2013.01.001
47. Feng L, Fong K-W, Wang J, Wang W, Chen J. RIF1 counteracts BRCA1-mediated end resection during DNA repair. *J Biol Chem.* (2013) 288:11135–43. doi: 10.1074/jbc.M113.457440
48. Ghezraoui H, Oliveira C, Becker JR, Bilham K, Moralli D, Anzilotti C, et al. 53BP1 cooperation with the REV7-shieldin complex underpins DNA structure-specific NHEJ. *Nature.* (2018) 560:122–7. doi: 10.1038/s41586-018-0362-1
49. Gupta R, Somyajit K, Narita T, Maskey E, Stanlie A, Kremer M, et al. DNA repair network analysis reveals shieldin as a key regulator of NHEJ and PARP inhibitor sensitivity. *Cell.* (2018) 173:972–88.e23. doi: 10.1016/j.cell.2018.03.050
50. Jaspers JE, Kersbergen A, Boon U, Sol W, van Deemter L, Zander SA, et al. Loss of 53BP1 causes PARP inhibitor resistance in Brca1-mutated mouse mammary tumors. *Cancer Discov.* (2013) 3:68–81. doi: 10.1158/2159-8290.CD-12-0049
51. Noordermeer SM, Adam S, Setiaputra D, Barazas M, Pettitt SJ, Ling AK, et al. The shieldin complex mediates 53BP1-dependent DNA repair. *Nature.* (2018) 560:117–21. doi: 10.1038/s41586-018-0340-7
52. Tkac J, Xu G, Adhikary H, Young JTF, Gallo D, Escribano-Diaz C, et al. HELB is a feedback inhibitor of DNA end resection. *Mol Cell.* (2016) 61:405–18. doi: 10.1016/j.molcel.2015.12.013
53. Xu G, Chapman JR, Brandsma I, Yuan J, Mistrik M, Bouwman P, et al. REV7 counteracts DNA double-strand break resection and affects PARP inhibition. *Nature.* (2015) 521:541–4. doi: 10.1038/nature14328
54. Zimmermann M, Lottersberger F, Buonomo SB, Sfeir A, de Lange T. 53BP1 regulates DSB repair using Rif1 to control 5′ end resection. *Science.* (2013) 339:700–4. doi: 10.1126/science.1231573
55. Christie EL, Pattnaik S, Beach J, Copeland A, Rashoo N, Fereday S, et al. Multiple ABCB1 transcriptional fusions in drug resistant high-grade serous ovarian and breast cancer. *Nat Commun.* (2019) 10:1–10. doi: 10.1038/s41467-019-09312-9
56. Rottenberg S, Jaspers JE, Kersbergen A, Van der Burg E, Nygren AO, Zander SA, et al. High sensitivity of BRCA1-deficient mammary tumors to the PARP inhibitor AZD2281 alone and in combination with platinum drugs. *Proc Natl Acad Sci USA.* (2008) 105:17079–84. doi: 10.1073/pnas.0806092105
57. Pettitt SJ, Rehman FL, Bajrami I, Brough R, Wallberg F, Kozarewa I, et al. A genetic screen using the PiggyBac transposon in haploid cells identifies Parp1 as a mediator of olaparib toxicity. *PLoS ONE.* (2013) 8:e61520. doi: 10.1371/journal.pone.0061520
58. Pettitt SJ, Krastev DB, Brandsma I, Dréan A, Song F, Aleksandrov R, et al. Genome-wide and high-density CRISPR-Cas9 screens identify point mutations in PARP1 causing PARP inhibitor resistance. *Nat Commun.* (2018) 9:1849. doi: 10.1038/s41467-018-03917-2
59. Gogola E, Duarte AA, de Ruiter JR, Wiegant WW, Schmid JA, de Bruijn R, et al. Selective LOSS Of PARG restores PARylation and counteracts PARP inhibitor-mediated synthetic lethality. *Cancer Cell.* (2018) 33:1078–93.e12. doi: 10.1016/j.ccell.2018.05.008
60. Cantor SB, Calvo JA. Fork protection and therapy resistance in hereditary breast cancer. *Cold Spring Harbor Symp Quant Biol.* (2017) 82:339–48. doi: 10.1101/sqb.2017.82.034413
61. Sidorova J. A game of substrates: replication fork remodeling and its roles in genome stability and chemo-resistance. *Cell Stress.* (2017) 1:115–33. doi: 10.15698/cst2017.12.114
62. Ray Chaudhuri A, Callen E, Ding X, Gogola E, Duarte AA, Lee J-E, et al. Replication fork stability confers chemoresistance in BRCA-deficient cells. *Nature.* (2016) 535:382–7. doi: 10.1038/nature18325
63. Schlacher K, Christ N, Siaud N, Egashira A, Wu H, Jasin M. Double-strand break repair-independent role for BRCA2 in blocking stalled replication fork degradation by MRE11. *Cell.* (2011) 145:529–42. doi: 10.1016/j.cell.2011.03.041
64. Schlacher K, Wu H, Jasin M. A distinct replication fork protection pathway connects Fanconi anemia tumor suppressors to RAD51-BRCA1/2. *Cancer Cell.* (2012) 22:106–16. doi: 10.1016/j.ccr.2012.05.015
65. Haaf T, Golub EI, Reddy G, Radding CM, Ward DC. Nuclear foci of mammalian Rad51 recombination protein in somatic cells after DNA damage and its localization in synaptonemal complexes. *Proc Natl Acad Sci USA.* (1995) 92:2298. doi: 10.1073/pnas.92.6.2298
66. Raderschall E, Golub EI, Haaf T. Nuclear foci of mammalian recombination proteins are located at single-stranded DNA regions formed after DNA damage. *Proc Natl Acad Sci USA.* (1999) 96:1921. doi: 10.1073/pnas.96.5.1921
67. Schmid JA, Berti M, Walser F, Raso MC, Schmid F, Krietsch J, et al. Histone ubiquitination by the DNA damage response is required for efficient DNA replication in unperturbed S phase. *Mol Cell.* (2018) 71:897–910.e8. doi: 10.1016/j.molcel.2018.07.011
68. Scully R, Chen J, Plug A, Xiao Y, Weaver D, Feunteun J, et al. Association of BRCA1 with Rad51 in MITOTIC AND MEIOTIC CELLS. *Cell.* (1997) 88:265–75. doi: 10.1016/S0092-8674(00)81847-4
69. Sirbu BM, McDonald WH, Dungrawala H, Badu-Nkansah A, Kavanaugh GM, Chen Y, et al. Identification of proteins at active, stalled, and collapsed replication forks using isolation of proteins on nascent DNA (iPOND) coupled with mass spectrometry. *J Biol Chem.* (2013) 288:31458–67. doi: 10.1074/jbc.M113.511337
70. Zellweger R, Dalcher D, Mutreja K, Berti M, Schmid JA, Herrador R, et al. Rad51-mediated replication fork reversal is a global response to genotoxic treatments in human cells. *J Cell Biol.* (2015) 208:563–79. doi: 10.1083/jcb.201406099
71. Guillemette S, Serra RW, Peng M, Hayes JA, Konstantinopoulos PA, Green MR, et al. Resistance to therapy in BRCA2 mutant cells due to loss of the nucleosome remodeling factor CHD4. *Genes Dev.* (2015) 29:489–94. doi: 10.1101/gad.256214.114
72. Lemacon D, Jackson J, Quinet A, Brickner JR, Li S, Yazinski S, et al. MRE11 and EXO1 nucleases degrade reversed forks and elicit MUS81-dependent fork rescue in BRCA2-deficient cells. *Nat Commun.* (2017) 8:860. doi: 10.1038/s41467-017-01180-5
73. Rondinelli B, Gogola E, Yücel H, Duarte AA, van de Ven M, van der Sluijs R, et al. EZH2 promotes degradation of stalled replication forks by recruiting MUS81 through histone H3 trimethylation. *Nat Cell Biol.* (2017) 19:1371. doi: 10.1038/ncb3626
74. Zellweger R, Lopes M. Dynamic architecture of eukaryotic DNA replication forks *in vivo*, visualized by electron microscopy. *Methods Mol Biol.* (2018) 1672:261–94. doi: 10.1007/978-1-4939-7306-4_19
75. Bensimon A, Simon A, Chiffaudel A, Croquette V, Heslot F, Bensimon D. Alignment and sensitive detection of DNA by a moving interface. *Science.* (1994) 265:2096. doi: 10.1126/science.7522347
76. Michalet X, Ekong R, Fougerousse F, Rousseaux S, Schurra C, Hornigold N, et al. Dynamic molecular combing: stretching the whole human genome for high-resolution studies. *Science.* (1997) 277:1518. doi: 10.1126/science.277.5331.1518
77. Parra I, Windle B. High resolution visual mapping of stretched DNA by fluorescent hybridization. *Nat Genet.* (1993) 5:17–21. doi: 10.1038/ng0993-17
78. Conti C, Saccà B, Herrick J, Lalou C, Pommier Y, Bensimon A. Replication fork velocities at adjacent replication origins are coordinately modified during DNA replication in human cells. *MBoC.* (2007) 18:3059–67. doi: 10.1091/mbc.e06-08-0689
79. Tuduri S, Crabbé L, Conti C, Tourrière H, Holtgreve-Grez H, Jauch A, et al. Topoisomerase I suppresses genomic instability by preventing interference between replication and transcription. *Nat Cell Biol.* (2009) 11:1315–24. doi: 10.1038/ncb1984
80. Vindigni A, Lopes M. Combining electron microscopy with single molecule DNA fiber approaches to study DNA replication dynamics. *Biophys. Chem.* (2017) 225:3–9. doi: 10.1016/j.bpc.2016.11.014

81. Norio P, Schildkraut CL. Visualization of DNA replication on individual epstein-barr virus episomes. *Science.* (2001) 294:2361. doi: 10.1126/science.1064603
82. Sirbu BM, Couch FB, Feigerle JT, Bhaskara S, Hiebert SW, Cortez D. Analysis of protein dynamics at active, stalled, and collapsed replication forks. *Genes Dev.* (2011) 25:1320–7. doi: 10.1101/gad.2053211
83. Leung KHT, El Hassan MA, Bremner R. A rapid and efficient method to purify proteins at replication forks under native conditions. *BioTechniques.* (2013) 55:204–6. doi: 10.2144/000114089
84. Söderberg O, Gullberg M, Jarvius M, Ridderstråle K, Leuchowius K-J, Jarvius J, et al. Direct observation of individual endogenous protein complexes *in situ* by proximity ligation. *Nat Methods.* (2006) 3:995–1000. doi: 10.1038/nmeth947
85. Roy S, Luzwick JW, Schlacher K. SIRF: quantitative *in situ* analysis of protein interactions at DNA replication forks. *J Cell Biol.* (2018) 217:1521. doi: 10.1083/jcb.201709121
86. Mutreja K, Krietsch J, Hess J, Ursich S, Berti M, Roessler FK, et al. ATR-mediated global fork slowing and reversal assist fork traverse and prevent chromosomal breakage at DNA interstrand cross-links. *Cell Rep.* (2018) 24:2629–42.e5. doi: 10.1016/j.celrep.2018.08.019
87. Byun TS, Pacek M, Yee M, Walter JC, Cimprich KA. Functional uncoupling of MCM helicase and DNA polymerase activities activates the ATR-dependent checkpoint. *Genes Dev.* (2005) 19:1040–52. doi: 10.1101/gad.1301205
88. Daigh LH, Liu C, Chung M, Cimprich KA, Meyer T. Stochastic endogenous replication stress causes ATR-triggered fluctuations in CDK2 activity that dynamically adjust global DNA synthesis rates. *Cell Syst.* (2018) 7:17–27.e3. doi: 10.1016/j.cels.2018.05.011
89. Zou L, Elledge SJ. Sensing DNA damage through ATRIP recognition of RPA-ssDNA complexes. *Science.* (2003) 300:1542–8. doi: 10.1126/science.1083430
90. Zou Y, Liu Y, Wu X, Shell SM. Functions of human replication protein A (RPA): from DNA replication to DNA damage and stress responses. *J Cell Physiol.* (2006) 208:267–73. doi: 10.1002/jcp.20622
91. Bhat KP, Cortez D. RPA and RAD51: fork reversal, fork protection, and genome stability. *Nat Struct Mol Biol.* (2018) 25:446–53. doi: 10.1038/s41594-018-0075-z
92. Sugiyama T, New JH, Kowalczykowski SC. DNA annealing by RAD52 protein is stimulated by specific interaction with the complex of replication protein A and single-stranded DNA. *Proc Natl Acad Sci USA.* (1998) 95:6049–54. doi: 10.1073/pnas.95.11.6049
93. Cortez D, Guntuku S, Qin J, Elledge SJ. ATR and ATRIP: partners in checkpoint signaling. *Science.* (2001) 294:1713–6. doi: 10.1126/science.1065521
94. Bétous R, Mason AC, Rambo RP, Bansbach CE, Badu-Nkansah A, Sirbu BM, et al. SMARCAL1 catalyzes fork regression and Holliday junction migration to maintain genome stability during DNA replication. *Genes Dev.* (2012) 26:151–62. doi: 10.1101/gad.178459.111
95. Ciccia A, Bredemeyer AL, Sowa ME, Terret M-E, Jallepalli PV, Harper JW, et al. The SIOD disorder protein SMARCAL1 is an RPA-interacting protein involved in replication fork restart. *Genes Dev.* (2009) 23:2415–25. doi: 10.1101/gad.1832309
96. Kolinjivadi AM, Sannino V, De Antoni A, Zadorozhny K, Kilkenny M, Técher H, et al. Smarcal1-mediated fork reversal triggers Mre11-dependent degradation of nascent DNA in the absence of Brca2 and stable Rad51 nucleofilaments. *Mol Cell.* (2017) 67:867–81.e7. doi: 10.1016/j.molcel.2017.07.001
97. Mijic S, Zellweger R, Chappidi N, Berti M, Jacobs K, Mutreja K, et al. Replication fork reversal triggers fork degradation in BRCA2-defective cells. *Nat Commun.* (2017) 8:859. doi: 10.1038/s41467-017-01164-5
98. Dungrawala H, Bhat KP, Le Meur R, Chazin WJ, Ding X, Sharan SK, et al. RADX promotes genome stability and modulates chemosensitivity by regulating RAD51 at replication forks. *Mol Cell.* (2017) 67:374–86.e5. doi: 10.1016/j.molcel.2017.06.023
99. Blastyák A, Hajdú I, Unk I, Haracska L. Role of double-stranded DNA translocase activity of human HLTF in replication of damaged DNA. *Mol Cell Biol.* (2010) 30:684–93. doi: 10.1128/MCB.00863-09
100. Vujanovic M, Krietsch J, Raso MC, Terraneo N, Zellweger R, Schmid JA, et al. Replication fork slowing and reversal upon DNA damage require PCNA polyubiquitination and ZRANB3 DNA translocase activity. *Mol Cell.* (2017) 67:882–90.e5. doi: 10.1016/j.molcel.2017.08.010
101. Achar YJ, Balogh D, Haracska L. Coordinated protein and DNA remodeling by human HLTF on stalled replication fork. *Proc Natl Acad Sci USA.* (2011) 108:14073–8. doi: 10.1073/pnas.1101951108
102. Flaus A, Martin DMA, Barton GJ, Owen-Hughes T. Identification of multiple distinct Snf2 subfamilies with conserved structural motifs. *Nucl Acids Res.* (2006) 34:2887–905. doi: 10.1093/nar/gkl295
103. Ciccia A, Nimonkar AV, Hu Y, Hajdu I, Achar YJ, Izhar L, et al. Polyubiquitinated PCNA recruits the ZRANB3 translocase to maintain genomic integrity after replication stress. *Mol Cell.* (2012) 47:396–409. doi: 10.1016/j.molcel.2012.05.024
104. Motegi A, Liaw H-J, Lee K-Y, Roest HP, Maas A, Wu X, et al. Polyubiquitination of proliferating cell nuclear antigen by HLTF and SHPRH prevents genomic instability from stalled replication forks. *Proc Natl Acad Sci USA.* (2008) 105:12411–6. doi: 10.1073/pnas.0805685105
105. Kile AC, Chavez DA, Bacal J, Eldirany S, Korzhnev DM, Bezsonova I, et al. HLTF's ancient HIRAN domain binds 3′ DNA ends to drive replication fork reversal. *Mol Cell.* (2015) 58:1090–100. doi: 10.1016/j.molcel.2015.05.013
106. Taglialatela A, Alvarez S, Leuzzi G, Sannino V, Ranjha L, Huang J-W, et al. Restoration of replication fork stability in BRCA1- and BRCA2-deficient cells by inactivation of SNF2-family fork remodelers. *Mol Cell.* (2017) 68:414–30.e8. doi: 10.1016/j.molcel.2017.09.036
107. Couch FB, Bansbach CE, Driscoll R, Luzwick JW, Glick GG, Bétous R, et al. ATR phosphorylates SMARCAL1 to prevent replication fork collapse. *Genes Dev.* (2013) 27:1610–23. doi: 10.1101/gad.214080.113
108. Baradaran-Heravi A, Raams A, Lubieniecka J, Cho KS, DeHaai KA, Basiratnia M, et al. SMARCAL1 deficiency predisposes to non-Hodgkin lymphoma and hypersensitivity to genotoxic agents *in vivo*. *Am J Med Genet Part A.* (2012) 158:2204–13. doi: 10.1002/ajmg.a.35532
109. Dhont L, Mascaux C, Belayew A. The helicase-like transcription factor (HLTF) in cancer: loss of function or oncomorphic conversion of a tumor suppressor? *Cell Mol Life Sci.* (2016) 73:129–47. doi: 10.1007/s00018-015-2060-6
110. Jones S, Stransky N, McCord CL, Cerami E, Lagowski J, Kelly D, et al. Genomic analyses of gynaecologic carcinosarcomas reveal frequent mutations in chromatin remodelling genes. *Nat Commun.* (2014) 5:5006. doi: 10.1038/ncomms6006
111. Kandoth C, Schultz N, Cherniack AD, Akbani R, Liu Y, Shen H, et al. Integrated genomic characterization of endometrial carcinoma. *Nature.* (2013) 497:67–73. doi: 10.1038/nature12113
112. MacKay C, Toth R, Rouse J. Biochemical characterisation of the SWI/SNF family member HLTF. *Biochem Biophys Res Commun.* (2009) 390:187–91. doi: 10.1016/j.bbrc.2009.08.151
113. Moinova HR, Chen W-D, Shen L, Smiraglia D, Olechnowicz J, Ravi L, et al. HLTF gene silencing in human colon cancer. *Proc Natl Acad Sci USA.* (2002) 99:4562–7. doi: 10.1073/pnas.062459899
114. Puccetti MV, Adams CM, Kushinsky S, Eischen CM. Smarcal1 and Zranb3 protect replication forks from Myc-induced DNA replication stress. *Cancer Res.* (2019) 79:1612–23. doi: 10.1158/0008-5472.CAN-18-2705
115. Bugreev DV, Rossi MJ, Mazin AV. Cooperation of RAD51 and RAD54 in regression of a model replication fork. *Nucleic Acids Res.* (2011) 39:2153–64. doi: 10.1093/nar/gkq1139
116. Fugger K, Mistrik M, Neelsen KJ, Yao Q, Zellweger R, Kousholt AN, et al. FBH1 catalyzes regression of stalled replication forks. *Cell Rep.* (2015) 10:1749–57. doi: 10.1016/j.celrep.2015.02.028
117. Machwe A, Xiao L, Groden J, Orren DK. The Werner and Bloom syndrome proteins catalyze regression of a model replication fork. *Biochemistry.* (2006) 45:13939–46. doi: 10.1021/bi0615487
118. Davies SL, North PS, Hickson ID. Role for BLM in replication-fork restart and suppression of origin firing after replicative stress. *Nat Struct Mol Biol.* (2007) 14:677–9. doi: 10.1038/nsmb1267
119. Kanagaraj R, Saydam N, Garcia PL, Zheng L, Janscak P. Human RECQ5beta helicase promotes strand exchange on synthetic DNA structures resembling a stalled replication fork. *Nucleic Acids Res.* (2006) 34:5217–31. doi: 10.1093/nar/gkl677

120. Gari K, Décaillet C, Delannoy M, Wu L, Constantinou A. Remodeling of DNA replication structures by the branch point translocase FANCM. *PNAS.* (2008) 105:16107–12. doi: 10.1073/pnas.0804777105
121. Blackford AN, Schwab RA, Nieminuszczy J, Deans AJ, West SC, Niedzwiedz W. The DNA translocase activity of FANCM protects stalled replication forks. *Hum Mol Genet.* (2012) 21:2005–16. doi: 10.1093/hmg/dds013
122. Schwab RA, Blackford AN, Niedzwiedz W. ATR activation and replication fork restart are defective in FANCM-deficient cells. *EMBO J.* (2010) 29:806–18. doi: 10.1038/emboj.2009.385
123. Yeo JE, Lee EH, Hendrickson EA, Sobeck A. CtIP mediates replication fork recovery in a FANCD2-regulated manner. *Hum Mol Genet.* (2014) 23:3695–705. doi: 10.1093/hmg/ddu078
124. Ying S, Hamdy FC, Helleday T. Mre11-dependent degradation of stalled DNA replication forks is prevented by BRCA2 and PARP1. *Cancer Res.* (2012) 72:2814–21. doi: 10.1158/0008-5472.CAN-11-3417
125. Ding X, Ray Chaudhuri A, Callen E, Pang Y, Biswas K, Klarmann KD, et al. Synthetic viability by BRCA2 and PARP1/ARTD1 deficiencies. *Nat Commun.* (2016) 7:12425. doi: 10.1038/ncomms12425
126. Murfuni I, De Santis A, Federico M, Bignami M, Pichierri P, Franchitto A. Perturbed replication induced genome wide or at common fragile sites is differently managed in the absence of WRN. *Carcinogenesis.* (2012) 33:1655–63. doi: 10.1093/carcin/bgs206
127. Thangavel S, Berti M, Levikova M, Pinto C, Gomathinayagam S, Vujanovic M, et al. DNA2 drives processing and restart of reversed replication forks in human cells. *J Cell Biol.* (2015) 208:545LP—62. doi: 10.1083/jcb.201406100
128. Ait Saada A, Lambert SAE, Carr AM. Preserving replication fork integrity and competence via the homologous recombination pathway. *DNA Repair.* (2018) 71:135–47. doi: 10.1016/j.dnarep.2018.08.017
129. Pepe A, West SC. MUS81-EME2 promotes replication fork restart. *Cell Rep.* (2014) 7:1048–55. doi: 10.1016/j.celrep.2014.04.007
130. Pond KW, de Renty C, Yagle MK, Ellis NA. Rescue of collapsed replication forks is dependent on NSMCE2 to prevent mitotic DNA damage. *PLoS Genet.* (2019) 15:e1007942. doi: 10.1371/journal.pgen.1007942
131. Sharma S, Brosh RMJ. Unique and important consequences of RECQ1 deficiency in mammalian cells. *Cell Cycle.* (2008) 7:989–1000. doi: 10.4161/cc.7.8.5707
132. Sharma S, Stumpo DJ, Balajee AS, Bock CB, Lansdorp PM, Brosh RMJ, et al. RECQL, a member of the RecQ family of DNA helicases, suppresses chromosomal instability. *Mol Cell Biol.* (2007) 27:1784–94. doi: 10.1128/MCB.01620-06
133. Seki M, Yanagisawa J, Kohda T, Sonoyama T, Ui M, Enomoto T. Purification of two DNA-dependent adenosinetriphosphatases having DNA helicase activity from HeLa cells and comparison of the properties of the two enzymes. *J Biochem.* (1994) 115:523–31. doi: 10.1093/oxfordjournals.jbchem.a124369
134. Thangavel S, Mendoza-Maldonado R, Tissino E, Sidorova JM, Yin J, Wang W, et al. Human RECQ1 and RECQ4 helicases play distinct roles in DNA replication initiation. *Mol Cell Biol.* (2010) 30:1382–96. doi: 10.1128/MCB.01290-09
135. Cybulski C, Carrot-Zhang J, Kluzniak W, Rivera B, Kashyap A, Wokolorczyk D, et al. Germline RECQL mutations are associated with breast cancer susceptibility. *Nat Genet.* (2015) 47:643–6. doi: 10.1038/ng.3284
136. Sun J, Wang Y, Xia Y, Xu Y, Ouyang T, Li J, et al. Mutations in RECQL gene are associated with predisposition to breast cancer. *PLoS Genet.* (2015) 11:e1005228. doi: 10.1371/journal.pgen.1005228
137. Viziteu E, Klein B, Basbous J, Lin Y-L, Hirtz C, Gourzones C, et al. RECQ1 helicase is involved in replication stress survival and drug resistance in multiple myeloma. *Leukemia.* (2017) 31:2104–13. doi: 10.1038/leu.2017.54
138. Ammazzalorso F, Pirzio LM, Bignami M, Franchitto A, Pichierri P. ATR and ATM differently regulate WRN to prevent DSBs at stalled replication forks and promote replication fork recovery. *EMBO J.* (2010) 29:3156–69. doi: 10.1038/emboj.2010.205
139. Rodriguez-Lopez AM, Jackson DA, Iborra F, Cox LS. Asymmetry of DNA replication fork progression in Werner's syndrome. *Aging Cell.* (2002) 1:30–9. doi: 10.1046/j.1474-9728.2002.00002.x
140. Hoa NN, Akagawa R, Yamasaki T, Hirota K, Sasa K, Natsume T, et al. Relative contribution of four nucleases, CtIP, Dna2, Exo1 and Mre11, to the initial step of DNA double-strand break repair by homologous recombination in both the chicken DT40 and human TK6 cell lines. *Genes Cells.* (2015) 20:1059–76. doi: 10.1111/gtc.12310
141. Paudyal SC, Li S, Yan H, Hunter T, You Z. Dna2 initiates resection at clean DNA double-strand breaks. *Nucleic Acids Res.* (2017) 45:11766–81. doi: 10.1093/nar/gkx830
142. Symington LS. End resection at double-strand breaks: mechanism and regulation. *Cold Spring Harb Perspect Biol.* (2014) 6:a016436. doi: 10.1101/cshperspect.a016436
143. Peng G, Dai H, Zhang W, Hsieh H-J, Pan M-R, Park Y-Y, et al. Human nuclease/helicase DNA2 alleviates replication stress by promoting DNA end resection. *Cancer Res.* (2012) 72:2802–13. doi: 10.1158/0008-5472.CAN-11-3152
144. Rhodes DR, Yu J, Shanker K, Deshpande N, Varambally R, Ghosh D, et al. ONCOMINE: a cancer microarray database and integrated data-mining platform. *Neoplasia.* (2004) 6:1–6. doi: 10.1016/S1476-5586(04)80047-2
145. Lai X, Broderick R, Bergoglio V, Zimmer J, Badie S, Niedzwiedz W, et al. MUS81 nuclease activity is essential for replication stress tolerance and chromosome segregation in BRCA2-deficient cells. *Nat Commun.* (2017) 8:15983. doi: 10.1038/ncomms15983
146. Hanada K, Budzowska M, Davies SL, van Drunen E, Onizawa H, Beverloo HB, et al. The structure-specific endonuclease Mus81 contributes to replication restart by generating double-strand DNA breaks. *Nat Struct Mol Biol.* (2007) 14:1096–104. doi: 10.1038/nsmb1313
147. Neelsen KJ, Zanini IMY, Herrador R, Lopes M. Oncogenes induce genotoxic stress by mitotic processing of unusual replication intermediates. *J Cell Biol.* (2013) 200:699LP—708. doi: 10.1083/jcb.201212058
148. Chen C-C, Feng W, Lim PX, Kass EM, Jasin M. Homology-directed repair and the role of BRCA1, BRCA2, and related proteins in genome integrity and cancer. *Annu Rev Cancer Biol.* (2018) 2:313–36. doi: 10.1146/annurev-cancerbio-030617-050502
149. Hashimoto Y, Ray Chaudhuri A, Lopes M, Costanzo V. Rad51 protects nascent DNA from Mre11-dependent degradation and promotes continuous DNA synthesis. *Nat Struct Mol Biol.* (2010) 17:1305–11. doi: 10.1038/nsmb.1927
150. Bryant HE, Petermann E, Schultz N, Jemth A-S, Loseva O, Issaeva N, et al. PARP is activated at stalled forks to mediate Mre11-dependent replication restart and recombination. *EMBO J.* (2009) 28:2601–15. doi: 10.1038/emboj.2009.206
151. Regairaz M, Zhang Y-W, Fu H, Agama KK, Tata N, Agrawal S, et al. Mus81-mediated DNA cleavage resolves replication forks stalled by topoisomerase I-DNA complexes. *J Cell Biol.* (2011) 195:739–49. doi: 10.1083/jcb.201104003
152. Ray Chaudhuri A, Hashimoto Y, Herrador R, Neelsen KJ, Fachinetti D, Bermejo R, et al. Topoisomerase I poisoning results in PARP-mediated replication fork reversal. *Nat Struct Mol Biol.* (2012) 19:417–23. doi: 10.1038/nsmb.2258
153. Sugimura K, Takebayashi S, Taguchi H, Takeda S, Okumura K. PARP-1 ensures regulation of replication fork progression by homologous recombination on damaged DNA. *J Cell Biol.* (2008) 183:1203LP—12. doi: 10.1083/jcb.200806068
154. Ghosal G, Chen J. DNA damage tolerance: a double-edged sword guarding the genome. *Transl Cancer Res.* (2013) 2:107–29. doi: 10.3978/j.issn.2218-676X.2013.04.01
155. Xie K, Doles J, Hemann MT, Walker GC. Error-prone translesion synthesis mediates acquired chemoresistance. *PNAS.* (2010) 107:20792–7. doi: 10.1073/pnas.1011412107
156. Bi X. Mechanism of DNA damage tolerance. *World J Biol Chem.* (2015) 6:48–56. doi: 10.4331/wjbc.v6.i3.48
157. Boldinova EO, Wanrooij PH, Shilkin ES, Wanrooij S, Makarova AV. DNA damage tolerance by eukaryotic DNA polymerase and primase PrimPol. *Int J Mol Sci.* (2017) 18:1584. doi: 10.3390/ijms18071584
158. Friedberg EC. Suffering in silence: the tolerance of DNA damage. *Nat Rev Mol Cell Biol.* (2005) 6:943–53. doi: 10.1038/nrm1781

159. McCulloch SD, Kunkel TA. The fidelity of DNA synthesis by eukaryotic replicative and translesion synthesis polymerases. *Cell Res*. (2008) 18:148–61. doi: 10.1038/cr.2008.4
160. Prakash S, Johnson RE, Prakash L. Eukaryotic translesion synthesis DNA polymerases: specificity of structure and function. *Annu Rev Biochem*. (2005) 74:317–53. doi: 10.1146/annurev.biochem.74.082803.133250
161. Friedberg EC, Lehmann AR, Fuchs RPP. Trading places: how do DNA polymerases switch during translesion DNA synthesis? *Mol Cell.* (2005) 18:499–505. doi: 10.1016/j.molcel.2005.03.032
162. Fujii S, Fuchs RP. Defining the position of the switches between replicative and bypass DNA polymerases. *EMBO J*. (2004) 23:4342–52. doi: 10.1038/sj.emboj.7600438
163. Fujii S, Fuchs RP. Interplay among replicative and specialized DNA polymerases determines failure or success of translesion synthesis pathways. *J Mol Biol*. (2007) 372:883–93. doi: 10.1016/j.jmb.2007.07.036
164. Baranovskiy AG, Lada AG, Siebler HM, Zhang Y, Pavlov YI, Tahirov TH. DNA polymerase δ and ζ switch by sharing accessory subunits of DNA polymerase δ. *J Biol Chem*. (2012) 287:17281–7. doi: 10.1074/jbc.M112.351122
165. Johnson RE, Prakash L, Prakash S. Pol31 and Pol32 subunits of yeast DNA polymerase δ are also essential subunits of DNA polymerase ζ. *Proc Natl Acad Sci USA*. (2012) 109:12455–60. doi: 10.1073/pnas.1206052109
166. Makarova AV, Burgers PM. Eukaryotic DNA polymerase ζ. *DNA Repair*. (2015) 29:47–55. doi: 10.1016/j.dnarep.2015.02.012
167. Makarova AV, Stodola JL, Burgers PM. A four-subunit DNA polymerase ζ complex containing Pol δ accessory subunits is essential for PCNA-mediated mutagenesis. *Nucl Acids Res*. (2012) 40:11618–26. doi: 10.1093/nar/gks948
168. Berquist BR, Wilson DM. Pathways for repairing and tolerating the spectrum of oxidative DNA lesions. *Cancer Lett*. (2012) 327:61–72. doi: 10.1016/j.canlet.2012.02.001
169. Bianchi J, Rudd SG, Jozwiakowski SK, Bailey LJ, Soura V, Taylor E, et al. PrimPol bypasses UV photoproducts during eukaryotic chromosomal DNA replication. *Mol Cell.* (2013) 52:566–73. doi: 10.1016/j.molcel.2013.10.035
170. García-Gómez S, Reyes A, Martínez-Jiménez MI, Chocrón ES, Mourón S, Terrados G, et al. PrimPol, an archaic primase/polymerase operating in human cells. *Mol Cell.* (2013) 52:541–53. doi: 10.1016/j.molcel.2013.09.025
171. Martínez-Jiménez MI, García-Gómez S, Bebenek K, Sastre-Moreno G, Calvo PA, Díaz-Talavera A, et al. Alternative solutions and new scenarios for translesion DNA synthesis by human PrimPol. *DNA Repair*. (2015) 29:127–38. doi: 10.1016/j.dnarep.2015.02.013
172. Bailey LJ, Bianchi J, Doherty AJ. PrimPol is required for the maintenance of efficient nuclear and mitochondrial DNA replication in human cells. *Nucl Acids Res.* (2019) 47:4026–38. doi: 10.1093/nar/gkz056
173. Guilliam TA, Brissett NC, Ehlinger A, Keen BA, Kolesar P, Taylor EM, et al. Molecular basis for PrimPol recruitment to replication forks by RPA. *Nat Commun.* (2017) 8:1–14. doi: 10.1038/ncomms15222
174. Kobayashi K, Guilliam TA, Tsuda M, Yamamoto J, Bailey LJ, Iwai S, et al. Repriming by PrimPol is critical for DNA replication restart downstream of lesions and chain-terminating nucleosides. *Cell Cycle.* (2016) 15:1997–2008. doi: 10.1080/15384101.2016.1191711
175. Quinet A, Tirman S, Jackson J, Šviković S, Lemaçon D, Carvajal-Maldonado D, et al. PRIMPOL-mediated adaptive response suppresses replication fork reversal in BRCA-deficient cells. *Mol Cell.* (2019) 77:461–474. doi: 10.1016/j.molcel.2019.10.008
176. Guilliam TA, Jozwiakowski SK, Ehlinger A, Barnes RP, Rudd SG, Bailey LJ, et al. Human PrimPol is a highly error-prone polymerase regulated by single-stranded DNA binding proteins. *Nucleic Acids Res.* (2015) 43:1056–68. doi: 10.1093/nar/gku1321
177. Keen BA, Jozwiakowski SK, Bailey LJ, Bianchi J, Doherty AJ. Molecular dissection of the domain architecture and catalytic activities of human PrimPol. *Nucleic Acids Res.* (2014) 42:5830–45. doi: 10.1093/nar/gku214
178. Zafar MK, Ketkar A, Lodeiro MF, Cameron CE, Eoff RL. Kinetic analysis of human PrimPol DNA polymerase activity reveals a generally error-prone enzyme capable of accurately bypassing 7,8-dihydro-8-oxo-2′-deoxyguanosine. *Biochemistry.* (2014) 53:6584–94. doi: 10.1021/bi501024u
179. Fumasoni M, Zwicky K, Vanoli F, Lopes M, Branzei D. Error-free DNA damage tolerance and sister chromatid proximity during DNA replication rely on the Polα/Primase/Ctf4 complex. *Mol Cell.* (2015) 57:812–23. doi: 10.1016/j.molcel.2014.12.038
180. Vanoli F, Fumasoni M, Szakal B, Maloisel L, Branzei D. Replication and recombination factors contributing to recombination-dependent bypass of DNA lesions by template switch. *PLoS Genet*. (2010) 6:e1001205. doi: 10.1371/journal.pgen.1001205
181. Zhang H, Lawrence CW. The error-free component of the RAD6/RAD18 DNA damage tolerance pathway of budding yeast employs sister-strand recombination. *Proc Natl Acad Sci USA*. (2005) 102:15954–9. doi: 10.1073/pnas.0504586102
182. Gonzalez-Huici V, Szakal B, Urulangodi M, Psakhye I, Castellucci F, Menolfi D, et al. DNA bending facilitates the error-free DNA damage tolerance pathway and upholds genome integrity. *EMBO J.* (2014) 33:327–40. doi: 10.1002/embj.201387425
183. Karras GI, Fumasoni M, Sienski G, Vanoli F, Branzei D, Jentsch S. Noncanonical role of the 9-1-1 clamp in the error-free DNA damage tolerance pathway. *Mol Cell.* (2013) 49:536–46. doi: 10.1016/j.molcel.2012.11.016
184. Ortiz-Bazán MÁ, Gallo-Fernández M, Saugar I, Jiménez-Martín A, Vázquez MV, Tercero JA. Rad5 plays a major role in the cellular response to DNA damage during chromosome replication. *Cell Rep*. (2014) 9:460–8. doi: 10.1016/j.celrep.2014.09.005
185. Moldovan G-L, Pfander B, Jentsch S. PCNA, the maestro of the replication fork. *Cell.* (2007) 129:665–79. doi: 10.1016/j.cell.2007.05.003
186. Masuda Y, Masutani C. Spatiotemporal regulation of PCNA ubiquitination in damage tolerance pathways. *Crit Rev Biochem Mol Biol.* (2019) 54:418–42. doi: 10.1080/10409238.2019.1687420
187. Branzei D, Szakal B. DNA damage tolerance by recombination: molecular pathways and DNA structures. *DNA Repair*. (2016) 44:68–75. doi: 10.1016/j.dnarep.2016.05.008
188. Masuda Y, Suzuki M, Kawai H, Hishiki A, Hashimoto H, Masutani C, et al. En bloc transfer of polyubiquitin chains to PCNA *in vitro* is mediated by two different human E2-E3 pairs. *Nucleic Acids Res.* (2012) 40:10394–407. doi: 10.1093/nar/gks763
189. Waters LS, Walker GC. The critical mutagenic translesion DNA polymerase Rev1 is highly expressed during G2/M phase rather than S phase. *Proc Natl Acad Sci USA*. (2006) 103:8971–6. doi: 10.1073/pnas.0510167103
190. Choe KN, Moldovan G-L. Forging ahead through darkness: PCNA, still the principal conductor at the replication fork. *Mol Cell.* (2017) 65:380–92. doi: 10.1016/j.molcel.2016.12.020
191. Papouli E, Chen S, Davies AA, Huttner D, Krejci L, Sung P, et al. Crosstalk between SUMO and ubiquitin on PCNA is mediated by recruitment of the helicase Srs2p. *Mol Cell.* (2005) 19:123–33. doi: 10.1016/j.molcel.2005.06.001
192. Pfander B, Moldovan G-L, Sacher M, Hoege C, Jentsch S. SUMO-modified PCNA recruits Srs2 to prevent recombination during S phase. *Nature.* (2005) 436:428–33. doi: 10.1038/nature03665
193. Hoege C, Pfander B, Moldovan G-L, Pyrowolakis G, Jentsch S. RAD6-dependent DNA repair is linked to modification of PCNA by ubiquitin and SUMO. *Nature.* (2002) 419:135–41. doi: 10.1038/nature00991
194. Moldovan GL, Dejsuphong D, Petalcorin MI, Hofmann K, Takeda S, Boulton SJ, et al. Inhibition of homologous recombination by the PCNA-interacting protein PARI. *Mol Cell.* (2012) 45:75–86. doi: 10.1016/j.molcel.2011.11.010
195. Zafar MK, Eoff RL. Translesion DNA synthesis in cancer: molecular mechanisms and therapeutic opportunities. *Chem Res Toxicol*. (2017) 30:1942–55. doi: 10.1021/acs.chemrestox.7b00157
196. Albertella MR, Lau A, O'Connor MJ. The overexpression of specialized DNA polymerases in cancer. *DNA Repair*. (2005) 4:583–93. doi: 10.1016/j.dnarep.2005.01.005
197. Stallons LJ, McGregor WG. Translesion synthesis polymerases in the prevention and promotion of carcinogenesis. *J Nucleic Acids*. (2010) 2010:643857. doi: 10.4061/2010/643857
198. Canitrot Y, Frechet M, Servant L, Cazaux C, Hoffmann JS. Overexpression of DNA polymerase beta: a genomic instability enhancer process. *FASEB J*. (1999) 13:1107–11. doi: 10.1096/fasebj.13.9.1107
199. Canitrot Y, Hoffmann JS, Calsou P, Hayakawa H, Salles B, Cazaux C. Nucleotide excision repair DNA synthesis by excess DNA polymerase beta:

a potential source of genetic instability in cancer cells. *FASEB J.* (2000) 14:1765–74. doi: 10.1096/fj.99-1063com
200. Nicolay NH, Helleday T, Sharma RA. Biological relevance of DNA polymerase β and translesion synthesis polymerases to cancer and its treatment. *Curr Mol Pharmacol.* (2012) 5:54–67. doi: 10.2174/1874467211205010054
201. Lemée F, Bergoglio V, Fernandez-Vidal A, Machado-Silva A, Pillaire M-J, Bieth A, et al. DNA polymerase theta up-regulation is associated with poor survival in breast cancer, perturbs DNA replication, and promotes genetic instability. *Proc Natl Acad Sci USA*. (2010) 107:13390–5. doi: 10.1073/pnas.0910759107
202. Ceppi P, Novello S, Cambieri A, Longo M, Monica V, Iacono ML, et al. Polymerase η mRNA expression predicts survival of non-small cell lung cancer patients treated with platinum-based chemotherapy. *Clin Cancer Res.* (2009) 15:1039–45. doi: 10.1158/1078-0432.CCR-08-1227
203. Teng K, Qiu M, Li Z, Luo H, Zeng Z, Luo R, et al. DNA polymerase η protein expression predicts treatment response and survival of metastatic gastric adenocarcinoma patients treated with oxaliplatin-based chemotherapy. *J Transl Med.* (2010) 8:126. doi: 10.1186/1479-5876-8-126
204. Wojtaszek JL, Chatterjee N, Najeeb J, Ramos A, Lee M, Bian K, et al. A small molecule targeting mutagenic translesion synthesis improves chemotherapy. *Cell.* (2019) 178:152–9.e11. doi: 10.1016/j.cell.2019.05.028
205. Actis ML, Ambaye ND, Evison BJ, Shao Y, Vanarotti M, Inoue A, et al. Identification of the first small-molecule inhibitor of the REV7 DNA repair protein interaction. *Bioorgan Med Chem.* (2016) 24:4339–46. doi: 10.1016/j.bmc.2016.07.026
206. Izuta S. Inhibition of DNA polymerase eta by oxetanocin derivatives. *Nucleic Acids Symp Ser.*(2006) 50:269–270. doi: 10.1093/nass/nrl134
207. Sail V, Rizzo AA, Chatterjee N, Dash RC, Ozen Z, Walker GC, et al. Identification of small molecule translesion synthesis inhibitors that target the Rev1-CT/RIR protein-protein interaction. *ACS Chem Biol.* (2017) 12:1903–12. doi: 10.1021/acschembio.6b01144
208. Xu X, Xie K, Zhang X-Q, Pridgen EM, Park GY, Cui DS, et al. Enhancing tumor cell response to chemotherapy through nanoparticle-mediated codelivery of siRNA and cisplatin prodrug. *Proc Natl Acad Sci USA*. (2013) 110:18638–43. doi: 10.1073/pnas.1303958110
209. Doles J, Oliver TG, Cameron ER, Hsu G, Jacks T, Walker GC, et al. Suppression of Rev3, the catalytic subunit of Polζ, sensitizes drug-resistant lung tumors to chemotherapy. *Proc Natl Acad Sci USA*. (2010) 107:20786–91. doi: 10.1073/pnas.1011409107
210. Buoninfante OA, Pilzecker B, Aslam MA, Zavrakidis I, van der Wiel R, van de Ven M, et al. Precision cancer therapy: profiting from tumor specific defects in the DNA damage tolerance system. *Oncotarget.* (2018) 9:18832–43. doi: 10.18632/oncotarget.24777
211. Lu C, Romo-Bucheli D, Wang X, Janowczyk A, Ganesan S, Gilmore H, et al. Nuclear shape and orientation features from H&E images predict survival in early-stage estrogen receptor-positive breast cancers. *Lab Invest.* (2018) 98:1438–48. doi: 10.1038/s41374-018-0095-7
212. Whitney J, Corredor G, Janowczyk A, Ganesan S, Doyle S, Tomaszewski J, et al. Quantitative nuclear histomorphometry predicts oncotype DX risk categories for early stage ER+ breast cancer. *BMC Cancer.* (2018) 18:610. doi: 10.1186/s12885-018-4448-9
213. Chakraborty S, Hosen Md. I, Ahmed M, Shekhar HU. Onco-multi-OMICS approach: a new frontier in cancer research. *Biomed Res Int.* (2018) 2018:9836256. doi: 10.1155/2018/9836256
214. Gallo Cantafio ME, Grillone K, Caracciolo D, Scionti F, Arbitrio M, Barbieri V, et al. From single level analysis to multi-omics integrative approaches: a powerful strategy towards the precision oncology. *High Throughput.* (2018) 7:33. doi: 10.3390/ht7040033
215. Lu M, Zhan X. The crucial role of multiomic approach in cancer research and clinically relevant outcomes. *EPMA J.* (2018) 9:77–102. doi: 10.1007/s13167-018-0128-8
216. Koboldt DC, Fulton RS, McLellan MD, Schmidt H, Kalicki-Veizer J, McMichael JF, et al. Comprehensive molecular portraits of human breast tumours. *Nature.* (2012) 490:61–70. doi: 10.1038/nature11412
217. Mertins P, Mani DR, Ruggles KV, Gillette MA, Clauser KR, Wang P, et al. Proteogenomics connects somatic mutations to signalling in breast cancer. *Nature.* (2016) 534:55–62. doi: 10.1038/nature18003
218. Boretto M, Maenhoudt N, Luo X, Hennes A, Boeckx B, Bui B, et al. Patient-derived organoids from endometrial disease capture clinical heterogeneity and are amenable to drug screening. *Nat Cell Biol.* (2019) 21:1041–51. doi: 10.1038/s41556-019-0360-z
219. Kim M, Mun H, Sung CO, Cho EJ, Jeon H-J, Chun S-M, et al. Patient-derived lung cancer organoids as *in vitro* cancer models for therapeutic screening. *Nat Commun.* (2019) 10:3991. doi: 10.1038/s41467-019-11867-6
220. Saito Y, Muramatsu T, Kanai Y, Ojima H, Sukeda A, Hiraoka N, et al. Establishment of patient-derived organoids and drug screening for biliary tract carcinoma. *Cell Rep.* (2019) 27:1265–76.e4. doi: 10.1016/j.celrep.2019.03.088
221. Sachs N, de Ligt J, Kopper O, Gogola E, Bounova G, Weeber F, et al. A living biobank of breast cancer organoids captures disease heterogeneity. *Cell.* (2018) 172:373–86.e10. doi: 10.1016/j.cell.2017.11.010
222. Duarte AA, Gogola E, Sachs N, Barazas M, Annunziato S, de Ruiter JR, et al. BRCA-deficient mouse mammary tumor organoids to study cancer-drug resistance. *Nat Methods.* (2018) 15:134–40. doi: 10.1038/nmeth.4535
223. Hall JM, Lee MK, Newman B, Morrow JE, Anderson LA, Huey B, et al. Linkage of early-onset familial breast cancer to chromosome 17q21. *Science.* (1990) 250:1684–9. doi: 10.1126/science.2270482
224. Capoluongo E. BRCA to the future: towards best testing practice in the era of personalised healthcare. *Eur J Hum Genet.* (2016) 24(Suppl 1):S1–2. doi: 10.1038/ejhg.2016.92
225. Nicolussi A, Belardinilli F, Mahdavian Y, Colicchia V, D'Inzeo S, Petroni M, et al. Next-generation sequencing of BRCA1 and BRCA2 genes for rapid detection of germline mutations in hereditary breast/ovarian cancer. *PeerJ.* (2019) 7:e6661. doi: 10.7717/peerj.6661
226. Cummings CA, Peters E, Lacroix L, Andre F, Lackner MR. The role of next-generation sequencing in enabling personalized oncology therapy. *Clin Transl Sci.* (2016) 9:283–92. doi: 10.1111/cts.12429
227. Cruz C, Castroviejo-Bermejo M, Gutiérrez-Enríquez S, Llop-Guevara A, Ibrahim YH, Gris-Oliver A, et al. RAD51 foci as a functional biomarker of homologous recombination repair and PARP inhibitor resistance in germline BRCA-mutated breast cancer. *Ann Oncol.* (2018) 29:1203–10. doi: 10.1093/annonc/mdy099
228. Di Virgilio M, Callen E, Yamane A, Zhang W, Jankovic M, Gitlin AD, et al. Rif1 prevents resection of DNA breaks and promotes immunoglobulin class switching. *Science.* (2013) 339:711–5. doi: 10.1126/science.1230624

Conflict of Interest: The authors declare that the research was conducted in the absence of any commercial or financial relationships that could be construed as a potential conflict of interest.

frontiers in Oncology

REVIEW
published: 28 July 2020
doi: 10.3389/fonc.2020.01256

The Therapeutic Potential of DNA Damage Repair Pathways and Genomic Stability in Lung Cancer

*Joshua T. Burgess[1], Maddison Rose[1], Didier Boucher[1], Jennifer Plowman[1], Christopher Molloy[1], Mark Fisher[1], Connor O'Leary[1,2], Derek J. Richard[1], Kenneth J. O'Byrne[1,2] and Emma Bolderson[1,2]**

[1] Cancer & Ageing Research Program, School of Biomedical Sciences, Institute of Health and Biomedical Innovation at the Translational Research Institute (TRI), Queensland University of Technology (QUT), Brisbane, QLD, Australia, [2] Princess Alexandra Hospital, Brisbane, QLD, Australia

Despite advances in our understanding of the molecular biology of the disease and improved therapeutics, lung cancer remains the most common cause of cancer-related deaths worldwide. Therefore, an unmet need remains for improved treatments, especially in advanced stage disease. Genomic instability is a universal hallmark of all cancers. Many of the most commonly prescribed chemotherapeutics, including platinum-based compounds such as cisplatin, target the characteristic genomic instability of tumors by directly damaging the DNA. Chemotherapies are designed to selectively target rapidly dividing cells, where they cause critical DNA damage and subsequent cell death (1, 2). Despite the initial efficacy of these drugs, the development of chemotherapy resistant tumors remains the primary concern for treatment of all lung cancer patients. The correct functioning of the DNA damage repair machinery is essential to ensure the maintenance of normal cycling cells. Dysregulation of these pathways promotes the accumulation of mutations which increase the potential of malignancy. Following the development of the initial malignancy, the continued disruption of the DNA repair machinery may result in the further progression of metastatic disease. Lung cancer is recognized as one of the most genomically unstable cancers (3). In this review, we present an overview of the DNA damage repair pathways and their contributions to lung cancer disease occurrence and progression. We conclude with an overview of current targeted lung cancer treatments and their evolution toward combination therapies, including chemotherapy with immunotherapies and antibody-drug conjugates and the mechanisms by which they target DNA damage repair pathways.

Keywords: lung cancer, DNA damage, DNA repair, cancer therapy, chemotherapy

OPEN ACCESS

Edited by:
Yitzhak Zimmer,
University Hospital Bern, Switzerland

Reviewed by:
Carlo V. Bruschi,
University of Salzburg, Austria
Zhi-Xiang Xu,
University of Alabama at Birmingham, United States

***Correspondence:**
Emma Bolderson
emma.bolderson@qut.edu.au

Specialty section:
This article was submitted to Molecular and Cellular Oncology, a section of the journal Frontiers in Oncology

Received: *17 April 2020*
Accepted: *17 June 2020*
Published: *28 July 2020*

Citation:
Burgess JT, Rose M, Boucher D, Plowman J, Molloy C, Fisher M, O'Leary C, Richard DJ, O'Byrne KJ and Bolderson E (2020) The Therapeutic Potential of DNA Damage Repair Pathways and Genomic Stability in Lung Cancer. Front. Oncol. 10:1256. doi: 10.3389/fonc.2020.01256

DNA DAMAGE REPAIR AND GENOMIC INSTABILITY IN LUNG CANCER

The integrity of cellular DNA is under continual stress, receiving over 30,000 damaging events per day (4). Damaged DNA bases and DNA single-strand breaks are the most abundant types of DNA damage. Although DNA double-strand breaks are less common, they are considered as the most deleterious types of DNA damage (5). Maintaining DNA integrity is essential to prevent cancer

development, which is accelerated by the accumulation of mutations. DNA breaks can arise from both endogenous and exogenous insults (6). Endogenous DNA damage can be induced by cellular processes, including somatic and meiotic recombination, and reactive oxygen species (ROS) that arise from normal cellular metabolism. Exogenous insults include cellular exposure to radiation, chemotherapeutic agents, and environmental carcinogenic compounds (7).

Lung cancers generally exhibit a unique genomic profile in contrast with other tumor types, with a high rate somatic mutation burden, second only to melanoma (8). The somatic lung cancer mutation rate was found to be much higher in smokers, 8–10 mutations/Mb, compared to <1 mutation/Mb in non-smokers, strongly supporting the causality of tobacco carcinogens (9). Highlighting the high genome instability in lung cancers, aneuploidy, (an abnormal number of chromosomes) is detected in over 60% of NSCLC cases (10) and genome duplication is observed in 30–50% of lung cancers (11).

The development of lung cancer is primarily thought to result from environmental provocation; however, there is data supporting that germline mutations in DNA repair genes increase the predisposition to the disease (12). Supporting this it has been shown that in ∼2.5% of all cancer, a germline mutation in a DNA repair gene was associated with cancer development (12).

DNA repair pathways are crucial to prevent the accumulation of DNA lesions and mutations that may promote tumorigenesis through the dysregulation of cell growth and death pathways. However, the gradual loss of genomic integrity can be accelerated by environmental factors such as carcinogens from cigarette smoke promoting the development of driver mutations, including oncogene activation and/or loss of tumor suppressor function, further increasing the likelihood of tumorigenesis.

Specifically, genomic instability promotes lung cancer pathogenesis by the constitutive activation of proto-oncogenes, including the members of the EGFR (ERBB), MYC, and RAS families, along with *PIK3CA*, *NKX2-1*, and *ALK*. Mutations (*KRAS*, *EGFR*, and PIK3CA) and amplifications (*MYC*, *EGFR*, *HER2*, *PIK3CA*, and *NKX2-1*) commonly activate these proto-oncogenes. In addition, translocations and inversions can also occur, positioning these genes under the control of constitutively active genes such as MYC or create chimeric proteins, such as the *ALK-EML4* fusion commonly observed in lung cancers (13, 14).

Probably the most significant exogenous factor contributing to lung cancer is the exposure of lung cells to cigarette smoke, which is well-known to significantly increase an individual's risk of developing lung cancer. Cigarette smoke is recognized as a major carcinogen, identified to contain 98 individual carcinogenic compounds (15). Many of these are predicted to be mutagenic via direct interaction with the DNA (16). If cells are unable to effectively repair these lesions, mutations may arise as a result of the carcinogenic exposure, potentially promoting tumorigenesis.

Once a DNA damage event is detected, it can be repaired by one or several of the DNA repair pathways: broadly defined as base excision repair (BER); direct repair (DR); homologous recombination (HR); mismatch repair (MMR); nucleotide excision repair (NER); or non-homologous end joining (NHEJ; as shown in **Figure 2**). Defective DNA repair mechanisms in cancer cells are often associated with poor patient prognosis due to enhanced disease progression. However, defects in DNA repair machinery may also provide an avenue to specifically target cancer cells due to increased sensitivity to anti-cancer therapies (17).

DNA REPAIR PATHWAYS

Nucleotide Excision Repair

Bulky DNA adducts caused by UV light and chemotherapeutic agents, such as Cisplatin, are repaired primarily through the nucleotide excision repair pathway (NER). This pathway is composed of a series of enzymatic reactions which are facilitated by over 30 proteins. Cisplatin and other platinum compounds bind to the DNA and form adducts, which lead to intrastrand or interstrand crosslinks (**Figure 1A**). These bulky adducts cause distortion of the DNA helix, blocking the replicative DNA polymerases and subsequently DNA replication and require the NER pathway (or the MMR pathway) for repair. These chemotherapeutic agents exploit differences in cellular proliferation and DNA repair pathways in cancerous cells to specifically target tumors.

As with the other DNA repair pathways, NER is a stepwise process initiated by DNA damage recognition; followed by recruitment of the pre-incision protein complex and DNA unwinding. This allows for excision of the damaged fragment and subsequent DNA repair and ligation [reviewed in (7)].

Depending on the DNA damage recognition step, the NER pathway is divided into two sub-pathways. Transcription coupled NER (TCR) is initiated by the stalling of transcription by RNA polymerase II promoting the subsequent recruitment of the Cockayne syndrome (CS) complementation group A and B to initiate repair (18, 19). During global genome NER (GGR), the XPC/hHR23B, DDB1, and DDB2/XPE complexes recognize the DNA lesions. Following damage recognition, TCR and GGR follow the same mechanism. The DNA helix is unwound by the TFIIH complex to enable access to the pre-incision complex (XPD, XPB, XPA, and XPG) (20, 21), opening the DNA double strand for the recruitment of RPA The damaged DNA is then excised, leading to removal of a patch of 24–32 base pairs, facilitated by XPG and the CPF-ERCC1 (excision repair cross-complementing enzyme group 1) endonucleases. DNA synthesis replaces the excised DNA in conjunction with PCNA and RPC, followed by the repair of the backbone through DNA ligase I (18).

Single nucleotide polymorphisms (SNPs) in NER associated proteins have been shown to have clear links to lung cancer patient survival and responsiveness to treatments. SNPs in NER proteins including ERCC1, ERCC6, POLD2, POLE, and XPA are associated with progression free survival. SNPs in other NER proteins, including ERCC6, GTF2H4, GTF2HA, MAT1, POLD1 are associated with overall survival (22, 23). Furthermore, decreased expression of XPG/ERCC5 and CSB/ERCC6 has been demonstrated to increase the risk of lung cancer (24).

Cisplatin sensitivity has been associated with SNPs and gene expression within the NER pathway. ERCC1 (excision repair cross-complementing enzyme group 1) is one such

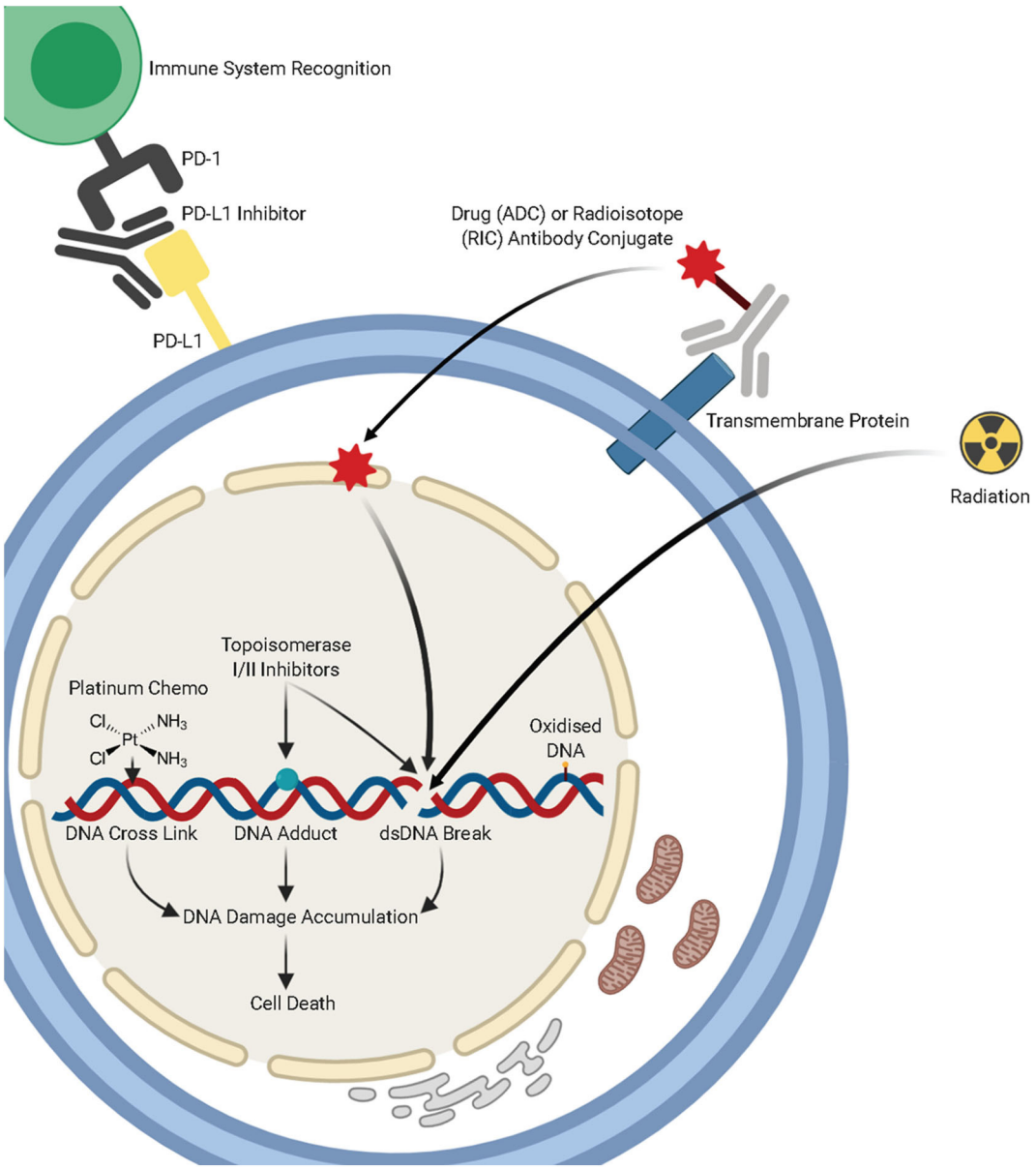

FIGURE 1 | A summary of lung cancer treatments, including chemotherapy, radiotherapy, immunotherapies, and antibody-drug conjugates and the mechanisms by which they target DNA damage repair pathways. Figure created with Biorender.

protein and functionally associates with XPF (xeroderma pigmentosum complementation group F) to incise damaged DNA (25).

ERCC2, another NER repair protein, is a helicase that unwinds DNA strands in the vicinity of a damaged site. ERCC2 mRNA expression has been shown to significantly correlate with cisplatin resistance in preclinical studies (26, 27). Cumulative evidence indicates that polymorphisms of the NER repair gene, ERCC5, could serve as pharmacogenomics biomarkers (28). In addition, a polymorphism in RRM1, a large regulatory subunit of ribonucleotide reductase, involved in the NER pathway, has been identified as a promising prognostic biomarker (29).

Mismatch Repair

DNA mismatch repair (MMR) is a conserved process responsible for the recognition and repair of mispaired bases generated during DNA replication and other DNA damage repair pathways. In addition to base mismatch, MMR can recognize other DNA lesions including DNA crosslinks induced by chemotherapeutic agents (30, 31).

The MMR process consists first of the damage recognition by the sliding clamp MutSα (MSH2/MSH6 heterodimer, for base mismatch) or MutSβ (MSH2/MSH3 heterodimer, for base insertion/deletion), followed recruitment of the MutLα complex (formed by MLH1 and PMS2) for the incision step. Exonuclease 1

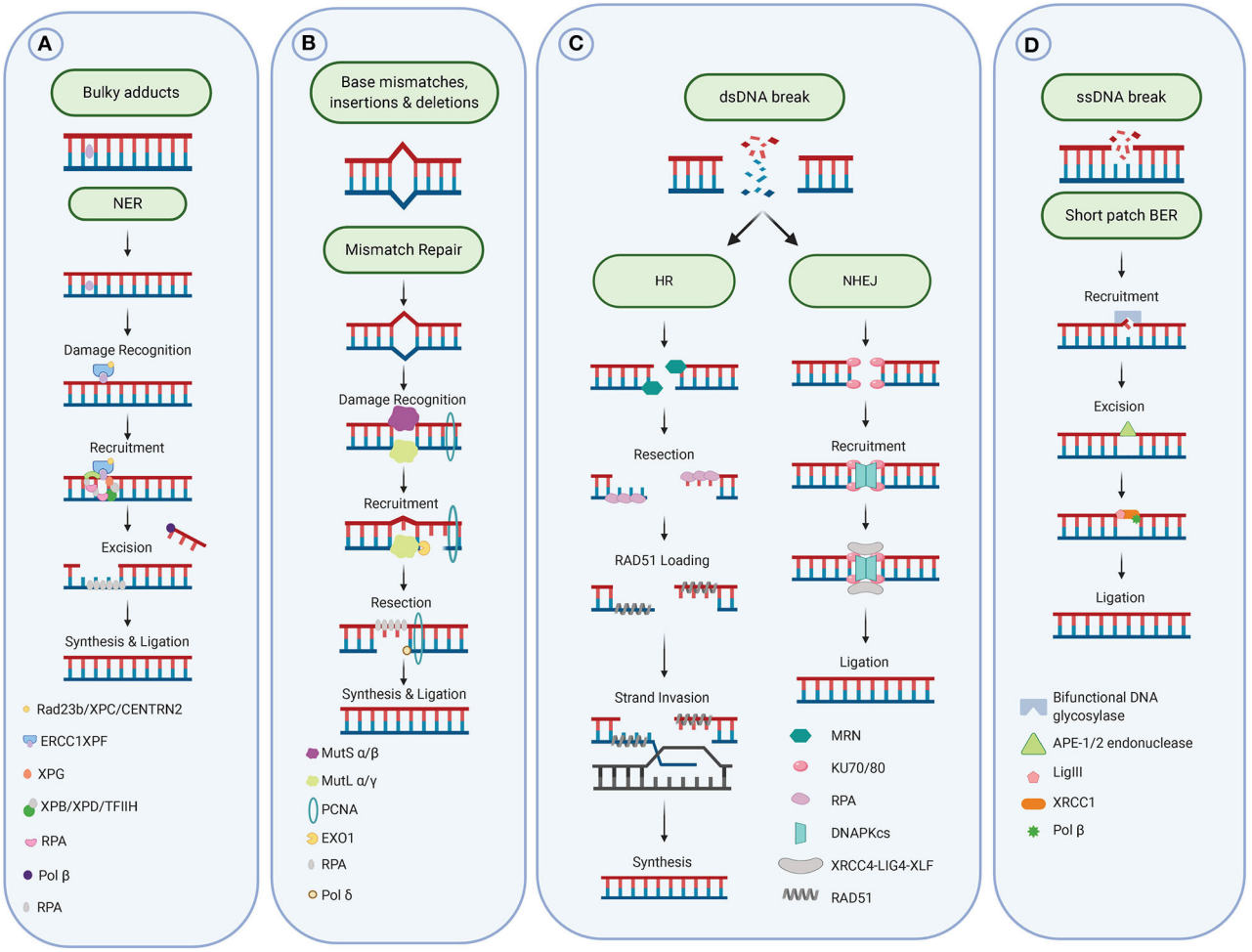

FIGURE 2 | DNA repair pathways. **(A)** Repair of bulky adducts via the Nucleotide excision repair pathway. **(B)** Repair of mismatches via the mismatch repair pathway. **(C)** Repair of DNA double-strand breaks via the homologous recombination and non-homologous end-joining pathways. **(D)** Repair of DNA single strand breaks and damaged and oxidized bases via the base excision repair pathway. Figure created with Biorender.

(EXO1) is then recruited to excise the damage, leaving a gap filled by DNA polymerase δ (Polδ). Finally, DNA ligase I closes the remaining nick on the newly synthesized strand [see for review (32), **Figure 2B**].

Inactivation of MMR can have wide ranging consequences due to its involvement in the repair of base substitution mismatches and insertion–deletion mismatches that escape DNA polymerase proofreading during replication (33). MMR proteins function in the activation of cell cycle checkpoints, supressing DNA lesions, and the initiation of apoptosis (34).

MMR proteins can be inactivated without causing cell lethality; however, this can lead to a significantly increased rate of genome-wide point mutations, resulting from unrepaired DNA synthesis errors. The mutator phenotype conferred by this loss of MMR activity contributes to the initiation and promotion of multi-stage carcinogenesis (35). MMR is dysregulated in non-small cell lung cancer, most frequently from mutations in the MSH2 and MLH1 genes, which are responsible for recognition of the mispaired nucleotides, deletions/insertions, and cisplatin-induced interstrand cross-links (36, 37). Decreased expression of MSH2 has been associated with increased cisplatin sensitivity (38).

In addition to mutations, mismatch repair may also be downregulated through epigenetic changes including hypermethylation of the MLH1 promoter, a defect occurring in 69% of non-small cell lung cancers, although it should be noted that this has also been disputed (39, 40). The prognostic significance of expression and methylation changes in these genes in non-small cell lung cancers is not well-understood and requires further study (41).

Base Excision Repair and Single-Strand Break Repair

Oxidative DNA damage has been shown to be a driver of carcinogenesis (42). Damage to bases within DNA requires the

base excision repair (BER) pathway for the effective repair of these lesions (**Figure 2D**). The BER pathway removes small covalent modifications such as those generated from reactive oxygen species (ROS) as a result of cellular metabolism or endogenous damage (43). Guanine, due to its chemical composition, is the most frequently oxidized base and following oxidation forms 8-oxo-7, 8-dihydro-guanine (8-oxoG) (44, 45). These lesions may result in G:C to A:T transversion during replication, due to the mis-pairing of 8-oxoG with cytosine of adenine nucleotides. Significantly these transversions are suggested to be one of the most common mutagenic features observed in many cancers (46, 47). Other types of damage involve alkylation or deamination (48).

The repair of these lesions involves the recognition and removal of the adduct by a specific DNA glycosylase (mono- or bi-functional), such as OGG1, NTH1, UNG, SMUG1, TDG, NEIL1, NEIL2, or NEIL3 [see for review (49)]. An AP-endonuclease, most commonly APE1, then catalyzes the hydrolysis of the site to generate a DNA single-strand break. This then activates the single-strand break repair pathway, which stimulates the poly-ADP ribose activity of PARP1. PARP1 uses NAD+ to catalyze the addition of long, branched PAR chains to onto serine, tyrosine and glutamic acid residues in the PARP1 automodification domain, in a process known as auto-ADP-ribosylation (50–54). This leads to further activation of PARP1 and thereby stimulates the PARP1-mediated poly-ADP-ribosylation of other repair proteins such as XRCC1 (X-ray repair cross-complementing protein 1). The nucleotide is then replaced by a DNA polymerase β and finally DNA ligase III repairs the DNA backbone (55). This process replaces a single nucleotide; however, long-patch BER is also possible where DNA polymerase δ/ε with PCNA replace a short sequence containing the damage (∼5 nucleotide). The endonuclease FEN1 resects the generated flap before final nick ligation by DNA ligase I. The reconstitution of long-patch-BER has demonstrated an absolute requirement for the endonuclease activity of FEN1, which, is often upregulated in cancers (56).

The reliance of tumor cells on BER pathways makes an attractive target for cancer therapy. Supporting this, elimination of N-Methylpurine DNA glycosylase (MPG) or inhibition of APE1 has been shown to increase sensitivity of cancer cells to alkylating chemotherapeutics (57). Several APE1 and Pol β inhibitors have also been developed and proved to be effective in cell line and mouse models; however, these have not yet progressed to human trials (58). PARP1 inhibitors have been approved as a human cancer therapy and will be discussed further in this review.

Mutations in key BER genes have been associated with an increased risk of lung cancer and decreased patient survival (59). Variants in the BER glycolyase and AP-endonuclease OGG1 and APEX1, respectively, have been shown to be associated with an increased risk of lung cancer (60–62). Variants in BER proteins have also been shown to associate with decreased patient survival, including; MDB4, a DNA binding protein, APE1, the primary endonuclease, OGG1, XRCC1 and Polymerase β variants (60–64).

DNA Double-Strand Break Repair

Regarded as potentially the most severe form of DNA damage, DNA double-strand breaks (DSBs) are induced by a variety of mechanisms. These include exogenous factors such as ionizing radiation and chemotherapeutic agents, or endogenous sources such as faulty DNA replication and oxidative stress induced by reactive oxygen species (ROS) during normal cellular metabolism (65). It is predicted that over 10 DSBs are induced per cell, per day and this can have severe consequences for cells, as failure to repair dsDNA breaks can lead to senescence or apoptosis. Furthermore, incorrect repair can result in genomic instability or mutation of critical regulatory genes and subsequently, tumorigenesis (66). Non-small cell lung cancers frequently exhibit mutations or loss of essential components of the DSB repair pathways (67, 68). Two main pathways are involved in the repair of DSBs; Homologous Recombination (HR) and Non-Homologous End Joining (NHEJ) [**Figure 1C**, (69)].

The two pathways are generally distinct from each other, however some of the repair machinery is involved in both pathways. NHEJ does not require a homologous template and involves the ligation of the two free DNA ends, without extensive resection, in contrast to HR. This ligation is initiated by the tight binding of the ring-shaped Ku70/Ku80 heterodimer to the two DSB ends to promote recruitment of DNA-dependent protein kinase (DNA-PK) and form an active catalytic complex (69). The bridging of the dsDNA break by the complex may initially enable DNA digestion or gap-filling by recruitment of the proteins Artemis (70), XLF (71), and PAXX (72), followed by induction of the Ligase IV/XRCC4 complex's DNA end ligation activity (66). The configuration of the DSB ends can lead to alternative NHEJ pathways [see for review (73)]. This process, which functions in all stages of the cell cycle, can result in the joining of cut DNA fragments from either a single gene or entirely separate chromosomes. Therefore, NHEJ is generally regarded as a more error prone method of DSB repair. NHEJ has been implicated in DNA translocation from one region or chromosome to another, having the potential to result in uncontrolled cell growth.

In late S and G2 phase, mammalian cells can repair dsDNA breaks by HR due to the availability of a homologous sister chromatid in close proximity to use as a template. HR requires the high fidelity matching of individual sequence bases to allow more accurate DNA repair than NHEJ, and without loss of bases (1, 74, 75). HR is initiated by the ATM-dependent recruitment of the Mre11-Rad50-NBS (MRN) complex. This serves to further activate ATM and promotes the further recruitment of other repair proteins, including MDC1, to the site of the break (76, 77). The MRN complex then resects DNA up to 3 kb from the dsDNA break site and in conjunction with Exo1 and Dna2, digests the DNA strand between the nick and DSB (78–80), exposing a section of single-stranded DNA (ssDNA) to which replication protein A (RPA) rapidly binds, promoting the recruitment of BRCA1 (81). Under the control of the BRCA1 and BRCA2 proteins (82), Rad51 then facilitates the search for a homologous DNA sequence and promotes the strand invasion to generate a D-loop. The resynthesis of the damaged strand is then completed by DNA polymerase eta, using the homologous sister chromatid

as template (83). The resulting Holliday junction is then resolved, by the 3′-flap endonuclease MUS81-EME1 or Gen1 resolvase (84, 85). Extensive degradation has also been observed at some DSBs, resulting from other mechanisms of repair called alternative-non-homologous end joining and single-strand annealing, both of which have the potential to cause mutagenic deletions (86, 87). However, it remains to be determined whether these alternative mechanisms of repair contribute toward lung tumorigenesis.

Similarly to many other cancer types, lung cancers display a high level of mutations in the tumor suppressor gene, TP53. TP53 has multiple faucets to its role in the maintenance of genome stability, including responding directly to DNA damage to promote repair and cell cycle arrest, the transcriptional regulation of DNA repair genes and the induction of apoptosis. In the absence of TP53 cells accumulate DNA damage and resist cell death. TP53 has been shown to be mutated in around 50% of all non-small-cell lung cancers (NSCLCs) and over 90% of small cell lung cancers (SCLCs). Since the presence of TP53 mutations have been detected in preneoplastic lesions in the lung, it has been hypothesized that the mutation of TP53 is likely to be an early event in the development of lung cancer (88).

In addition to TP53 mutations, mutations in the DSB repair kinase ATM, were identified in 6.12% of NSCLC. Mutations were also prevalent in other key DNA repair proteins including, TP53, BRCA2, EGFR, and PARK2 (12). There was an increased incidence of familial cancer syndromes associated with these mutations (89). Germline mutations in DNA repair pathway genes, similar to other solid tumors, are the most common subclass of genes associated with an increase in NSCLC predisposition (12).

Mutations in several DNA damage response genes, including PARP1, BRCA1, ATM, and TP53 have been shown to be associated with cancer progression and metastasis. The presence of DDR gene mutations has been linked with an increased tumor mutational burden in NSCLC. This study also showed that mutations in DNA repair genes were not mutually exclusive as 77% had a mutation in two or more genes associated with DNA repair. PARP1 and ATM mutations increase metastatic potential, likely due to their association with SNAIL-1, a master regulator of the epithelial-mesenchymal transition required for metastasis. Mutations in BRCA1 disrupt DSB repair via HR, increasing the mutation rate, and subsequently increasing the risk of tumorigenesis (90–92).

Mutations in DNA repair genes have been associated with a differential tumor response to cancer therapy. Mutations or changes in expression of genes that have been associated with chemotherapy sensitivity of NSCLC include TP73, MDM2, PTWN, PIK3, DNPK1, and DNA-PKcs (93). The treatment of NSCLC tumors possessing DNA-PK, TP53, and PTEN mutations with radiation similarly alters sensitivity in a mutant dependent manner (93). Mutations of MDM2 and TP53 have been associated with an increase in patient survival in lung adenocarcinoma (93).

Lung cancer has been well-characterized as possessing one of the most aggressive mutation rates of all cancers. Supporting this an average mutation rate of 4.21 mutations per megabase was identified in a screen of somatic mutations in protein kinase genes from 210 cancer cell lines (46). Sequencing of 188 primary lung adenocarcinomas identified 26 mutated genes, including several known tumor suppressor genes including TP53, KRAS, CDKN2A, and STK11 (LKB protein). High mutation rates in DNA repair genes, including CDNK2 (p16) and RB were also shown via whole-genome and transcriptome sequencing of lung cancers (9, 40). As mentioned above mutations in STK11/LKB1 and consequential disruption of AMPK signaling pathways are amongst the most frequent aberrations in lung cancers [reviewed in (94)]. Both LKB1 and AMPK have been suggested to have roles in DNA repair pathways, however the full extent of the influence of LKB1 downregulation on DNA repair pathways in lung cancer has not yet been explored (95, 96).

Translocations, which can result from errors in repairing DSBs, are also common in lung cancers, with gene fusions in the tyrosine kinases ALK and ROS1 being the first identified, targetable driver rearrangements in NSCLC. Fusions in other kinases have also been established as targetable, oncogenic drivers, including RET, NTRK, EGFR, and BRAF (97).

DNA REPAIR PATHWAYS AS THERAPEUTIC TARGETS

The recommended frontline treatment for patients with stage I–III NSCLC is surgery. For inoperable locally advanced tumors, the current standard of care involves concurrent radiotherapy and doublet chemotherapy followed by 1 year of adjuvant immunotherapy, Durvalumab. Therapies for the treatment of advanced lung cancer have become more targeted to the individual tumor, utilizing advances in molecular target technologies based on genomic abnormalities detected in the tumor tissue. It is estimated that up to 69% of patients with advanced NSCLC could have alterations in one or more molecular targets that could guide their treatment (98). These include EGFR activating mutations, KRAS, BRAF, HER2, and MET mutations, ROS1, ALK, RET, and NTRK rearrangements. EGFR, ALK, ROS-1, and BRAF positive tumors now have clinically applicable targeted specific therapies [reviewed in (99)] which offers superior patient outcomes and an improved toxicity profile compared to standard platinum doublet based chemotherapy. Clinical trials are currently underway investigating compounds that specifically target KRAS, HER2, MET, RET, and NTRX alterations in NSCLC. These compounds, if proven efficacious, will dramatically expand the treatment landscape for these patients. Single agent pembrolizumab, platinum-based doublet therapy with or without immunotherapy are current options in the first line for patients that do not fit an identified targeted therapy. Treatment decisions on the most appropriate choice will have to be balanced across a number of factors including assessment on the extent of tumor PD-L1 expression, patient co-morbidities, patient performance status, extent of disease as well as patient preference. This, together with other agents targeting DNA repair and/or genome

instability, along with the emerging immunotherapies are discussed further, below.

CHEMOTHERAPIES—DNA DAMAGING AGENTS

Platinum Therapy

Platinum doublet therapy has been a frontline therapy for lung cancer since the 1990's. This therapy consists of platinum compounds in combination with several third generation chemotherapeutic drugs, including; cisplatin/carboplatin in combination with gemcitabine, pemetrexed, docetaxel, or paclitaxel (100). It has been generally accepted that the main mechanism of action of platinum compounds as a cancer therapy is by crosslinking the purine bases within DNA, causing DNA damage. In rapidly growing cancer cells this leads to inhibition of DNA replication, cell division, and eventual cell death. Other suggested contributions of platinum compounds to cellular toxicity also include; oxidative stress, modulation of calcium signaling, and activation of several other kinases and signaling pathways [reviewed in (101)]. The emergence of personalized therapies and the toxicity and subsequent side-effects of platinum therapy have led to a reduction in their use. However, until a more effective treatment is found for tumors without an identified biomarker mutation or translocation, platinum treatment is likely to remain a mainstay of lung cancer treatment.

Topoisomerase Inhibitors

Topoisomerase inhibitors are commonly used in combination with platinum agents for treatment of small cell lung cancer (SCLC). First line treatment for SCLC widely involves the topoisomerase II inhibitor, etoposide in combination with platinum therapy. The topoisomerase II enzyme functions to cleave double-stranded DNA and topoisomerase II inhibitors such as etoposide inhibit this activity leading to stable protein-linked DSBs in DNA and subsequent cell death in rapidly dividing cancer cells (102). Topoisomerase I functions to induce single-strand breaks in the DNA to reduce torsional stain on the DNA helix. Relapsed refractory SCLC is commonly treated with the topoisomerase I inhibitors topotecan or irinotecan, following resistance to platinum and topoisomerase II targeting therapies. Inhibition of topoisomerase I, by topotecan or irinotecan prevents repair of these single-strand breaks that are then converted into double-strand breaks in the S-phase of the cell cycle leading to tumor cell death.

DNA-Damage Targeted Therapies

Despite the advances made in "personalized medicine" for the treatment of lung cancers, new treatments have generally not been suitable for the majority of patients, due to a lack of mutations identified in targetable genes. Of further concern, patients inevitably develop resistance to these targeted therapies through an additional mutation in the target gene or initiation of a downstream signaling pathway that stimulates tumor growth. Therefore, although significant progress has been made in lung cancer treatment in recent years, new treatment strategies are urgently required. Several proteins involved in the DNA damage response have been identified as emerging targets for cancer treatment, including; PARP1, ATR, and Chk1.

PARP Inhibitors

The term "synthetic lethality" describes how perturbation of one gene is compatible with cell viability; however, simultaneous disruption of two genes results in cell death (103). In cancer treatments, synthetic lethality can be used to exploit tumor-driven mutations and protein expression alterations to induce cancer-specific cell death [reviewed in (104)]. This treatment specifically targets the tumor cells over the normal cells, which reduces toxic side-effects for patients and improves quality of life during treatment.

The most recognized example of synthetic lethality used in cancer therapy is the use of PARP inhibitors in homologous recombination deficient tumors (105, 106). Inhibition of the PARP enzymes results in PARP immobilization at DNA single-strand breaks and homologous recombination repair is required for replication forks to bypass this lesion. Diminished capacity to complete functional homologous recombination confers cell death following treatment with PARP inhibitors. The breast cancer associated proteins BRCA1/2 function in the repair of DNA via homologous recombination; therefore, PARP inhibitors are approved for treatment of BRCA1/2 mutated breast, ovarian, and pancreas cancer (107). The first PARP inhibitor to be approved by the European Medicines Agency in 2014 was Olaparib (Lynparza; AstraZeneca, London, UK), which is currently used as maintenance therapy for patients with BRCA1/2 mutated ovarian cancer following platinum-based chemotherapy. Subsequently, Niraparib and Talazoparib were also approved for use in a maintenance therapy setting. Several other potent PARP inhibitors are in late clinical trial development including, Veliparib. There are 416 PARP inhibitor clinical trials currently listed on clinicaltrials.gov, including 40 in lung cancer, indicating the potential of this treatment.

Although PARP inhibitor treatment in patients with a range of tumor types with germline BRCA1/2 mutations have shown to be effective, such mutations are only found in ∼5% of patients with lung cancer (108). It is now clear that clinical efficacy would be beneficial beyond this niche population of patients. The need for a definitive biomarker for PARP inhibitor sensitivity has been well-documented (109) and a number of strategies have been explored to predict tumor sensitivity to PARP inhibitors, including unsuccessful attempts to identify predictive biomarkers for homologous recombination-deficient tumors (110). In terms of lung cancer, it has been suggested that high levels of DNA repair inhibiting proteins, such as SLFN11, and low levels of DNA repair promoting proteins, including ATM, may be a superior predictive biomarkers to BRCA1/2 mutations in small cell lung cancer (111, 112).

Significantly, tumors with mutations in the DNA repair protein PTEN account for 4–8% of all NSCLCs and it has been

shown that PTEN mutant tumor cells are sensitive to PARP inhibitors, expanding the number of lung cancer patients this therapy may benefit (113, 114). While PARP inhibitors use in BRCA1/2 mutated tumors remains the best characterized treatment based on synthetically lethality, numerous other synthetic lethal interactions have been identified using RNAi screens, based on other mutations found in lung cancer, including mKRAS and EGFR mutations [summarized in (115)].

Although several combination treatment lung cancer clinical trials, with PARP inhibitors are underway, these trials are still in their early stages and the majority data or trial outcomes are not publically available. However, a recent trial published data, showing the safety and activity of a combination treatment of the PARP inhibitor Olaparib with the DNA damaging alkylating agent temozolomide in patients with relapsed SCLC. The combination was confirmed as safe and active, with an overall response (defined as >30% decrease in the sum of the longest diameter of target legions) in 41.7% of patients and median overall survival of 8.5 months (116). It has also been suggested that a combination of PARP1 inhibitors with immunotherapies may also be an effective combination treatment for lung cancers, particularly in tumors with other DNA repair defects, such as ERCC1 deficiency (117).

PARP inhibitors have also been implicated as a radiosensitizer in NSCLC. Since radiation therapy is the first-line treatment in patients with locally advanced NSCLC, this could have significant implications for their treatment (118, 119).

THE DNA DAMAGE RESPONSE AND IMMUNOTHERAPIES

Immune-Checkpoint Inhibitors

The treatment of lung cancer through immunotherapies, including immune checkpoint inhibitors, and targeted antibodies, has dramatically expanded over recent years. Checkpoint inhibitors which target PD-1 and PDL-1 are considered a standard first and second-line treatment in lung cancer. These immunotherapies block the PD-1 checkpoint to enable the immune system to recognize and target cancer cells. There are now multiple antibodies that are raised against anti-PD1 or anti-PD-L1, including Atezolizumab, Avelumab, Durvalumab, Pembrolizumab, and Nivolumab (120).

Although immunotherapies do not directly target DNA damage repair, DNA damage, and genome instability has been shown to induce changes in the tumor microenvironment and stimulate the generation of neoantigens on cancer cells, increasing the tumor response to immunotherapies. This has led to the hypothesis that DNA damaging agents, such as cisplatin, may increase the efficacy of immunotherapies. Indeed, clinical and preclinical data have shown that chemotherapy can induce PD-L1 expression on tumor cells (121–123).

Testing of PD-L1 expression has rapidly become standard for newly diagnosed patients with advanced NSCLC. A high number of mutations in a tumor, known as the tumor mutation burden, is also associated with an increased response rate to immunotherapy. Similarly, microsatellite instability, also associated with genome instability, is also linked with a better response to immunotherapy. Many commercial laboratories now offer a comprehensive gene sequencing report comprising of the PD-L1 expression, tumor mutation burden, and microsatellite instability status of tumors (124).

In light of the above, the treatment of lung cancer patients with immunotherapies in combination with chemotherapy has shown improvement in patient survival and tumor response rate as such it has now become the standard of care for first-line treatment in several lung cancer subtypes (125–128). Pembrolizumab as a single agent was compared to standard platinum doublet chemotherapy in the first line setting in patient with advanced NSCLC in those with a tumor PD-L1 expression >50%. Updated analysis revealed a median overall survival improvement of 15.8 months in favor of pembrolizumab reported in this group. Based on this study single agent pembrolizumab is favored over platinum based chemotherapy in those with a PD-L1 >50%. A phase 2 randomized study using the combination of pembrolizumab plus carboplatin and pemetrexed demonstrated an objective response rate of 55% in the combination compared to 29% in chemotherapy alone, p:0.0016, supporting the use of a DNA damaging agent in combination with immunotherapy (129). A later phase III randomized placebo controlled trial confirmed the addition of pembrolizumab to chemotherapy led to a significant improvement in median progression free survival (8.8 vs. 4.9 months) and overall survival (12 months overall survival: 69.2 vs. 49.4%) in advanced non-squamous NSCLC. Similar findings have also been observed in another double-blind phase III trial in treatment-naive patients with metastatic squamous NSCLC. In this study, pembrolizumab was combined with carboplatin and either paclitaxel or nab-paclitaxel. In the total population median overall survival was 15.9 months in the combination (chemo-immunotherapy) vs. 11.3 months in the standard arm (130). This constitutes level one evidence for the use of combination chemo-immunotherapy and is considered as an option for the first-line treatment of patients in squamous and non-squamous advanced NSCLC, irrespective of the tumor PD-L1 status (131).

Antibody Drug Conjugates

Antibody-drug conjugates (ADCs) are a rapidly developing area of targeted therapy in lung cancers [reviewed in (132)]. ADCs consist of monoclonal antibodies that are covalently bound to a cytotoxic chemical. These immuno-conjugates are designed to have greater cancer cells toxicity whilst minimizing off target effects on normal cells. The ADCs are now in their third generation through linker optimization, which allows for lower de-conjugation rate in circulation whilst still having a potent impact on cancer cells.

The development of ADCs is limited by the identification of a specific target antigen on the cell surface which has high expression in tumors and low or no expression in normal tissue. The toxic warhead is still a limiting factor based on a small number of cytotoxic drug families, similarly to other cancer therapies, inducing DNA damage or inhibiting microtubule formation. Difficulties arise with the selection of drugs with requirements for retaining potency following

linkage whilst maintaining solubility. Compounds that target DNA include Calicheamicins which induce DNA double-strand breaks, Duocarmycins which alkylate DNA, Benzodiazepines which bind DNA to induce crosslinks and Camptothecin analogs inhibiting DNA topoisomerase I (119, 133, 134). Other ADC warheads include Auristatins, Maytansinoids, and Tubulysins which aim to prevent cancer cell proliferation by inhibiting tubulin assembly (135–138).

Several ADC have been developed that contain compounds that induce DNA damage, as discussed below. These ADC have shown promise for potential treatment of lung cancer, however it should be noted that none of these are currently licensed for use. For example, Sacituzumab Govitecan (IMMU-132) which utilizes an antibody against the transmembrane glycoprotein, Trop-2 (which is highly expressed in epithelial malignancies), conjugated with SN-38, the active metabolite of the topisomerase I inhibitor, irinotecan. In preclinical models, IMMU-132 was shown to deliver 136 fold more SN-38 than irinotecan (139). Clinical trials have shown an overall response rate of between 14 and 31% with IMMU-132 in NSCLC and SCLC (139).

SGN-15 is an ADC targeting topoisomerase II, using the drug Doxorubicin linked to a monoclonal antibody against the carbohydrate antigen Lewis-Y. In a phase II trial comparing SGN-15 in combination with docetaxel to docetaxol treatment alone in NSCLC patients, the overall response rate was 6% for the combination vs. 21% for docetaxol alone. However, the overall survival was greater in the combination treatment (140).

Rovalpituzumab Tesirine (Rova-T) consists of an antibody against delta-like ligand DLL-3 conjugated to pyrrolo-benzodiazepine dimer toxin (a DNA damaging agent). In a phase I trial, SCLC patients had a 18% overall response rate to Rova-T. An improved response rate of 38% was also observed in patients with high DLL3 expression (141). Another phase II trial showed a 14% overall response rate in SCLC patients with DLL3 high expression and 12% overall (142).

Although DNA damage inducing ADCs are not currently approved for treatment of lung cancer, the combination of ADCs with other therapies is under investigation. The treatment of patients with immunotherapy through the targeting of programmed cell death 1 ligand 1 (PDL1) or cytotoxic T lymphocyte antigen 4 (CTLA4) along with ADCs, has shown potential in several tumor types. ADC targeted therapy is rapidly advancing but there is still much to learn in terms of resistance and toxicity before this class of therapy can be fully utilized.

Radiotherapy

Radiation therapy is an effective anti-cancer therapy which induces DNA damage by targeting the DNA to induce multiple forms of damage, including double and single-strand breaks and oxidative lesions. Furthermore, indirect ionization involves interaction with water molecules surrounding DNA to produce radical oxygen species (ROS). These ROS also generate further DNA single-strand breaks, DNA DSBs, and oxidized DNA bases, this leads to cell death in genomically unstable tumors (143).

Radiation therapy is commonly utilized in the treatment of several cancers, including lung cancer. It is still considered a first-line therapy in the treatment of non-small cell lung cancer (NSCLC). However, small cell lung cancer is primarily treated with chemotherapy, although combination radiotherapy and chemotherapy is used as a second line therapy (144). Radiation therapy for lung cancer has evolved over time to increase the accuracy of the X-ray dose delivered to the tumor, subsequently decreasing toxicity to adjacent tissues (145).

Dose fractionation and 3-Dimensional conformal radiation therapy (3DCRT, using CT images) significantly improved radiation treatment (146). The development of multileaf collimators allowing modulation of the X-ray beam dose-rate led to intensity-modulated radiation therapy (IMRT, characterized by a static delivery) and volumetric-modulated arc therapy (VMAT, with a dynamic delivery), which improved the target volume accuracy and led to less organ toxicity (147, 148).

Potential mechanisms of radiation resistance include mutations in EGFR and RAS, increased expression of MDM2 and Livin α, or decreased TP54I3 expression (149, 150). Various XRCC1 mutations have been identified to increase and decrease radio sensitivity in NSCLC (43, 151, 152). Blood-based microRNAs (miRNAs) have been identified as potential biomarkers to elucidate the tumor response to radiotherapy (153).

The field of radiation therapy is still evolving, notably with the development of stereotactic ablative radiation therapy [SBRT or SABR, used by the CyberKnife system (154)], where a very high dose is locally delivered using 3DCRT or IMRT (155). Radiation therapy can also be used in combination with sensitizing drugs (156). The molecules used target DNA [such as Cisplatin (157) or Paclitaxel (158)], DNA repair (PARP inhibitor) (159), or growth factors receptors (e.g., Epidermal Growth Factor Receptor blockade by the drug Cetuximab) (160).

Radioimmunoconjugates

Similarly to some ADCs, radioimmunoconjugates (RICs) are designed to induce DNA-damage specifically in tumor cells, in order to induce cell death. In this case, radionuclides are conjugated via a linker to a monoclonal antibody in order to deliver a dose of radiation specifically to tumor cells expressing a specific cell-surface antigen [reviewed in (161)]. Although a promising area of tumor therapy, RIC therapy has several limitations, due to the radioactive conjugates involved. The pharmacokinetic biodistribution is dependent on the conjugated antibody and this leads to a dose rate two orders of magnitude below conventional external beam radiation therapy, which may limit the use of RICs (162). Although this type of therapy has shown promise in several cancer types, there are no published studies in lung cancer thus far.

CONCLUSIONS

Lung cancer is a highly unstable cancer with genomic instability being a primary driver of the disease. The highly genetically diverse lung cancers are driven by the exposure to DNA damage

from both exogenous and endogenous sources. Although the loss of the normal DNA repair machinery and accumulation of mutations initially drives the tumor progression, it also provides a targetable defect for therapeutic intervention. Such agents that target these defects have been shown to be effective against lung cancer, including combining traditional therapies, such as platinum agents and radiotherapy, and more recently with targeted therapies, such as immunotherapies. Future research efforts are likely to involve refining these combination treatments to overcome the development of tumor resistance to treatments and to improve survival outcomes for patients. Further study of agents that target DNA damage and repair pathways, such as PARP1 inhibitors and ADCs linked to DNA damaging agents are vital to determine their regulatory and subsequent approval for use in the clinic. It is also likely that the further characterization of DNA repair proteins and pathways will drive the quest for new lung cancer therapeutics targets in subsequent years.

AUTHOR CONTRIBUTIONS

JB, MR, DB, JP, CM, MF, CO'L, DR, KO'B, and EB contributed to the writing and editing of the manuscript. MR made the figures. All authors contributed to the article and approved the submitted version.

FUNDING

This work was supported by a grant from the Princess Alexandra Hospital Research Foundation and a Queensland Senior Clinical Research Fellowship (KO'B). JB is supported by an Advance Queensland Early-Career Research Fellowship.

REFERENCES

1. Lee J-K, Choi Y-L, Kwon M, Park PJ. Mechanisms and consequences of cancer genome instability: lessons from genome sequencing studies. *Annu Rev Pathol.* (2016) 11:283–312. doi: 10.1146/annurev-pathol-012615-044446
2. Ahmad S. Platinum-DNA interactions and subsequent cellular processes controlling sensitivity to anticancer platinum complexes. *Chem Biodivers.* (2010) 7:543–66. doi: 10.1002/cbdv.200800340
3. Negrini S, Gorgoulis VG, Halazonetis TD. Genomic instability an evolving hallmark of cancer. *Nat Rev Mol Cell Biol.* (2010) 11:220–8. doi: 10.1038/nrm2858
4. Hoeijmakers JHJ. DNA damage, aging, and cancer. *N Engl J Med.* (2009) 361:1475–85. doi: 10.1056/NEJMra0804615
5. Ciccia A, Elledge SJ. The DNA damage response: making it safe to play with knives. *Mol Cell.* (2010) 40:179–204. doi: 10.1016/j.molcel.2010.09.019
6. Tubbs A, Nussenzweig A. Endogenous DNA damage as a source of genomic instability in cancer. *Cell.* (2017) 168:644–56. doi: 10.1016/j.cell.2017.01.002
7. Melis JPM, Van Steeg H, Luijten M. Oxidative DNA damage and nucleotide excision repair. *Antioxidants Redox Signal.* (2013) 18:2409–19. doi: 10.1089/ars.2012.5036
8. Kandoth C, McLellan MD, Vandin F, Ye K, Niu B, Lu C, et al. Mutational landscape and significance across 12 major cancer types. *Nature.* (2013) 502:333–9. doi: 10.1038/nature12634
9. Govindan R, Ding L, Griffith M, Subramanian J, Dees ND, Kanchi KL, et al. Genomic landscape of non-small cell lung cancer in smokers and never-smokers. *Cell.* (2012) 150:1121–34. doi: 10.1016/j.cell.2012.08.024
10. Choma D, Daurès JP, Quantin X, Pujol JL. Aneuploidy and prognosis of non-small-cell lung cancer: a meta-analysis of published data. *Br J Cancer.* (2001) 85:14–22. doi: 10.1054/bjoc.2001.1892
11. Bielski CM, Zehir A, Penson AV, Donoghue MTA, Chatila W, Armenia J, et al. Genome doubling shapes the evolution and prognosis of advanced cancers. *Nat Genet.* (2018) 50:1189–95. doi: 10.1038/s41588-018-0165-1
12. Parry EM, Gable DL, Stanley SE, Khalil SE, Antonescu V, Florea L, et al. Germline mutations in DNA repair genes in lung adenocarcinoma. *J Thorac Oncol.* (2017) 12:1673–8. doi: 10.1016/j.jtho.2017.08.011
13. Varella-Garcia M. Chromosomal and genomic changes in lung cancer. *Cell Adh Migr.* (2010) 4:100–6. doi: 10.4161/cam.4.1.10884
14. Tosato V, Grüning NM, Breitenbach M, Arnak R, Ralser M, Bruschi CV. Warburg effect and translocation-induced genomic instability: Two yeast models for cancer cells. *Front Oncol.* (2013) 2:212. doi: 10.3389/fonc.2012.00212
15. Pezzuto F, Fortarezza F, Lunardi F, Calabrese F. Are there any theranostic biomarkers in small cell lung carcinoma? *J Thorac Dis.* (2019) 11(Suppl 1):S102–S12. doi: 10.21037/jtd.2018.12.14
16. Hang B. Formation and repair of tobacco carcinogen-derived bulky DNA adducts. *J Nucleic Acids.* (2010) 2010:709521. doi: 10.4061/2010/709521
17. Helleday T, Petermann E, Lundin C, Hodgson B, Sharma RA. DNA repair pathways as targets for cancer therapy. *Nat Rev Cancer.* (2008) 8:193–204. doi: 10.1038/nrc2342
18. Vermeulen W. Dynamics of mammalian NER proteins. *DNA Repair (Amst).* (2011) 10:760–71. doi: 10.1016/j.dnarep.2011.04.015
19. Kamileri I, Karakasilioti I, Garinis GA. Nucleotide excision repair: new tricks with old bricks. *Trends Genet.* (2012) 28:566–73 doi: 10.1016/j.tig.2012.06.004
20. Cadet J, Douki T, Gasparutto D, Ravanat JL. Oxidative damage to DNA: formation, measurement and biochemical features. *Mutat Res.* (2003) 531:5–23. doi: 10.1016/j.mrfmmm.2003.09.001
21. Bowden NA. Nucleotide excision repair: Why is it not used to predict response to platinum-based chemotherapy? *Cancer Lett.* (2014) 346:163–71. doi: 10.1016/j.canlet.2014.01.005
22. Song X, Wang S, Hong X, Li X, Zhao X, Huai C, et al. Single nucleotide polymorphisms of nucleotide excision repair pathway are significantly associated with outcomes of platinum-based chemotherapy in lung cancer. *Sci Rep.* (2017) 7:11785. doi: 10.1038/s41598-017-08257-7
23. Grenda A, Błach J, Szczyrek M, Krawczyk P, Nicoś M, Kuznar Kaminska B, et al. Promoter polymorphisms of TOP2A and ERCC1 genes as predictive factors for chemotherapy in non-small cell lung cancer patients. *Cancer Med.* (2020) 9:605–14. doi: 10.1002/cam4.2743
24. Cheng L, Spitz MR, Hong WK, Wei Q. Reduced expression levels of nucleotide excision repair genes in lung cancer: A case-control analysis. *Carcinogenesis.* (2000) 21:1527–30. doi: 10.1093/carcin/21.8.1527
25. Olaussen KA, Dunant A, Fouret P, Brambilla E, André F, Haddad V, et al. DNA repair by ERCC1 in non-small-cell lung cancer and cisplatin-based adjuvant chemotherapy. *N Engl J Med.* (2006) 355:983–91. doi: 10.1056/NEJMoa060570
26. Weaver DA, Crawford EL, Warner KA, Elkhairi F, Khuder SA, Willey JC. ABCC5, ERCC2, XPA and XRCC1 transcript abundance levels correlate with cisplatin chemoresistance in non-small cell lung cancer cell lines. *Mol Cancer.* (2005) 4:18. doi: 10.1186/1476-4598-4-18
27. Aloyz R, Xu ZY, Bello V, Bergeron J, Han FY, Yan Y, et al. Regulation of cisplatin resistance and homologous recombinational repair by the TFIIH subunit XPD. *Cancer Res.* (2002) 62:5457–62.
28. Huang D, Zhou Y. Nucleotide excision repair gene polymorphisms and prognosis of non-small cell lung cancer patients receiving platinum-based chemotherapy: a meta-analysis based on 44 studies. *Biomed Rep.* (2014) 2:452–62. doi: 10.3892/br.2014.282
29. Mlak R, Krawczyk P, Ramlau R, Kalinka-Warzocha E, Wasylecka-Morawiec M, Wojas-Krawczyk K, et al. Predictive value of ERCC1 and RRM1 gene

single-nucleotide polymorphisms for first-line platinum- and gemcitabine-based chemotherapy in non-small cell lung cancer patients. *Oncol Rep.* (2013) 30:2385–98. doi: 10.3892/or.2013.2696
30. Colussi C, Parlanti E, Degan P, Aquilina G, Barnes D, Macpherson P, et al. The Mammalian Mismatch Repair pathway removes DNA 8-oxodGMP incorporated from the oxidized dNTP pool. *Curr Biol.* (2002) 12:912–18. doi: 10.1016/S0960-9822(02)00863-1
31. Russo MT, Blasi MF, Chiera F, Fortini P, Degan P, Macpherson P, et al. The oxidized deoxynucleoside triphosphate pool is a significant contributor to genetic instability in mismatch repair-deficient cells. *Mol Cell Biol.* (2004) 24:465–74. doi: 10.1128/MCB.24.1.465-474.2004
32. Liu D, Keijzers G, Rasmussen LJ. DNA mismatch repair and its many roles in eukaryotic cells. *Mutat Res - Rev Mutat Res.* (2017) 773:174–87. doi: 10.1016/j.mrrev.2017.07.001
33. Umar A, Boland CR, Terdiman JP, Syngal S, de la Chapelle A, Rüschoff J, et al. Revised Bethesda Guidelines for hereditary nonpolyposis colorectal cancer (Lynch syndrome) and microsatellite instability. *J Natl Cancer Inst.* (2004) 96:261–8. doi: 10.1093/jnci/djh034
34. Kunkel TA, Erie DA. DNA MISMATCH REPAIR. *Annu Rev Biochem.* (2005) 74:681–710. doi: 10.1146/annurev.biochem.74.082803.133243
35. Loeb LA, Loeb KR, Anderson JP. Multiple mutations and cancer. *Proc Natl Acad Sci U S A.* (2003) 100:776–81. doi: 10.1073/pnas.0334858100
36. Bischoff J, Ignatov A, Semczuk A, Schwarzenau C, Ignatov T, Krebs T, et al. HMLH1 promoter hypermethylation and MSI status in human endometrial carcinomas with and without metastases. *Clin Exp Metastasis.* (2012) 29:889–900. doi: 10.1007/s10585-012-9478-0
37. Van Puijenbroek M, Middeldorp A, Tops CMJ, Van Eijk R, Van Der Klift HM, Vasen HFA, et al. Genome-wide copy neutral LOH is infrequent in familial and sporadic microsatellite unstable carcinomas. *Fam Cancer.* (2008) 7:319–30. doi: 10.1007/s10689-008-9194-8
38. Kamal NS, Soria JC, Mendiboure J, Planchard D, Olaussen KA, Rousseau V, et al. MutS homologue 2 and the long-term benefit of adjuvant chemotherapy in lung cancer. *Clin Cancer Res.* (2010) 16:1206–15. doi: 10.1158/1078-0432.CCR-09-2204
39. Safar AM, Spencer H, Su X, Coffey M, Cooney CA, Ratnasinghe LD, et al. Methylation profiling of archived non-small cell lung cancer: a promising prognostic system. *Clin Cancer Res.* (2005) 11:4400–5. doi: 10.1158/1078-0432.CCR-04-2378
40. Do H, Wong NC, Murone C, John T, Solomon B, Mitchell PL, et al. A critical re-assessment of DNA repair gene promoter methylation in non-small cell lung carcinoma. *Sci Rep.* (2014) 4:4186. doi: 10.1038/srep04186
41. Cooper WA, Kohonen-Corish MRJ, Chan C, Kwun SY, McCaughan B, Kennedy C, et al. Prognostic significance of DNA repair proteins MLH1, MSH2 and MGMT expression in non-small-cell lung cancer and precursor lesions. *Histopathology.* (2008) 52:613–22. doi: 10.1111/j.1365-2559.2008.02999.x
42. Nikolaev A, Yang ES. The impact of DNA repair pathways in cancer biology and therapy. *Cancers (Basel).* (2017) 9:126. doi: 10.3390/cancers9090126
43. Kelsey CR, Jackson IL, Langdon S, Owzar K, Hubbs J, Vujaskovic Z, et al. Analysis of single nucleotide polymorphisms and radiation sensitivity of the lung assessed with an objective radiologic endpoin. *Clin Lung Cancer.* (2013) 14:267–74. doi: 10.1016/j.cllc.2012.10.006
44. Lindahl T. Instability and decay of the primary structure of DNA. *Nature.* (1993) 362:709–15. doi: 10.1038/362709a0
45. van Loon B, Markkanen E, Hübscher U. Oxygen as a friend and enemy: how to combat the mutational potential of 8-oxo-guanine. *DNA Repair (Amst).* (2010) 9:604–16. doi: 10.1016/j.dnarep.2010.03.004
46. Greenman C, Stephens P, Smith R, Dalgliesh GL, Hunter C, Bignell G, et al. Patterns of somatic mutation in human cancer genomes. *Nature.* (2007) 446:153–8. doi: 10.1038/nature05610
47. Shibutani S, Takeshita M, Grollman AP. Insertion of specific bases during DNA synthesis past the oxidation-damaged base 8-oxodG. *Nature.* (1991) 349:431–4. doi: 10.1038/349431a0
48. Cadet J, Douki T, Ravanat JL. Measurement of oxidatively generated base damage in cellular DNA. *Mutat Res.* (2011) 711:3–12. doi: 10.1016/j.mrfmmm.2011.02.004
49. Dizdaroglu M, Coskun E, Jaruga P. Repair of oxidatively induced DNA damage by DNA glycosylases: mechanisms of action, substrate specificities and excision kinetics. *Mutat Res.* (2017) 771:99–127. doi: 10.1016/j.mrrev.2017.02.001
50. Hammerman PS, Voet D, Lawrence MS, Voet D, Jing R, Cibulskis K, et al. Comprehensive genomic characterization of squamous cell lung cancers. *Nature.* (2012) 489:519–25. doi: 10.1038/nature11404
51. Leidecker O, Bonfiglio JJ, Colby T, Zhang Q, Atanassov I, Zaja R, et al. Serine is a new target residue for endogenous ADP-ribosylation on histones. *Nat Chem Biol.* (2016) 12:998–1000. doi: 10.1038/nchembio.2180
52. Tao Z, Gao P, Liu HW. Identification of the ADP-ribosylation sites in the PARP-1 automodification domain: analysis and implications. *J Am Chem Soc.* (2009) 131:14258–60. doi: 10.1021/ja906135d
53. Alemasova EE, Lavrik OI. Poly(ADP-ribosyl)ation by PARP1: reaction mechanism and regulatory proteins. *Nucleic Acids Res.* (2019) 47:3811–27. doi: 10.1093/nar/gkz120
54. Leslie Pedrioli DM, Leutert M, Bilan V, Nowak K, Gunasekera K, Ferrari E, et al. Comprehensive ADP-ribosylome analysis identifies tyrosine as an ADP-ribose acceptor site. *EMBO Rep.* (2018) 19:e45310. doi: 10.15252/embr.201745310
55. Robertson AB, Klungland A, Rognes T, Leiros I. DNA Repair in mammalian cells: base excision repair: the long and short of it. *Cell Mol Life Sci.* (2009) 66:981–93. doi: 10.1007/s00018-009-8736-z
56. Petermann E, Keil C, Oei SL. Roles of DNA ligase III and XRCC1 in regulating the switch between short patch and long patch BER. *DNA Repair (Amst).* (2006) 5:544–55. doi: 10.1016/j.dnarep.2005.12.008
57. Adhikari S, Choudhury S, Mitra P, Dubash J, Sajankila S, Roy R. Targeting base excision repair for chemosensitization. *Anticancer Agents Med Chem.* (2012) 8:351–7. doi: 10.2174/187152008784220366
58. Gavande NS, Vandervere-Carozza PS, Hinshaw HD, Jalal SI, Sears CR, Pawelczak KS, et al. DNA repair targeted therapy: the past or future of cancer treatment? *Pharmacol Ther.* (2016) 160:65–83. doi: 10.1016/j.pharmthera.2016.02.003
59. Broustas CG, Lieberman HB. DNA damage response genes and the development of cancer metastasis. *Radiat Res.* (2014) 181:111–30. doi: 10.1667/RR13515.1
60. Cai L, Fu Y, Zhang Y. APE1 Asp148Glu polymorphism and lung cancer susceptibility. *Tumor Biol.* (2014) 35:5237–44. doi: 10.1007/s13277-014-1681-y
61. Xu Z, Yu L, Zhang X. Association between the hOGG1 Ser326Cys polymorphism and lung cancer susceptibility: a meta-analysis based on 22,475 subjects. *Diagn Pathol.* (2013) 8:144. doi: 10.1186/1746-1596-8-144
62. Wei W, He XF, Qin JB, Su J, Li SX, Liu Y, et al. Association between the OGG1 Ser326Cys and APEX1 Asp148Glu polymorphisms and lung cancer risk: a meta-analysis. *Mol Biol Rep.* (2012) 39:11249–62. doi: 10.1007/s11033-012-2035-8
63. Peng Y, Li Z, Zhang S, Xiong Y, Cun Y, Qian C, et al. Association of DNA base excision repair genes (OGG1, APE1 and XRCC1) polymorphisms with outcome to platinum-based chemotherapy in advanced nonsmall-cell lung cancer patients. *Int J Cancer.* (2014) 135:2687–96. doi: 10.1002/ijc.28892
64. Wallace SS, Murphy DL, Sweasy JB. Base excision repair and cancer. *Cancer Lett.* (2012) 327:73–89. doi: 10.1016/j.canlet.2011.12.038
65. Helleday T, Eshtad S, Nik-Zainal S. Mechanisms underlying mutational signatures in human cancers. *Nat Rev Genet.* (2014) 15:585–98. doi: 10.1038/nrg3729
66. Lieber MR. The mechanism of double-strand DNA break repair by the nonhomologous DNA end-joining pathway. *Annu Rev Biochem.* (2010) 79:181–211. doi: 10.1146/annurev.biochem.052308.093131
67. Birkelbach M, Ferraiolo N, Gheorghiu L, Pfäffle HN, Daly B, Ebright MI, et al. Detection of impaired homologous recombination repair in NSCLC cells and tissues. *J Thorac Oncol.* (2013) 8:279–86. doi: 10.1097/JTO.0b013e31827ecf83
68. Tan W, Guan H, Zou LH, Wang Y, Liu XD, Rang WQ, et al. Overexpression of TNKS1BP1 in lung cancers and its involvement in homologous recombination pathway of DNA double-strand breaks. *Cancer Med.* (2017) 6:483–93. doi: 10.1002/cam4.995

69. Lieber MR, Yu K, Raghavan SC. Roles of nonhomologous DNA end joining, V(D)J recombination, and class switch recombination in chromosomal translocations. *DNA Repair (Amst).* (2006) 5:1234–45. doi: 10.1016/j.dnarep.2006.05.013
70. Gerodimos CA, Chang HHY, Watanabe G, Lieber MR. Effects of DNA end configuration on XRCC4-DNA ligase IV and its stimulation of Artemis activity. *J Biol Chem.* (2017) 292:13914–924. doi: 10.1074/jbc.M117.798850
71. Graham TGW, Carney SM, Walter JC, Loparo JJ. A single XLF dimer bridges DNA ends during nonhomologous end joining. *Nat Struct Mol Biol.* (2018) 25:877–84. doi: 10.1038/s41594-018-0120-y
72. Ochi T, Blackford AN, Coates J, Jhujh S, Mehmood S, Tamura N, et al. PAXX, a paralog of XRCC4 and XLF, interacts with Ku to promote DNA double-strand break repair. *Science.* (2015) 347:185–8. doi: 10.1126/science.1261971
73. Chang HHY, Pannunzio NR, Adachi N, Lieber MR. Non-homologous DNA end joining and alternative pathways to double-strand break repair. *Nat Rev Mol Cell Biol.* (2017) 18:495–506. doi: 10.1038/nrm.2017.48
74. Khanna KK, Jackson SP. DNA double-strand breaks: signaling, repair and the cancer connection. *Nat Genet.* (2001) 27:247–54. doi: 10.1038/85798
75. Shrivastav M, De Haro LP, Nickoloff JA. Regulation of DNA double-strand break repair pathway choice. *Cell Res.* (2008) 18:134–47. doi: 10.1038/cr.2007.111
76. Xie A, Hartlerode A, Stucki M, Odate S, Puget N, Kwok A, et al. Distinct roles of chromatin-associated proteins MDC1 and 53BP1 in mammalian double-strand break repair. *Mol Cell.* (2007) 28:1045–57. doi: 10.1016/j.molcel.2007.12.005
77. Lee JH, Paull TT. ATM activation by DNA double-strand breaks through the Mre11-Rad50-Nbs1 complex. *Science.* (2005) 308:551–4. doi: 10.1126/science.1108297
78. Richard DJ, Cubeddu L, Urquhart AJ, Bain A, Bolderson E, Menon D, et al. HSSB1 interacts directly with the MRN complex stimulating its recruitment to DNA double-strand breaks and its endo-nuclease activity. *Nucleic Acids Res.* (2011) 39:3643–51. doi: 10.1093/nar/gkq1340
79. Richard DJ, Savage K, Bolderson E, Cubeddu L, So S, Ghita M, et al. HSSB1 rapidly binds at the sites of DNA double-strand breaks and is required for the efficient recruitment of the MRN complex. *Nucleic Acids Res.* (2011) 39:1692–702. doi: 10.1093/nar/gkq1098
80. Lamarche BJ, Orazio NI, Weitzman MD. The MRN complex in double-strand break repair and telomere maintenance. *FEBS Lett.* (2010) 584:3682–95. doi: 10.1016/j.febslet.2010.07.029
81. Ma CJ, Gibb B, Kwon Y, Sung P, Greene EC. Protein dynamics of human RPA and RAD51 on ssDNA during assembly and disassembly of the RAD51 filament. *Nucleic Acids Res.* (2017) 45:749–61. doi: 10.1093/nar/gkw1125
82. Cousineau I, Abaji C, Belmaaza A. BRCA1 regulates RAD51 function in response to DNA damage and suppresses spontaneous sister chromatid replication slippage: implications for sister chromatid cohesion, genome stability, and carcinogenesis. *Cancer Res.* (2005) 65:11384–91. doi: 10.1158/0008-5472.CAN-05-2156
83. Mcllwraith MJ, Vaisman A, Liu Y, Fanning E, Woodgate R, West SC. Human DNA polymerase η promotes DNA synthesis from strand invasion intermediates of homologous recombination. *Mol Cell.* (2005) 20:783–92. doi: 10.1016/j.molcel.2005.10.001
84. Boddy MN, Gaillard PHL, McDonald WH, Shanahan P, Yates JR, Russell P. Mus81-Eme1 are essential components of a Holliday junction resolvase. *Cell.* (2001) 107:537–48. doi: 10.1016/S0092-8674(01)00536-0
85. Punatar RS, Martin MJ, Wyatt HDM, Chan YW, West SC. Resolution of single and double Holliday junction recombination intermediates by GEN 1. *Proc Natl Acad Sci U S A.* (2017) 114:443–50. doi: 10.1073/pnas.1619790114
86. Guirouilh-Barbat J, Huck S, Bertrand P, Pirzio L, Desmaze C, Sabatier L, et al. Impact of the KU80 pathway on NHEJ-induced genome rearrangements in mammalian cells. *Mol Cell.* (2004) 14:611–23. doi: 10.1016/j.molcel.2004.05.008
87. Bennardo N, Cheng A, Huang N, Stark JM. Alternative-NHEJ is a mechanistically distinct pathway of mammalian chromosome break repair. *PLoS Genet.* (2008) 4:e1000110. doi: 10.1371/journal.pgen.1000110
88. Tammemagi MC, McLaughlin JR, Bull SB. Meta-analyses of p53 tumor suppressor gene alterations and clinicopathological features in resected lung cancers. *Cancer Epidemiol Biomarkers Prev.* (1999) 8:625–34.
89. Kennedy RD, D'Andrea AD. DNA repair pathways in clinical practice: lessons from pediatric cancer susceptibility syndromes. *J Clin Oncol.* (2006) 24:3799–808. doi: 10.1200/JCO.2005.05.4171
90. Leng XF, Chen MW, Xian L, Dai L, Ma GY, Li MH. Combined analysis of mRNA expression of ERCC1, BAG-1, BRCA1, RRM1 and TUBB3 to predict prognosis in patients with non-small cell lung cancer who received adjuvant chemotherapy. *J Exp Clin Cancer Res.* (2012) 31:25. doi: 10.1186/1756-9966-31-25
91. Miao J, Zhang W, Hu X, Chen S, Hu B, Li H. Clinical evaluation of postoperative chemotherapy based on genetic testing in patients with stage IIIA non-small cell lung cancer. *Thorac Cancer.* (2016) 7:44–9. doi: 10.1111/1759-7714.12272
92. Zhang Q, Zhu X, Zhang L, Sun S, Huang J, Lin Y. A prospective study of biomarker-guided chemotherapy in patients with non-small cell lung cancer. *Cancer Chemother Pharmacol.* (2014) 74:839–46. doi: 10.1007/s00280-014-2513-x
93. Wang C, Nie H, Li Y, Liu G, Wang X, Xing S, et al. The study of the relation of DNA repair pathway genes SNPs and the sensitivity to radiotherapy and chemotherapy of NSCLC. *Sci Rep.* (2016) 6:26526. doi: 10.1038/srep26526
94. Kullmann L, Krahn MP. Controlling the master - Upstream regulation of the tumor suppressor LKB1. *Oncogene.* (2018) 37:3045–57. doi: 10.1038/s41388-018-0145-z
95. Wang YS, Chen J, Cui F, Wang H, Wang S, Hang W, et al. LKB1 is a DNA damage response protein that regulates cellular sensitivity to PARP inhibitors. *Oncotarget.* (2016) 7:73389–401. doi: 10.18632/oncotarget.12334
96. Sanli T, Steinberg GR, Singh G, Tsakiridis T. AMP-activated protein kinase (AMPK) beyond metabolism: a novel genomic stress sensor participating in the DNA damage response pathway. *Cancer Biol Ther.* (2014) 15:156–69. doi: 10.4161/cbt.26726
97. Farago AF, Azzoli CG. Beyond ALK and ROS1: RET, NTRK, EGFR and BRAF gene rearrangements in non-small cell lung cancer. *Transl Lung Cancer Res.* (2017) 6:550–9. doi: 10.21037/tlcr.2017.08.02
98. Tsao AS, Scagliotti GV, Bunn PA, Carbone DP, Warren GW, Bai C, et al. Scientific advances in lung cancer 2015. *J Thorac Oncol.* (2016) 11:613–38. doi: 10.1016/j.jtho.2016.03.012
99. Hirsch FR, Scagliotti GV, Mulshine JL, Kwon R, Curran WJ, Wu YL, et al. Lung cancer: current therapies and new targeted treatments. *Lancet.* (2017) 389:299–311. doi: 10.1016/S0140-6736(16)30958-8
100. Bodor JN, Kasireddy V, Borghaei H. First-line therapies for metastatic lung adenocarcinoma without a driver mutation. *J Oncol Pract.* (2018) 14:529–35. doi: 10.1200/JOP.18.00250
101. Dasari S, Bernard Tchounwou P. Cisplatin in cancer therapy: molecular mechanisms of action. *Eur J Pharmacol.* (2014) 740:364–78. doi: 10.1016/j.ejphar.2014.07.025
102. Chan BA, Coward JIG. Chemotherapy advances in small-cell lung cancer. *J Thorac Dis.* (2013) 5(Suppl 5):S565–S78. doi: 10.3978/j.issn.2072-1439.2013.07.43
103. Dobzhansky T. Genetics of natural populations; recombination and variability in populations of *Drosophila pseudoobscura*. *Genetics.* (1946) 31:269–90.
104. O'Neil NJ, Bailey ML, Hieter P. Synthetic lethality and cancer. *Nat Rev Genet.* (2017) 18:613–23. doi: 10.1038/nrg.2017.47
105. Bryant HE, Schultz N, Thomas HD, Parker KM, Flower D, Lopez E, et al. Specific killing of BRCA2-deficient tumours with inhibitors of poly(ADP-ribose) polymerase. *Nature.* (2005) 434:913–7. doi: 10.1038/nature03443
106. Farmer H, McCabe H, Lord CJ, Tutt AHJ, Johnson DA, Richardson TB, et al. Targeting the DNA repair defect in BRCA mutant cells as a therapeutic strategy. *Nature.* (2005) 434:917–21. doi: 10.1038/nature03445
107. Tutt A, Robson M, Garber JE, Domchek SM, Audeh MW, Weitzel JN, et al. Oral poly(ADP-ribose) polymerase inhibitor olaparib in patients with BRCA1 or BRCA2 mutations and advanced breast cancer: a proof-of-concept trial. *Lancet.* (2010) 376:235–44. doi: 10.1016/S0140-6736(10)60892-6
108. Fang W, Cai X, Zhou H, Wang Y, Zhang Y, Hong S, et al. BRCA1/2 germline mutations and response to PARP inhibitor treatment in lung cancer. *J Clin Oncol.* (2019) 37:e13007. doi: 10.1200/JCO.2019.37.15_suppl.e13007

109. Ganguly B, Dolfi SC, Rodriguez-Rodriguez L, Ganesan S, Hirshfield KM. Role of biomarkers in the development of PARP inhibitors. *Biomark Cancer.* (2016) 8(Suppl 1):15–25. doi: 10.4137/BIC.S36679
110. Lord CJ, Ashworth A. BRCAness revisited. *Nat Rev Cancer.* (2016) 16:110–20. doi: 10.1038/nrc.2015.21
111. Stewart CA, Tong P, Cardnell RJ, Sen T, Li L, Gay CM, et al. Dynamic variations in epithelial-to-mesenchymal transition (EMT), ATM, and SLFN11 govern response to PARP inhibitors and cisplatin in small cell lung cancer. *Oncotarget.* (2017) 8:28575–87. doi: 10.18632/oncotarget.15338
112. Pietanza MC, Waqar SN, Krug LM, Dowlati A, Hann CL, Chiappori A, et al. Randomized, double-blind, phase II study of temozolomide in combination with either veliparib or placebo in patients with relapsed-sensitive or refractory small-cell lung cancer. *J Clin Oncol.* (2018) 36:2386–94. doi: 10.1200/JCO.2018.77.7672
113. Dillon L, Miller T. Therapeutic targeting of cancers with loss of PTEN function. *Curr Drug Targets.* (2014) 15:65–79. doi: 10.2174/1389450114666140106100909
114. Mendes-Pereira AM, Martin SA, Brough R, McCarthy A, Taylor JR, Kim JS, et al. Synthetic lethal targeting of PTEN mutant cells with PARP inhibitors. *EMBO Mol Med.* (2009) 1:315–22. doi: 10.1002/emmm.200900041
115. Leung AWY, de Silva T, Bally MB, Lockwood WW. Synthetic lethality in lung cancer and translation to clinical therapies. *Mol Cancer.* (2016) 15:61. doi: 10.1186/s12943-016-0546-y
116. Farago AF, Yeap BY, Stanzione M, Hung YP, Heist RS, Marcoux JP, et al. Combination olaparib and temozolomide in relapsed small-cell lung cancer. *Cancer Discov.* (2019) 9:1372–87. doi: 10.1158/2159-8290.CD-19-0582
117. Chabanon RM, Muirhead G, Krastev DB, Adam J, Morel D, Garrido M, et al. PARP inhibition enhances tumor cell-intrinsic immunity in ERCC1-deficient non-small cell lung cancer. *J Clin Invest.* (2019) 129:1211–28. doi: 10.1172/JCI123319
118. Jiang Y, Verbiest T, Devery AM, Bokobza SM, Weber AM, Leszczynska KB, et al. Hypoxia potentiates the radiation-sensitizing effect of olaparib in human non-small cell lung cancer xenografts by contextual synthetic lethality. *Int J Radiat Oncol Biol Phys.* (2016) 95:772–81. doi: 10.1016/j.ijrobp.2016.01.035
119. Owonikoko TK, Zhang G, Deng X, Rossi MR, Switchenko JM, Doho GH, et al. Poly (ADP) ribose polymerase enzyme inhibitor, veliparib, potentiates chemotherapy and radiation *in vitro* and *in vivo* in small cell lung cancer. *Cancer Med.* (2014) 3:1579–94. doi: 10.1002/cam4.317
120. Grenda A, Nicoś M, Szczyrek M, Krawczyk P, Kucharczyk T, Jarosz B, et al. MicroRNAs aid the assessment of programmed death ligand 1 expression in patients with non-small cell lung cancer. *Oncol Lett.* (2019) 17:5193–200. doi: 10.3892/ol.2019.10207
121. Sheng J, Fang W, Yu J, Chen N, Zhan J, Ma Y, et al. Expression of programmed death ligand-1 on tumor cells varies pre and post chemotherapy in non-small cell lung cancer. *Sci Rep.* (2016) 6:20090. doi: 10.1038/srep23850
122. Sakai H, Takeda M, Sakai K, Nakamura Y, Ito A, Hayashi H, et al. Impact of cytotoxic chemotherapy on PD-L1 expression in patients with non-small cell lung cancer negative for EGFR mutation and ALK fusion. *Lung Cancer.* (2019) 127:59–65. doi: 10.1016/j.lungcan.2018.11.025
123. Rojkó L, Reiniger L, Téglási V, Fábián K, Pipek O, Vágvölgyi A, et al. Chemotherapy treatment is associated with altered PD-L1 expression in lung cancer patients. *J Cancer Res Clin Oncol.* (2018) 144:1219–26. doi: 10.1007/s00432-018-2642-4
124. Walk EE, Yohe SL, Beckman A, Schade A, Zutter MM, Pfeifer J, et al. The cancer immunotherapy biomarker testing landscape. *Arch Pathol Lab Med.* (2019) 144:706–24. doi: 10.5858/arpa.2018-0584-CP
125. Reck M, Rodriguez-Abreu D, Robinson AG, Hui R, Csöszi T, Fülöp A, et al. Pembrolizumab versus chemotherapy for PD-L1-positive non-small-cell lung cancer. *N Engl J Med.* (2016) 375:1823–33. doi: 10.1056/NEJMoa1606774
126. McGranahan N, Furness AJS, Rosenthal R, Ramskov S, Lyngaa R, Saini SK, et al. Clonal neoantigens elicit T cell immunoreactivity and sensitivity to immune checkpoint blockade. *Science.* (2016) 351:1463–9. doi: 10.1126/science.aaf1490
127. Antonia SJ, Brahmer JR, Gettinger SN, Chow LQM, Juergens RA, Shepherd FA, et al. Nivolumab (anti-PD-1; BMS-936558, ONO-4538) in combination with platinum-based doublet chemotherapy (PT-DC) in advanced non-small cell lung cancer (NSCLC). *J Clin Oncol.* (2014) 32:8113. doi: 10.1200/jco.2014.32.15_suppl.8113
128. Sandler AB, Nemunaitis J, Denham C, Von Pawel J, Cormier Y, Gatzemeier U, et al. Phase III trial of gemcitabine plus cisplatin versus cisplatin alone in patients with locally advanced or metastatic non-small-cell lung cancer. *J Clin Oncol.* (2000) 18:122. doi: 10.1200/JCO.2000.18.1.122
129. Langer CJ, Gadgeel SM, Borghaei H, Papadimitrakopoulou VA, Patnaik A, Powell SF, et al. Carboplatin and pemetrexed with or without pembrolizumab for advanced, non-squamous non-small-cell lung cancer: a randomised, phase 2 cohort of the open-label KEYNOTE-021 study. *Lancet Oncol.* (2016) 17:1497–508. doi: 10.1016/S1470-2045(16)30498-3
130. Paz-Ares L, Luft A, Vicente D, Tafreshi A, Gümüş M, Mazières J, et al. Pembrolizumab plus chemotherapy for squamous non-small-cell lung cancer. *N Engl J Med.* (2018) 379:2040–51. doi: 10.1056/NEJMoa1810865
131. Gandhi L, Rodríguez-Abreu D, Gadgeel S, Esteban E, Felip E, De Angelis F, et al. Pembrolizumab plus chemotherapy in metastatic non-small-cell lung cancer. *N Engl J Med.* (2018) 378:2078–92. doi: 10.1056/NEJMoa1801005
132. Pacheco JM, Camidge DR. Antibody drug conjugates in thoracic malignancies. *Lung Cancer.* (2018) 124:260–9. doi: 10.1016/j.lungcan.2018.07.001
133. Shor B, Gerber HP, Sapra P. Preclinical and clinical development of inotuzumab-ozogamicin in hematological malignancies. *Mol Immunol.* (2015) 67(2 Pt A):107–16. doi: 10.1016/j.molimm.2014.09.014
134. Jeffrey SC, Burke PJ, Lyon RP, Meyer DW, Sussman D, Anderson M, et al. A potent anti-CD70 antibody-drug conjugate combining a dimeric pyrrolobenzodiazepine drug with site-specific conjugation technology. *Bioconjug Chem.* (2013) 24:1256–63. doi: 10.1021/bc400217g
135. Lambert JM, Chari RVJ. Ado-trastuzumab emtansine (T-DM1): An antibody-drug conjugate (ADC) for HER2-positive breast cancer. *J Med Chem.* (2014) 57:6949–64. doi: 10.1021/jm500766w
136. Beck A, Reichert JM. Antibody-drug conjugates present and future. *MAbs.* (2014) 6:15–7. doi: 10.4161/mabs.27436
137. Maderna A, Doroski M, Subramanyam C, Porte A, Leverett CA, Vetelino BC, et al. Discovery of cytotoxic dolastatin 10 analogues with N-terminal modifications. *J Med Chem.* (2014) 57:10527–43. doi: 10.1021/jm501649k
138. Li JY, Perry SR, Muniz-Medina V, Wang X, Wetzel LK, Rebelatto MC, et al. A biparatopic HER2-targeting antibody-drug conjugate induces tumor regression in primary models refractory to or ineligible for HER2-targeted therapy. *Cancer Cell.* (2016) 29:117–29. doi: 10.1016/j.ccell.2015.12.008
139. Heist RS, Guarino MJ, Masters G, Purcell WT, Starodub AN, Horn L, et al. Therapy of advanced non-Small-cell lung cancer with an SN-38-Anti-Trop-2 drug conjugate, sacituzumab govitecan. *J Clin Oncol.* (2017) 35:2790–97. doi: 10.1200/JCO.2016.72.1894
140. Ross HJ, Hart LL, Swanson PM, Rarick MU, Figlin RA, Jacobs AD, et al. A randomized, multicenter study to determine the safety and efficacy of the immunoconjugate SGN-15 plus docetaxel for the treatment of non-small cell lung carcinoma. *Lung Cancer.* (2006) 54:69–77. doi: 10.1016/j.lungcan.2006.05.020
141. Rudin CM, Pietanza MC, Bauer TM, Ready N, Morgensztern D, Glisson BS, et al. Rovalpituzumab tesirine, a DLL3-targeted antibody-drug conjugate, in recurrent small-cell lung cancer: a first-in-human, first-in-class, open-label, phase 1 study. *Lancet Oncol.* (2017) 18:42–51. doi: 10.1016/S1470-2045(16)30565-4
142. Carbone DP, Morgensztern D, Le Moulec S, Santana-Davila R, Ready N, Hann CL, et al. Efficacy and safety of rovalpituzumab tesirine in patients with DLL3-expressing, ≥3rd line small cell lung cancer: results from the phase 2 TRINITY study. *J Clin Oncol.* (2018) 36:8507–07. doi: 10.1200/JCO.2018.36.15_suppl.8507
143. Burkart W, Jung T, Frasch G. Damage pattern as a function of radiation quality and other factors. *C R Acad Sci III.* (1999) 322:89–101. doi: 10.1016/S0764-4469(99)80029-8
144. Jeremic B, Gomez-Caamano A, Dubinsky P, Cihoric N, Casas F, Filipovic N. Radiation therapy in extensive stage small cell lung cancer. *Front Oncol.* (2017) 7:169. doi: 10.3389/fonc.2017.00169

145. Diwanji TP, Mohindra P, Vyfhuis M, Snider JW, Kalavagunta C, Mossahebi S, et al. Advances in radiotherapy techniques and delivery for non-small cell lung cancer: Benefits of intensity-modulated radiation therapy, proton therapy, and stereotactic body radiation therapy. *Transl Lung Cancer Res.* (2017) 6:131–47. doi: 10.21037/tlcr.2017.04.04
146. Vijayakumar S, Chen GTY. Implementation of three dimensional conformal radiation therapy: Prospects, opportunities, and challenges. *Int J Radiat Oncol Biol Phys.* (1995) 33:979–83. doi: 10.1016/0360-3016(95)02060-8
147. Selek U, Bölükbaşi Y, Welsh JW, Topkan E. Intensity-modulated radiotherapy versus 3-dimensional conformal radiotherapy strategies for locally advanced non-small-cell lung cancer. *Balkan Med J.* (2014) 31:286–94. doi: 10.5152/balkanmedj.2014.14529
148. Macchia G, Deodato F, Cilla S, Cammelli S, Guido A, Ferioli M, et al. Volumetric modulated arc therapy for treatment of solid tumors: current insights. *Onco Targets Ther.* (2017) 2017:3755–72. doi: 10.2147/OTT.S113119
149. Li T, Kung HJ, Mack PC, Gandara DR. Genotyping and genomic profiling of non-small-cell lung cancer: implications for current and future therapies. *J Clin Oncol.* (2013) 31:1039–49. doi: 10.1200/JCO.2012.45.3753
150. Heist RS, Zhou W, Chirieac LR, Cogan-Drew T, Liu G, Su L, et al. MDM2 polymorphism, survival, and histology in early-stage non-small-cell lung cancer. *J Clin Oncol.* (2007) 25:2243–7. doi: 10.1200/JCO.2006.08.8914
151. Du Y, Su T, Zhao L, Tan X, Chang W, Zhang H, et al. Associations of polymorphisms in DNA repair genes and MDR1 gene with chemotherapy response and survival of non-small cell lung cancer. *PLoS One.* (2014) 9:e99843. doi: 10.1371/journal.pone.0099843
152. Chen J, Zhao QW, Shi GM, Wang LR. XRCC1 Arg399Gln and clinical outcome of platinum-based treatment for advanced non-small cell lung cancer: a meta-analysis in 17 studies. *J Zhejiang Univ Sci B.* (2012) 13:875–83. doi: 10.1631/jzus.B1200083
153. Deig CR, Mendonca MS, Lautenschlaeger T. Blood-based nucleic acid biomarkers as a potential tool to determine radiation therapy response in non-small cell lung cancer. *Radiat Res.* (2017) 187:333–8. doi: 10.1667/RR14613.1
154. Brown WT, Wu X, Fayad F, Fowler JF, Amendola BE, García S, et al. CyberKnife® radiosurgery for stage I lung cancer: results at 36 months. *Clin Lung Cancer.* (2007) 8:488–92. doi: 10.3816/CLC.2007.n.033
155. Ma L, Wang L, Tseng CL, Sahgal A. Emerging technologies in stereotactic body radiotherapy. *Chinese Clin Oncol.* (2017) 6(Suppl 2):S12. doi: 10.21037/cco.2017.06.19
156. Kumar SS, Higgins KA, McGarry RC. Emerging therapies for stage III non-small cell lung cancer: Stereotactic body radiation therapy and immunotherapy. *Front Oncol.* (2017) 7:197. doi: 10.3389/fonc.2017.00197
157. Stinchcombe TE. Combined modality therapy for stage III non-small cell lung cancer. *Oncologist.* (2006) 11:809–823. doi: 10.1634/theoncologist.11-7-809
158. Higgins KA, Pillai RN, Chen Z, Tian S, Zhang C, Patel P, et al. Concomitant chemotherapy and radiotherapy with SBRT boost for unresectable stage III non-small cell lung cancer: a phase I study. *J Thorac Oncol.* (2017) 12:1687–95. doi: 10.1016/j.jtho.2017.07.036
159. de Haan R, Pluim D, van Triest B, van den Heuvel M, Peulen H, van Berlo D, et al. Improved pharmacodynamic (PD) assessment of low dose PARP inhibitor PD activity for radiotherapy and chemotherapy combination trials. *Radiother Oncol.* (2018) 126:443–9. doi: 10.1016/j.radonc.2017.10.017
160. Liu TC, Jin X, Wang Y, Wang K. Role of epidermal growth factor receptor in lung cancer and targeted therapies. *Am J Cancer Res.* (2017) 7:187–202.
161. Bourgeois M, Bailly C, Frindel M, Guerard F, Chérel M, Faivre-Chauvet A, et al. Radioimmunoconjugates for treating cancer: recent advances and current opportunities. *Expert Opin Biol Ther.* (2017) 17:813–9. doi: 10.1080/14712598.2017.1322577
162. Pouget JP, Lozza C, Deshayes E, Boudousq V, Navarro-Teulon I. Introduction to radiobiology of targeted radionuclide therapy. *Front Med.* (2015) 2:12. doi: 10.3389/fmed.2015.00012

Conflict of Interest: KO'B and DR are founders of CARP Pharmaceuticals. EB, DR, and KO'B are founders of Carpe Vitae Pharmaceuticals. EB, JB, KO'B, and DR are inventors on patent applications filed by Queensland University of Technology.

The remaining authors declare that the research was conducted in the absence of any commercial or financial relationships that could be construed as a potential conflict of interest.

Advantages of publishing in Frontiers

OPEN ACCESS
Articles are free to read for greatest visibility and readership

FAST PUBLICATION
Around 90 days from submission to decision

HIGH QUALITY PEER-REVIEW
Rigorous, collaborative, and constructive peer-review

TRANSPARENT PEER-REVIEW
Editors and reviewers acknowledged by name on published articles

Frontiers
Avenue du Tribunal-Fédéral 34
1005 Lausanne | Switzerland

Visit us: www.frontiersin.org
Contact us: frontiersin.org/about/contact

REPRODUCIBILITY OF RESEARCH
Support open data and methods to enhance research reproducibility

DIGITAL PUBLISHING
Articles designed for optimal readership across devices

FOLLOW US
@frontiersin

IMPACT METRICS
Advanced article metrics track visibility across digital media

EXTENSIVE PROMOTION
Marketing and promotion of impactful research

LOOP RESEARCH NETWORK
Our network increases your article's readership